Ramionics (Theory of Everything): Calculating Alpha, the Constants of Physics, and Quantum Gravity from the Geometry of Spacetime

Ramionics — Theorem Contents

Theorem 0: Definition of Physics
Theorem 1: Real Quantity
Theorem 2: Decomposition
Theorem 3: Contact and Repulsion
Theorem 4: Computability and Observability
Theorem 5: Energy
Theorem 6: Equilibrium and Conservation of Energy
Theorem 7: The Escaping Nature of Energy and the Force Equilibrium of Ramions
Theorem 8: The Sphericity of Ramions and Entropy
Theorem 9: The MES State
Theorem 10: Heisenberg's Uncertainty Principle
Theorem 11: Derivation of the Principles of Newtonian Physics from the Theorems of Ramionics
Theorem 12: A Second Proof of Theorem 5
Theorem 13: Isotropy — Another Proof of the Sphericity of Ramions
Theorem 14: Another Proof of the Balance Between Linear and Rotational Energy
Theorem 15: Proof of the Principle of Matter–Energy Equivalence
Theorem 16: Rotational Inertia
Theorem 17: Kissing Number
Theorem 18: The Universe Is Three-Dimensional and Cubic-Crystalline
Theorem 19: FCC Cubic-Crystal Calculations
Theorem 20: The Ramion Energy Equation, Gravitational and Electric Potentials, and the Origin of Relativity
Theorem 21: Proof of the Principle of the Constancy of the Speed of Light
Theorem 22: Calculation of the Speed of Light and Mechanical Definition of Planck's Constant
Theorem 23: The Nature of Mass and Gravity
Theorem 24: The Nature of Charge and the Electric Field; From Ramion Geometry to the Possibility of Modeling the Strong Interaction
Theorem 25: The Twelve-Ball Model
Theorem 26: Ball Equations and Potential Quantization Factors η
Theorem 27: Electric Potential and the Energy of Particles in the Same Family
Theorem 28: Packaging and Generation Classification of Charged Particles (Fermions and Leptons) and Uncharged Particles (Neutrinos)
Theorem 29: Antimatter and Matter–Antimatter Asymmetry
Theorem 30: Geometric Calculation of Alpha
Theorem 31: Calculation of the Gyromagnetic Factor
Theorem 32: Calculation of the Gravitational Constant
Theorem 33: Calculation of the Hubble Constant
Theorem 34: Calculations of Gravity, Relativity, and Dark Matter

Theorem 34: Gravity, Relativity, and Dark Matter — Conclusion
Theorem 35: Electromagnetism
Theorem 36: Muon and Tau Calculations
Theorem 37: Relativistic Dynamics
Theorem 38: Gravitational Time Dilation and Light Deflection
Theorem 39: Strong and Weak Forces, Entropy Equilibrium, and Matter–Energy Exchange
Theorem 40: The Dimensions and Shape of the Universe and Entanglement
Theorem 41: Masses of Quarks, the Proton, and the Neutron
Theorem 42: Calculation of Inertia in Hadrons
Theorem 43: Proton Radius
Theorem 44: Quark Chromatics (Color Charge and Its Geometric Model in Ramionics)

Author: Ramin Khosravi

Website for the latest published revision: https://Ramionics.com/

Email: Ramionics@gmail.com

Introduction and Nomenclature

Fundamental Questions

The **fine-structure constant**, denoted by α, is one of the most fundamental dimensionless constants in physics and determines the strength of the electromagnetic interaction. It is defined by the following relation:

[0.1] $\alpha = K.q_e^2/(\hbar.c)$

Here, K is Coulomb's constant, q_e is the elementary electric charge, $\hbar = h/(2\pi)$ is the reduced Planck constant, and c is the speed of light in vacuum.

The experimentally determined inverse of this constant is approximately:

; $\alpha^{-1} \approx 137.035999177$

Despite the remarkable success of quantum electrodynamics (QED) in calculating phenomena that depend on this constant, its fundamental value is not calculated from first principles in the Standard Model of physics; instead, it enters the theory as an empirical parameter. Although various theoretical models have been proposed to explain its value, no generally accepted and validated model has yet independently derived it from the fundamental principles of physics. Thus, an independent geometrical calculation of the fine-structure constant remains an important and fundamental problem in theoretical physics.

Why does the fine-structure constant have precisely this value? Could this number be a necessary consequence of the geometry of spacetime and the structure of the electron?

More generally, from what principles do the fundamental constants of physics originate—including the speed of light (c), Coulomb's constant (K), Planck's constant (h), the electron gyromagnetic factor (g_e), the gravitational constant (G), the rest energies of the electron (E_e) and proton, and cosmic scales ranging from the electron radius to the Hubble radius (R_h) and the radius of the observable universe (R_u)? What deeper relationships exist among these quantities and their ratios, including the fine-structure constant (α)?

What is the nature of energy, matter, antimatter, electric charge, electric force, dark matter, dark energy, gravity, and, more generally, the four fundamental forces of nature? How does spacetime curvature arise? Most fundamentally, **what exactly are space and time themselves, and what structure or fabric do they possess?**

Ramionics is a physical theory of everything that formulates answers to these fundamental questions within a unified framework based on the **geometry of energy–spacetime**. In this theory, energy, matter, forces, fundamental constants, and space and time themselves are different manifestations of a geometrical structure governed by common principles. Ramionics describes the universe as a **face-centred cubic (FCC)** lattice of fundamental, discrete, spherical units of energy that touch one another, called **Ramions**.

Ramions exist in **SuperSpace**, an environment with infinitely many or very many dimensions, zero or negligible energy density, and an infinite or extremely high propagation speed for energy and light.

Ramions present their energy in the form of space and time. The regions of SuperSpace remaining between the Ramion spheres are called **NonSpace**.

A small fraction of the universe's energy also propagates as radiation, such as photons, across the Ramion lattice at the speed of light. Ramions have variable and even non-integer spacetime dimensions; in this universe, however, they have on average three spatial dimensions and one temporal dimension, and calculations involving these dimensions are performed by straightforward multiplication and division.

Ramion: Rotational And Linear Absolute Energy, Antimatter And Matter

Every Ramion has a finite, positive energy called E_r. The lowest Ramion energy is called the reference energy E_s. The index s comes from the following expression:

Ⓢettled, Ⓢpherical, Ⓢymmetric, Ⓢtandard Ramions at far Ⓢteady-Ⓢtate ⓈSpace

The energy of each Ramion is expressed relative to the reference energy by the factor N:

[0.2] $E_r = N.E_s$, $N \geq 1$

The parameter N is the common metric of energy, space, and time.

A Brief Example of Ramionics Calculations

The following is an example of results obtained in Ramionics. The derivations and proofs of these relations are examined in detail in their respective sections.

Figure [0.3]. The kissing number in three-dimensional space is 12: twelve equal spheres can simultaneously touch a central sphere without overlapping. If the central sphere is placed at the centre of a cube, the centres of the twelve neighbouring spheres lie at the midpoints of the cube’s twelve edges.

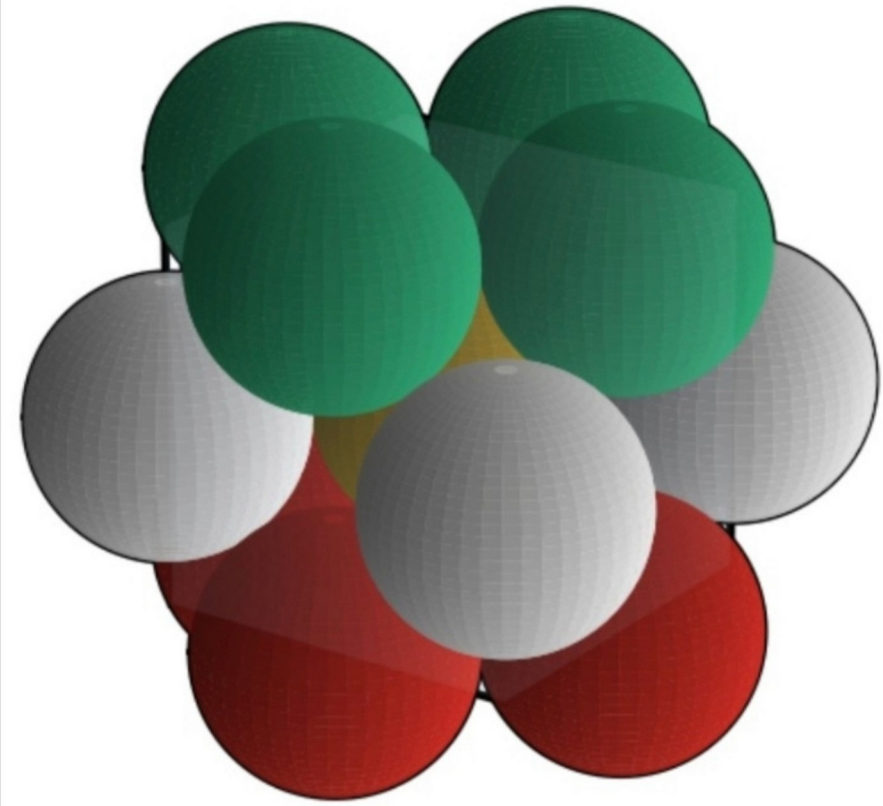

Figure [0.4]. This illustration shows one complete central sphere and twelve quarter-spheres inside a cube. The cube demonstrates the spatial packing fraction:

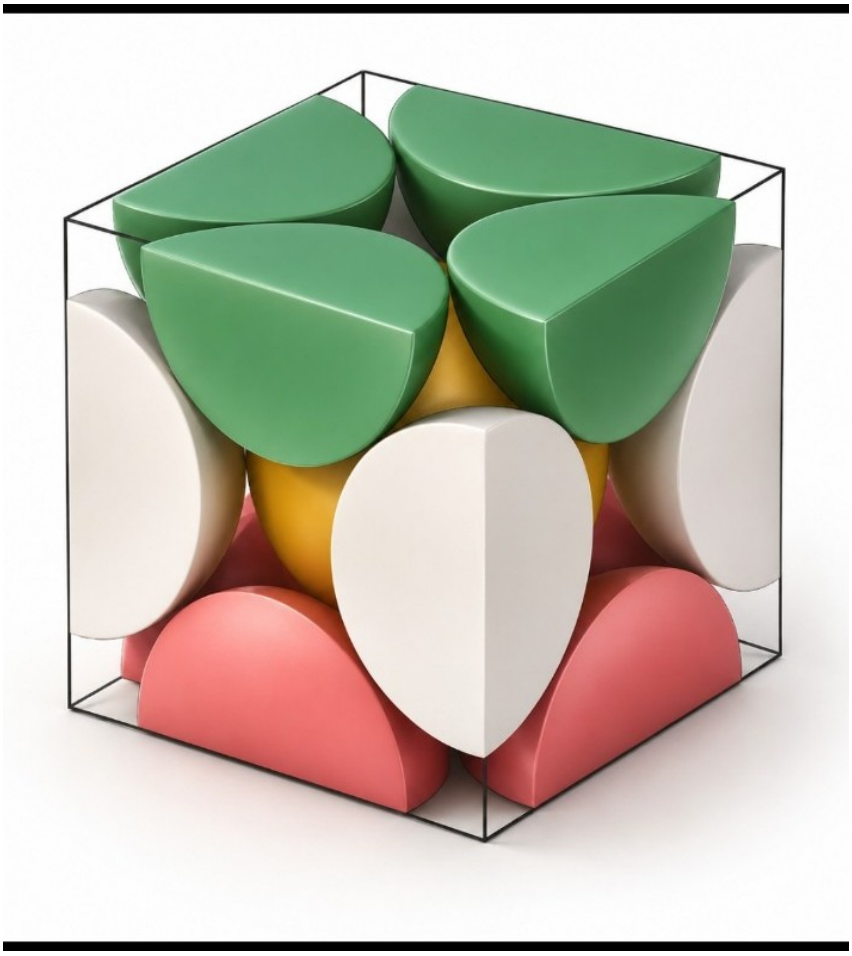

[0.4] $\varphi=\pi/(3\sqrt{2}) \approx 0.74$

From this geometry, γ, the radial freedom factor, and β, the surface coverage factor—the fraction of the surface of a larger sphere lying inside the volumes of the smaller spheres—are obtained as follows:

[0.5] $\varphi = (10/8)/(3\gamma^3)$, $\gamma \approx 0.826$

[0.6] $\beta=(10/8)/(2\gamma^2)=\sqrt[3]{(5\pi^2)/4} \approx 0.917$

The genetic code of the electron family and its growth pathway

In Ramionics, electron formation begins with an initial arrangement of 12 Ramions touching one another. The growth and combination pathway of Ramions forming the electron is expressed by:

[0.7] $\mathring{N} = 4^0 \cdot 4 \cdot 4 \cdot 6 \cdot 6 \cdot 4 \cdot 4 \cdot 2 \cdot 2 = 36864$

This relation, derived from the Euclidean geometry of spacetime, indicates that two stages of fourfold combination, two stages of sixfold combination, another two stages of fourfold combination, and finally two stages of twofold combination form the electron's energy wavefunction.

Geometrical transformation of the genetic code during fermion separation

When fermions separate from the shared 12-ball structure, the change in rotational inertia and characteristic speed determines the geometrical factor $\pi^2/10$ through conservation of rotational energy. The final number of Ramions in each ball is obtained after this transformation and geometrical quantisation:

[0.8] $N_e = \mathrm{Ceil}_{30}((\pi^2/10)\mathring{N}) = 36390$

Derivation of the fine-structure constant

[0.9] $\alpha^{-1} = (1-1/N_e)40\pi/\beta$

; $\alpha^{-1} = 160\sqrt[3]{}(\pi/5)(1-1/N_e)$

; $\alpha^{-1} \approx 137.03599920783327$

These relations indicate that the fine-structure constant has this same value in every three-dimensional universe. More importantly, the geometrical structure and energy equilibrium of Ramions explain why the rest energy of the electron and its related fermions is constant throughout the universe.

Family-Index Standard

The default family index for particle parameters such as N, ħ, α, and K is the electron family. The exceptions are c and c̊, whose default index is s.

Consequently, when the family index is not explicitly written, parameters in the first group refer to the electron family unless another family is specified in the text.

Particle-Notation Standard

Neutrino: ν

Example: the largest neutrino produced during formation of the electron family:

; $\acute{\nu}_e = \nu_{480}$

This denotes a neutrino with an energy of 480 Ramions on each ball.

Electron family:

; e_0=Naryon of electron family, e_1=d=Down , e_2=u=Up , e_3=e=Electron

Hadrons:

; p=Proton=(udu), n=Neutron=(dud)

Muon family:

; m_1=Strange, m_2=Charm, m_3=m=Muon(μ)

Tau family:

; t_1=Bottom , t_2=Top , t_3=t=Tau(τ)

The symbols above refer to ordinary matter. Particles with index c = 3 are leptons with a full negative charge; particles with index c = 1 have charge −⅓ relative to the lepton of the same family, while particles with index c = 2 have charge +⅔.

For antiparticles, the same symbols are used with a tilde accent:

; $\tilde{e}_1 = \tilde{d}$ = Anti-Down , $\tilde{e}_2 = \tilde{u}$ = Anti-Up , $\tilde{e}_3 = \tilde{e}$ = Anti-Electron

; $\tilde{n}$ = ($\tilde{d}\tilde{u}\tilde{d}$) =Anti-Neutron

; $\tilde{p}$ = ($\tilde{u}\tilde{d}\tilde{u}$) = Anti-Proton

; $\tilde{m}_1$ = Anti-Strange, $\tilde{m}_2$ = Anti-Charm, $\tilde{m}_3 = \tilde{m}$ = Anti-Muon(μ^+)

; $\tilde{t}_1$ = Anti-Bottom , $\tilde{t}_2$ = Anti-Top , $\tilde{t}_3 = \tilde{t}$ = Anti-Tau(τ^+)

The energy of each antiparticle equals that of its corresponding particle, so no additional energy notation is needed.

Positron energy: E_e

Scaling Factors

These seven quantities are called **scaling factors**, rather than physical constants, because they define units such as m, s, kg, and J.

[0.11] $c = 2.99792458_{(10)}^{8}$ m/s

[0.12] $h = 6.62607015_{(10)}^{-34}$ J.s

; $\hbar = h/(2\pi)$

; $\hbar = 1.05457181764616_{(10)}^{-34}$

The exact Ramion energy calculated from the experimental energies of the electron, proton, and neutron is:

[0.13] $E_s = \{\theta_e\} \times 9.3723441902457$ eV

The approximate Ramion energy, calculated using only the electron energy, is just 1.47 parts per billion higher than the exact value:

; Approximated $E_s \approx \{\theta_e\}(E_{ex}/54522) \approx \{\theta_e\} \times 9.37234420399105$ eV

Electron rest energy in units of E_s, distinguished by model:

; $E_{es(A/B)} = E_e / E_{s(A/B)} = 54522$

; $E_{es(C/D)} = E_e / E_{s(C/D)} = 54585$

Thus, the electron energy in both scaling conventions is:

; $E_e = 0.510998949940581$ MeV

At present, instead of scaling time by the caesium-133 hyperfine transition frequency, Ramionics uses energy scaling with E_s. In models A/B, the electron energy is $54522E_s$; in models C/D, it is $54585E_s$:

; $f_{cs133ht} = f_{cs} = 9.19263177_{(10)}^{9}$ Hz

[0.14] $q_e = 1.602176634_{(10)}^{-19}$ Coulomb

Boltzmann's constant defines the kelvin:

[0.15] $K_\beta = 1.380649_{(10)}^{-23}$ J/K

Avogadro's constant defines the mole:

[0.16] $N_{av} = 6.02214076_{(10)}^{23}$ 1/mol

The luminous efficacy of monochromatic radiation at a frequency of $540_{(10)}^{12}$ Hz defines the candela:

[0.17] $K_{cd} = 683$ lm.W^{-1}

; 1 lm = 1 cd.sr

At $540_{(10)}^{12}$ Hz, 1 cd corresponds to a radiant intensity of 1/683 W.sr^{-1} in the specified direction.

The seven factors above suffice to define the metre, second, joule or kilogram, electric charge in coulombs, temperature in kelvins, amount of substance in moles, and luminous intensity in candelas.

Ramionics geometrically calculates all physical constants and parameters of the universe and particles—including the fine-structure constant, Coulomb's and gravitational constants, the gyromagnetic factor, and particle charge, mass, radius, and structure—using only the scaling factors.

Even f_{cs} and K_β should, in theory, be calculable from h, c, and E_s. Thus these three scaling factors alone, which are needed to define the three units of energy, space, and time (joule or kilogram,

metre, and second), should permit geometrical calculation of all constants and formulas of physics, because Ramionics models the universe as energy capsules—Ramions—that present space and time.

Experimental Values

The index x signifies an **experimental** or **external** value outside Ramionics, including experimental, theoretical, computational, or combined results such as QED or QCD.

Ramionics does not use these values as inputs. It calculates its own values solely from the geometry of the universe, modelled as a face-centred cubic lattice of Ramions—the only real particles—together with two fundamental equations: conservation of energy and the balance between linear and rotational energy components. The calculated results are then compared with these external values.

CODATA 2022; the default year index is 2022:

[0.19] $\alpha_x^{-1} = 137.035999177 \pm 21_{(10)}{}^{-9}$

; $g_{ex} = 2.00231930436092 \pm 36_{(10)}{}^{-14}$

; $E_{ex} = 0.51099895069 \pm 16_{(10)}{}^{-11}$ MeV

; $E_{px} = 938.27208943 \pm 29_{(10)}{}^{-8}$ MeV

; $E_{nx} = 939.56542194 \pm 48_{(10)}{}^{-8}$ MeV

; $G_x = 6.67430_{(10)}{}^{-11} \pm 15_{(10)}{}^{-16}$ $m^3 \cdot kg^{-1} \cdot s^{-2}$

CODATA 2018 and earlier:

[0.20] $\alpha_{x2018}^{-1} = 137.035999084 \pm 21_{(10)}{}^{-9}$

; $g_{ex2018} = 2.00231930436256 \pm 35_{(10)}{}^{-14}$

; $E_{ex2018} = 0.51099895000 \pm 15_{(10)}{}^{-11}$ MeV

; $E_{px2018} = 938.27208816 \pm 29_{(10)}{}^{-8}$ MeV

; $E_{nx2018} = 939.56542052 \pm 54_{(10)}{}^{-8}$ MeV

; $G_{x2014} = 6.67408_{(10)}{}^{-11} \pm 31_{(10)}{}^{-16}$ $m^3 \cdot kg^{-1} \cdot s^{-2}$

CODATA 2022 data compared with 2018:

; $\Delta\alpha_{x2022}^{-1} = 4.428\sigma_{2018}$

; $\Delta E_{ex2022} = 4.600\sigma_{2018}$

; $\Delta E_{px2022} = 4.379\sigma_{2018}$

; $\Delta E_{nx2022} = 2.630\sigma_{2018}$

History of the electron g-factor in CODATA:

; $g_{ex2018} = 2.00231930436256 \pm 35_{(10)}{}^{-14}$

; $g_{ex2014} = 2.00231930436182 \pm 52_{(10)}{}^{-14}$

; $g_{ex2010} = 2.00231930436153 \pm 53_{(10)}{}^{-14}$

; $g_{ex2006} = 2.0023193043622 \pm 15_{(10)}{}^{-13}$

; $g_{ex2002} = 2.0023193043718 \pm 75_{(10)}{}^{-13}$

Changes in g_e relative to the uncertainty of the preceding adjustment:

; $\Delta g_{ex2022} = -4.686\sigma_{2018}$

; $\Delta g_{ex2018} = +1.423\sigma_{2014}$

; $\Delta g_{ex2014} = +0.547\sigma_{2010}$

; $\Delta g_{ex2010} = -0.446\sigma_{2006}$

; $\Delta g_{ex2006} = -1.280\sigma_{2002}$

Theorem 0: Definition of Physics

The four axioms implicit in the very definition of physics, which are the only axioms of Ramionics.

The definition of physics is: (1) knowledge of the reality of the universe; (2) knowledge of the reality of the components of the universe; (3) knowledge of the truth of the relationships among the components of the universe; and (4) knowledge of the truth of the parameters of the universe (including the parameters of its components and the parameters of the relationships among them).

This definition encompasses four postulates or fundamental principles (axioms): (1) The universe is real; or, if it is not real (for example, if it is someone's simulation, dream, or imagination), it is justified to assume that it is real. (2) The universe consists of real components; or it is justified in making that assumption. (3) The components of the universe genuinely interact with one another; that is, they exchange force and torque or, more generally, energy and information; or it is justified to assume this. (4) The universe is genuinely computable and observable at every instant and has computable processes; or it is justified to assume this.

These four principles are defined as the fundamental principles within the Ramionics framework and form the basis for the subsequent theorems.

Using only these simple, minimal principles 1 through 4, the corresponding philosophical-geometrical Theorems 1 through 4, and then Theorems 5 and 6, Ramionics calculates the geometrical fabric of spacetime. From there, by simple calculations, it calculates the fine-structure constant and even quantum gravity.

On this basis, Ramionics has absolutely no axiom other than the definition of physics itself. Under a different definition of physics, these four principles—and, if necessary, Theorems 1 through 6—may instead be regarded as the axioms of Ramionics.

Ramionics is a triangle with three sides: physics, philosophy, and experience. The intersection of physics and philosophy is mathematics. The part of mathematics that connects mathematics to philosophy is logic and fields such as set theory. The part connecting mathematics to physics is algebra and geometry. The third part is pure mathematics, which both provides a foundation for the other two parts and gradually reveals its role in physics and philosophy. For example, in Ramionics the mass of the electron arises from prime and Mersenne numbers (such as $2^5-1 = 31$, where both 5 and 31 are prime); for this reason, the electron's mass is constant throughout the universe. This represents the entry of Mersenne numbers from pure mathematics into one of the most important foundations of physics.

Experience is the axis connecting physics to philosophy: its intersection with physics is reality, and its intersection with philosophy is truth.

Now imagine a circle comprising philosophy, mathematics (from logic to algebra and geometry), physics, reality, experience, and truth. Ramionics examines each of these six foundations with reference to the other five. For example, it examines physics on the basis of reality, experience, truth, philosophy, and mathematics, while simultaneously examining mathematics on the basis of philosophy and physics. With this approach it calculates the kissing number for different dimensions (the kissing number is needed to calculate the fabric of spacetime in universes whose spatial and temporal dimensions differ from 3 and 1).

Definitions of the real and the true: Real things are self-subsisting and independent. True things depend for their existence on real things; examples include properties such as the colour or length of a pencil, which depend on the existence of the pencil itself and immediately cease to fall within the domain of truth when it no longer exists. Reality concerns existence or nonexistence and whether something is real; truth concerns correctness or incorrectness and the quantity, quality, or attributes of a real thing. Nevertheless, a correct proposition does not necessarily refer to something true, because correct propositions or things based on what is unreal are classified as virtual, rather than true, under this definition.

Definition of a system: A partition or subset of the components of the universe, usually with strong interconnections, having one or more inputs X (effects it receives from other components of the universe), one or more outputs Y (effects it exerts on other components), and usually several parameters describing its status or state S. The complement of this subset—that is, the remaining components of the universe—is itself a system. The feedback relationship between the two systems is such that the output of the first system is an input to the complementary system, and the output of the complementary system is an input to the first. For computational simplicity, feedback is usually restricted to those components of the universe that are more strongly connected to the system.

Definition of system computability: Computability means that, at an instant, if the analyst possesses the necessary parameters in S and X for each output y, the analyst can calculate that output. The more required parameters the analyst knows, and the more accurately they are known, the more accurately the analyst can calculate y. Thus computability means that the parameters of a system at every instant are subject to calculation and accounting.

Definition of system observability: If the analyst has S at time t_0 and X from t_0 to t_1, the analyst must be able to calculate S and Y over that interval; hence the process of change in the parameters is computable. Not needing X or S before t_0 means that all past effects on the system are reflected in its state at t_0 and that no additional hidden memory is involved. Not needing X or S after t_1 also expresses the causality of the system and its independence from the future.

The universe itself is therefore a closed system: its vectors X, Y, and S—or all of its parameters—reduce to S alone and encompass all interconnected components. Consequently, computability of the universe means that its unknown parameters can be calculated from the necessary known parameters; observability means that, if all parameters of the universe were known, its parameter states could be estimated or predicted over intervals into the past and future, depending on the accuracy of that knowledge.

In this framework, the intersection of physics and experience lies in sensations, observations, and experiments; the intersection of philosophy and experience lies in perceptions. Experience supplies sensory data, and perception arises through comparison and interpretation of these data in connection with previous knowledge. Each of the three domains—physics, philosophy, and experience—also has its own independent territory in addition to its overlaps with the others.

Detailed Explanation

Definition of Ramionics

Ramionics is a triangle whose sides are physics (nature and the study of nature), philosophy (reflection and thought), and experience. The intersection of physics and philosophy is mathematics; the intersection of experience and physics is sensation and observation; and the intersection of experience and philosophy is understanding (perception).

Branches of mathematics such as logic and set theory are the language of philosophy. Since physics has three important pillars—{quantities and their measurement}, {analysis of changes in

quantities}, and {the conception and visualisation of these quantities and their changes as qualities}—branches of mathematics such as number theory, differential calculus, and geometry are the language of physics. Other branches of mathematics currently have no direct application in physics or philosophy but may acquire one in the future. For example, Ramionics physics holds that the structure of fermion packets is founded on Mersenne primes, while the geometry of the universe is based on the kissing number, a concept in discrete geometry.

In this triangle, “experience” is considered an independent axis extending from sensations and observations toward perceptions and intuition. At the level of sensation and observation, data are primarily received through the senses. These data become perceptions, however, when they are placed in the appropriate location in the mind (that is, precisely the appropriate physical location in the brain's neural network), compared with previous information—whether sensory or perceptual—and the relationships among them are evaluated. The outcome of this cognitive process may be the confirmation and reinforcement of previous information, its correction and revision, or the generation of new questions.

Accordingly, the intersection of physics and experience appears in “sensation and experiment,” where experience takes objective form as an experiment. Similarly, the intersection of experience and philosophy lies in “perception,” where empirical data enter the realm of interpretation and meaning.

Philosophy, like mathematics, also has domains that move away from physics, mathematics, and even formal structures and approach emotions, feelings, and intuition. This indicates that each side of the triangle has its own independent extent in addition to the areas it shares with the others.

If the sides—physics, philosophy, and experience—and the three corners or overlapping regions—mathematics, observations, and perceptions—are imagined as a hexagon or circle, Ramionics treats each of these six elements on the basis of the intersection and reflection of the other five. Ramionics is a physics defined on the basis of nature, sensations, experience, perception, philosophy, logic, and mathematical tools such as numbers, differentials, and geometry, ultimately returning to nature. Ramionics is a mathematics connected to physics and philosophy, and a philosophy grounded in physics, experience, and mathematics.

Theorem 1: Real Quantity

If the universe is real, it possesses at least one real and absolute quantity.

If the universe is real, it has at least one real quantity. To begin with, examining phenomena such as positive feedback, amplification or resonance, the butterfly effect, and emergence shows that a change or fluctuation (at macroscopic or quantum scales) in a real quantity is necessary to produce a true effect on the universe. But nothing real can arise from a collection of unreal things, however complex.

This is because reality, in the domain of logic, is imposed; it does not propagate through spacetime like a quality or exhibit relativity or dependence on an observer. It is therefore discrete rather than continuous, variable, or susceptible to fluctuations. This discreteness refers to the binary condition of being real or not being real, not to discreteness in the value of a real quantity; the continuity or discreteness of the quantity itself is examined in Section 2. The emergence of real things from unreal things is thus not merely improbable (with absolutely zero probability), but one level further removed: it is impossible. It is ruled out not only in the domains of probability and estimation but also in the domain of possibility.

A real quantity does not depend on any other quantity; therefore its value is also independent and absolute, not relative. The independence of real quantities likewise means that they are absolute rather than relative. This nonrelativity does not concern units of measurement: obviously, changing the measurement unit or scaling of any quantity changes its numerical value.

If all quantities were relative, with each defined in terms of another quantity, the chain of definitions would have no independent foundation. This logical circularity or infinite regress is inconsistent with the assumption that at least one real and absolute quantity exists. This argument concerns logic and mathematics; by itself it makes no judgment about circularity or infinite regress in space, time, causality, or existence.

Detailed Explanation

If the universe is real, it possesses at least one real and absolute quantity.

If the universe, or anything at all, is real (that is, self-subsisting and absolute rather than dependent or relative), it possesses at least one real quantity (absolute and self-subsisting rather than dependent on hypothetical or virtual lines and fields). The basis of this argument is that the universe consists of quantities and qualities, and qualities are relative and often rest upon and are supported by quantities. If quantities were also all relative, there would be no place for reality, which is absolute. If all quantities were relative, each quantity would be defined in terms of another, forming a logical chain without a foundation. No determinate, absolute value could then be defined.

This theorem says only that {circularity and infinite regress} are invalid in {the domains of logic and mathematics}; it offers no opinion on {space, time, causality, and existence}. For example, in {the absence, disturbance, or closure of space or time}, one cannot necessarily say {if A is ahead of B, B cannot be ahead of A}; but under any circumstances one can say {if the number A is greater than B, then B cannot be greater than A}.

A real entity, as opposed to {an unreal entity, whether true (Truth) or virtual (Virtual)}, is a self-subsisting and independent entity as opposed to one that rests on and depends on another; it is objective as opposed to abstract, mental, imaginary, theoretical, conceptual, philosophical, logical, mathematical, or geometrical; absolute as opposed to relative; independent of an observer as opposed to requiring an observer; an object as opposed to a subject; real and actual as opposed to merely correct and surreal.

The only difference between the true and the virtual is that a true entity rests on a real entity, whereas a virtual entity rests on unreal entities or other virtual entities.

Reality means {a correct proposition about a real entity}, and truth means {a correct proposition about a true entity}. Therefore, reality and truth themselves, being propositions, are neither of them real.

Theorem 2: Decomposition

If the constituents of the universe are real, the universe possesses at least one real quantity that is decomposed, that is, encapsulated.

If the universe consists of real constituents, then at least one discrete or encapsulated real quantity exists in the universe.

This discreteness does not require fixed or rigid boundaries. Even if the boundaries of the constituents are wavelike and disturbed, distinguishing real constituents requires at least one encapsulated real quantity, because in pure continuity no boundary arises by which independent constituents can be distinguished.

These capsules themselves, namely Ramions, must repel one another, because if they were neutral or attractive they would sooner or later merge, and in a continuum there is no separability into constituents. Even in the neutral case, the universe's continual turbulence and changes would, over time, cause Ramions to penetrate one another and their boundaries to disappear. Their internal constituents must therefore repel one another as well. Thus Ramions must press against one another or, beyond that, may even be continually expanding.

If the constituents of these Ramions are themselves continuous—that is, differentials of that real quantity—there is no universe made up of separate constituents inside them. If, instead, their constituents are discrete, meaning separate particles, each Ramion in this universe could itself be another universe, and this universe could be a Ramion of another universe: nested universes. For the model's present calculations these two possibilities make no difference, because even in the discrete case the number of particles within each Ramion is so large that there is no difference between summation and integration.

Explanation: The discreteness discussed in this theorem concerns the separation and distinctness of the Ramions constituting this universe, not whether the internal constituents of an individual Ramion are continuous or discrete. Both possibilities remain open for the internal structure of Ramions. In this argument, repulsion is invoked to preserve the separation of real constituents, and is extended to the internal constituents of a Ramion regardless of their continuity or discreteness. The resulting mutual pressure between Ramions also makes their expansion possible.

Theorem 3: Contact and Repulsion

The capsules of real quantity throughout the universe are in a state of mutual tangency and pushing (repulsion).

On the one hand, the capsules of real quantity must repel one another: without repulsion, their independent boundaries would disappear through attraction or gradual intermixing. On the other hand, the real transfer of energy, force, light, and information requires contact and slight indentation between capsules. Repulsion therefore does not mean an absence of contact; rather, it means resistance to further indentation. Attraction, by contrast, is described here as increased indentation and greater intermixing. The indentation must remain sufficiently limited that the capsules stay at the boundary between tangential contact and overlap.

If the constituents of the universe are genuinely connected to their surroundings everywhere, they can genuinely exchange energy (or information). Since Theorem 2 established that Ramions press against one another or may even expand, Ramions are present everywhere in the universe.

To set aside, for the moment, the complications of spatial curvature and the expansion of space, we may say that between any two particles anywhere in the universe there must be a number of particles forming a chain in which every two adjacent particles can exchange energy, light, and information. Geometrically, this means that between any two points in the universe one must be able to find a sequence of points such that a line can be drawn between each pair of adjacent points.

This replaces the simpler statement that any two particles anywhere in the universe must be able to exchange energy, light, and information—that is, geometrically, that a line must be drawable between any two points in the universe.

Ramions are everywhere in the universe: space is filled with them, or more precisely, they are filled with space. Yet between Ramions, as between fruits in a bag, something empty remains. This region is called **NonSpace**. The combination of Space and NonSpace is called **SuperSpace**. As will be shown more precisely in Theorem 18, SuperSpace has infinitely many or very many dimensions, zero or

negligible energy density, and an infinite or extremely high speed of light. Many universes may exist within SuperSpace, separated from one another or occupying different dimensions—that is, parallel universes.

Theorem 4: Computability and Observability

For its real quantities, the universe possesses at least one equilibrium equation and one conservation equation.

In this framework, the computability of the universe requires two fundamental relations based on absolute quantities: a conservation relation to establish global properties and an equilibrium relation to describe constituents and details. These relations complement one another, and relative quantities alone cannot provide an independent foundation for them.

Conservation of a quantity means that its sum over the entire universe remains constant.

If the universe is computable, equations must hold in physics. Every equation contains an equality sign; that equality arises from another physical equation, and ultimately at least one equilibrium equation must hold between real quantities or presentations of real quantities, forming a point of connection between physics and mathematics.

Thus at least one fundamental equilibrium equation must link mathematical relations to the real quantities of the universe. It is not necessary that every equation in physics directly be an equilibrium equation.

By a **presentation**, consider, for example, the perimeter P and area S of a circle. An equilibrium equation between these two presentations is:

$4\pi S = P^2$

If the universe is observable, something real must remain constant over time. In other words, if equations hold between derivatives and consequently between integrals, the constant of integration must be determined from somewhere else. Therefore, at least one real quantity—or the sum of several real quantities or their presentations—must be conserved.

Comparing states of the universe at different times requires a real, stable reference, which in this framework is expressed through the conservation of a real quantity.

Theorem 5: Energy

Energy is the only real quantity.

In Ramionics, energy is defined as motion and as the universe's sole real, self-subsisting, absolute quantity. Space, time, and their numbers of dimensions are not properties imposed upon a Ramion; rather, in the model they emerge from interactions between capsules of energy.

The definition of any physical quantity is either manifestly related to space (for example, something involving length, area, volume, or a vector), manifestly related to time (for example, something containing a derivative, integral, or a time differential), or implicitly related to spacetime (such as temperature, which itself arises from molecular motion). Consequently, space and time must either be real quantities or be demonstrably derived from some real quantity.

Neither space can create time nor time create space; furthermore, neither has meaning without the other. Hence neither can be an independent real quantity. Without space there is no motion, so time is neither measurable nor meaningful. If space existed but time did not, the temporal separation between any two points of space would be either zero or infinite, rendering spatial separation

meaningless. Both are therefore unreal (and thus relative), yet true rather than virtual. Accordingly, mass or energy must be assumed to be the real quantity.

Mass is fundamentally defined here by a tendency toward rest. Even gravity, which arises from mass, generates motion only temporarily and transiently, until the collision ends; its enduring response is rest. If a mass m revolves around M, this is because m originally had a velocity that would have carried it linearly toward infinity, but it became trapped by gravity. Viewed from afar, it has become stationary relative to the motion it would have had without gravity.

Energy, which tends toward motion and indeed is motion itself, therefore provides the answer, since it gives meaning to both space and time.

Consider a Ramion—that is, energy (or, for easier visualization, compressed mass)—made up of constituents that may be particles or differentials of energy (or mass). These constituents intrinsically move. Their motion has two forms: linear and rotational; oscillations and other familiar motions are also reduced to these two forms within this framework. Linear motion, like the motion of gas molecules (or springlike molecules wound around themselves in several dimensions, with their ends connected and moving in all dimensions), generates pressure and hence space. Rotational motion creates rotation and a reference for time. These two components do not interfere with each other: increasing the pressure inside a balloon does not generate rotation; likewise, increasing a wheel's rotational speed or torque, assuming its axle is not loose, does not generate a lateral force around it. Every Ramion is therefore both a quantum and a vessel or capsule of energy, space, and time.

Each rotational axis constitutes one dimension of time; under ordinary conditions there is one. The difference from a clock is that the rotation of a Ramion advances time, whereas time advances a clock's hands.

The numbers of spatial and temporal dimensions are not written into a Ramion's identity, since its only real quantity is energy. It is the interactions and decisions of Ramions themselves that determine how many dimensions of space and time they create.

In this model, the linear–radial component of energy is regarded as the source of pressure, space, mass, relativity, and gravity; the rotational–angular component is regarded as the source of time, torque, electric charge, and electrical, magnetic, and electromagnetic phenomena. These assignments are mechanical assumptions of the Ramionics framework, examined in subsequent theorems.

Ramions differ from balloons attached to one another in that Ramions produce space by presenting energy in SuperSpace, whereas balloons occupy pre-existing space. Balloons are also filled with air molecules, while Ramions consist of pure energy. A balloon's membrane is made of a different substance from its contents and has the same number of dimensions as the balloon—three (regarding its surface as two-dimensional is only an approximation). By contrast, a Ramion's membrane is made of the same substance as its contents, namely energy, but has exactly one fewer dimension.

Detailed explanation:

In the mechanical description, a spherical capsule of energy is considered. The linear motion of its constituents, like collisions between gas molecules, exerts pressure on a membrane also made of energy and having one fewer dimension. This picture is used to explain the presentation and expansion of space. In this framework, the energy of Ramions is also proposed as a source of dark energy; this is not a result proved solely by the gas analogy.

To explain the rotational component, the analogy of a clock hand is used. Unlike a clock, however, in the Ramionics model the rotation of the capsule is considered to create the reference for time rather than merely measure it. Rotation around multiple axes is also proposed as a possibility for multidimensional time. This description further assumes that linear motion alone does not produce time, and rotational motion alone does not produce pressure or space.

The supplementary formulation also explains the name **Ramion** using the English phrase “Rotational_electrical Linear_gravitational Real Absolute energy Anti Matter And Matter Ion,” and presents the model's overall aim as describing the origins of space, time, mass, electric charge, and fundamental forces through capsules of energy.

Theorem 6: Equilibrium and Conservation of Energy

According to Theorem 5, the only real quantity in the universe is energy, with only two components or presentations: linear and rotational. Therefore, by Theorem 4, and because at the most fundamental level there is no preference between these two nonzero components, the only possible equilibrium and conservation equations are that linear and rotational energies are equal and their sum is conserved throughout the universe. A better formulation is:

The universe's only real quantity is energy, which is conserved and has two equal linear and rotational presentations corresponding to space and time. This equilibrium holds for every Ramion and even for every constituent of a Ramion. Thus the rule of conservation of energy is established, not as an axiom but as a theorem; likewise, the energy of any constituent of a Ramion or of the entire Ramion is:

E_r=2(Linear Energy)=2(½$\mathring{m}_r.\mathring{c}_r^2$)=$\mathring{m}_r.\mathring{c}_r^2$

In this framework, conservation of energy means that the total energy of all Ramions throughout the universe remains constant:

; $\sum \mathring{E}_r$ = constant

The ring above E denotes the internal space of each Ramion. The equilibrium between the linear and rotational components of energy is written:

; $\hat{E} = \check{E} = ½\mathring{E}$

In Ramionics notation, $\hat{E}$ and $\check{E}$ represent linear and rotational energy, respectively:

; $E_{(Linear)} = E_{(L)} = \hat{E}$

; $E_{(Rotational)} = E_{(R)} = \check{E}$

Under the assumptions of the theorem, this equilibrium is extended to the constituents of every Ramion, to each Ramion itself, and to the entire universe.

This is also the principle of equivalence between matter and energy, which is established as a theorem rather than assumed as an axiom.

Ramionics therefore has only two fundamental equations: conservation of energy and balance between the linear and rotational components of the energy of every Ramion, or even any part of it.

The linear component of energy produces pressure and consequently space, relativity, and quantized gravity, without singularities or hypothetical spacetime curvature.

The rotational component of energy produces time, torque, electricity, magnetism, and electromagnetism.

Thus Ramions are atoms or capsules of energy, space, and time; balance in the distribution of energy between the linear and rotational components means balance between the presentation of space and the presentation of time.

Detailed explanation:

In the philosophical account of this theorem, energy or motion is regarded as the essence and substance of the universe. In the model's view, because a Ramion itself creates space and time, no independent external agent is assumed to disturb the balance between its two energy components. The supplementary formulation also considers extending these two relations to other possible real universes; here, that extension is a theoretical possibility, not a conclusion independent of the theorem's premises.

Theorem 7: The Escaping Nature of Energy and the Force Equilibrium of Ramions

The preceding theorems indicate that every Ramion is a vessel of energy, and this energy naturally tends to spread: it seeks to increase both the size of the Ramion and its number of dimensions. Consequently, each Ramion tends to transfer its energy to the surrounding Ramions and reach the minimum possible energy, zero. But the surrounding Ramions have the same tendency and resist it. Thus the fabric of spacetime arises from the equilibrium of forces among Ramions, and repulsion is the foundation of physics (and it will be shown that gravity itself arises from this repulsion).

Theorem 8: The Sphericity of Ramions and Entropy

The d-dimensional sphere is the most complete and simplest geometrical shape among d-dimensional bodies.

Geometrically, completeness means that among all d-dimensional volumes, the sphere encloses the greatest volume for a given surface area, or requires the least surface area for a given volume: it has the greatest volume-to-surface ratio. Physically, this means that, for a given amount of gas at a given pressure, or a given amount of energy at a given energy density, the sphere exerts the least force on its membrane. In other words, if a membrane has a specified pressure tolerance, the spherical state can store the greatest amount of energy. A balloon, for example, reaches the greatest possible volume under the same pressure when spherical. This property expresses the sphere's maximum efficiency in energy storage.

The sphere is also the most symmetrical geometrical shape. Geometrically, symmetry means simplicity: the least information needed to describe structure, position, and orientation. Physically, greater symmetry (meaning a more uniform distribution of forces) and a smaller information burden (meaning fewer sharp corners and edges) both reduce the maximum pressure at different points in the system. Hence maximum symmetry—disorder, entropy—like minimum energy, is a natural tendency of everything. The tendency of systems to carry the least order and energy is the macroscopic, large-scale expression of this tendency of Ramions.

In short, the completeness of the sphere means minimizing the total force exerted on its membrane, while its symmetry means distributing that force more uniformly, thereby minimizing the maximum stress or pressure.

To clarify the issue of information, suppose we wish to order the manufacture of a shape from a particular material. A sphere is the simplest option, because it is specified by a single parameter: diameter or radius. Even a cube needs more information: its side length or diagonal, and the

number six to specify its six-faced structure. A rectangular cuboid needs additional parameters, such as length, width, and height.

In terms of spatial position, in a d-dimensional space every body requires d coordinates to specify its position. Apart from the sphere, however, bodies also depend on $d(d-1)/2$ additional parameters to specify rotations about axes, that is, their spatial orientation:

Roll: rotation about the x-axis. **Pitch:** rotation about the y-axis. **Yaw:** rotation about the z-axis.

Thus, in the balanced and average state, the spherical shape is the most natural and stable shape for Ramions.

Now take the center of a Ramion as the origin of a coordinate system and call that Ramion layer zero. The Ramions tangent to it are called layer 1, those tangent to layer 1 are called layer 2, and so on. Thus, according to Theorem 3, all Ramions in the universe can be addressed by a unique layer number.

The universe's natural tendency concerns not only the sphericity of each Ramion but also the sphericity of every surrounding layer of Ramions.

The conclusion is that each individual Ramion, and the universe as a whole, tends toward minimum energy and maximum symmetry—entropy and disorder. Each Ramion additionally tends to attain the minimum possible energy; however, because of energy conservation, one cannot assume that the entire universe also tends toward minimum total energy.

Theorem 9: The MES State

Except for the conservation and linear–rotational energy-equilibrium equations, all other equations and calculations are subject to turbulence.

Energy or motion constitutes the capsules that are the life of the universe. The universe is therefore intrinsically oscillatory, wavelike, turbulent, dynamic, and changing—not static. In addition, the universe is filled with gravitational, electromagnetic, and neutrino radiation. On the other hand, the universe is intrinsically discrete and quantized, because it consists of capsules of energy.

Accordingly, every physical quantity and every equation, apart from the two laws of conservation and equilibrium, is wavelike and disturbed. These two Ramionics equations permit the calculation of such waves and disturbances, as well as calculations in the MES state, which is the default state.

Definition of MES: Mean and probable; enduring and equilibrated; stable.

Mean &: probable equilibrium stable

For example, consider the spherical shape of Ramions. If one were hypothetically to film a single Ramion over a long period, or photograph a large number of Ramions at one instant, the result—the mean or most probable shape—would be a sphere. Furthermore, this would also be the most enduring, balanced, stable, and equilibrium-like shape after the transient period. In this terminology, the shape of a Ramion in the MES state is spherical, or the sphere is the most MES-like shape of a Ramion.

Theorem 10: Heisenberg's Uncertainty Principle

On the basis of Theorems 6 through 8, every quantity (except total energy, the linear component of energy, or the rotational component of energy) faces an intrinsic limit on measurement precision:

The product of the measurement error of a quantity and the measurement error of the rate of change of that same quantity cannot fall below a threshold.

If that quantity is the position of a particle, this relation is called Heisenberg's uncertainty principle.

Theorem 11: Derivation of the Principles of Newtonian Physics from the Theorems of Ramionics

The energy of a Ramion, and its shorter representation, are defined as follows:

[11.1] $\mathring{E}_r = E_{(}\text{Linear}_{)} + E_{(}\text{Rotational}_{)} = E_{(}L_{)} + E_{(}R_{)}$

[11.2] $\mathring{E}_r = \hat{E} + \check{E}$

These symbols are also used to distinguish other linear and rotational parameters. The subscript r denotes a Ramion. The subscript R denotes the rotational component, and L the linear component. The parameter r is the radius of a Ramion, whereas R is the distance of any point in the universe from the center of the Ramion, taken as the coordinate origin. The parameter $\vec{r}$ is the position vector.

The subscript s denotes Ramions possessing the minimum energy:

[11.3] $\mathring{E}_s = \min(\mathring{E}_r)$

Linear energy defines space, and rotational energy defines time.

Position

With the definition of space, the position vector and angle are defined:

[11.4] $\vec{r} = x\,\vec{\imath} + y\,\vec{\jmath} + z\,\vec{k} = (x, y, z)$

[11.5] θ = (arc length)/(radius)

Here $\vec{\imath}$, $\vec{\jmath}$, and $\vec{k}$ are unit vectors along the coordinate axes.

A vector is like a number with as many components as the number of spatial dimensions or degrees of freedom of a problem. Since, in matrix notation using [ ], columns within a row are separated by spaces without commas, while rows are separated by commas, it is preferable to regard a vector as a column of numbers containing several rows separated by commas.

A vector is a one-dimensional generalization of an ordinary number (or scalar, or zero-dimensional quantity), just as a line is a one-dimensional generalization or extension of a zero-dimensional point. A matrix generalizes a vector and may have more than one dimension.

[11.6] [x, y, z] = (x, y, z)

Velocity

Once time t and the variables x, y, z, and θ have been defined, their derivatives with respect to t define linear and angular velocity:

[11.7] $\vec{v} = d\vec{r}/dt = v_x\,\vec{\imath} + v_y\,\vec{\jmath} + v_z\,\vec{k} = (v_x, v_y, v_z)$

[11.8] $v_x = dx/dt$, $v_y = dy/dt$, $v_z = dz/dt$

[11.9] $\vec{\omega} = (d\theta/dt)\,\vec{n}$

The vector $\vec{n}$ is the unit vector along the rotation axis.

The positive direction of $\vec{\omega}$ is determined by the right-hand rule: if the fingers of the right hand curl in the direction of rotation, the thumb indicates the direction of $\vec{\omega}$. Equivalently, when viewed along the positive direction of the $\vec{n}$ axis, the rotation appears counterclockwise.

[11.10] $|\vec{v}| = \sqrt{(v_x^2 + v_y^2 + v_z^2)}$

Here speed is the scalar magnitude of velocity.

Acceleration

[11.11] $\vec{a} = d\vec{v}/dt = a_x \vec{\imath} + a_y \vec{\jmath} + a_z \vec{k} = (a_x, a_y, a_z)$

[11.12] $\vec{\alpha} = d\vec{\omega}/dt$

[11.13] $a_x = d^2x/dt^2$, $a_y = d^2y/dt^2$, $a_z = d^2z/dt^2$

Force and Torque

[11.14] $\vec{F} = \pm \nabla \hat{E}$

Definition of the gradient:

[11.15] $\nabla \hat{E} = (d\hat{E}/dx, d\hat{E}/dy, d\hat{E}/dz)$

[11.16] $\vec{\tau} = \pm (d\check{E}/d\theta)\, \vec{n}$

The positive or negative sign depends on whether energy is transferred into or out of the system.

The relation between torque and the vector product of radius and tangential force, for a small portion of energy or mass undergoing rotational motion, is:

[11.17] $\vec{\tau} = d\check{E}/d\theta = r \times (d\check{E}/(r\, d\theta)) = r \times F_{(rot)}$

[11.18] $\check{F} = F_{(Rotational)} = F_{(Tangent)} = F_t$

[11.19] Default $F = \hat{F} = F_{(Linear)} = F_{(L)} = F_{(Pressure)} = F_p$

The designation $\vec{\tau}$ is taken from periodic or temporal phenomena, or *Time*, but is also consistent with *Tangent*.

Definition of Moment of Inertia

Linear inertia, briefly called mass (m), and rotational-angular moment of inertia, briefly called inertia (I), are defined by:

[11.20] $m = |\vec{F}|/|\vec{a}|$

[11.21] $I = |\vec{\tau}|/|\vec{\alpha}|$

Summary of the Derivation of Newton's Principles

For the constituents of a Ramion regarded as a body, and by extension for bodies throughout the universe, the preceding definitions and relations imply the following.

First, if energy does not change, the time derivative of linear and rotational velocity is zero. Consequently, the body moves with constant linear velocity in a fixed direction and rotates with constant angular velocity about a fixed axis.

Second, the spatial derivative of energy, namely force, is proportional to the time derivative of linear velocity; and the angular derivative of energy, namely torque, is proportional to the time derivative of angular velocity.

Third, whenever two bodies exert forces on one another, conservation of energy requires that the energy gained by one equals the energy lost by the other. Thus, the force of either body is the negative of the force of the other.

Accordingly, the principles of Newtonian physics are established inside a Ramion, that is, among its constituents, and always hold there. The same Newtonian relations outside the Ramion give rise to relativity and gravitation. In other words, outside rather than inside a Ramion, Newtonian equations must be replaced by more accurate relativistic relations at high gravitational fields and speeds.

Detailed Derivation

Momentum

Linear momentum is defined as the product of linear inertia (mass) and linear velocity. Correspondingly, rotational (angular) momentum is defined as the product of rotational inertia I and rotational (angular) velocity:

[11.22] $\hat{p} = m \cdot \vec{v}$

[11.23] $\check{p} = I \cdot \vec{\omega} = \vec{L} = \vec{J}$

The letter p derives from the Latin *ponderum* or *pondus*, meaning weight or heaviness. Angular momentum is also represented by L or J. Taking the time derivatives (rates of change) of these momenta gives force and torque:

[11.24] $d\hat{p}/dt = m \cdot d\vec{v}/dt = m \cdot \vec{a} = \vec{F}$

[11.25] $d\check{p}/dt = I \cdot d\vec{\omega}/dt = I \cdot \vec{\alpha} = \vec{\tau}$

Energy as a Function of Velocity

The rate of change of linear energy with respect to position equals force, that is, mass multiplied by acceleration:

[11.26] $d\hat{E}/dL = \hat{F} = m \cdot dv/dt$

A change of variables shows that the derivative of energy with respect to velocity equals mass multiplied by velocity:

[11.27] $d\hat{E}/dv = m \cdot dL/dt = m \cdot v$

Integrating the preceding relation yields:

[11.28] $\hat{E} = ½\ m \cdot v^2$

The same procedure applies to rotational energy:

[11.29] $d\check{E}/d\theta = \tau = I \cdot d\omega/dt$

[11.30] $d\check{E}/d\omega = I \cdot \omega$

[11.31] $\check{E} = ½\ I \cdot \omega^2$

Constant Acceleration and Velocity

[11.32] $a = dv/dt = dv/dL \cdot dL/dt = dv/dL \cdot v$

[11.33] $\int a\ dL = \int v\ dv$

[11.34] $v^2 - v_0^2 = 2\ a\ L$

Similarly, for rotational motion with constant angular acceleration:

[11.35] $\omega^2 - \omega_0^2 = 2\ \alpha\ \theta$

Centripetal Acceleration and Apparent Centrifugal Force

Consider the position vector in an inertial reference frame:

[11.36] $\vec{r}(t) = r\ (\cos(\omega t), \sin(\omega t))$

Velocity:

[11.37] $\vec{v} = d\vec{r}/dt = r\ \omega\ (-\sin(\omega t), \cos(\omega t))$

Speed:

[11.38] $|\vec{v}| = r\ \omega$

Acceleration:

[11.39] $\vec{a} = d\vec{v}/dt = -r\,\omega^2\,(\cos(\omega t), \sin(\omega t)) = -\omega^2\,\vec{r}$

Therefore:

[11.40] $\vec{a} = -\omega^2\,\vec{r}$, $a_{(c)} = \omega^2\,r = v^2/r$

In an inertial reference frame, this centripetal acceleration and force are real:

[11.41] $\vec{F} = m\,.\,\vec{a} = -m\,.\,\omega^2\,\vec{r}$

In a frame rotating with angular velocity ω, however, centrifugal acceleration and force are apparent:

[11.42] $F_{(centrifugal)} = +m\,.\,\omega^2\,\vec{r}$

Coriolis Acceleration

To describe motion in a rotating frame, one must consider the transformation of time derivatives between inertial and rotating frames. For an arbitrary vector $\vec{A}$:

[11.43] $(d\vec{A}/dt)_{(inertial)} = (d\vec{A}/dt)_{(rot)} + \vec{\omega} \times \vec{A}$

This relation shows that the actual change (in the inertial frame) consists of two parts: the change in the rotating frame and the effect of the frame's rotation.

For the position vector:

[11.44] $\vec{v}_{(inertial)} = \vec{v}_{(rel)} + \vec{\omega} \times \vec{r}$

Here $\vec{v}_{(rel)}$ is the body's velocity relative to the rotating frame.

Taking the time derivative:

[11.45] $\vec{a}_{(inertial)} = \vec{a}_{(rel)} + 2\,\vec{\omega} \times \vec{v}_{(rel)} + \vec{\omega} \times (\vec{\omega} \times \vec{r})$

This relation contains three important physical terms:

[11.46] $a_{(Coriolis)} = 2\,\vec{\omega} \times \vec{v}_{(rel)}$

[11.47] $a_{(centrifugal)} = \vec{\omega} \times (\vec{\omega} \times \vec{r})$

Consequently, Coriolis acceleration appears only when the body has a relative velocity in the rotating frame; its direction is perpendicular to $\vec{\omega}$ and $\vec{v}_{(rel)}$.

Gyroscopic Effect

For a rotating rigid body, the principal quantity is angular momentum:

[11.48] $\vec{L} = I\,.\,\vec{\omega}$

If an external torque acts:

[11.49] $\vec{\tau} = d\vec{L}/dt$

When the magnitude of $\vec{L}$ is constant but its direction changes:

[11.50] $d\vec{L}/dt = \Omega \times \vec{L}$

Here Ω is the angular velocity of precession.

Substituting into the torque relation:

[11.51] $\vec{\tau} = \Omega \times \vec{L}$

Taking the magnitude of this relation:

[11.52] $|\Omega| = |\vec{\tau}|/|\vec{L}|$

This result shows that, under torque, the rotation axis begins to precess instead of falling. This is gyroscopic stability.

Here $\vec{\omega}$ is the body's angular velocity relative to the inertial frame; Ω is the angular velocity of change in the direction of the rotation axis; and $\vec{v}_{(\mathrm{rel})}$ is the body's velocity relative to the rotating frame.

The Coriolis and gyroscopic phenomena both arise from the analysis of motion in non-inertial reference frames. The former concerns translational motion in a rotating frame, whereas the latter concerns the angular momentum of rigid bodies.

Integral Relation for Moment of Inertia

For a particle of mass dm at distance r from the axis:

[11.53] $v = \omega \times r$

Note that × denotes the vector product. Its rotational energy is:

[11.54] $dĚ = ½\ dm\ .\ v^2 = ½\ dm\ .\ (r^2\omega^2)$

For the entire body:

[11.55] $Ě = \int ½\ r^2\omega^2\ dm$

Since ω is the same for the entire body:

[11.56] $Ě = ½\omega^2 \int r^2\ dm$

Definition of rotational energy:

[11.57] $Ě = ½\ I\ .\ \omega^2$

Comparing the two relations:

[11.58] $I = \int r^2\ dm$

Here r is the perpendicular distance from the rotation axis in an inertial frame, or in the frame in which the axis is defined, and ω is the angular velocity of the rigid body relative to that same frame.

Effective Radius

Dividing the preceding relation by the total mass:

[11.59] $I/m = (1/m) \int r^2\ dm$

An effective radius may be defined:

[11.60] $r_e\int^2 = (1/m)\ \square\ \ r^2\ dm$

Thus:

[11.61] $I = m\ .\ r_e\mathit{//}^2$

The quantity $r_e\mathit{//}$ has an important physical interpretation: it is the distance at which concentrating the entire mass would produce the same rotational inertia.

Power, Pressure, Stress, and Strain

Power is the change in energy attributable to something per unit time. Its unit is joules per second, or watts.

[11.62] $E = \int \mathrm{Power}\ dt$

Pressure is force per unit area. Its unit is newtons per square meter, or pascals.

[11.63] $F = \int \mathrm{Pressure}\ dS$

In this article, momentum is represented by lowercase p and pressure by uppercase P.

Stress, σ, measured in pascals (Pa), comprises three cases: (1) normal stress, including tension and compression—pressure is its isotropic form in fluids—and their combination in bending; (2) parallel stress, including shear or simple sliding and torsion; and (3) combined normal and parallel stress.

Strain, denoted ε, is the relative deformation of a body.

Hooke's relation, in which E_γ is Young's modulus for a given material, is:

[11.64] $\sigma = E_\gamma \cdot \varepsilon$

Compare this with a spring, whose behavior depends on the shape of the body and the material:

[11.65] $F = k_s \cdot x$

If a rod of Young's modulus E_γ, radius r, and length L is formed into a spring of radius R, its spring constant is:

[11.66] $k_s = (E_\gamma \cdot \pi r^4)/(4 R^2 L)$

If a strip of Young's modulus E_γ, width b, thickness t, and length L is formed into a torsion spring, its torsional stiffness is:

[11.67] $k_s = (E_\gamma \cdot b t^3)/(12 L)$

Theorem 12: A Second Proof of Theorem 5

A systematic examination of physical quantities shows that all quantities can be classified into two general categories: those associated with linear motion and those associated with rotational motion.

The domain of {linear–radial–pressure–gravitational energy} includes linear velocity, linear acceleration, linear inertia (mass m), linear force, linear momentum, pressure, relativity, and gravitation. The domain of {rotational–angular–tangential–torque–electrical energy} includes angular velocity, angular acceleration, rotational inertia I, tangential force F_t, torque, angular momentum, and electrical charge, field, force, and energy, as well as magnetic and electromagnetic quantities.

Apart from energy, none of these quantities individually possesses a simultaneously linear and rotational nature. For example, velocity, acceleration, force, or momentum in their linear and tangential forms are {perpendicular} to one another and therefore share no common component. Consequently, mass and electric charge, and their corresponding forces, are also independent of one another.

Consider, however, a linear spring, a torsion spring, a charged battery, or a dam filled with water (that is, charged with gravitational energy, which is fundamentally linear energy). Energy is readily exchanged among them. Energy therefore has a nature beyond the distinction between linear and rotational forms and encompasses both.

Energy is consequently the only quantity that can serve, absolutely and fundamentally, as the origin and source of other physical quantities and as the basis for their definition and explanation. It is therefore the only real quantity.

Theorem 13: Isotropy — Another Proof of the Sphericity of Ramions

If the universe exhibits isotropy or radial symmetry—that is, if physical formulas and constants, such as the speed of light, appear identical in every direction—then the measures of real quantities must be spherical {in the form of MES, or more precisely than MES}. In other words, measures that behave identically in every direction must possess spherical symmetry.

Theorem 14: Another Proof of the Balance Between Linear and Rotational Energy

Since Ramions are containers of spacetime, at least within the computational framework of a distant observer, distinctions of direction, distance, and linear velocity disappear:

[14.1] $\hat{c} = \check{c} = \mathring{c}$

Here $\mathring{c}$ is the speed of transmission of energy or light inside a Ramion and is proportional to the speed of light c as it passes through the Ramion's space.

Furthermore, because a Ramion is a container of spacetime, all its constituents perceive the same radius r and angular velocity ω. Consequently, their tangential velocities are equal:

[14.2] $\check{c} = r \cdot \omega = \mathring{c}$

Therefore, from relations (1) and (2):

[14.3] $\hat{c} = \check{c} = r \cdot \omega = \mathring{c}$

The linear energy of each constituent is:

[14.4] $\hat{E} = ½\, m \cdot \mathring{c}^2$

Its rotational energy is:

[14.5] $\check{E} = ½\, I \cdot \omega^2$

Substituting:

[14.6] $I = \mathring{m} \cdot r^2$

And using relation (2):

[14.7] $\check{E} = ½\, \mathring{m} \cdot r^2 \cdot \omega^2 = ½\, \mathring{m} \cdot \mathring{c}^2$

It follows that:

[14.8] $\hat{E} = \check{E}$

This is precisely the balance between linear and rotational energy. It shows that equality of these two components may be inferred not only from their definition but also from the spacetime structure of a Ramion.

To understand how all constituents of a Ramion perceive the same radius and angular velocity, consider the inertia of a point mass, a ring perpendicular to the axis of rotation, or a rod or thin cylinder parallel to the rotation axis. In all these cases, every point perceives the same radius and angular velocity.

Theorem 15: Proof of the Principle of Matter–Energy Equivalence

Theorems 8 and 14 independently show that:

[15.1] $\check{E} = ½\, \mathring{m} \cdot r^2 \cdot \omega^2 = ½\, \mathring{m} \cdot \mathring{c}^2 = \hat{E}$

Consequently:

[15.2] $\mathring{E}_r = 2\,(½\, \mathring{m} \cdot \mathring{c}^2) = \mathring{m} \cdot \mathring{c}^2$

Theorem 16: Rotational Inertia

Rotational inertia (moment of inertia) of familiar bodies with uniform surface or volume distributions

Point mass at distance R from the rotation axis:

[16.1] $I = m R^2$, point mass

Thin ring about its central axis:

[16.2] $I = m R^2$, thin ring central axis

Thin cylindrical shell about its central axis:

[16.3] $I = m R^2$, thin cylindrical shell

Thin rod parallel to the rotation axis at distance R:

[16.4] $I = m R^2$, thin rod parallel axis

The preceding four equations mean precisely that the effective radius equals the radius of the body itself.

Ring about its own diameter:

[16.5] $I = \frac{1}{2} m R^2$, ring about diameter

Solid cylinder about its central axis:

[16.6] $I = \frac{1}{2} m R^2$, solid cylinder

Disk about an axis perpendicular to its plane:

[16.7] $I = \frac{1}{2} m R^2$, disk central axis

Disk about its own diameter:

[16.8] $I = \frac{1}{4} m R^2$, disk about diameter

Thin rod about its center, perpendicular to its length:

[16.9] $I = \frac{1}{12} m L^2$, rod center perpendicular

Spherical shell:

[16.10] $I = \frac{2}{3} m R^2$, spherical shell

Solid sphere:

[16.11] $I = \frac{2}{5} m R^2$, solid sphere

Important calculations in Ramionics for determining mass moment, electric moment, and the gyromagnetic factor:

Consider twelve equal spheres of radius R, tangent to one another and to an imaginary spherical cavity of the same radius. Call each sphere a ball. The centers of every two balls symmetric about the center form a pair and lie on an axis passing through the center of the body, namely the center of the cavity. Accordingly, divide each ball into two hemispheres: the far hemisphere (away from the center) and the near hemisphere (toward the center). At the center of each ball, define a local spherical coordinate system whose z-axis coincides with the radius extending outward from the center of the body. Use it to visualize the far and near hemispheres and the equatorial plane.

Inertia for a uniform mass distribution on the surfaces of the spheres:

[16.12] $Iws = \frac{10}{3} m R^2$

On the volumes of the spheres:

[16.13] $Iwv = \frac{46}{15} m R^2$

On the equatorial plane, the disk common to the far and near hemispheres:

[16.14] $Iwdisk = 3 m R^2$

On the surfaces of the far hemispheres:

[16.15] $Ihw = \frac{14}{3}\ m\ R^2$

On the surfaces of the far hemispheres, but in the differential case: the inertia of the mass on a far hemisphere minus the inertia of an equal mass on the near hemisphere:

[16.16] $IhwD = \frac{8}{3}\ m\ R^2$

And two further inertias assuming a distribution weighted by cos(θ), defined in the local coordinates of the corresponding sphere:

[16.17] $IhwCos = \frac{46}{9}\ m\ R^2$

Differential case:

[16.18] $IhwCosD = \frac{32}{9}\ m\ R^2$

Detailed derivation

In this section, the inertias are calculated directly from their integral definition:

[16.19] $I = \int r^2\ dm$

This equation states that the contribution of each mass element to the total inertia is proportional to the square of its distance from the rotation axis. Consequently, the spatial distribution of mass is the principal determinant of inertia: as mass lies farther from the axis, its contribution increases quadratically.

For continuous distributions, depending on the distribution type, dm is expressed in surface or volume form:

[16.20] $I = \int r^2\ \sigma\ dA$

[16.21] $I = \int r^2\ \rho\ dV$

If the surface or volume density is uniform, calculating the inertia reduces to determining an effective radius. The total mass is then treated as being located at an effective distance from the axis corresponding to the root-mean-square distance.

[16.22] $I = m\ R_{(eff)}^2$

[16.23] $R_{(eff)}^2 = (1/m) \int r^2\ dm$

For a uniform surface distribution:

[16.24] $R_{(eff)}^2 = (1/A) \int r^2\ dS$

For a uniform volume distribution:

[16.25] $R_{(eff)}^2 = (1/V) \int r^2\ dV$

Important theorems:

Parallel Axis Theorem

If the rotation axis does not pass through the center of mass, the total inertia equals the inertia about the center of mass plus a term proportional to the square of the distance between the new axis and the center of mass. This term is always positive and increases the inertia. The relationship is independent of the body's shape and depends only on its mass and the distance. Conditions of validity: the two axes must be parallel; one must pass through the center of mass; the body must be rigid; and d must be the perpendicular separation between the axes.

[16.26] $I = Icm + m\ d^2$

Euler's Inertia Tensor Theorem

Inertia is a second-rank tensor, diagonal in the principal-axis coordinate system, where its components become independent; this simplifies the analysis of rotational motion. Conditions of validity: the body must be rigid, the mass distribution known, the axes must pass through a common point, and the principal axes must be chosen. The following equations do not hold simultaneously: each is valid only for its corresponding planar case.

[16.27] $I_x + I_y = I_z$

This equation holds for a planar body in the xy-plane, or when the z-component of every mass element is zero.

[16.28] $I_x + I_z = I_y$

This equation holds for a planar body in the xz-plane, or when the y-component of every mass element is zero.

[16.29] $I_y + I_z = I_x$

This equation holds for a planar body in the yz-plane, or when the x-component of every mass element is zero.

Euler's Direction-Cosine Theorem of Inertia

The inertia about an arbitrary axis is a weighted sum of the inertias about the principal axes, with weights equal to the squares of the corresponding direction cosines. This relationship expresses the directional dependence of inertia. Conditions of validity: the axes must be principal axes, or the tensor must be diagonal, and the arbitrary axis must be a unit axis.

[16.30] $I = I_x \cos^2\theta_x + I_y \cos^2\theta_y + I_z \cos^2\theta_z$

[16.31] $\cos^2\theta_x + \cos^2\theta_y + \cos^2\theta_z = 1$

Maxwell's Perpendicular Axis Theorem

For planar bodies, the inertia about the perpendicular axis equals the sum of the inertias about two mutually perpendicular axes in the plane. Conditions of validity: the body must be planar, its mass must lie in one plane, and all three axes must pass through a common point.

[16.32] $I_z = I_x + I_y$

Axis Transformation Theorem (Otto Mohr)

This relationship describes how inertia changes when the coordinate system rotates within a plane and includes the product-of-inertia term. Conditions of validity: the transformation must take place in a plane and the axes must share a common origin.

[16.33] $I(\theta) = I_x \cos^2\theta + I_y \sin^2\theta - 2\, I_{xy} \sin\theta \cos\theta$

[16.34] $I_{xy}(\theta) = (I_y - I_x) \sin\theta \cos\theta + I_{xy} (\cos^2\theta - \sin^2\theta)$

Thin ring about its diameter

Linear density:

[16.35] $dm = (m / 2\pi R) \,.\, R\, d\theta$

Distance from the axis:

[16.36] $r = R \sin\theta$

Substitution:

[16.37] $I = \int_0^{2\pi} (R^2 \sin^2\theta) \,.\, (m / 2\pi R) \,.\, R\, d\theta$

[16.38] $I = \frac{1}{2}\, m\, R^2$

This result shows that the mean squared distance of the ring's points from its diameter is half the square of the radius.

Disk about an axis perpendicular to its plane

Surface density:

[16.39] $dm = (m / \pi R^2) \cdot 2\pi r \, dr$

[16.40] $I = \int_0^R r^2 \cdot (m / \pi R^2) \cdot 2\pi r \, dr$

[16.41] $I = (2m / R^2) \int_0^R r^3 \, dr = \frac{1}{2} m R^2$

Here the mass distribution extends from the center to the outer radius, and the mean squared distance equals half the square of the radius.

Disk about its diameter

[16.42] $I = \int_0^{2\pi} \int_0^R (r^2 \sin^2\theta) \cdot (m / \pi R^2) \cdot r \, dr \, d\theta$

[16.43] $I = \frac{1}{4} m R^2$

This result follows from the planar symmetry, which halves the inertia relative to the axis perpendicular to the disk.

Spherical shell

Surface density:

[16.44] $dm = (m / 4\pi R^2) \cdot (R^2 \sin\theta \, d\theta \, d\varphi)$

[16.45] $I = \int_0^{2\pi} \int_0^{\pi} (R^2 \sin^2\theta) \cdot (m / 4\pi R^2) \cdot R^2 \sin\theta \, d\theta \, d\varphi$

[16.46] $I = \frac{2}{3} m R^2$

Here the distribution of mass over the sphere's surface makes the mean squared distance greater than for the disk.

Solid sphere

Volume density:

[16.47] $dm = (m / (\frac{4}{3} \pi R^3)) \cdot r^2 \sin\theta \, dr \, d\theta \, d\varphi$

[16.48] $I = \int_0^R \int_0^{\pi} \int_0^{2\pi} (r^2 \sin^2\theta) \cdot dm$

This integral includes the contribution from every point in the volume and has a stronger dependence on the internal radii.

[16.49] $I = \frac{2}{5} m R^2$

This result shows that, compared with a shell, some of the mass is closer to the axis and the inertia is reduced.

Ramionics calculations for twelve spheres

In this calculation, the total mass m is distributed uniformly among twelve spheres. The distances of their centers are considered in groups of four and eight.

[16.50] $m_1 = m / 12$

The four middle spheres lie at a distance of twice the radius from the axis.

[16.51] $d_4 = 2R$

The other eight spheres lie at a distance of the square root of two times the radius.

[16.52] $d_8 = \sqrt{2} \, R$

Inertia of twelve spherical shells

The inertia of the four spheres includes intrinsic and axis-translation contributions.

[16.53] $I_{4s} = 4 \, . \, (⅔ \, (m/12) \, R^2 + (m/12)(2R)^2)$

The inertia of the eight spheres is calculated using their smaller distance from the axis.

[16.54] $I_{8s} = 8 \, . \, (⅔ \, (m/12) \, R^2 + (m/12)(\sqrt{2} \, R)^2)$

The total inertia is the sum of the contributions from both groups.

[16.55] $Iws = I_{4s} + I_{8s}$

The final result is the total surface inertia of the system.

[16.56] $Iws = ¹⁰⁄₃ \, m \, R^2$

Inertia of twelve solid spheres

The volume inertia of the four spheres is calculated taking their internal mass distribution into account.

[16.57] $I_{4v} = 4 \, . \, (⅖ \, (m/12) \, R^2 + (m/12)(2R)^2)$

The contribution of the other eight spheres is included in the volume inertia.

[16.58] $I_{8v} = 8 \, . \, (⅖ \, (m/12) \, R^2 + (m/12)(\sqrt{2} \, R)^2)$

The total inertia is the sum of both groups.

[16.59] $Iwv = I_{4v} + I_{8v}$

The final result is the total volume inertia of the system.

[16.60] $Iwv = ⁴⁶⁄₁₅ \, m \, R^2$

Inertia of the equatorial planes of twelve spheres

The general formula for one disk follows by combining Euler's theorem with the parallel-axis theorem:

[16.61] $I = M \, D^2 + (M \, R^2 / 4)(2 \cos^2\theta + \sin^2\theta)$

Mass of each disk:

[16.62] $M = m / 12$

Calculation for four disks

The angle θ is 90° and the distance D is 2R.

[16.63] $\cos^2\theta = 0 \, , \, \sin^2\theta = 1$

[16.64] $Icenter = (M \, R^2 / 4)(1)$

[16.65] $Icenter = (m/12)(R^2/4)$

[16.66] $Ishift = (m/12)(2R)^2 = (m/12)(4R^2)$

[16.67] $Ione = (m/12)(4R^2) + (m/48)R^2$

[16.68] $Ione = ¹⁷⁄₄₈ \, m \, R^2$

For four disks:

[16.69] $I_4 = 4 \, . \, (¹⁷⁄₄₈ \, m \, R^2)$

[16.70] $I_4 = ¹⁷⁄₁₂ \, m \, R^2$

Calculation for eight disks

The angle θ is 45° and the distance D is $\sqrt{2}$ R.

[16.71] $\cos^2\theta = ½ \, , \, \sin^2\theta = ½$

[16.72] Icenter = (M R^2 / 4)(2 . ½ + ½)

[16.73] Icenter = (M R^2 / 4)(3/2)

[16.74] Icenter = (m/12)(3/8 R^2)

[16.75] Ishift = (m/12)(√2 R)² = (m/12)(2R^2)

[16.76] Ione = (m/12)(2R^2) + (m/12)(3/8 R^2)

[16.77] Ione = 19/96 m R^2

For eight disks:

[16.78] I_8 = 8 . (19/96 m R^2)

[16.79] I_8 = 19/12 m R^2

Total sum

[16.80] I = I_4 + I_8

[16.81] I = (17/12 + 19/12) m R^2

[16.82] Iwdisk = I = 3 m R^2

Inertia of twelve spherical hemishells

Assumption: the total mass m is distributed separately over the twelve far hemishells, and another mass m is distributed over the twelve near hemishells.

Mass of each hemishell:

[16.83] M = m / 12

Calculation of the inertia of one hemishell

From the general definition:

[16.84] I = ∫ r^2 dm

For a hemishell whose center lies at distance d from the axis:

[16.85] r^2 = $|\vec{R} + \vec{d}|^2$

Expansion:

[16.86] r^2 = R^2 + d^2 + 2 ($\vec{R}$. $\vec{d}$)

Substitution into the integral:

[16.87] I = ∫ R^2 dm + ∫ d^2 dm + 2 ∫($\vec{R}$. $\vec{d}$) dm

Simplification:

[16.88] ∫ d^2 dm = M d^2

The integral ∫ r^2 dm is Icm:

[16.89] Icm = 2/3 M R^2

Coupling term:

[16.90] ∫ ($\vec{R}$. $\vec{d}$) dm = d R∫(R cosα) dm

For a hemishell:

[16.91] ∫ (R cosα) dm = M (R/2) sinθ

Therefore:

[16.92] 2 ∫($\vec{R}$. $\vec{d}$) dm = M d R sinθ

Resulting base formula:

Far hemishell:

[16.93] $I_{far} = M\,(d^2 + \tfrac{2}{3} R^2 + d\,R \sin\theta)$

Near hemishell:

[16.94] $I_{near} = M\,(d^2 + \tfrac{2}{3} R^2 - d\,R \sin\theta)$

Calculation for four hemishells

[16.95] $d = 2R$

[16.96] $\theta = 90°$

[16.97] $\sin\theta = 1$

Far hemishells:

[16.98] $I4_{far} = 4 \cdot (m/12) \cdot ((2R)^2 + \tfrac{2}{3} R^2 + 2R \cdot R)$

[16.99] $I4_{far} = \tfrac{20}{9}\, m\, R^2$

Near hemishells:

[16.100] $I4_{near} = 4 \cdot (m/12) \cdot ((2R)^2 + \tfrac{2}{3} R^2 - 2R \cdot R)$

[16.101] $I4_{near} = \tfrac{8}{9}\, m\, R^2$

Calculation for eight hemishells

[16.102] $d = \sqrt{2}\, R$

[16.103] $\theta = 45°$

[16.104] $\sin\theta = \sqrt{2} / 2$

Far hemishells:

[16.105] $I8_{far} = 8 \cdot (m/12) \cdot ((\sqrt{2}\, R)^2 + \tfrac{2}{3} R^2 + (\sqrt{2}\, R)\, R \cdot (\sqrt{2}/2))$

[16.106] $I8_{far} = \tfrac{22}{9}\, m\, R^2$

Near hemishells:

[16.107] $I8_{near} = 8 \cdot (m/12) \cdot ((\sqrt{2}\, R)^2 + \tfrac{2}{3} R^2 - (\sqrt{2}\, R)\, R \cdot (\sqrt{2}/2))$

[16.108] $I8_{near} = \tfrac{10}{9}\, m\, R^2$

Total sum

Far hemishells:

[16.109] $I_{hwfar} = \tfrac{14}{3}\, m\, R^2$

Near hemishells:

[16.110] $I_{hwnear} = 2\, m\, R^2$

Combined total for both sets:

[16.111] $I_{tot} = \tfrac{20}{3}\, m\, R^2$

If a mass m/2 were placed on the twelve near hemishells and another m/2 on the twelve far hemishells, the coefficient in the preceding equation would be halved, consistent with the same coefficient 10/3 calculated for Iws.

Difference:

[16.112] $I_{hwD} = \tfrac{8}{3}\, m\, R^2$

Inertia of twelve spheres with a point mass at the center of each sphere:

Mass of each sphere:

[16.113] $m_1 = m / 12$

Four spheres at distance 2R from the axis:

[16.114] $I_4 = 4 . (m/12) . (2R)^2$

[16.115] $I_4 = ⅔ m R^2$

Eight spheres at distance √2 R from the axis:

[16.116] $I_8 = 8 . (m/12) . (\sqrt{2} R)^2$

[16.117] $I_8 = ⅔ m R^2$

Total sum:

[16.118] $I = I_4 + I_8$

Thus, the twelve-center point-mass model gives:

[16.119] $Iwpoint = ⅘ m R^2$

This equals the differential inertia of the twelve spherical hemishells.

Inertia of twelve cosine-weighted spherical hemishells

Inertia of a cosine-weighted spherical hemishell (with precise angle notation)

In this section, the inertia of a cosine-weighted spherical hemishell is derived and calculated with precise angle notation, so that no ambiguity remains between the angle of a point and the angle of the rotation axis.

Definition of the coordinate system

Position vector of a point on the shell:

[16.120] $\vec{r}(\theta,\varphi) = (R \sin\theta \cos\varphi , R \sin\theta \sin\varphi , R \cos\theta)$

In this definition:

θ is the angle between the radius and the z-axis.

φ is the angle in the xy-plane.

Domains:

[16.121] $0 \leq \theta \leq \pi/2$

[16.122] $0 \leq \varphi \leq 2\pi$

Surface element:

[16.123] $dS = R^2 \sin\theta \, d\theta \, d\varphi$

Definition of cosine-weighted density

Surface density:

[16.124] $\rho(\theta) = \rho_0 \cos\theta$

Determination of the density coefficient

Total mass:

[16.125] $M = \iint \rho \, dS$

[16.126] $M = \rho_0 \int_0\{2\pi\} \int_0\{\pi/2\} \cos\theta . R^2 \sin\theta \, d\theta \, d\varphi$

[16.127] $M = \rho_0 R^2 . (2\pi) . (½)$

[16.128] $M = \rho_0 \pi R^2$

[16.129] $\rho_0 = M / (\pi R^2)$

Definition of the rotation axis

[16.130] $\hat{e} = (\sin\alpha , 0 , \cos\alpha)$

[16.131] $\hat{p} = (-\cos\alpha , 0 , \sin\alpha)$

[16.132] $A = d\ \hat{p}$

Distance from the axis

[16.133] $L^2 = | (\vec{r} - A) - ((\vec{r} - A) . \hat{e})\ \hat{e} |^2$

Which simplifies to:

[16.134] $L^2 = R^2 + d^2 - 2d\ (\vec{r} . \hat{p})\ r - (\vec{r} . \hat{e})^2$

Definition of inertia

[16.135] $I = \iint L^2\ \rho\ dS$

[16.136] $I = M(R^2 + d^2) - 2d \iint (\vec{r} . \hat{p})\ \rho\ dS\ r - \iint r(\vec{r} . \hat{e})^2\ \rho\ dS$

Calculation of the linear term

[16.137] $\vec{r} . \hat{p} = R(-\sin\theta \cos\varphi \cos\alpha + \cos\theta \sin\alpha)$

[16.138] $\iint r(\vec{r} . \hat{p})\ \rho\ dS = \frac{2}{3}\ M\ R \sin\alpha$

Calculation of the quadratic term

[16.139] $\vec{r} . \hat{e} = R(\sin\theta \cos\varphi \sin\alpha + \cos\theta \cos\alpha)$

[16.140] $\iint r(\vec{r} . \hat{e})^2\ \rho\ dS = (M\ R^2 / 4)(1 + \cos^2\alpha)$

Final simplification

[16.141] $I = M(R^2 + d^2) - (\frac{4}{3})\ M\ d\ R \sin\alpha - (M\ R^2 / 4)(1 + \cos^2\alpha)$

[16.142] $R^2 - (R^2/4)(1 + \cos^2\alpha) = (R^2/4)(2 + \sin^2\alpha)$

Final base formula

Far hemishell:

[16.143] $Ifar = M\ [\ d^2 + (R^2/4)(2 + \sin^2\alpha) + (\frac{4}{3})\ d\ R \sin\alpha\ ]$

Near hemishell:

[16.144] $Inear = M\ [\ d^2 + (R^2/4)(2 + \sin^2\alpha) - (\frac{4}{3})\ d\ R \sin\alpha\ ]$

Calculations for the twelve-hemishell configuration

Mass of each hemishell:

[16.145] $M = m / 12$

Group of four

[16.146] $d = 2R$

[16.147] $\alpha = 90°$

[16.148] $\sin\alpha = 1$

Far hemishell:

[16.149] $I4far = 4 . (m/12) . [\ 4R^2 + (\frac{3}{4})R^2 + (\frac{8}{3})R^2\ ]$

[16.150] $I4far = \frac{89}{36}\ m\ R^2$

Near hemishell:

[16.151] $I4near = 4 . (m/12) . [\ 4R^2 + (\frac{3}{4})R^2 - (\frac{8}{3})R^2\ ]$

[16.152] $I4near = \frac{25}{36}\ m\ R^2$

Group of eight

[16.153] $d = \sqrt{2}\,R$

[16.154] $\alpha = 45°$

[16.155] $\sin\alpha = \sqrt{2} / 2$

Far hemishell:

[16.156] $I8far = 8 \,.\, (m/12) \,.\, [\, 2R^2 + (5/8)R^2 + (4/3)R^2 \,]$

[16.157] $I8far = 95/36\ m\ R^2$

Near hemishell:

[16.158] $I8near = 8 \,.\, (m/12) \,.\, [\, 2R^2 + (5/8)R^2 - (4/3)R^2 \,]$

[16.159] $I8near = 31/36\ m\ R^2$

Final results

[16.160] $IhwCosfar = 46/9\ m\ R^2$

[16.161] $IhwCosnear = 14/9\ m\ R^2$

[16.162] $Itot = 20/3\ m\ R^2$

[16.163] $IhwCosD = 32/9\ m\ R^2$

Theorem 17: Kissing Number

[17.1] $k_m(d) = k_f(d).k_{full}(d)$

[17.2] $k_{full}(d) = (2d)2^{(d/2)}$: full kissing number

[17.3] $k_f(d) = ½+cc(d)/2$: kissing factor

[17.4] $cc(d) = \cos^2(\pi.\log_4{}^2(d/6))$

Criteria:

1&2: base-dimension condition:

[17.5] $k_1 = 2$, $k_2 = 6$

2d: divisibility by 2d:

[17.6] $k \bmod (2d) = 0$, for $d > 2$

2k: recursive upper bound:

[17.7] $k(d) \leq 2k(d-1)$, for $d > 2$

GF: greatest-factor condition:

[17.8] $GF(k/d) \leq 1 + d/2$

GF1: first-power condition for the greatest factor:

[17.9] $Power(GF(k/d)) = 1$

GFA: optional first-power condition for all larger factors:

[17.10] $Power(p) = 1$, for every prime $p > 3$ dividing k/d

Parity: even-power balancing condition:

[17.11] $Power_2(k) \geq Count(\text{odd powers of primes} > 2)$

no2: condition excluding pure powers of 2: $k \neq 2^n$

Kissing-number table: dimensions 1 through 33

The following table reports the continuous quantities k_f, k_{full} and k_m; the upper and lower discrete candidates k_u and k_d; and the selected kissing number k. Alternatives under the optional GFA condition are enclosed in square brackets. The reference values k_r are provided only for comparison and do not enter the model calculations. For dimensions above 24, accepting a model output does not constitute a mathematical proof of the kissing number.

Table:

For each dimension d, calculate k_f, k_{full} and their product k_m. Report the nearest valid integers above k_m and at or below k_m that satisfy the kissing-number conditions as k_u and k_d, and report their ratios to k_{full} as k_{uf} and k_{df}. Different results under GFA are displayed in square brackets.

The kissing number is k_d, except in exceptional cases: dimensions 1 and 2, where k_d is zero; or cases of the form 164^n where k_{full} is an integer and, as with 44^n or 24×4^n, k_{uf} is not greater than 1. In these cases the kissing number k is k_u.

Other parameters:

Pk: sum of the exponents of the prime factors of kissing number k.

SPk: sum of Pk values for the prime factors of d, weighted by their exponents in d.

k′ = k/d

Pk′: sum of the exponents of the prime factors of k′.

SPk′: sum of Pk′ values for the prime factors of d, weighted by their exponents in d.

k″ = k^2/d

Pk″: sum of the exponents of the prime factors of k″.

SPk″: sum of Pk″ values for the prime factors of d, weighted by their exponents in d.

q=... s(d,q)=...

Description: Ramionics kissing-number model with continuous k_m.Range: 1 to 33.

Format: GFA alternatives are shown inside [].

Definitions:

k = kissing number. Pk = sum of prime-factor exponents of k. SPk = sum of Pk values of prime factors of d, counted with their powers in d.

k' = k/d. Pk' = sum of prime-factor exponents of k'. SPk' = sum of Pk' values of prime factors of d, counted with their powers in d.

k″ = k^2/d. Pk″ = sum of prime-factor exponents of k″. SPk″ = sum of Pk″ values of prime factors of d, counted with their powers in d.

Parameters:

k_r = reference kissing number or reference range.

k_f = kissing factor.

k_{full} = full geometric kissing capacity.

k_m = k_f*k_{full}.

k_u = first valid integer above k_m.

k_d = first valid integer at or below k_m.

k = selected final kissing number.

q = optimized FCC side dimension.

s(d,q) = Comb(d,q)*2^(d-q).

GF and GF1 are mandatory. GFA is optional.

Each dimension is printed immediately after completion.

d=1 k_r=2=2

$k_{\not f}$=0.630261155583177 $k_{\not f ull}$=2.82842712474619 k_m=1.78264774812534$k_{u\not f}$=0.707106781186547 k_u=2 =k ✓✓

k_u=2=2

$k_{d\not f}$=0 k_d=0

k_d=0=0

q=0 s(d,q)=2

k=2 Pk=1 SPk=0

k'=2 Pk'=1 SPk'=0

k''=4 Pk''=2 SPk''=0

d=2 k_r=2.3=6

$k_{\not f}$=0.576616696016245 $k_{\not f ull}$=8 k_m=4.61293356812996

$k_{u\not f}$=0.75 k_u=6 =k ✓✓

k_u=6=2.3

$k_{d\not f}$=0 k_d=0

k_d=0=0

q=- s(d,q)=- ; no q satisfies s(d,q)>=6

k=6 Pk=2 SPk=(2)

k'=3 Pk'=1 SPk'=(1)

k''=18 Pk''=3 SPk''=(3)

d=3 k_r=2^2.3=12

$k_{\not f}$=0.75 $k_{\not f ull}$=16.9705627484771 k_m=12.7279220613579

$k_{u\not f}$=1.06066017177982 k_u=18

k_u=18=2.3^2

$k_{d\not f}$=0.707106781186547 k_d=12 =k ✓✓

k_d=12=2^2.3

q=1 s(d,q)=12

k=12 Pk=3 SPk=(3)

k'=4 Pk'=2 SPk'=(2)

k''=48 Pk''=5 SPk''=(5)

d=4 k_r=2^3.3=24

$k_{\not f}$=0.964748237111439 $k_{\not f ull}$=32 k_m=30.8719435875661

$k_{u\not f}$=1.5 k_u=48

k_u=48=2^4.3

$k_{d/}$=0.75 k_d=24 =k ✓✓

k_d=24=2^3.3

q=2 s(d,q)=24

k=24 Pk=4 SPk=4

k'=6 Pk'=2 SPk'=2

k″=144 Pk″=6 SPk″=6

d=5 40<=K_r<=44

$k_{/}$=0.998525066277834 $k_{/ull}$=56.5685424949238 k_m=56.4851076439842$k_{u/}$=1.06066017177982 k_u=60

k_u=60=2^2.3.5

$k_{d/}$=0.707106781186547 k_d=40 =k ✓✓

k_d=40=2^3.5

q=3 s(d,q)=40

k=40 Pk=4 SPk=(4)

k'=8 Pk'=3 SPk'=(3)

k″=320 Pk″=7 SPk″=(7)

d=6 72<=K_r<=78

$k_{/}$=1 $k_{/ull}$=96 k_m=96

$k_{u/}$=1.125 k_u=108

k_u=108=2^2.3^3

$k_{d/}$=0.75 k_d=72 =k ✓✓

k_d=72=2^3.3^2

q=3 s(d,q)=160

k=72 Pk=5 SPk=5

k'=12 Pk'=3 SPk'=3

k″=864 Pk″=8 SPk″=8

d=7 126<=K_r<=134

$k_{/}$=0.999245930710152 $k_{/ull}$=158.391918985787 k_m=158.272480503919$k_{u/}$=1.06066017177982 k_u=168

k_u=168=2^3.3.7

$k_{d/}$=0.795495128834866 k_d=126 =k ✓✓

k_d=126=2.3^2.7

q=4 s(d,q)=280

k=126 Pk=4 SPk=(4)

k'=18 Pk'=3 SPk'=(3)

k″=2268 Pk″=7 SPk″=(7)

d=8 k_r=2^4.3.5=240

$k_{/}$=0.990904054973683 $k_{/ull}$=256 k_m=253.671438073263

$k_{u/}$=1.125 k_u=288

k_u=288=2^5.3^2

$k_{d/}$=0.9375 k_{d}=240 =k ✓✓

k_{d}=240=2^{4}.3.5

q=5 s(d,q)=448

k=240 Pk=6 SPk=6

k'=30 Pk'=3 SPk'=3

k″=7200 Pk″=9 SPk″=9

d=9 306<=K_r<=380

$k_{/}$=0.964748237111439 $k_{/ull}$=407.293505963451 k_{m}=392.935691865177$k_{u/}$=1.06066017177982 k_{u}=432

k_{u}=432=2^{4}.3^{3}

$k_{d/}$=0.883883476483184 k_{d}=360 =k ✓✓

k_{d}=360=2^{3}.3^{2}.5

q=6 s(d,q)=672

k=360 Pk=6 SPk=6

k'=40 Pk'=4 SPk'=4

k″=14400 Pk″=10 SPk″=10

d=10 500<=K_r<=566

$k_{/}$=0.914407439371962 $k_{/ull}$=640 k_{m}=585.220761198055

$k_{u/}$=0.9375 k_{u}=600

k_{u}=600=2^{3}.3.5^{2}

$k_{d/}$=0.84375 k_{d}=540 =k ✓✓

k_{d}=540=2^{2}.3^{3}.5

q=7 s(d,q)=960

k=540 Pk=6 SPk=6

k'=54 Pk'=4 SPk'=4

k″=29160 Pk″=10 SPk″=10

d=11 582<=K_r<=870

$k_{/}$=0.840313948045895 $k_{/ull}$=995.606347910659 k_{m}=836.621900912361$k_{u/}$=0.883883476483184 k_{u}=880

k_{u}=880=2^{4}.5.11

$k_{d/}$=0.795495128834866 k_{d}=792 =k ✓✓

k_{d}=792=2^{3}.3^{2}.11

q=8 s(d,q)=1320

k=792 Pk=6 SPk=(6)

k'=72 Pk'=5 SPk'=(5)

k″=57024 Pk″=11 SPk″=(11)

d=12 840<=K_r<=1355

$k_{/}$=0.75 $k_{/ull}$=1536 k_{m}=1152

$k_{u/}$=0.84375 k_{u}=1296

k_{u}=1296=2^{4}.3^{4}

$k_{d/}$=0.703125 k_{d}=1080 =k ✓✓

k_{d}=1080=2^3.3^3.5

q=9 s(d,q)=1760

k=1080 Pk=7 SPk=7

k'=90 Pk'=4 SPk'=4

k''=97200 Pk''=11 SPk''=11

d=13 1154<=K_r<=2064

$k_{/}$=0.656404798540402 $k_{/ull}$=2353.25136778883 k_m=1544.68548998835$k_{u/}$=0.662912607362388 k_u=1560

k_u=1560=2^3.3.5.13

$k_{d/}$=0.618718433538229 k_{d}=1456 =k ✓✓

k_{d}=1456=2^4.7.13

q=10 s(d,q)=2288

k=1456 Pk=6 SPk=(6)

k'=112 Pk'=5 SPk'=(5)

k''=163072 Pk''=11 SPk''=(11)

d=14 1606<=K_r<=2562

$k_{/}$=0.574829050905242 $k_{/ull}$=3584 k_m=2060.18731844439

$k_{u/}$=0.625 k_u=2240

k_u=2240=2^6.5.7

$k_{d/}$=0.5625 k_{d}=2016 =k ✓✓

k_{d}=2016=2^5.3^2.7

q=11 s(d,q)=2912

k=2016 Pk=8 SPk=6

k'=144 Pk'=6 SPk'=4

k''=290304 Pk''=14 SPk''=10

d=15 2564<=K_r<=2728

$k_{/}$=0.519408522619839 $k_{/ull}$=5430.58007951269 k_m=2820.68957606841$k_{u/}$=0.530330085889911 k_u=2880

k_u=2880=2^6.3^2.5

$k_{d/}$=0.497184455521791 k_{d}=2700 =k ✓✓

k_{d}=2700=2^2.3^3.5^2

q=12 s(d,q)=3640

k=2700 Pk=7 SPk=7

k'=180 Pk'=5 SPk'=5

k''=486000 Pk''=12 SPk''=12

d=16 k_r=2^5.3^3.5=4320

$k_{/}$=0.500001676023753 $k_{/ull}$=8192 k_m=4096.01372998658

$k_{u/}$=0.52734375 k_u=4320 =k ✓✓

k_u=4320=2^5.3^3.5

$k_{𝒹𝒻}$=0.4921875 $k_{𝒹}$=4032

$k_{𝒹}$=4032=$2^6.3^2.7$

q=13 s(d,q)=4480

k=4320 Pk=9 SPk=8

k'=270 Pk'=5 SPk'=4

k''=1166400 Pk''=14 SPk''=12

d=17 5346<=K_r<=6528

$k_{𝒻}$=0.520174338717182 $k_{𝒻_{ull}}$=$1.23093148468954_{(10)^4}$ k_m=6402.98971054541

$k_{u𝒻}$=0.530330085889911 k_u=6528

k_u=6528=$2^7.3.17$

$k_{𝒹𝒻}$=0.497184455521791 $k_{𝒹}$=6120 =k ✓✓

$k_{𝒹}$=6120=$2^3.3^2.5.17$

q=13 s(d,q)=38080

k=6120 Pk=7 SPk=(7)

k'=360 Pk'=6 SPk'=(6)

k''=2203200 Pk''=13 SPk''=(13)

d=18 7398<=K_r<=10668

$k_{𝒻}$=0.576616696016245 $k_{𝒻_{ull}}$=18432 k_m=$1.06281989409714_{(10)^4}$

$k_{u𝒻}$=0.615234375 k_u=11340

k_u=11340=$2^2.3^4.5.7$

$k_{𝒹𝒻}$=0.5625 $k_{𝒹}$=10368 =k ✓✓

$k_{𝒹}$=10368=$2^7.3^4$

q=14 s(d,q)=48960

k=10368 Pk=11 SPk=8

k'=576 Pk'=8 SPk'=5

k''=5971968 Pk''=19 SPk''=13

d=19 10668<=K_r<=17064

$k_{𝒻}$=0.65996309160744 $k_{𝒻_{ull}}$=$2.75149390695309_{(10)^4}$ k_m=$1.8158844253718_{(10)^4}$

$k_{u𝒻}$=0.662912607362388 k_u=18240

k_u=18240=$2^6.3.5.19$

$k_{𝒹𝒻}$=0.618718433538229 $k_{𝒹}$=17024 =k ✓✓

$k_{𝒹}$=17024=$2^7.7.19$

q=15 s(d,q)=62016

k=17024 Pk=9 SPk=(9)

k'=896 Pk'=8 SPk'=(8)

k''=15253504 Pk''=17 SPk''=(17)

d=20 17400<=K_r<=40960

$k_{𝒻}$=0.75669451297644 $k_{𝒻_{ull}}$=40960 k_m=$3.0994207251515_{(10)^4}$

$k_{u\not f}$=0.7734375 k_u=31680

k_u=31680=2^6.3^2.5.11

$k_{d\not f}$=0.751953125 $k_{d\not}$=30800 =k ✓✓

$k_{d\not}$=30800=2^4.5^2.7.11

q=16 s(d,q)=77520

k=30800 Pk=8 SPk=8

k'=1540 Pk'=5 SPk'=5

k″=47432000 Pk″=13 SPk″=13

d=21 27720<=K_r<=67584

$k_{\not f}$=0.851635780403766 $k_{\not f_{ull}}$=6.08224968905421$_{(10)^4}$ k_m=5.17986146054824$_{(10)^4}$

$k_{u\not f}$=0.870072797163135 k_u=52920

k_u=52920=2^3.3^3.5.7^2

$k_{d\not f}$=0.850737846115065 $k_{d\not}$=51744 =k ✓✓

$k_{d\not}$=51744=2^5.3.7^2.11

q=17 s(d,q)=95760

k=51744 Pk=9 SPk=7

k'=2464 Pk'=7 SPk'=5

k″=127497216 Pk″=16 SPk″=12

d=22 49896<=K_r<=89112

$k_{\not f}$=0.930521888074261 $k_{\not f_{ull}}$=90112 k_m=8.38511883781478$_{(10)^4}$

$k_{u\not f}$=0.9375 k_u=84480

k_u=84480=2^9.3.5.11

$k_{d\not f}$=0.90234375 $k_{d\not}$=81312 =k ✓✓

$k_{d\not}$=81312=2^5.3.7.11^2

q=18 s(d,q)=117040

k=81312 Pk=9 SPk=8

k'=3696 Pk'=7 SPk'=6

k″=300529152 Pk″=16 SPk″=14

d=23 126720<=K_r<=237168

$k_{\not f}$=0.982178299383656 $k_{\not f_{ull}}$=1.33230231284045$_{(10)^5}$ k_m=1.30855841989054$_{(10)^5}$

$k_{u\not f}$=0.994368911043582 k_u=132480

k_u=132480=2^7.3^2.5.23

$k_{d\not f}$=0.972271824131503 $k_{d\not}$=129536 =k ✓✓

$k_{d\not}$=129536=2^9.11.23

q=19 s(d,q)=141680

k=129536 Pk=11 SPk=(11)

k'=5632 Pk'=10 SPk'=(10)

k″=729546752 Pk″=21 SPk″=(21)

d=24 k_r=$2^4.3^3.5.7.13$=196560

$k_{\not f}$=1 $k_{\not f_{ull}}$=196608 k_m=196608

$k_{u\not f}$=1.007080078125 k_u=198000[199584]

k_u=198000=$2^4.3^2.5^3.11$[199584=$2^5.3^4.7.11$]

$k_{d\not f}$=0.999755859375 k_d=196560 =k ✓✓

k_d=196560=$2^4.3^3.5.7.13$

q=19 s(d,q)=1360128

k=196560 Pk=10 SPk=9

k'=8190 Pk'=6 SPk'=5

k″=1609826400 Pk″=16 SPk″=14

d=25 K_r=unreferenced

$k_{\not f}$=0.98258217269588 $k_{\not f_{ull}}$=$2.8963093757401_{(10)^5}$ k_m=$2.84586195921415_{(10)^5}$

$k_{u\not f}$=0.987463571383558 k_u=286000

k_u=286000=$2^4.5^3.11.13$

$k_{d\not f}$=0.978831896808526 k_d=283500 =k ✓✓

k_d=283500=$2^2.3^4.5^3.7$

q=20 s(d,q)=1700160

k=283500 Pk=10 SPk=8

k'=11340 Pk'=8 SPk'=6

k″=3214890000 Pk″=18 SPk″=14

d=26 K_r=unreferenced

$k_{\not f}$=0.933515610177573 $k_{\not f_{ull}}$=425984 k_m=$3.97662713685883_{(10)^5}$

$k_{u\not f}$=0.9375 k_u=399360

k_u=399360=$2^{11}.3.5.13$

$k_{d\not f}$=0.93310546875 k_d=397488[393120] =k ✓✓

k_d=397488=$2^4.3.7^2.13^2$[393120=$2^5.3^3.5.7.13$]

q=21 s(d,q)=2104960

k=397488[393120] Pk=9[11] SPk=8

k'=15288[15120] Pk'=7[9] SPk'=6

k″=6076796544[5943974400] Pk″=16[20] SPk″=14

d=27 K_r=unreferenced

$k_{\not f}$=0.860487221270566 $k_{\not f_{ull}}$=$6.25602825159861_{(10)^5}$ k_m=$5.38323236640825_{(10)^5}$

$k_{u\not f}$=0.861786389571105 k_u=539136

k_u=539136=$2^9.3^4.13$

$k_{d\not f}$=0.854535782928079 k_d=534600[532224] =k ✓✓

k_d=534600=$2^3.3^5.5^2.11$[532224=$2^8.3^3.7.11$]

q=22 s(d,q)=2583360

k=534600[532224] Pk=11[13] SPk=9

k'=19800[19712] Pk'=8[10] SPk'=6

k″=10585080000[10491199488] Pk″=19[23] SPk″=15

d=28 K_r=unreferenced

k_f=0.773907031164757 k_{full}=917504 k_m=7.10062796721789$_{(10)^5}$

k_{uf}=0.777587890625 k_u=713440[720720]

k_u=713440=2^5.5.7^3.13[720720=2^4.3^2.5.7.11.13]

k_{df}=0.7734375 k_d=709632 =k ✓✓

k_d=709632=2^{10}.3^2.7.11

q=23 s(d,q)=3144960

k=709632 Pk=14 SPk=8

k'=25344 Pk'=11 SPk'=5

k″=17984913408 Pk″=25 SPk″=13

d=29 K_r=unreferenced

k_f=0.685315566900786 k_{full}=1.34388755034341$_{(10)^6}$ k_m=9.209870584145$_{(10)^5}$

k_{uf}=0.69122449996849 k_u=928928

k_u=928928=2^5.7.11.13.29

k_{df}=0.683628626342463 k_d=918720 =k ✓✓

k_d=918720=2^6.3^2.5.11.29

q=24 s(d,q)=3800160

k=918720 Pk=11 SPk=(11)

k'=31680 Pk'=10 SPk'=(10)

k″=29105049600 Pk″=21 SPk″=(21)

d=30 K_r=unreferenced

k_f=0.605815248592141 k_{full}=1.96608$_{(10)^6}$ k_m=1.19108124395204$_{(10)^6}$

k_{uf}=0.609375 k_u=1198080

k_u=1198080=2^{11}.3^2.5.13

k_{df}=0.604248046875 k_d=1188000[1182720] =k ✓✓

k_d=1188000=2^5.3^3.5^3.11[1182720=2^{10}.3.5.7.11]

q=25 s(d,q)=4560192

k=1188000[1182720] Pk=12[14] SPk=9

k'=39600[39424] Pk'=9[11] SPk'=6

k″=47044800000[46627553280] Pk″=21[25] SPk″=15

d=31 K_r=unreferenced

k_f=0.544727151841525 k_{full}=2.87313890073418$_{(10)^6}$ k_m=1.56507677024202$_{(10)^6}$

k_{uf}=0.545349199650465 k_u=1566864

k_u=1566864=2^4.3^5.13.31

k_{df}=0.543795498226959 k_d=1562400[1547520] =k ✓✓

k_d=1562400=2^5.3^2.5^2.7.31[1547520=2^8.3.5.13.31]

q=26 s(d,q)=5437152

k=1562400[1547520] Pk=11[12] SPk=(11)[(12)]

k'=50400[49920] Pk'=10[11] SPk'=(10)[(11)]

k″=78744960000[77252198400] Pk″=21[23] SPk″=(21)[(23)]

d=32 K_r=unreferenced

k_{f}=0.508613039331216 k_{full}=$4.194304_{(10)^6}$ k_m=$2.13327770531908_{(10)^6}$

k_{uf}=0.5126953125 k_u=2150400[2154240]

k_u=2150400=$2^{12}.3.5^2.7$[2154240=$2^8.3^2.5.11.17$]

k_{df}=0.5084228515625 k_d=2132480[2129920] =k ✓✓

k_d=2132480=$2^9.5.7^2.17$[2129920=$2^{15}.5.13$]

q=27 s(d,q)=6444032

k=2132480[2129920] Pk=13[17] SPk=10

k'=66640[66560] Pk'=8[12] SPk'=5

k″=142108467200[141767475200] Pk″=21[29] SPk″=15

d=33 K_r=unreferenced

k_{f}=0.50073425326403 k_{full}=$6.11700540156309_{(10)^6}$ k_m=$3.06299413196373_{(10)^6}$

k_{uf}=0.502708727249811 k_u=3075072

k_u=3075072=$2^{10}.3.7.11.13$

k_{df}=0.499903433012926 k_d=3057912 =k ✓✓

k_d=3057912=$2^3.3^5.11^2.13$

q=28 s(d,q)=7594752

k=3057912 Pk=11 SPk=9

k'=92664 Pk'=9 SPk'=7

k″=283358357568 Pk″=20 SPk″=16

Conditions checked: 1&2, 2d, GF_on_k_over_d, GF1_on_k_over_d, parity, no2

Optional condition checked: GFA_on_k_over_d.

For d > 24, final k is marked accepted because no reference range is used.

Downward scan reports k_d=0 and k_{df}=0 if no valid kd exists.

Final one-line report preserves [] options only when they belong to the selected side.

SPk, SPk', and SPk″ are computed from d factorization, not from k factorization.

All reported nonzero values passed their active conditions.

Final kissing numbers:

k_1=2 k_2=6 k_3=12 k_4=24 k_5=40 k_6=72 k_7=126 k_8=240 k_9=360 k_{10}=540 k_{11}=792 k_{12}=1080 k_{13}=1456 k_{14}=2016 k_{15}=2700 k_{16}=4320 k_{17}=6120 k_{18}=10368 k_{19}=17024 k_{20}=30800 k_{21}=51744 k_{22}=81312 k_{23}=129536 k_{24}=196560 k_{25}=283500 k_{26}=397488[393120] k_{27}=534600[532224] k_{28}=709632 k_{29}=918720 k_{30}=1188000[1182720] k_{31}=1562400[1547520] k_{32}=2132480[2129920] k_{33}=3057912

Detailed discussion:

The kissing-number problem and the maximum dimensional-density problem

In d-dimensional space, every arrangement of beads (equal d-dimensional spheres of radius r) fills a characteristic relative volume φ of its containing space. This is the occupancy, coverage, compression, or packing factor, and φ depends on the arrangement. The arrangement also has an average number of beads tangent to any given bead, called the kissing number or contact number, denoted k; this too depends on the arrangement.

The greatest relative volume attainable by the densest possible lattices in d-dimensional space is denoted φ_d and called the dimensional density of dimension d; it is a function of d. Likewise, the maximum number of spheres that can touch one sphere is called the kissing number k_d of that dimension, also a function of d.

The kissing conjecture, for any dimension d, consists of three proposed statements: (1) every lattice attaining the maximum φ also attains the maximum k; (2) every lattice attaining the maximum k also attains the maximum φ; (3) for d greater than 2, a cubic lattice can always be found that attains both the maximum φ and the maximum k.

In three dimensions, the kissing conjecture is associated here with Kepler's conjecture of approximately 1611, which was proved in 2014 after about 400 years. In any case, the three-dimensional proof is sufficient for formulating the three-dimensional universe in Ramionics.

[17.12] FCC = CPC Lattice = Face Centered Cubic = Cubic Packed Configuration

That is, similar cells in the form of d-dimensional cubes with maximal filling of their edges and diagonals; geometrically, these have maximum simplicity, symmetry and isotropy and, physically, the greatest softness, understood here as the greatest resistance to fracture and separation.

History of the kissing number and dimensional density

$k_1 = 2$

$k_2 = 6$

$k_3 = 12$; 1611, conjecture by Johannes Kepler 1998, proof by Thomas Hales 2014, formal proof (Flyspeck), Fulkerson Prize (2009, Hales)

$k_4 = 24$; 1979, Oleg Musin (final proof 2003)

k_5: $40 \le k_5 \le 44$; 1953, John Leech 2003, upper bound Oleg Musin

k_6: $72 \le k_6 \le 78$; 1953, John Leech (lower bound) 2003, Oleg Musin (upper bound improvement)

k_7: $126 \le k_7 \le 134$; 1953, John Leech 2000s, numerical improvements

$k_8 = 240$ 1967; John Leech (Leech lattice) 2016, optimality proof by Maryna Viazovska 2017, Salem Prize 2022, Fields Medal

k_9: $306 \le k_9 \le 380$; 1990s–2000s, semidefinite programming

k_{10}: $500 \le k_{10} \le 566$; 2000–2010, SDP improvements

k_{11}: $582 \le k_{11} \le 870$; 2000–2010, Henry Cohn and collaborators

k_{12}: $840 \le k_{12} \le 1355$

k_{13}: $1154 \le k_{13} \le 2064$

k_{14}: $1606 \le k_{14} \le 2562$

k_{15}: $2564 \le k_{15} \le 2728$

$k_{16} = 4320$; 1988 Boris Venkov

k_{17}: $5346 \le k_{17} \le 6528$

k_{18}: $7398 \le k_{18} \le 10668$

k_{19}: $10668 \leq k_{19} \leq 17064$

k_{20}: $17400 \leq k_{20} \leq 40960$

k_{21}: $27720 \leq k_{21} \leq 67584$

k_{22}: $49896 \leq k_{22} \leq 89112$

k_{23}: $126720 \leq k_{23} \leq 237168$; SDP bounds (Henry Cohn, Noam Elkies, Christine Bachoc et al.)

$k_{24} = 196560$; 1968, John Leech 2016, final proof by Maryna Viazovska, Henry Cohn, Abhinav Kumar, Stephen Miller, Danylo Radchenko 2022, Fields Medal

In summary, the exact kissing number has so far been established by proof in only seven dimensions—1, 2, 3, 4, 8, 16 and 24. For the remaining dimensions, relatively tight bounds are known only through dimension 24; beyond this, the bounds have been estimated approximately as follows:

[17.13] $k(d) \approx 2^{(0.401\ d)}$

Reference table: values or ranges proved or calculated to date using geometric and numerical methods

Reference table of Kissing number d1 to d24:

(3) (2), (6), (12), (24), 40 to 44, 72 to 78, 126 to 134, (240), 306 to 380, 500 to 566, 582 to 870, 840 to 1355, 1154 to 2064, 1606 to 2562, 2564 to 2728, (4320), 5346 to 6528, 7398 to 10668, 10668 to 17064, 17400 to 40960, 27720 to 67584, 49896 to 89112, 126720 to 237168, (196560)

The maximum dimensional density φ has been proved in only five dimensions:

[17.14] $\varphi_1 = 1$

[17.15] $\varphi_2 = \pi/(2\sqrt{3}) = 0.90689968$

[17.16] $\varphi_3 = \pi/(3\sqrt{2}) = 0.74048049$

[17.17] $\varphi_8 = \pi^4/384 = 0.25366951$

[17.18] $\varphi_{24} = \pi^{12}/12! = 0.00192957$

Geometric algorithm

In a d-dimensional cube of side a, place spheres of radius r at its center and at the greatest possible number of edge midpoints.

If contact is maximal, then for at least one diagonal of dimension Q, its entire length lies within the spheres: that diagonal equals the diameter of the central sphere plus two radii of the surrounding spheres. Therefore:

[17.19] $a\sqrt{Q} = 4r$

Take the cube center as the coordinate origin and represent the vectors to the edge midpoints using coordinates ±1. Then:

[17.20] $a = 2$

[17.21] $t = \text{threshold} = (2r)^2 = Q$

If the squared distance between two centers (DistanceSquare) is denoted diss, the indentation or penetration depth is:

[17.22] $\text{Indentation} = 2r - \sqrt{\text{diss}} = \sqrt{Q} - \sqrt{\text{diss}}$

The conditions for two spheres to overlap or to be tangent are:

[17.23] $\text{Indentation} > 0$; $\text{Indentation} = 0$

These conditions can be evaluated without square roots.

[17.24] Q − diss > 0 , Q − diss = 0

A simple measure of overlap severity is also available without calculating square roots: Q − diss.

For each dimension d, searching Q from 2 to d yields a separate kissing number for each Q. The largest z is the kissing number for d, and its associated Q is called the full kissing diameter.

The algorithm for finding k can operate on individual spheres or pairs (a pair consists of centers whose coordinates are all sign-reversed). Independently, it can be subtractive or additive.

Subtractive model: rank first by the number of overlaps and then by overlap severity, or first by severity and then by the number of overlaps: two cases.

The additive model can be simple (based on minimum or maximum distance) or combined, treating sisters (those sharing a zero coordinate) and relatives (those not sharing a zero coordinate) separately with minimum- or maximum-distance models: six cases.

There are 16 cases in total.

For every dimension, test all algorithms. Any algorithm producing an incorrect answer in a dimension is not used for higher dimensions.

In every algorithm, also check and count overlaps with the central sphere.

The d-dimensional volume of a d-dimensional sphere of radius r and its (d−1)-dimensional boundary area:

[17.25] V(d) = π^(d/2)/Γ(d/2 + 1) . r^d

[17.26] S(d) = 2π^(d/2)/Γ(d/2) . r^(d−1)

[17.27] V(d) = S(d) . r / d

Recurrence relations:

[17.28] V(2) = π , V_3 = 4π/3 , V(d) = (2π/d) . V(d−2)

[17.29] S(2) = 2π, S(3) = 4π , S(d) = (2π/(d−2)) . S(d−2)

In d-dimensional space, the maximum volume of a cube inscribed in the unit sphere, with the cube corners touching the sphere:

[17.30] √d . a = 1

[17.31] a = 1/√d

Cube side length:

[17.32] L = 2a = 2/√d

Cube volume:

[17.33] V_cube = L^d

[17.34] V_cube = (2/√d)^d

[17.35] V_cube = 2^d/d^(d/2)

[17.36] V_cube(d) = 2^d/d^(d/2)

Logarithmic algorithm:

The kissing-number conditions are named rather than numbered:

Condition 1&2: Elementary geometry shows that the kissing numbers in dimensions 1 and 2 are 2 and 6. These values are not affected by the conditions imposed in higher dimensions; rather, they

influence the higher-dimensional conditions, preserving factors 2 and/or 3, since each dimension is obtained by extending lower dimensions.

The reason k_1 is 2 is that a one-dimensional sphere is a line segment of length 2r, with a zero-dimensional boundary consisting of points; at maximum packing it touches two other such spheres.

The reason k_2 is 6 is that two-dimensional spheres, namely circles, can be reconstructed with triangular cells, and six circles fit around each circle in two-dimensional space: each triangle angle is 180/3 degrees and the complete circle is 360 degrees.

Condition 2d: for d greater than 2, the kissing number is divisible by 2d.

For FCC, 2d is the number of (d−1)-dimensional faces of a d-dimensional cube. For example, a three-dimensional cube has six two-dimensional faces.

For dimension 2, as already stated, k_1 and k_2 are elementary results unaffected by higher-dimensional conditions. Indeed, k_2 is divisible only by d, not 2d, because it is based on triangles rather than a two-dimensional cube (square).

Condition 2k: since dimension d is obtained by extending dimension d−1:

[17.37] k(d) <= 2 . k(d−1) for d>2

Consequently:

[17.38] k <= 3 . 2^(d−1)

Condition GF (Greatest Factor): in k/d, the greatest factor other than 2 and 3 is less than or equal to 1+d/2.

Condition GF1: in k/d, the greatest factor other than 2 and 3 has exponent one.

Optional condition GFA: in k/d, all factors other than 2 and 3 have exponent one. This produces a special type of symmetric lattice of the same name, which is reported if its answer differs from that of the principal lattice (that is, if k differs). The GF1 and GFA conditions ensure the largest powers for the fundamental factors 2 and 3 appearing in k_1 and k_2; they were inspired by the electron genetic code.

Parity condition: in k, the exponent of factor 2 is at least the number of non-2 prime factors with odd exponents. Thus the kissing number can be expressed as the product of 1 or 2 and a number of factors 2p, where p is prime. These three conditions were inspired by the electron genetic code in Ramionics and the capacities 2, 6, 10 and 14 of atomic orbitals.

Condition no2 means that k is not a pure power of 2.

The kissing factor $k_{\not f}$ compensates for dimensional interference at high dimensions through the greatest possible symmetry in the dimensional distribution of spheres.

[17.39] $k_m(d) = k_{\not f}(d) \cdot k_{\not f ull}(d)$

[17.40] $k_{\not f ull}(d) = (2d)2^{(d/2)}$: kissing full number

[17.41] $k_{\not f}(d) = 1/2+cc(d)/2$: kissing factor

[17.42] $cc(d) = (\cos^2(\pi \cdot (\log_4{}^2(d/6))^g))^t$

For calculating k, the cosine function with g=t=1 is sufficient. More complex parameters than k require functions more complex than cc and ss, with values other than 2 for g and t:

[17.43] $ss(d) = (\sin^2(\pi \cdot (\log_4{}^2(d/6))^g))^t$

In this case, the dimension $6\times2^{(\sqrt{2})}$ has the minimum $k_{\not f}$ and, surprisingly, is close to the integer 16.

[17.44] $6 \cdot 2^{(\sqrt{2})} = 15.99086485614$

Use the reference values k_r only for the final comparison, not for calculating k_m, k_u, $k_{\mathcal{A}}$ or k.

Theorem 18: The Universe Is Three-Dimensional and Cubic-Crystalline

Face-centered cubic (FCC) layering: In an FCC arrangement, designate one bead as the central bead, or layer zero, and take its center as the origin of the d-dimensional spherical coordinate system of the FCC crystal lattice. Define layer one as the beads tangent to layer zero, and, generally, define layer n as the collection of beads tangent to layer $n-1$. The centers of the first-layer beads lie on a sphere of radius 2r. In subsequent layers, the layer shapes—that is, the distributions of bead centers—deviate slightly from the ideal sphere. Except in dimensions one and two, however, the shapes of large layers again tend toward the ideal sphere. The number of beads in layer n is:

[18.1] $L(n,d) = \sum_{k=0}^{d} \{(-1)^k \cdot C(d,k) \cdot C(n(d-2k)+d-1, d-1)\}$

Where Ramionics physics and kissing geometry intersect: The greater likelihood of three-dimensional universes, and dimension 3 for this universe, is not an intrinsic, predetermined property of ramions; rather, it results from a collective process under pressure. Subjected to intense pressure from mutual contacts, ramions tend toward a state in which contact is maximized and the parameter x is minimized. This state occurs precisely in three-dimensional space. Thus, three-dimensionality is not an initial assumption but a consequence of the dynamics and interactions among ramions.

Two-dimensional space is unique in two respects: first, its cells are triangular rather than square; second, the shape of its layers remains hexagonal from the second layer onward.

One-dimensional space is also unique because the beads of each layer—two line segments on opposite sides of the central segment—are disconnected, whereas in higher dimensions the beads of each layer are connected.

Theorem 19: FCC Cubic-Crystal Calculations

Number of ramions in layer n:

[19.1] $L(n) = 10n^2 + 2$

Total number of ramions through layer n:

[19.2] $T(n) = (10n^3 + 15n^2 + 11n + 3)/3$

; $IT(n)$: Ceil(Inversed function of T)

Volume occupancy factor: For ramions, φ is the factor by which space is created out of SuperSpace. The intervals between ramions are NonSpace: without location or time, and empty of energy (or having a very low energy density). Consequently, the speed of light there is infinite (or nearly infinite). Ramionics uses this NonSpace to explain different forms of entanglement as well as the curvature of time.

In the face-centered cubic (FCC) arrangement, the cubic cell can be represented by twelve sphere centers at the midpoints of its edges and one sphere center at the cube center. Each edge sphere is shared among four cells; therefore, the effective number of spheres per cell is 12/4+1, or four spheres. A translation of the origin makes this representation equivalent to the conventional FCC representation.

Let the radius of each sphere be r and the cube edge length be a. The cube's face diagonal equals four sphere radii. Therefore:

; $\sqrt{2}a = 4r$

; $a = 2\sqrt{2}r$

; $V_{cu\beta e} = a^3 = 16\sqrt{2}r^3$

The total volume of the four effective spheres, divided by the cell volume, determines the volumetric packing coefficient φ:

; $V_{spheres} = 4(4\pi r^3/3) = 16\pi r^3/3$

; $\varphi = V_{spheres}/V_{cu\beta e} = (16\pi r^3/3)/(16\sqrt{2}r^3) = \pi/(3\sqrt{2})$

Thus, approximately 74.048 percent of the volume in the ideal arrangement is occupied by spheres. For a large spherical region of radius R, neglecting boundary effects, the approximate number of spheres follows from the volume ratio:

; $V = 4\pi R^3/3$

; $N(R) \approx \varphi(R/r)^3$

In the layer-counting model of Ramionics, the population of layer n is $L_{(n)}=10n^2+2$. For large n, the dominant term is $10n^2$, and the cumulative total is approximately $10n^3/3$. Defining the effective radial step by $R=2\gamma rn$ and equating the volumetric and layer counts:

; $N(n) \approx 10n^3/3$

; $n = R/(2\gamma r)$

; $\varphi(R/r)^3 = (10/3)(R/(2\gamma r))^3$

; $\varphi = 10/(24\gamma^3)$

; $\gamma = \sqrt[3]{(10/(24\varphi))} = \sqrt[3]{(10\sqrt{2}/(8\pi))}$

To calculate the effective surface coverage coefficient β, compare the surface area of the large sphere with the population scale of layer n:

; $A = 4\pi R^2 = 16\pi\gamma^2 r^2 n^2$

; $\beta = 10n^2/(16\gamma^2 n^2) = 10/(16\gamma^2) = \sqrt[3]{(5\pi^2)}/4$

Accordingly, φ is the volumetric packing coefficient, γ the effective radial-step coefficient, and β the effective surface-coverage coefficient. The calculation of φ follows directly from the geometry of the FCC arrangement; deriving γ and β additionally depends on the layer-counting law and the large-n approximation.

[19.3] $\varphi = \pi/(3\sqrt{2})$

; $\varphi = 0.740480489693061$

Radial freedom factor: γ

[19.4] $\varphi = (10/8)/(3\gamma^3)$

; $\gamma = \sqrt[3]{((10/8)/(3\varphi))} = \sqrt[3]{(10\sqrt{2}/(8\pi))}$

; $\gamma = 0.825578509501464$

Surface coverage factor: β

[19.5] $\beta = (10/8)/(2\gamma^2) = \sqrt[3]{(5\pi^2)}/4$

; $\beta = 0.916987168493568$

Sphericity and stability factor, zeta: ζ

[19.6] $\zeta = \varphi/(\gamma^3 4/3) = \varphi^2/(\beta\gamma^2 8/9) = \pi^2/10$

; $\zeta = 0.986960440108936$

Approximations:

[19.7] $2\beta^8 = 0.999852793457834$

; $\varphi^7 2^{10}/5^3 = 0.999966117180411$

Surface-bisecting radius of first-layer ramions:

[19.8] $R_{sh} = \sqrt{5}\, r_r$

Overlap of two spheres of radii r and R with center separation D:

[19.9] $d = R+r-D$

; $V_{common} = V_c = \pi d^2[(R+r-d)^2 + 2(R+r-d)(R+r) - 3(R-r)^2]/[12(R+r-d)]$

; $d = 2r$, $V_c = (4/3)\pi R^3/2$, $x = R_v/r$ gives:

; $3x^4 - 16x^3 + 18x^2 + 11 = 0$

Volume-bisecting radius of the first FCC layer:

; $R_{vh} = 2.12191578090306\, r_r$

Surface-Bisecting Radius in Arbitrary Layers

To extend the surface-bisecting radius from the first layer to layer n, an interpolation model was proposed in the archive. It satisfies both the condition $R_{sh}(1)=\sqrt{5}r$ and the asymptotic behavior $R_{sh}(n)\approx 2\gamma rn$:

; $R_{sh}(n) = r\sqrt{(4\gamma^2 n^2+5-4\gamma^2)}$

This relation is constructed by matching the two conditions and, by itself, does not constitute an exact geometric proof for every FCC layer. Its derivation and supplementary relations appear under “Details” below.

Details:

In the archived cubic-crystal calculations, φ, γ, and β were derived from the cubic cell and the approximation for counting large layers. The relations for these three coefficients have already been given in the main text of this theorem and are not repeated here.

Surface-bisecting radius

In discrete FCC geometry, the surface-bisecting radius R_{sh} specifies the effective position of a layer's surface relative to the structure's center. This radius must satisfy both the geometry of the first layer and the limiting FCC behavior at large distances.

For the first layer, the surface-bisecting radius follows from geometry:

; $R_{sh}(1) = \sqrt{5}r$

On the other hand, at large distances, the radial spacing of layers approaches the geometric coefficient γ, and the radius of the center of layer n behaves as:

; $R_c(n) \approx 2r\gamma n$

Therefore, to construct a single relation satisfying both conditions, the surface-bisecting radius is defined in radical form:

; $R_{sh}(n) = r\sqrt{((2\gamma n)^2+C)}$

The constant C is determined from the exact first-layer condition:

; $5 = 4\gamma^2+C$

Consequently:

; $C = 5-4\gamma^2$

The complete relation for the surface-bisecting radius is thus obtained:

; $R_{sh}(n) = r\sqrt{(4\gamma^2 n^2 + 5 - 4\gamma^2)}$

For the first layer, this relation satisfies the geometric condition exactly:

; $R_{sh}(1) = \sqrt{5}r$

Furthermore, the ratio of the surface-bisecting radius to the radius of the layer center tends to unity at large distances:

; $\text{Lim}\ \{n \to \infty\}\ \{R_{sh}(n)/(2r\gamma n)\} = 1$

The amount by which the surface-bisecting radius extends beyond the asymptotic radius of the layer center is:

; $\delta(n) = r[\sqrt{(4\gamma^2 n^2 + 5 - 4\gamma^2)} - 2\gamma n]$

Rationalizing the expression:

; $\delta(n) = r(5 - 4\gamma^2)/[\sqrt{(4\gamma^2 n^2 + 5 - 4\gamma^2)} + 2\gamma n]$

And at large distances:

; $\delta(n) \approx r(5 - 4\gamma^2)/(4\gamma n)$

Thus, the extension of the surface-bisecting radius is appreciable in the initial layers, decreases as n increases, and tends to zero at large distances. At the same time, the surface-bisecting radius approaches the asymptotic behavior $2r\gamma n$.

This relation will subsequently be treated as the interpolation model for the surface-bisecting radius.

Fermion Generations

Theorem 20: The Ramion Energy Equation, Gravitational and Electric Potentials, and the Origin of Relativity

For general Ramions r:

[20.1] $E_r = \hat{E}_r + \check{E}_r,\ \hat{E}_r = \check{E}_r,\ E_r = 2\hat{E}_r = 2\check{E}_r$

; $E_r = 2\hat{E}_r = 2(\tfrac{1}{2}\mathring{m}_r.\mathring{c}_r^2) = \rho_r.V_r = 2P_r.V_r = 2r_r.F_r/3 = 2(\tfrac{1}{2}G_r m_r^2/r_r)$

; $E_r = 2\check{E}_r = 2(\tfrac{1}{2}I_r.\omega_r^2) = 2T.\Delta\theta_r = 2T \times 1\text{Rad} = \{1/\theta_p\}2(\tfrac{1}{2}K_r q_r^2/r_r)$

Force clarification: F_r is not the gravitational force; rather, it is the total outward force of the Ramion shell.

Mass clarification: m_r is a hypothetical mass in the point approximation; that is, mass is assumed to be concentrated on the surface of a Ramion's 12 balls.

Notation: r as a principal parameter denotes the Ramion radius, whereas r as a subscript denotes a general Ramion. R as a principal parameter denotes the distance from the center of the Ramion selected as the spatial origin, whereas R as a subscript denotes rotational motion.

$\hat{E}$: linear energy; $\check{E}$: rotational energy.

The preceding relationships hold for every Ramion, including s Ramions. Therefore, replacing the general subscript r with the reference subscript s gives:

; $E_s = \hat{E}_s + \check{E}_s,\ \hat{E}_s = \check{E}_s,\ E_s = 2\hat{E}_s = 2\check{E}_s$

; $E_s = 2\hat{E}_s = 2(\tfrac{1}{2}\mathring{m}_s.\mathring{c}_s^2) = \rho_s.V_s = 2P_s.V_s = 2r_s.F_s/3 = 2(\tfrac{1}{2}G_s m_s^2/r_s)$

; $E_s = 2\check{E}_s = 2(½I_s.\omega_s^2) = 2T.\Delta\theta_s = 2T\times 1Rad = \{1/\theta_p\}2(½K_s q_s^2/r_s)$

Rotational energy is equivalent to the work performed by torque T through one radian.

E_s is the smallest E_r in the entire universe and is the reference energy. Thus, a particular N is defined for each Ramion:

[20.2] $E_r = N.E_s$, $E_{rs}=N$, $N \geq 1$

Therefore, N is the Ramion energy metric. However, Ramions within the cubic-ball lattice must also maintain force equilibrium. Thus, if a Ramion has energy metric N, then, according to the fundamental energy–radius–force relation:

[20.3] $E_r = 2r_r.F_r/3$

The same N must also scale the radius:

[20.4] $r_r = N.r_s = N\hbar_s\mathring{c}_s/E_s$, $r_{rs}=N$

Consequently, N is also the Ramion spatial metric.

The mapping from the reference Ramion toward a Ramion, ball, or particle of energy $N.E_s$ in the universe's cubic-ball lattice is called **Ramion projection**. The inverse transformation is called **back-projection**.

Thus, energy and space both have the projection factor N.

However, within the same Ramion, surface area and volume increase by projection factors N^2 and N^3, respectively, whereas its energy increases only by N. Therefore, relative or local energy density has projection factor N^{-2}:

[20.5] $A_r = N^2.A_s$, $V_r = N^3.V_s$,$\rho_r = \rho_s/N^2$

The fundamental Ramion energy relation also shows that energy density is always twice the pressure:

[20.6] $\rho_r = 2P_r$

Pressure therefore has the same N^{-2} projection.

As a result, $\mathring{c}_r$—the rotational or linear speed of Ramion components—and consequently c_r both decrease by projection factor N^2:

[20.7] $P_r = P_s/N^2$, $\mathring{c}_r = \mathring{c}_s/N^2$,$c_r = c_s/N^2$

Because the spatial projection is N while the speed-of-light projection is N^{-2}, time is consequently dilated with projection factor 1/N.

Planck constant: $\hbar_{rs}=N^4$.

Local relative mass: $\mathring{m}_{rs}=N^5$.

Gravitational constant: $G_{rs}=N^{-8}$.

Local relative internal Coulomb constant: $\mathring{K}_{rs}=N^0$.

This decrease in local pressure is known as gravity and constitutes a simple yet precise explanation of quantum gravity.

From the reference Ramion, or a Ramion with smaller N, a Ramion—or the physics of a Ramion—with larger N appears larger and slower: spatial expansion and time dilation. Viewed in the opposite direction, length contraction and faster passage of time appear.

Different Ramions, or different observers, always measure one another's speed of light to be the same, because each observer measures the other's distance using their own time scale (or the other's time using their own distance). This is the principle of the invariance of the speed of light.

Completion of Structural Potentials and Mass Projection

In the fundamental energy relation, the assumed mass distribution matters: for a uniform volume distribution, the sphere's gravitational self-energy has coefficient 3/5, whereas for a surface distribution the coefficient is 1/2. The fundamental relation in the original text employs the surface approximation corresponding to mass concentrated on the surfaces of 12 balls. Accordingly, the volume coefficient must not be substituted without changing the assumed distribution.

; $\hat{E}_{r(volume)} = (3/5)G_r\mathring{m}_r^2/r_r$

; $\hat{E}_{r(surface)} = (1/2)G_r\mathring{m}_r^2/r_r$

In the electric-potential model, positive and negative Ramion charges are treated as two disks on opposite sides of the equatorial plane. Assuming each newly added charge element sees the previous charge at effective distance r_r, the structural energy of each part follows from the charge-assembly integral. The precise interpretation of the total coefficient must remain consistent with the definitions of $\check{E}_r$ and K_r in the original fundamental relation.

; $U_{e(disk)} = \int_0^{q_r} (K_r/r_r)Q.dQ = (1/2)K_rq_r^2/r_r$

Absolute mass assigned to energy and local relative mass arising from internal speed are two different definitions in this model. Mapping E_r to $N.E_s$ and $\mathring{c}_r$ to $\mathring{c}_s/N^2$ changes local mass by N^5, while mass defined relative to a fixed reference speed changes by N. This distinction must not be confused with equivalence between the two mass definitions.

The proposed mechanical interpretation of gravity in this framework is a reduction of local pressure with increasing N and the creation of a pressure gradient between adjacent regions. A reduction in pressure alone does not prove the direction of attraction; the force direction depends on the spatial pressure distribution and boundary conditions.

Exploratory Factors θ

The seven θ factors are exploratory factors for further investigation of sensitivities, derivatives, drifts, approximations, and even possible future corrections: θ_p concerns the structural electric potential of a Ramion; θ_c concerns the projection of the internal speed of light to the external speed; θ_h concerns Planck-constant projection; θ_k concerns Coulomb-constant projection; and $\theta_{\mathscr{g}}$ concerns gravitational-constant projection and also supports any new calculation of the half-radius of a particle black hole's surface layer.

The factor θ_r concerns the Ramion radius: for example, if photon energy is assumed to include linear energy equal to its rotational energy, its value is 2; otherwise, it is 1.

The factor θ_e concerns Ramion energy: if the magnetic inertia d:63 is assumed to have been counted in calculating electron rest energy, Ramion energy equals electron rest energy divided by $3N/2-63$, namely 54522, and θ_e equals 1. Otherwise, Ramion energy equals electron rest energy divided by 54585 and θ_e equals 54522/54585, namely 0.998845836768343. In proton- and neutron-mass calculations, the first assumption applies to models A/B and the second to models C/D.

Because every version of the equations includes all identified factors and quantizations relating to inertia, potential, energy, space, time, and cubic-ball geometry in the projections, the reference value of every exploratory θ factor is 1:

; $\theta_p=\theta_c=\theta_h=\theta_k=\theta_{\mathscr{g}}=\theta_e=\theta_r=1$

Possible changes to factors in these domains are likely to arise from powers of 2, 3, 5, π, φ, β, γ or parameters η, and hence lie approximately between 0.1 and 10, unless they include a power of N. At the same time, the θ variations are not independent; for example, the general fine-structure-constant relation shows:

$\theta_r\theta_h/(\theta_p\theta_k)=1$

It may also be necessary, because of spatial projection, to divide both θ_k and θ_h by N, or both by N^2. In the first case, θ_g must be divided by N^2, G_s and the Ramion radius r_s must be multiplied by N, and the spatial energy densities ρ_s and ρ_u must be divided by N^3. In the second case, θ_g must be divided by N^4, G_s and r_s must be multiplied by N^2, and energy densities ρ_s and ρ_u must be divided by N^6.

Details

The following text records the step-by-step calculations and non-repetitive supplementary explanations from Theorem 20, preserving the sequence of reasoning and prioritizing the notation of the main text. Old archive equation numbers have been converted to unnumbered lines solely to avoid reference conflicts. Where notation or coefficients differ, the fundamental relation of the main text takes precedence.

According to the preceding theorems, the total energy of a Ramion is defined as the sum of two rotational and linear components:

Here Ě denotes rotational energy and Ê denotes linear energy.

The magnitude of linear speed and the magnitude of angular speed of all Ramion energy components are represented by č, the effective energy speed within a Ramion; each energy component possesses linear energy corresponding to this speed for its equivalent mass:

Energy stored under constant pressure P on the Ramion, namely V, is expressed as follows:

In the relation between linear energy and linear force, the number 3, as in the Friedmann relation, is the number of spatial dimensions. r, A, and V denote the Ramion radius, surface area, and volume, respectively.

The letter F is used by default for linear–radial–pressure–gravitational force.

Definition of Gravitational Potential

The energy expended to overcome the repulsion between m_1 and m_2 and bring them from infinite separation to r, which is stored as potential in their energy arrangement, is also denoted by U as a structural gravitational or electric potential. Here the analysis denote structural gravitational potential by Ê and structural electric potential by Ě.

For repulsion between energy components or their equivalent masses, the calculation gives volume potential analogously to a uniformly charged sphere:

; $\rho = \mathring{m}/(4/3\pi r^3)$

; $m(x) = 4/3\pi x^3\rho$

; $\mathit{d}m = 4\pi x^2\rho.\mathit{d}x$

; $\mathit{d}\hat{E} = G_r.m(x).\mathit{d}m/x$

; $\mathit{d}\hat{E} = G_r.(4/3\pi x^3\rho).(4\pi x^2\rho.\mathit{d}x)/x$

; $\mathit{d}\hat{E} = (16/3)\pi^2.G_r.\rho^2.x^4.\mathit{d}x$

; $\hat{E} = \int_0^r\{(16/3)\pi^2.G_r.\rho^2.x^4.\mathit{d}x\}$

; $\hat{E} = (16/3)\pi^2.G_r.\rho^2.(r^5/5)$

; $\rho^2 = 9\mathring{m}^2/(16\pi^2r^6)$

; $\hat{E} = 3/5.G_r.\mathring{m}^2/r$

The preceding relation applies to volumetric mass density. If density is assumed to reside on the Ramion surface:

; $\hat{E} = ½G_r.m̊^2/r$

; ℅ = ratio of volume to surface gravitational potential energy

The subsequent derivation shows that this same repulsion appears as attraction outside the Ramion because of relativistic effects.

Now the expression is the analogous dual relations for rotational energy:

; $\tau = đ\check{E}/đ\theta$

; $\check{E} = \theta.\tau = \theta.r.F_t$

Definition of Electric Potential

For a sphere with charge q:

The energy spent overcoming the repulsion between q_1 and q_2 and bringing them from infinite separation to r is stored as potential in their arrangement:

; $\check{E} = K_r.q_1.q_2/r$

Thus, to assemble charge from zero to q_r:

; $đ\check{E} = (K_r/r).Q.đQ$

; $\check{E} = ∫\{0 \text{ to } q_r\}\{(K_r/r).Q.đQ\}$

; $\check{E} = ½K_r.q_r^2/r$

Considering the existence of two hemispheres, the total energy becomes:

; $\check{E} = K_r.q_r^2/r$

For an object containing both positive and negative charges, the mutual repulsion of positive charges and the mutual repulsion of negative charges must be added, and the attraction between positive and negative charges subtracted. However, for the Ramion, the charge modeling the torque on each hemisphere has only positive potential. Moreover, because the Ramion generates spacetime, as seen in the discussion of angular speed, all charges perceive an equal radius r.

Thus, the representation uses the Ramion's electric charges $\pm q_r$ as two positive and negative disks on opposite sides of the equatorial circle.

Each differential charge sees the entire preceding charge as a point at the disk center at radius r. Therefore, relations 23–25, originally written for a charged sphere of charge q_r, also hold for the Ramion with charges $\pm q_r$.

Summary of Ramion Relations

The summary of relations within the Ramion universe, which at least in this model is entirely Newtonian, is as follows:

All parameters in the preceding relations concern a single Ramion and carry subscript r, which was omitted for simplicity.

In the principal parameter names, r is the Ramion radius, while R is the distance of any point in the universe from the center of the Ramion assumed to be the origin of the SuperSpace coordinate system.

In parameter subscripts, R and L mean Rotational and Linear, whereas r and s refer, respectively, to any arbitrary Ramion E_r and the reference Ramion E_s, which is at rest and has the lowest E_r in the universe, with radius r_s.

Volumetric energy density is ρ; hence:

Every Ramion, to maintain force equilibrium throughout the lattice of Ramions constituting the universe, keeps its radius—that is, the radius of the space it itself creates—proportional to its energy.

Ramion components, or energy differentials, may actually be continuous or discrete. If discrete, it is entirely possible that each Ramion is itself a universe and that this universe is another universe's Ramion. This hierarchy may perhaps be infinite, closed, or entangled, because it is not constrained by spacetime such that circularity or infinite regress would apply to it.

In any event, even if Ramion components are discrete, their number—that is, the number of particles in each Ramion—is so large that they can be treated as continuous for ordinary calculations.

Because total energy has increased by a factor N while volume has increased by N^3, volumetric energy density decreases.

On the other hand, given the pressure–density relation:

Local relativistic pressure likewise decreases as follows:

Remarkably, Ramion energy has increased while local relativistic pressure has decreased. This change of sign is precisely the moment at which gravity changes from repulsion within Ramions to attraction outside them, and the remarkable moment when quantum gravity occurs.

Since all dynamical processes within a Ramion, including energy propagation and information transfer, depend on pressure, reduced pressure leads to a reduction in the characteristic speed of these processes. Consequently, the effective speed of light inside a Ramion scales as follows:

Time Dilation

An increase in radius according to $r_r = N.r_s$ signifies an increase in the length scale, equivalent to a smaller unit of length in the local measurement frame. Simultaneously, $t_r = t_s/N$ indicates an enlarged unit of time and hence time dilation. In this framework, effective light speed also scales as $\mathring{c}_r = \mathring{c}_s/N^2$, directly resulting from the simultaneous changes in spatial and temporal scales.

Explanation:

When a Ramion receives more energy, its effective rotational speed decreases. This reduction in rotational speed means an increase in the local time scale: time passes more slowly. Consequently, distances or spatial scales appear larger from the local observer's perspective, effectively opening up space to accommodate more energy.

Now, using the fundamental energy relation:

And applying the scalings:

The speed of light decreases when passing through higher-energy Ramions.

When Ramion energy doubles, $\mathring{m}_r$, its local or relative mass, increases 32-fold, but absolute mass m in E/c^2 only doubles.

For electric charge as well, given the potential relation:

; $\mathring{E} \propto q^2/r$

; $q_r = N.q_s$

That is, electric charge increases proportionally to N. This equation links charge conservation to energy conservation.

Theorem 21: Proof of the Principle of the Constancy of the Speed of Light

The principle of the constancy of the speed of light states that the speed of light has a constant value for all observers, under all circumstances, independently of the state of the source or the observer.

Within the Ramionics framework, this principle follows directly from the simultaneous scaling of space and time with energy. Any Ramion whose energy is N times that of the reference becomes N times larger, while time within it passes N times more slowly. Consequently, the effective speed of light in that Ramion decreases by a factor of $1/N^2$.

Nevertheless, when an observer measures the reference speed of light, the observer either measures the reduced distance on the reference side using their own slowed time, or compares the enlarged distance on their own side with the faster time on the reference side. In both cases, the spatial and temporal changes cancel one another exactly, and the final observed speed of light remains the same universal constant.

Likewise, when two Ramions with different energies observe one another, each measures the speed of light on the other side as that same universal constant. Thus, the constancy of the speed of light is not an independent principle but a direct consequence of space and time scaling together with energy in the Ramionics structure.

Theorem 22: Calculation of the Speed of Light and Mechanical Definition of Planck's Constant

$\mathring{c}$ is the rotational or linear speed of the energy components inside a Ramion; c is the linear speed of light in the cubic-belief space (Bavar-Cubic space). The default subscript for c and $\mathring{c}$ is s, whereas the default family subscript for particle parameters is e.

[22.1] $c_r=\{\theta_c\}\mathring{c}_r/\varphi$, $c_s=c$, $\mathring{c}_s=\{1/\theta_c\}\varphi c$

For a Ramion with energy NE_s, both speeds have the Ramionic mapping N^{-2}:

[22.2] $c_r/c_s=\mathring{c}_r/\mathring{c}_s=1/N^2$

Thus N, as the metric of energy, space, and time, is greater near a black hole than in the distant field, while pressure is lower. Quantum gravity therefore arises simply from a pressure gradient, analogously to the Archimedean force or as expressed through Gauss's relation.

Distribution of Mass and Electric Charge over the Surfaces of Twelve Bals

The distributions of mass and electric charge over the surfaces of the twelve Bals are uniform and cosine-shaped, respectively. The corresponding inertias—or, proportionally, the masses and magnetic moments—therefore have the following factors for $M.r^2$ and $Q.r^2$, where r is the Bal radius:

[22.3] Iws=10/3, IhwCosD =32/9

Planck's Constant

As soon as a Ramion receives additional linear energy beyond that of its neighbors, it increases the number of spatial dimensions. If it receives additional rotational energy, it creates a second axis of rotation perpendicular to the first, thereby creating the second dimension of time. The first axis is electrical and the second is magnetic.

[22.4] $\partial\theta/\partial t=\partial\theta/\partial t_1+\partial\theta/\partial t_2$

[22.5] $\omega_{(}total_{)}=\omega+\omega_m$

The total rotational energy after creation of the second axis is:

[22.6] $\check{E}_r+\Delta E_{(}rot_{)}=½I_r(\omega+\omega_m)^2$

The additional rotational energy of the second axis is $\Delta E_{(}rot_{)}$.

[22.7] $E_m=\{\theta_r\}½I_r((\omega+\omega_m)^2-\omega^2)$

[22.8] $(\omega+\omega_m)^2=\omega^2+2.\omega.\omega_m+{\omega_m}^2$

[22.9] $E_m=\{\theta_r\}½I_r(2.\omega.\omega_m+{\omega_m}^2)$

[22.10] $E_m=\{\theta_r\}I_r.\omega.\omega_m(1+\omega_m/(2\omega))$

Therefore, creation of the second axis and the second temporal dimension introduces the linear term $I_r.\omega.\omega_m$ into the additional energy.

Mechanical definition of the reduced Planck constant:

[22.11] $\hbar_r=I_r.\omega_r$

[22.12] $\hbar_r.\omega_r=I_r.{\omega_r}^2$

[22.13] $\hbar_r.\omega_r=E_r$

[22.14] $\omega_r=\mathring{c}_r/r_r$

[22.15] $\hbar_r=E_r r_r/\mathring{c}_r=I_r.\omega_r$

Complete photon-energy relation:

Using the mechanical definition of $\hbar_r$ in the relation for additional rotational energy:

[22.16] $E_m=\{\theta_r\}\hbar_r.\omega_m(1+\omega_m/(2\omega))$

[22.17] $E_m=\{\theta_r\}(\hbar_r.\omega_m+\hbar_r.{\omega_m}^2/(2\omega))$

In the low-energy limit:

[22.18] $\omega_m \ll \omega$

[22.19] $E_m\approx\{\theta_r\}\hbar_r.\omega_m$

The Ramionic mapping of Planck's constant follows directly from $E_r/E_s=N$, $r_r/r_s=N$, and $\mathring{c}_r/\mathring{c}_s=N^{-2}$:

[22.20] $\hbar_r/\hbar_s=N^4$

For mapping from a Ramion to a Bal, the rotational-inertia ratio produces a factor of 5:

[22.21] $I_e/I_{\mathscr{e}}=(10/3)/(⅔)=5$

The factor φ converts the internal linear-rotational speed of a Ramion or Bal into the measured speed of light in the cubic-belief space. Thus, before mapping the Bal to the particle:

[22.22] $\hbar_{\mathscr{e}}=\hbar_s 5\varphi N^4=\{\theta_r^{-1}\}\hbar_{s(1)}5\varphi N^4$

Mapping from one Bal to the complete particle includes two independent factors of 12.

For the first factor of 12, the inertia coefficient 10/3 associated with the particle's larger radius has already been introduced at the Bal stage. The remaining factor of 12 arises because the mass of the complete particle is 12 times the mass of one Bal, thereby introducing the corresponding factor of 12 into the rotational inertia.

The second factor of 12 arises independently from ω. The particle experiences greater time dilation than one Bal; consequently, its rotational period acquires the corresponding factor of 12, which introduces the second factor of 12 into the mapping of Planck's constant.

In addition, all the energy emitted by the electron is treated as rotational energy, introducing an independent factor of 2.

The complete mapping is therefore:

[22.23] $\hbar_e/\hbar_s=\{\theta_r\theta_h/\theta_c\}N^4 2\times 12^2 5\varphi$

[22.24] $\hbar_s=\{\theta_c/(\theta_r\theta_h)\}\hbar_e/[N^4 2\times 12^2 5\varphi]$

[22.25] $\hbar_s=\{\theta_r^{-1}\}5.63990549106575_{(10)^{-56}}$ J.s

The stable Ramion radius follows directly from the mechanical Planck relation:

[22.26] $r_s=\hbar_s\mathring{c}_s/E_s=\{\theta_r^{-1}\}\hbar_{s(1)}\mathring{c}_s/E_s$

[22.27] $r_s=\{\theta_r^{-1}\theta_e^{-1}\}8.33772422647155_{(10)^{-30}}$ m

The energy density of a stable Ramion is:

[22.28] $\rho_s=E_s/((4/3)\pi r_s^3)=\{\theta_r^3\}E_s/((4/3)\pi r_{s(1)}^3)$

[22.29] $\rho_s=\{\theta_r^3\theta_e^4\}6.18482525983801_{(10)^{68}}$ J/m^3

The mean energy density of the universe:

[22.30] $\rho_u=\varphi\rho_s=\{\theta_r^3\}\varphi\rho_{s(1)}$

[22.31] $\rho_u=\{\theta_r^3\theta_e^4\}4.57974243707115_{(10)^{68}}$ J/m^3

Supplementary Explanations of Speed, Photons, and Quantization

In the geometric interpretation of the model, the ratio between the internal speed of energy and the observed speed of light derives from the fraction of the path traversed through the occupied space of the FCC lattice. This argument assumes an almost delay-free passage through NonSpace. Nevertheless, the general speed relation and its correction factors remain those of [22.1] in the main text; the simplified geometric argument must not replace the coefficient $\{\theta_c\}$.

In the photon-transfer model, receipt of additional rotational energy is associated with the appearance of a second rotational axis perpendicular to the first, electrical axis. In comparison with a rigid-body model having two independent axes, the appearance of the linear term in the additional energy depends on the composition of angular velocities and the assumptions concerning the second temporal dimension. The exact relations and factor $\{\theta_r\}$ are given in [22.7] through [22.19].

In the discussion of the stable energy of a Bal, the quantization convention of this version is **Ceil$_{30}$**. The archived quantization relation is interpreted only according to this convention; the alternative Ceil$_{10}$ form is not accepted in this version.

Detailed Explanation

Volume Occupancy Factor and the Ratio of the Two Speeds of Light

In the FCC structure, Ramions do not occupy the entire volume of hyperspace. Those portions of hyperspace not occupied by the space generated by Ramions are called NonSpace.

In NonSpace, the energy density is zero or very close to zero. Consequently, the speed of energy propagation there is infinite or almost infinite, and the transit-time delay is practically zero. The observed speed of light c is therefore greater than its internal speed $\mathring{c}$ inside a Ramion.

To calculate the ratio of these two speeds, consider a very long, thin column along the path of light through hyperspace. If the column is sufficiently thin, the fraction of its volume lying inside Ramions equals the fraction of its axial length passing through Ramion space.

This ratio is the FCC volume occupancy factor:

; $\varphi = \pi/(3\sqrt{2})$

Light therefore travels inside Ramions along only the fraction φ of its path, and all of its time delay arises in this portion. In the remaining portion of the path, namely NonSpace, transit time is practically zero.

Hence:

; $\mathring{c}_s = \varphi.c_s$

And because:

; $c_s = c$

For an E_s Ramion:

; $\mathring{c}_s = \varphi.c$

Or equivalently:

; $c = \mathring{c}_s/\varphi$

Thus φ is not merely a geometric volume occupancy coefficient; it directly determines the ratio of the internal speed of light in a Ramion to its observed linear speed in the FCC lattice.

Origin of the Factor $\pi^2/10$ and the Stable Energy of Particles

The factor $\pi^2/10$ is obtained from a combined analysis of inertia, conservation of rotational energy, and the geometric factor φ during fermionic separation.

Before separation, the common moment of inertia of the twelve-Bal structure is:

; $I_{(before)} = 12.(½mr^2) = 6mr^2$

After separation of the fermion from the common cavity, the moment of inertia changes to:

; $I_{(after)} = (10/3)mr^2$

During the same process, the characteristic speed changes by the factor φ. Therefore, conservation of rotational energy gives the effective energy-transfer coefficient:

; $(I_{(before)}/I_{(after)}).\varphi^2 = (6/(10/3)).\varphi^2 = (18/10)\varphi^2 = \pi^2/10$

Thus, if $\mathring{N}$ is the particle's genetic growth code, the continuous value of the energy of each Bal before quantization is:

; $\acute{N} = (\pi^2/10)\mathring{N}$

In the FCC structure, the number of Ramions in layer n is:

; $L(n) = 10n^2 + 2$

In sufficiently large layers, the number of Ramions per layer is approximately a multiple of ten. Therefore, for particle energy to be distributed stably among the Ramions of each layer, the energy value of each Bal must be quantized upward to the next multiple of ten:

; $N = Ceil_{30}((\pi^2/10)\mathring{N})$

Consequently, the energy of a stable twelve-Bal structure is:

; $E = 12N.E_s$

The energy of stable particles thus follows directly from FCC geometry, the particle's genetic growth code, conservation of energy, inertia, and layer-by-layer quantization.

Energy Exchange in the Ramionic Lattice and the Origin of the Photon

If a large amount of energy is exchanged with a network of Ramions—that is, supplied to or removed from them—neighboring Ramions act collectively by changing their radii, balancing force and energy throughout the lattice.

But if a small amount of energy reaches scattered Ramions, the receiving Ramions cannot, by increasing their radii alone, create the space required to retain that energy stably. They must therefore pass the excess energy to the Ramions ahead of them.

This continuous transfer of energy from one Ramion to the next is the passage of energy manifested as a photon.

In a Ramion, the first axis of energy rotation defines the electric field. Upon receiving a small amount of additional energy, a second rotational axis perpendicular to the first appears, corresponding to the magnetic field.

These two mutually perpendicular rotations form the electromagnetic-wave structure and transfer the additional energy as a photon from one Ramion to the next.

Result for a Classical Rigid-Body Model

If a Ramion were an ordinary rigid body situated in pre-existing spacetime, rather than itself generating space and time, then upon absorbing additional rotational energy about the second axis, the energies of the two independent axes would simply add.

Because the moments of inertia about both axes are equal, the additional rotational energy would be:

; $E_m = \frac{1}{2} I.\omega_m^2 = \frac{1}{2} E_0.(\omega_m/\omega)^2$

Therefore:

; $E_m \propto \omega_m^2$

Thus, if a Ramion were a classical rigid body, the relation for the energy of the second axis, and consequently Planck's relation, would also be quadratic: photon energy would be proportional to the square of angular frequency rather than to angular frequency itself.

In such a model, there would be no natural mechanical mechanism for the emergence of a linear energy–frequency relation.

This fundamental difference shows that a Ramion cannot be modeled as a classical rigid body in a pre-established spacetime.

Priority of Energy Laws over the Dimensions of Space and Time

In Ramionics, a Ramion is both a quantum of energy and a generator of space and time. Accordingly, when it receives or loses energy, it does not merely change its rotational or linear speed: the effective dimensions of space and time themselves change in order to preserve the universe's two fundamental relations.

These two fundamental relations are:

Conservation of energy in the universe.

Complete equilibrium between linear and rotational energy.

These two relations, proved in the earliest theorems of Ramionics, are more fundamental even than the number of dimensions of space and time.

A Ramion never tolerates an imbalance between linear and rotational energy in response to received positive or negative energy. Whenever rotational energy begins to increase, the Ramion immediately increases the number of temporal dimensions to prevent an imbalance. Whenever linear energy tends to increase, the Ramion immediately increases the number of spatial dimensions to prevent an imbalance.

If rotational energy increases—that is, rotation becomes greater and the effective radius smaller, as in the process associated with Planck's constant—the number of temporal dimensions increases from one. Conversely, if the linear-energy share increases, the number of spatial dimensions increases from three.

Because energy reception and emission among Ramions are continuous or nearly continuous, the effective numbers of spatial and temporal dimensions can also change continuously over short intervals, even taking noninteger and fractional values.

For this reason, in Ramionics the universe has three spatial dimensions and one temporal dimension only in the mean-equilibrium state, MES. Three spatial dimensions and one temporal dimension are not immutable, higher-order numbers of the universe; rather, they are the average values of a system that constantly adjusts its effective dimensions to preserve energy conservation and equilibrium between linear and rotational energy.

By virtue of the properties of energy, Ramions tend toward higher spatial dimensions, but energy density compels them to tolerate lower dimensions. Fewer than three spatial dimensions are unsuitable: in one dimension the layers are discrete, and in two dimensions the layers are hexagonal and hence nonspherical. On the other hand, a single temporal dimension is preferred because of its lower entropy.

The three-dimensional structure of space and one-dimensional structure of time are therefore the stable, average state of the universe. During disturbances and energy exchange, however, the effective dimensions can change to preserve the two fundamental relations.

The Second Temporal Dimension and the Electromagnetic Wave

Upon receiving a small amount of rotational energy, the Ramion structure changes so that a new rotational axis is created.

The first axis is the main axis of energy rotation and corresponds to the electric field. The second axis is perpendicular to the first and corresponds to the magnetic field.

In this state, instead of one temporal dimension—that is, one unique time parameter—there are two independent components of angular evolution corresponding to the two rotational axes and thus to two temporal dimensions.

The time derivative of the angle therefore appears as the sum of two components:

$$; \partial\theta/\partial t = \partial\theta/\partial t_1 + \partial\theta/\partial t_2$$

In terms of angular velocities:

$$; \omega_{(total)} = \omega + \omega_m$$

The total rotational energy is therefore:

$$; \check{E}_0 + E_m = \tfrac{1}{2} I.(\omega + \omega_m)^2$$

The additional energy relative to the initial state is:

$$; E_m = \tfrac{1}{2} I.((\omega + \omega_m)^2 - \omega^2)$$

The exact expansion is:

$$; (\omega + \omega_m)^2 = \omega^2 + 2.\omega.\omega_m + \omega_m^2$$

Consequently:

$$; E_m = \tfrac{1}{2} I.(2.\omega.\omega_m + \omega_m^2)$$

And, after factorization:

$$; E_m = I.\omega.\omega_m.(1 + \omega_m/(2\omega))$$

Creating the second temporal dimension thus causes the linear term $I.\omega.\omega_m$—which was absent from the sum of energies of two independent axes of an ordinary rigid body—to appear and dominate the quadratic term at low energies.

Projection of Planck's Constant with N^4

For a Ramion with N times the reference Ramion's energy:

; $E_r = N.E_s$

Under the Ramionics projection laws, its radius also increases by a factor of N:

; $r_r = N.r_s$

Meanwhile, the internal energy speed decreases by the factor $1/N^2$:

; $\mathring{c}_r = \mathring{c}_s/N^2$

Now, from the mechanical definition of Planck's constant:

; $\hbar_r = E_r.r_r/\mathring{c}_r$

Substituting the projection relations gives:

; $\hbar_r = (N.E_s).(N.r_s)/(\mathring{c}_s/N^2)$

Therefore:

; $\hbar_r = N^4.(E_s.r_s/\mathring{c}_s)$

And because:

; $\hbar_s = E_s.r_s/\mathring{c}_s$

It follows that:

; $\hbar_r = N^4.\hbar_s$

Thus, when energy is N times E_s, the local or relative Planck constant becomes N^4 times as large, because energy and radius each increase by N, while the internal speed of light decreases by $1/N^2$.

The power N^4 in Planck's constant is therefore not an independent assumption; it follows directly from its mechanical definition and the projections of energy, radius, and internal speed in a Ramion.

Theorem 23: The Nature of Mass and Gravity

Because ramions constitute space, the only way to define mass is for the ramions within a spherical region of space to be destroyed and explode, with their energy subsequently disseminated throughout the universe in accordance with energy conservation.

Matter is not a concentration of energy. Rather, it is the explosion and destruction of a number of ramions within a spherical region of space, after which their energy spreads throughout space, with a greater share distributed among the nearer layers. A spherical cavity, or black hole, is left at the center of the energy distribution and thus within the fabric of spacetime.

The only difference between the central black holes of subatomic particles and galactic black holes is their scale; their mathematical formulation is the same.

In this model, the released energy first reaches the ramions of adjacent layers. Since absorbing energy requires an increase in a ramion's radius, and the FCC geometrical arrangement restricts this increase, each ramion absorbs only part of the energy it receives and passes the remainder to the next layer. This layer-by-layer transmission produces a nonuniform distribution of energy around the central region.

Within the Ramionics framework, an increase in the energy metric near the center is accompanied by a decrease in the local effective pressure. The resulting pressure gradient is therefore the proposed mechanism of attraction. In this description, the central cavity is a region of nonspace, rather than a geometrical singularity.

Details:

To explain the stability of the central cavity, the surrounding ramions can be compared to the components of a thrust arch that support one another. This analogy is descriptive and does not, by itself, prove geometrical stability.

In a supplementary hypothesis in the archive, ramions opposite one another on the surface of the central cavity might be entangled through extremely small structures permitting rapid transfer of force and information, thereby maintaining force and torque equilibrium. Extending this mechanism to entanglement between different particles is also proposed in the archive; this interpretation still requires quantitative derivation and independent testing.

Theorem 24: The Nature of Charge and the Electric Field; From Ramion Geometry to the Possibility of Modeling the Strong Interaction

Abstract

This theorem first reviews accepted definitions of electric charge, the electric field, electromagnetism, and the strong interaction in contemporary physics. It then presents the proposed Ramionics mechanism for a mechanical interpretation of charge, local particle polarization, quark color, and the high strength of short-range interactions. The geometrical part retains the volume of intersection of two ramions, the cross-sectional area, energy, and the energy derivative without omitting the existing relations. A distinction must be maintained between calculated geometrical results, the mechanical hypothesis of Ramionics, and experimental predictions that have not yet been derived.

Part One: Significance, Definitions, and the Current State of Physics

1. Significance of the Problem

In particle physics, electric charge determines electromagnetic interaction, whereas the color charge of quarks plays a different role in quantum chromodynamics (QCD). Understanding why short-range interactions among hadronic constituents are very strong, how zero net charge can coexist with internal structure, and how interaction strength depends on scale is important for connecting particle geometry with forces.

2. Charge and the Electric Field in the Standard Description

Electric charge is a conserved quantity and a source of the electromagnetic field. The electron has charge $-q$ and the positron $+q$; up and down quarks have charges $+\frac{2}{3}q$ and $-\frac{1}{3}q$, respectively. Electrical neutrality does not necessarily imply the absence of internal structure or electromagnetic moments. However, the standard neutrino has zero net electric charge, and its weak interaction is described in the Standard Model through the W and Z bosons.

For two point charges in vacuum, Coulomb's law in the electrostatic approximation is:

; $F_e=K.q_1q_2/r^2$

The magnitude of the field produced by a point charge, disregarding the directional sign, is:

; $|E|=K.|q|/r^2$

The fine-structure constant specifies the dimensionless strength of electromagnetic interaction:

; $\alpha=K.q^2/(\hbar c)$

; $\alpha^{-1}\approx137.035999177$

This is the low-energy reference value. In precise quantum calculations, the effective electromagnetic coupling varies with energy scale. A static electric field in standard physics does not require continuous emission of real photons; in quantum field theory, static interactions can be described in terms of virtual exchange. This distinction is essential when comparing the standard description with the Ramionics interpretation.

3. The Strong Interaction and Color Charge

In QCD, quarks have three color states, conventionally called red, green, and blue; these names do not refer to optical colors. Gluons carry the color field, and their self-interactions are related to color confinement and asymptotic freedom. Observed hadronic states are overall color-neutral, although their constituent quarks carry color charge.

The strong coupling α_{st} depends on the energy scale Q. Its reference value near the Z-boson mass is approximately 0.118. It becomes smaller at high energies, whereas at low hadronic energy scales a simple perturbative approximation is generally insufficient. At one-loop order, for a fixed number of active flavors:

; $\alpha_{st}(Q) \approx \alpha_{st}(Q_0)/[1+\alpha_{st}(Q_0)\beta_0/(2\pi).\ln(Q/Q_0)]$

; $\beta_0 = 11 - 2n_f/3$

In the color-singlet quark–antiquark channel at short distances, the Coulombic potential approximation is:

; $U_{st}(r) \approx -C_f \alpha_{st} \hbar c/r$

; $C_f = 4/3$

; $|F_{st}(r)| \approx C_f \alpha_{st} \hbar c/r^2$

These relations are QCD approximations within their appropriate regime, not universal fixed laws at all distances. At hadronic distances, the confining potential and nonperturbative effects become important. Common ratios quoted for the strengths of fundamental forces, including comparisons on the order of 10^{38} with gravity, depend on the particle, distance, and comparison convention; they must not replace a quantitative prediction under specified conditions.

4. The Problem Ramionics Seeks to Solve

The objective of Ramionics in this theorem is to propose a common geometrical origin for net charge, local polarization, quark color, and the difference between near-field and far-field strengths. Achieving this objective requires the model to reproduce not only charge counting, but also the potential, force direction, dependence on distance and energy scale, and ultimately hadronic data. In what follows, every definite geometrical result is distinguished from the physical hypotheses.

Part Two: The Proposed Ramionics Mechanism

5. Twelve-Ball Geometry and Six Rotational Axes

Based on the twelve-ball structure introduced in the twelve-ball theorem and the formulations of Theorems 39 and 44, a particle consists of twelve balls arranged in six opposing pairs. Three mutually perpendicular pairs provide three distinct geometrical classes. In the Ramionics convention, the direction of rotation and the effective signs of the balls are associated with the arrangement of net charge and the local field. Each pair can contribute an effective q/6 to charge counting. This is a model convention and is not yet equivalent to deriving the SU(3) gauge theory.

In this model, a neutrino may possess balls with positive and negative effective signs at very short distances, while its total charge remains zero. Consequently, the overall neutrality of a particle does not rule out hypothetical locally directional effects. This hypothesis must be tested against

experimental limits on neutrino charge and electromagnetic moments, and must not be mistaken for proof of nonzero neutrino electric charge.

From the model's perspective, quarks likewise possess positive and negative local arrangements. In addition, three distinct classes of rotational axes are proposed as candidates for the origin of the three color states. For quarks, color is assumed to depend on the orientation of modified axes relative to three orthogonal pairs. In the six-axis convention of this model, the electron has six negative contributions of the same sign. Its configuration therefore does not exhibit the quark's threefold color structure under this criterion and is consequently classified as **colorless**. This statement concerns QCD color, not the absence of the electron's electromagnetic charge or field.

6. Near Field, Far Field, and the Question of Force Strength

Ramionics associates field magnitude and effective constants with the energy metric and spacetime structure of the particle, using the parameter N. In the gravity-projection treatment of Theorems 32 and 39, there is a specific dependence on N^8:

; $G=144K_{\mathscr{g}}G_s/[N^8(1-1/N)]$

Within the same convention, keeping all other factors constant, this relation yields:

; $G_s/G=N^8(1-1/N)/(144K_{\mathscr{g}})$

Thus **N^8 is the principal scaling factor in this projection, but the exact force ratio is not simply N^8**. Geometrical coefficients, effective masses, distance, and the definition of force also matter. Nor does this relation alone establish that the QCD strong force is exactly N^8 times the gravitational force. Such a claim would require an independent derivation of the short-range quark potential and color coupling without fitting experimental data.

The mechanical hypothesis of Ramionics is that, at short distances, direct ball-to-ball interactions occur before the field has undergone full geometrical dilution, whereas the macroscopic gravitational field is a weakened projection of the same structure. Any possible dependence of electric-field strength and α on the metric N must also be completed through an explicit relation, correct dimensional analysis, and separate experimental testing. The gravitational N^8 dependence does not, by itself, determine the law governing variation of α.

7. Mechanical Mechanism of Charge and Magnetism

In the Ramionics picture, every rotating ramion has an axis, two conventional poles, and an equatorial plane. The north pole is designated positive. Adjacent ramions form a common region V_c at their contact or slight interpenetration. When like poles approach one another, rotational directions in the contact region may become opposite and, in this interpretation, be associated with reduced overlap and repulsion; the reverse arrangement is associated with attraction. The analogy to friction between rotating surfaces is purely mechanical and does not imply ordinary dissipative friction in vacuum.

In this framework, a static electric field is explained through alignment of the rotations of environmental ramions and local changes in their arrangement. In the same picture, the photon is interpreted as an excitation or wave of ramion rotational energy, rather than as an independent elementary particle. This interpretation differs from the standard photon description and requires experimental testing. Magnetism is linked to the rotation of the principal electric axis about a second axis, termed the magnetic axis, with its additional energy represented by E_m. The hypothesis of a second dimension of time and the exclusive fundamentality of energy are hypothetical components of the Ramionics framework; they do not follow from sphere-intersection geometry alone.

8. Exact Geometrical Model of the Intersection Region and Energy

The following geometrical calculations are retained from the earlier formulation of Theorem 24. Here d is the penetration depth and dist is the distance between centers. The opposing directions of change of these two variables are essential when interpreting the force sign.

Volume of intersection of two ramions (two spheres with penetration d)

Consider two spheres of radii r_1 and r_2, with center-to-center distance dist.

Penetration depth:

[24.1] $d = r_1 + r_2 - dist$

[24.2] $dist = r_1 + r_2 - d$

Geometrical definition of the intersection plane

The common plane of the two spheres is at a distance x from the center of the first sphere:

[24.3] $x = (dist^2 + r_1^2 - r_2^2)/(2.dist)$

Cap heights:

[24.4] $h_1 = r_1 - x$

[24.5] $h_2 = r_2 - (dist - x)$

Integral formula for the intersection volume

The intersection volume is the sum of two spherical caps:

[24.6] $V_c = \int \{r_1 - h_1 \text{ to } r_1\}\{\pi.(r_1^2 - z^2).dz\} + \int \{r_2 - h_2 \text{ to } r_2\}\{\pi.(r_2^2 - z^2).dz\}$

Alternatively, in a more symmetric form with a local change of variable:

[24.7] $V_c = \int_0(h_1)\{\pi.(2.r_1.z - z^2).dz\} + \int_0(h_2)\{\pi.(2.r_2.z - z^2).dz\}$

Closed-form result of the integrals

[24.8] $V_c = \pi.(h_1^2.(r_1 - h_1/3) + h_2^2.(r_2 - h_2/3))$

Radius of the intersection circle:

[24.9] $a = \sqrt{(r_1^2 - x^2)}$

The distance from the first sphere's center to the intersection plane is x.

Area of the circle in the intersection plane:

[24.10] $A_c = \pi.(r_1^2 - ((dist^2 + r_1^2 - r_2^2)/(2.dist))^2)$

Special case: $r_1 = r_2 = r$

In this case:

[24.11] $x = dist/2$

[24.12] $h = r - dist/2 = d/2$

Area of the circle in the intersection plane:

[24.13] $A_c = \pi.(r.d - d^2/4)$

Intersection volume:

[24.14] $V_c = 2.\int_0(h)\{\pi.(2.r.z - z^2).dz\}$

Result:

[24.15] $V_c = 2.\pi.(h^2.(r - h/3))$

Substituting h = d/2:

[24.16] $V_c = 2.\pi.((d/2)^2.(r - d/6))$

Simplified form:

[24.17] $V_c = (\pi.d^2.(3.r - d))/6$

Physical interpretation in the Ramion model

In this framework, d is the indentation depth, and the intersection volume V_c represents the degree of spatial overlap and, consequently, the amount of released energy or change in potential between two ramions.

Increasing d increases V_c and consequently decreases the potential.

Decreasing d decreases V_c and consequently increases the potential.

If the volumetric energy density of the two ramions is ρ, the energy of the common region follows directly from its intersection volume:

[24.18] $E_{(Common)} = E_e = \rho.V_c$

Using relation [24.17]:

[24.19] $V_c = (\pi.d^2.(3.r - d))/6$

Consequently:

[24.20] $E_e(d) = \rho.(\pi.d^2.(3.r - d))/6$

Derivative of energy with respect to d

Force is the negative derivative of energy with respect to distance.

[24.21] $\partial E_e/\partial d = \rho.(\pi/6).\partial/\partial d[d^2.(3.r - d)]$

[24.22] $\partial E_e/\partial d = \rho.\pi.(r.d - d^2/2) = -F$

For small penetration depths

[24.23] $V_c = (\pi.d^2.(3.r - d))/6 \approx \pi.r.d^2/2$

[24.24] $A_c = \pi.(r.d - d^2/4) \approx \pi.r.d$

[24.25] $V_c/A_c = d/2$

[24.26] $F = -\rho.\pi.(r.d - d^2/2) \approx -\rho.\pi.r.d$

[24.27] $-F/A_c = \rho = E/V$

That is, the surface density of electric force becomes equal to the volumetric energy density.

Physical interpretation

This force arises directly from the increase or decrease in the overlap volume.

For small d, the r.d term dominates and the force grows approximately linearly with d.

For larger d, the d^2 term reduces the rate of increase of the force, and nonlinear behavior appears.

This is precisely the behavior expected of an interaction arising from volumetric overlap: increasing penetration initially produces a rapid increase in released energy, but with further penetration a geometrical saturation effect appears.

In Ramionics, electric force depends directly on the geometrical structure of the intersection of two ramions and is derived from the geometry of the universe itself, without requiring an independently defined field.

9. From Intersection Volume to a Strong-Force Model

Relations [24.1] through [24.27] specify the common volume, contact cross-sectional area, energy associated with the assumed density ρ, and its derivative. This calculation supplies a geometrical core for defining a short-range interaction. Nevertheless, converting it into the strong force requires precisely specifying the potential energy U in terms of the actual center-to-center distance, rotational orientations, quark type, and color state. Since d decreases as dist increases, the definition of the force sign must be consistent with the potential and coordinate conventions. Relation [24.22] is retained as the sign convention of the original text and should not be interpreted as a radial force without this qualification.

To extend the model, interaction energy may be considered a function of overlap geometry, local signs, threefold axes, and the particle metric. Such a function has not yet been derived in this theorem. In particular, it must be clarified why quarks of the same color and different colors behave differently, how the colorless hadronic state forms, and how the model can be compatible with asymptotic freedom at short distances and confinement at larger distances.

10. Required Tests and Limitations

To turn the mechanical interpretation into a quantitative theory comparable with QCD, the following steps are necessary: determining a directional potential function from overlap energy; deriving the color factor instead of importing its standard value; determining the running of the coupling with energy; deriving the force scale and range and predicting the force for specified color states; and comparing predictions with hadron spectra, scattering, and experimental neutrino constraints. In the absence of these steps, the proposed geometrical origin of color and the N^8 factor constitute a definite theoretical research program, not experimental proof of the strong interaction.

Conclusion

In this formulation, Theorem 24 proceeds from a review of charge and fields in contemporary physics to the twelve-ball structure of Ramionics. It then shows how local polarization of a neutral particle, three geometrical axes for quark color, and the absence of color in the electron can be proposed within a common mechanical picture. The geometrical relations for the intersection of two spheres constitute the calculated and testable portion of this proposal. The N^8 dependence in the gravitational projection motivates investigation of the difference between near and far fields, but quantitatively identifying it with the strong force requires independent derivation and testing. The fuller discussion of color appears in Theorem 44, and the discussion of force unification in Theorem 39.

Theorem 25: The Twelve-Ball Model

In the far field, all linear and rotational energy dispersed throughout space is modeled on 12 balls surrounding a black hole of the same radius, corresponding to the twelve Ramions of the first face-centered cubic layer.

Formation of Particle Structure and Energy Distribution

In the Ramionics model, the conversion of energy into matter is described as the collapse of one or more Ramions due to intense fluctuations and possible resonance of gravitational, electromagnetic, or neutrino waves. The energy of collapsed Ramions propagates through the lattice, and nearby Ramions receive a greater share of the region's energy. The reverse process is the conversion of matter into energy. This mechanism is a mechanical hypothesis of the model and must not be regarded as established without an independent calculation.

For force and torque equilibrium, the collapsed region is assumed in this model to be spherical or approximately spherical. Collapse of FCC layers is treated as discrete: each layer either collapses completely or remains stable. The first stable layer forms a shell around the central cavity, which contains no Ramions. Within this framework, particle black-hole structures and cosmic black holes are related in their proposed mechanism, although their size and energy scales differ.

Concentrating mass or energy at the center of the cavity is only a computational approximation. In the model's more fundamental description, no Ramion exists inside the cavity; energy is distributed around it and throughout the lattice. For computing an effective field, energy may also be distributed over the cavity surface. This surface approximation is more consistent with the empty interior than an assumed volumetric distribution. In this picture, gravitation and electromagnetism are behaviors of the linear and rotational portions of energy, not two independent substances or energies.

The single-center approximation is insufficient to describe torque equilibrium and charge arrangement. Consequently, in the more complete model, effective energy is distributed over twelve balls surrounding the cavity. Each ball carries part of the structure's linear and rotational energy. This model is an effective representation of energy distribution in space and does not necessarily imply the existence of twelve independent material spheres.

Under the geometric convention of this model, signed charge density, or the rotational contribution, on each ball's surface is described as proportional to cos(θ): it has a positive maximum at the north pole, is zero at the equator, and reaches a negative maximum at the south pole. By contrast, the pressure or gravitational contribution is assumed uniform in the surface approximation. The cosine distribution is a modeling assumption and does not follow from the definition of torque alone.

Net charge appears when the signed arrangement of the balls becomes asymmetric relative to the neutral state. In the neutral state, six balls with positive contributions and six with negative contributions form symmetric pairs. Changing the arrangement of independent axes produces the quantized charge states described later in this theorem.

Stability requires simultaneous force and torque equilibrium. In the model's relativistic description, changes in energy and radius enter force equilibrium; for torque equilibrium, rotations of opposing balls must cancel one another. **The convention for rotational direction is the same as in the original text of this theorem:** viewed from the center, two opposite balls rotate in opposite directions, whereas from the corresponding two exterior viewpoints they appear to rotate in the same direction and carry charges of the same sign.

The electric potential contribution is subtracted from the full energy of the neutral state when calculating rest energy. Representing this reduction by a negative term does not imply physically negative mass or energy; it is an energy-potential accounting convention. The rotational contribution and the assumed cosine distribution play a role in interpreting this potential.

Throughout charge counting, **q** is the family's full charge, each ball contributes q/12, and each axis contributes q/6. Thus the archival convention Q does not replace q in the original text. The seven charge values and the procedure for reversing axis signs remain those given below in the original text.

Fundamental Particle Structure

The twelve-ball model offers a simple explanation for the stability of particle electric charges at 0, −⅓, +⅔, and −3/3 for matter particles. The signs are reversed for antimatter.

Let q be the magnitude of the electron's full charge. Each electron ball carries 1/12 of q. In a stable state, each opposing pair of balls must cancel the other's torque so that the particle structure

remains in torque equilibrium. Therefore, when viewed from the center, the two opposing balls must rotate in opposite directions. However, when observed from outside at two corresponding points, each near one ball, their rotational directions are the same; that is, they carry electric charge of the same sign.

The particle therefore has six axes, or six pairs of balls, each carrying either $+q/6$ or $-q/6$. In the neutral state, these signs alternate and the total charge is zero. At extremely short distances, the contribution of each individual ball remains distinguishable; approaching a positive ball of a neutral particle therefore produces a locally positive contribution, and the reverse applies to a negative ball.

Relative to the neutral state, reversing one positive axis creates a total charge of $-q/3$. Reversing two negative axes creates $+2q/3$. Reversing all three positive axes creates $-q$.

These three states correspond, respectively, to the down quark, the up quark, and the electron. The three opposite states constitute their antiparticles. Together with the neutral state, there are seven possible stable electric-charge states. In the electron family, the neutral structure is the electron-family narion, denoted e_0, which is its own antiparticle. Each family therefore contains seven stable particles. They have identical structure, radius, and total energy; their only difference is the orientation of the balls, which generates a different ball potential U. This potential is subtracted from the full energy—that is, the neutral-state energy—to obtain the rest energy.

For quarks, a particle's rotation axis may belong to three distinct classes of axes, whereas all axes are equivalent for the electron.

Thus these three classes of quark axes correspond to the three QCD colors, while quark flavor is associated with family and charge.

Theorem 26: Ball Equations and Potential Quantization Factors η

A ball obeys the fundamental Ramion equations, but its second-degree structural potentials, q^2 and $\mathring{m}^2$, are divided by the discrete potential factor η^2.

Explanation for $Q=Nq$:

[26.1] $E_{(}continuous_{)}=KQ^2/(2r)=KN^2q^2/(2r)$

[26.2] $E_{(}discrete_{)}=Kq^2/r\sum_{n=0}^{N-1}n=KN_{(}N-1_{)}q^2/(2r)$

Therefore:

[26.3] $\eta^2=E_{(}discrete_{)}/E_{(}continuous_{)}=1-1/N$, $\eta=\sqrt{(1-1/N)}$

[26.4] $1/\eta^2=1/(1-1/N)$, $\eta_{\mathscr{m}}=\sqrt{(1-1/(\mathscr{m}N))}$

; Default $\eta=\eta_1$

Relative $\eta_{\mathscr{m}}$ for one particle: $\eta_{12/9}$, $\eta_{12/4}$, $\eta_{12/1}$, $\eta_{6/1}$, $\eta_{4/1}$, $\eta_{2/1}$.

Relative $\eta_{\mathscr{m}}$ for two particles: $\eta_{6/1me}=\eta_{6/1m}/\eta_{6/1e}=\eta_{6/1m}/\eta_{6/1}$; similarly for t.

Basis of Discrete Counting and the Energy Convention

The ball model is an effective description of energy propagation and interaction within the Ramion lattice. Each ball consists of a large number of Ramions, and the energy of pairwise interactions must be counted using a discrete sum. The first Ramion already carries its initial energy; adding it creates no new interaction pair with preceding Ramions. The sum therefore starts at zero. This explains the convention for counting pairs and is not, by itself, an independent proof of energy conservation.

According to [26.1] and [26.2], for N Ramions with charge q, constant K, and reference radius r, the interaction sum contains $N(N-1)/2$ pairs; the corresponding continuous approximation uses $N^2/2$ instead. Hence η^2 is the ratio of discrete to continuous energy. The archival relations [26.8] and [26.9], which omitted the factor ½ on both sides, are inconsistent with the definition [26.2] if interpreted as absolute energies; only their ratio remains correct. The convention retaining ½ in the main text is authoritative.

Distinguishing the Energy Factor from the Effective Interaction Constant

If K is the same constant in both the continuous and discrete models, the energy calculated by discrete counting is η^2 times the continuous energy. But if the target energy is held fixed and the effective constant is extracted from that energy, the factor applied to the effective constant is the reciprocal. These two calculation methods must not be used simultaneously in one equation as two independent corrections.

; $K_{(}effective_{)}=K_{(}reference_{)}/\eta^2$

; $G_{(}effective_{)}=G_{(}reference_{)}/\eta^2$

In these two relations, the reference and effective constants must correspond to the same energy definition and interaction geometry. The gravitational factor can be transferred in this form only if the same pair-counting structure and normalization convention apply. Under an alternative convention, when the interaction constant does not appear in the formula, the reciprocal factor can be assigned to an effective charge or mass. This is merely a reparameterization of the same quadratic product, not an independent change in actual charge or mass.

; $q_{(}effective_{)}=Nq_s/\eta$

; $\mathring{m}_{(}effective_{)}=N\mathring{m}_s/\eta$

These effective relations do not replace the convention for the ball's actual charge in Theorem 30. There, the structural charge of each ball is mapped using N and that of the twelve-ball particle using 12N. Likewise, the archival ball-energy relation that simultaneously introduced $K_{\mathscr{n}}\eta^2$ and $G_{\mathscr{n}}\eta^2$ into the potentials must not be added as another independent equality without specifying whether those constants are “reference” or “effective.” The factor ½ in electric potential and the geometric coefficient ⅗ in gravitational energy must also be retained according to the conventions of Theorem 20.

Generalization to Ball Counts and Interactions Between Two Families

In [26.4], $\mathscr{n}$ denotes the number of participating components. Thus η_1, η_6, and η_{12} are defined for one, six, and twelve components, respectively. Ratios such as $\eta_{12/9}$, $\eta_{12/4}$, and $\eta_{6/1}$ are ratios of two coefficients and must not be confused with the coefficient of a single set.

In interactions between two different families, each side contributes its own correction. To avoid confusing the family subscript with the ball-count subscript, the mutual correction factor is expressed as a product of the corresponding coefficients:

; $K_{(}mutual_{)}=K_{(}reference_{)}/(\eta_{(}family1_{)}\eta_{(}family2_{)})$

; $G_{(}mutual_{)}=G_{(}reference_{)}/(\eta_{(}family1_{)}\eta_{(}family2_{)})$

This expression is valid only under the effective-constant convention. Under the effective-charge or effective-mass convention, each η factor must enter the corresponding quantity only once. The special ratios for the electron, muon, and tau families presented at the beginning of the theorem remain unchanged.

Connection to the Fine-Structure Constant

Under its older convention, before the introduction of the seven θ factors, the archive used $\alpha=\beta/[40\pi(1-1/N)]$ with N=36390 and β=0.9169871684935677, reporting $\alpha^{-1}=137.035999207833$. The current reference is [30.12] in the main article, which employs θ_p, θ_k, θ_r, and θ_h in the specific combination used to calculate α. The absence of the other θ factors from that relation does not mean they are removed from the seven-factor framework. The archival formula becomes equivalent to the current formula only under the condition $\theta_p\theta_k/(\theta_r\theta_h)=1$; this condition does not follow from the archive and must not be assumed without proof. The archive's reported numerical value is only the result of the older convention, not an independent recalculation with all θ factors.

In the calculation reported in the archive, the experimental value $\alpha_x^{-1}=137.035999177$ with uncertainty 0.000000021 was compared, yielding a difference of +1.468251σ for N=36390 under the inverse-alpha difference convention. For N=36389 and N=36391, the reported differences were −3.459800σ and +6.396030σ, respectively. The sign and difference convention in Theorem 30 is authoritative; that theorem gives −1.46825075418451σ for the alpha difference. This sign discrepancy arises from comparing alpha versus comparing inverse alpha, not from a different N. The geometric derivation of N is explained in Theorem 28; experimental agreement alone does not prove that model selection is independent of experimental data.

Further explanation:

In the effective ball interpretation, gravitational and electromagnetic effects propagate at the speed of light; in the proposed more fundamental description, energy itself moves through the lattice. For example, in a hypothetical scenario where a central mass is annihilated, the rearrangement of surrounding energy and fields is not instantaneous and requires propagation time. Re-formation of the same initial structure from dispersed energy is an additional hypothesis and does not follow solely from propagation delay.

The apparently continuous exchange of energy among very many Ramions has two proposed interpretations: fundamental continuity of energy constituents, or discreteness on a scale far smaller than the computational resolution. The nested-universe hypothesis, according to which each Ramion may itself be an independent universe and this universe may in turn form part of a larger structure, belongs to the second interpretation. Questions about whether this chain is infinite or cyclic are raised in the archive, but they are not established consequences of the η relations. The distinction between a logical cycle and a closed physical structure is also discussed within this hypothetical framework.

Theorem 27: Electric Potential and the Energy of Particles in the Same Family

1. The Twelve-Ball FCC Structure

In Ramionics, the fundamental structure of a particle consists of a center and twelve balls corresponding to the twelve immediate neighbors in three-dimensional FCC geometry.

The structural energy of each ball is N units of E_s, and the complete structural energy of a neutral particle is 12N units of E_s. According to the fundamental equilibrium, half of each ball's energy is linear–mechanical and the other half is rotational–electrical. Under the model's normalized electrical-distribution convention, the electrical energy allocated to each ball is N/12, and to each half-ball N/24. At the same time, under the structural-energy convention, the rotational share of each ball is N/2. Therefore, the allocated electrical energy N/12 and the total rotational energy N/2 are not

the same quantity, and the conversion between these two conventions must be explicit when calculating potential.

Thus, the complete structural energy of a neutral particle, or naryon, is:

[27.1] $\mathbb{E}_{0s}=12N$

[27.2] $\mathbb{E}_{0s}=24(N/2)$

Each ball has two electrical half-balls with opposite poles; consequently, the twelve-ball structure contains twenty-four electrical half-balls. The allocated electrical energy of each half-ball under the electrical convention is N/24. In the potential relations, N/2 is the “normalized axial potential unit,” not the electrical energy allocated to one half-ball. This distinction allows the coefficients 12 and 9 to be reported under a consistent convention.

2. Six Independent Axes and Charge Discreteness

The twelve balls form six opposing pairs. In terms of torque equilibrium, each pair shares one dependent axis.

In the neutral arrangement, three axes have a positive sign and three axes have a negative sign.

Reversing the electrical direction of one, two, or three axes produces one-third, two-thirds, or full charge.

The number of reversed axes is represented by c:

[27.3] $c\in\{0,1,2,3\}$

[27.4] $|q|/q_e=c/3$

The positive or negative sign of charge is independent of its magnitude and is determined by rotational orientation.

3. First Derivation of the 12+9 Model

3.1. The Linear Coefficient 12

To produce a fully charged arrangement, the orientations of twelve effective half-balls on the reference surface are adjusted.

Under the electrical-distribution convention, each half-ball contributes N/24. In calculating potential, the electrical contributions on the reference surface are mapped to a normalized axial unit whose reference energy is N/2. Thus, 12 in the following relation is the number of effective axial units and must not be confused with the energy of twelve individual half-balls.

Therefore:

[27.5] $\mathbb{U}_{12}=12(N/2)$

Since full charge is obtained by reversing three axes, the linear contribution per axis is four reference units.

[27.6] $\mathbb{U}_{l}=4c(N/2)$

3.2. The Quadratic Coefficient 9

In the fully charged arrangement, six half-balls reverse direction.

Under projection onto the black-hole surface of radius r, these six half-balls become three equivalent pairs. In this derivation, Q is the reference charge of one effective half-ball pair on the surface at r, and $Q_{e/\!/}$ is the projected charge of the three pairs. The ball and black-hole radii are equal; hence the radius cancels in the energy ratio:

[27.7] $Q_{e\not{/}\not{/}}=3Q$

In this projection, the reference radius is fixed and equals the radius of the ball and black hole. Electric potential energy is proportional to the square of charge:

[27.8] $\mathbb{U}\propto Q^2/R$

Therefore, the quadratic coefficient for full charge is:

[27.9] $(Q_{e\not{/}\not{/}}/Q)^2=3^2=9$

And the corresponding energy is:

[27.10] $\mathbb{U}_9=9(N/2)$

Consequently, the full electric potential is:

[27.11] $\mathbb{U}_{3s}=(12+9)(N/2)$

[27.12] $\mathbb{U}_{3s}=21N/2$

4. Second Derivation of the 12+9 Model

In this derivation, the calculation uses the zero-equipotential sphere at radius 2r; in the first derivation, the same arrangement was projected onto the black-hole surface at radius r. In both derivations, r is the common radius of the ball and black hole.

The radius of the reference surface is twice the ball radius:

[27.13] $R_0=2R_{\not{e}}$

To charge the surface fully, twelve charged hemispheres are considered.

Since each ball has two electrical hemispheres, the effective surface charge is six times the reference charge of one ball:

[27.14] $Q_{e\not{/}\not{/}}=6Q$

Given the quadratic dependence of energy on charge and its inverse dependence on radius:

[27.15] $\mathbb{U}_{18}/(N/2)=6^2/2=18$

On the zero-equipotential sphere, the inner and outer half-shells appear symmetrically in the initial count. The effective contribution to the external potential is the outer half-shell; hence a second geometric factor of 1/2 is applied. Therefore:

[27.16] $\mathbb{U}_9=18(N/2)/2$

[27.17] $\mathbb{U}_9=9(N/2)$

Adding the baseline component of twelve half-balls:

[27.18] $\mathbb{U}_{3s}=12(N/2)+9(N/2)$

[27.19] $\mathbb{U}_{3s}=21N/2$

Both derivations yield the same geometric coefficient, 12+9.

5. Generalization to Fractional Charges

For c reversed axes, the number of reoriented axial units is proportional to c. At the same fixed radius r, the accumulated effective charge is also proportional to c, and the interaction energy is proportional to its square. Thus, the linear contribution varies with c, and the interaction contribution varies with c^2.

[27.20] $\mathbb{U}_l=4c(N/2)$

[27.21] $\mathbb{U}_p=c^2(N/2)$

Consequently:

[27.22] $\mathbb{U}_{cs}=(4c+c^2)(N/2)$

[27.23] $\mathbb{U}_{cs}=c(4+c)(N/2)$

The zero-alpha rest energy is obtained by subtracting the electric potential from the neutral structural energy:

[27.24] $\mathbb{E}_{cs}=12N-\mathbb{U}_{cs}$

[27.25] $\mathbb{E}_{cs}=(24-4c-c^2)(N/2)$

c	Particle family	Charge magnitude	Linear	Quadratic	Potential	Rest energy
0	Naryon	0	0	0	0	12N
1	Down-type quark	1/3	4	1	5N/2	19N/2
2	Up-type quark	2/3	8	4	6N	6N
3	Charged lepton	1	12	9	21N/2	3N/2

For the electron family:

[27.26] $\mathbb{E}_{es}=3N/2$

[27.27] $\mathbb{E}_{us}=6N$

[27.28] $\mathbb{E}_{\mathscr{A}s}=19N/2$

6. Energy Ratios

[27.29] $\mathbb{E}_{us}/\mathbb{E}_{es}=4$

[27.30] $\mathbb{E}_{\mathscr{A}s}/\mathbb{E}_{es}=19/3$

[27.31] $\mathbb{E}_{es}/\mathbb{E}_{\mathscr{A}s}=3/19$

The ratio of naryon energy to electron energy:

[27.32] $\mathbb{E}_{\mathbf{0}s}/\mathbb{E}_{es}=8$

The share of the electron's electric potential in the naryon's structural energy:

[27.33] $\mathbb{U}_{3s}/\mathbb{E}_{\mathbf{0}s}=7/8$

7. Magnetic Inertia

In Theorem 31, it is shown that, for the electron-family metric:

[27.34] $N=36390$

Particle	Zero-alpha energy	Magnetic correction	Corrected energy
Electron	54585	63	54522
Up quark	218340	42	218298
Down quark	345705	21	345684
Naryon	436680	—	—

Corrected energy is denoted by E, and zero-alpha energy by $\mathbb{E}$.

[27.35] $E_{es}=54585-63=54522$

[27.36] $E_{us}=218340-42=218298$

[27.37] $E_{\mathcal{A}_s}=345705-21=345684$

The magnetic correction is derived in Theorem 31. The geometric packet calculation in Theorem 28 uses zero-alpha energy; therefore, the magnetic correction is not introduced at that stage.

Theorem 28: Packaging and Generation Classification of Charged Particles (Fermions and Leptons) and Uncharged Particles (Neutrinos)

1. Formation of the Central Cavity

In the Ramionics model, the conversion of energy into matter begins with the release of energy from ramions and the collapse of layers of the FCC lattice.

During this process, a central cavity forms. The surrounding layers resist further collapse until a retaining layer stops it.

Because of geometric symmetry, the cavity is regarded as approximately spherical. Its energy deficit relative to the original lattice can conventionally be represented by a corresponding negative energy.

External energy and lattice disturbances can initiate the collapse.

2. Cumulative FCC Geometry

The kissing number of the three-dimensional FCC lattice:

[28.1] $k_3=12$

Number of ramions in layer n:

[28.2] $L_0=1$

[28.3] $L_n=10n^2+2$

Cumulative number of ramions through layer n:

[28.4] $T_n=1+\sum_{k=1}^{n}L_k$

[28.5] $T_n=(10n^3+15n^2+11n)/3+1$

n	L_n	T_n
0	1	1
1	12	13
3	92	147
7	492	1415
15	2252	12431
31	9612	104223
63	39692	853567
127	161292	6909055
255	650252	55597311
511	2611212	446083583
1023	10465292	3573900287

3. The Largest–Most-Similar Rule and Three Numerical Stability Criteria

3.1. The Largest–Most-Similar Rule

According to the largest–most-similar rule, the particles of a packet—that is, the energy-distribution functions surrounding a shared black hole—must be the largest and most similar particles possible.

This rule is associated with a tendency toward greater symmetry and a more balanced energy distribution, and applies to fermionic and neutrino packets.

3.2. First Criterion: High Factorization of the Retaining-Layer Number

The retaining-layer number is denoted by S.

The retaining layer should have as many suitable factors as possible, so that the linear and rotational energies, forces, and torques acting on the shared black hole are distributed more evenly.

In a binary growth structure, powers of 2 are preferred for the retaining-layer number.

3.3. Second Criterion: Low Factorization of the Number of Packet Particles

The number of particles in the packet is denoted by P.

According to the largest–most-similar rule, P should have as few factors as possible and preferably be prime.

If P is composite, the particles can be divided into equal groups and recombined to form larger particles.

A prime number does not permit such a nontrivial equal partition and is therefore preferred for packet stability.

3.4. Third Criterion: Preference for Base 2 in S and P

Base 2 is preferred for three reasons.

First, binary growth is the simplest path for successive particle combinations.

Second, a 2×2×2 arrangement along the three spatial axes provides suitable symmetry for distributing forces and torques.

Third, doubling the linear size quadruples the surface area and increases the volume eightfold. This feature is consistent with binary, quaternary, and octonary growth of the structure.

Simultaneous combination of more particles requires greater coordination and orientation; hence binary combination is the model's preferred path.

3.5. Consequence of the Three Criteria

[28.6] $S=2^{s}$

[28.7] $S-1=2^{s}-1$

[28.8] $P=2^{p}-1$

The three structural preferences—high factorization of the retaining layer, low factorization of particle number, and base-2 growth—are imposed simultaneously, yielding $S=2^{s}$ and $P=2^{p}-1$. Once these three preferences are met, **positive residual energy is a mandatory condition for acceptance**. Among accepted candidates, the sole comparison and ranking criterion is **the smallest percentage of residual energy relative to the total energy released through the last collapsed layer S−1**; the ratio to the energy of the stopping layer is not a ranking criterion.

[28.9] $R_{res}=100(T_{(}S-1_{)}-\mathbb{E}_{/\!/(S)})/T_{(}S-1_{)}$, $T_{(}S-1_{)}-\mathbb{E}_{/\!/(S)}>0$

Under this convention, S is the retaining-layer number, S−1 is the last collapsed-layer number, and P is the number of particles in the packet.

The packet particle counts belong to the family of Mersenne numbers, with Mersenne primes receiving greater preference.

The three criteria above are numerical rules for selecting packets. Energy balance and the conditions of packet formation constitute independent, supplementary examinations.

4. Definition of the Generation Number

The generation number is defined by the code S//P.

By expressing S and P as powers of 2, the generation code is written in the compact form s/p.

This symbol is a generation code, not mathematical division.

For example, generation 7/5 denotes a retaining-layer index of 7 and a particle-count index of 5.

[28.10] $S=2^7=128$

[28.11] $P=2^5-1=31$

The last collapsed layer is 127.

5. The Mersenne Barrier and Growth Factors

During ordinary growth, an increase of one unit in s is accompanied by an increase of one unit in p.

When the expected number of particles becomes composite, they may combine into larger groups. This obstacle is called the Mersenne barrier.

For example:

[28.12] $2^4-1=15=3\times5$

In a Mersenne retreat, s increases while p remains constant.

The genetic-code factors are:

4^0: The initial factor, with numerical value one.

4: Ordinary growth, increasing both s and p by one unit.

6: Mersenne retreat associated with the factor 3; s increases while p remains constant.

8: Mersenne leap; s increases while p remains constant.

2_e: The electrical factor of a charged packet.

2_r: The residual-energy factor, incorporated into the code according to energy capacity.

The electrical and residual factors are independent and are not included in the counting of s and p.

6. General Structure of the Genetic Code

If the numbers of factors 4, 6, and 8 are n_4, n_6, and n_8, respectively:

[28.13] $p=n_4$

[28.14] $s=n_4+n_6+n_8$

[28.15] $n_6+n_8=s-p$

The genetic code is written as a product of growth factors, and their order also indicates the chronological growth sequence.

A charged packet contains one factor 2_e. A neutrino packet does not contain this factor.

The factor 2_r is independent of the electrical factor.

7. Narion and Packet Charging

A narion is the initial neutral fermion and the common structure of family members before electric charge is specified.

Upon charging, family members become charged leptons, up quarks, down quarks, and their corresponding antiparticles.

Charging changes the ratio of the rest energy of the charged packet to that of the neutral packet.

For generation 7/5, this ratio is exactly one-half.

8. Genetic Code of Generation 7/5

The growth path of the electron family contains five factors of 4 and two factors of 6.

Genetic code:

[28.16] $\mathring{N}_e=4^0.4.4.6.6.4.4.2_e.2_r$

[28.17] $\mathring{N}_e=36864$

Numbers of growth factors:

[28.18] $n_4=5$, $n_6=2$, $n_8=0$

[28.19] $s=7$, $p=5$

This code identifies generation 7/5 of the electron family.

9. Seven-Stage Growth Path

Generation	s	p	Stopper	Particles	Genetic N	Packet energy	Released energy	Residual
1/1	1	1	2	1	1	12	13	1
2/2	2	2	4	3	4	144	147	3
3/3	3	3	8	7	16	1344	1415	71
4/3	4	3	16	7	96	8064	12431	4367
5/3	5	3	32	7	2304	96768	104223	7455
6/4	6	4	64	15	9216	829440	853567	24127
7/5	7	5	128	31	36864	6856704	6909055	52351

This table shows the stage-by-stage path before geometric projection and quantization.

Two Mersenne retreats occur in generations 4/3 and 5/3.

10. Fermionic Composition of Generation 7/5

The electron-family packet contains 31 fermions.

Particle-count condition:

[28.20] $N_u+N_{\not d}+N_e=31$

Electric-charge neutrality condition:

[28.21] $2N_u-N_{\not d}-3N_e=0$

Selected composition:

[28.22] $N_u=15$, $N_{\not d}=9$, $N_e=7$

To determine the final composition, the condition for forming three-quark hadrons is also imposed. Because the down quark, with charge $-⅓$, has greater rest energy than the up quark, with charge

+⅔, in this model, a neutron containing two down quarks is heavier than a proton containing one down quark. Among the integer, nonnegative, electrically neutral packet compositions, the smallest deviation from symmetry of the protonic composition is obtained with **one neutron**; a zero-neutron state is incompatible with the integer particle-count constraints for a 31-fermion packet. Thus the selected composition is 7 protons, 1 neutron, and 7 electrons. This selection is made at the fermionic-composition level; calculation of the hadronic-stage layering is not addressed in this theorem.

[28.23] $15u+9d+7e \rightarrow 7p+1n+7e$

This composition contains fifteen up quarks, nine down quarks, and seven electrons.

In the hadronic structure, the corresponding composition is seven protons, one neutron, and seven electrons.

11. Energy of Charged and Neutral Packets

Using the zero-alpha energies of Theorem 27:

[28.24] $\mathbb{E}_{\not{f}_s}=15(6N)+9(19N/2)+7(3N/2)$

[28.25] $\mathbb{E}_{\not{f}_s}=186N$

Energy of thirty-one neutral narions:

[28.26] $\mathbb{E}_{0p}=31(12N)=372N$

Energy ratio:

[28.27] $\mathbb{E}_{\not{f}_s}/\mathbb{E}_{0p}=1/2$

Thus the zero-alpha energy of the charged packet of generation 7/5 is half that of the corresponding neutral packet.

12. Inverse Cumulative Layer Function

For an input value Q, IT determines the first layer whose cumulative capacity is at least Q.

[28.28] $IT(Q)=\min\{n\in\mathbb{N}:T_n\geq Q\}$

Cumulative capacity of the resulting layer:

[28.29] $TIT(Q)=T_{(IT(Q))}$

Excess amount:

[28.30] $EIT(Q)=TIT(Q)-Q$

Percentage excess relative to the total T of the resulting layer:

[28.31] $EITP(Q)=100EIT(Q)/TIT(Q)$

Every IT report records the layer number, capacity T, excess amount, and percentage excess relative to T.

13. Derivation of the Geometric Factor $\pi^2/10$

Rotational moment of inertia of the common twelve-ball structure:

Before separation, twelve balls participate in a shared black hole. In the effective rotational-distribution model, each ball contributes $\frac{1}{2}mr^2$; therefore the inertia of the common structure is 12 times the contribution of each ball. After separation, the inertia of the fermion, with mass distributed uniformly over the surfaces of twelve balls and their geometry, acquires the coefficient 10/3 relative to mr^2. At the same time, the conversion coefficient from the characteristic internal speed to the geometric FCC speed is φ. In conservation of rotational energy, the inertia ratio is

multiplied by the square of the speed ratio; hence the transfer coefficient ζ is obtained. This explanation is the same mechanical derivation found in the article's archival sections.

[28.32] $I_c=6mr^2$

Moment of inertia of the fermion after separation:

[28.33] $I_{\not f}=(10/3)mr^2$

FCC geometric coefficient:

[28.34] $\varphi=\pi/(3\sqrt{2})$

From the ratio of moments of inertia and geometric conversion:

[28.35] $\zeta=(6/(10/3))\varphi^2$

[28.36] $\zeta=\pi^2/10$

; $\zeta=(12(1/2)/(10/3))(\pi/(3\sqrt{2}))^2=\pi^2/10$

This factor is the geometric projection of the initial genetic code onto the electron-family metric.

14. Metric Projection and Quantization

The function $Ceil_n$ returns the first multiple of n greater than the input, $Floor_n$ returns the first multiple of n less than the input, and $Round_n$ returns the nearest multiple of n; an input already exactly divisible by n remains unchanged.

The metric N counts the E_s ramions on each ball of the twelve-ball structure, and the complete structural energy of the assembly is 12N. The continuous value resulting from projection, before quantization, is:

[28.37] $\acute{N}=(\pi^2/10)\mathring{N}$

[28.38] $N=Quant_n(\acute{N})$

[28.39] $\mathring{N}=36864$, $\acute{N}\approx 36383.3096641758$

In FCC geometry, the dominant term in the population of distant layers is $10n^2$. Therefore base 10 is selected for balancing the distribution of forces and torques and stabilizing linear and rotational contributions. If each ball independently distributes energy among the 12 neighbors in the first layer, the least common multiple of 10 and 12 is 60. If the entanglement of opposite balls is included, six independent axes remain, and the least common multiple of 10 and 6 is 30; geometrically, each ball sees half of the directional universe.

[28.40] LCM(10,12)=60

[28.41] LCM(10,6)=30

If the metric oscillates between two consecutive multiples of 60, their average is:

[28.42] $(Floor_{60}(\acute{N})+Ceil_{60}(\acute{N}))/2=30+Floor_{60}(\acute{N})$

Among Round, Floor, and Ceil with bases 1, 10, 30, and 60, the five selected functions that yield the metric 36390 for the electron family are:

[28.43] $Quant_n(\acute{N})\in\{Ceil_{10}(\acute{N}),Ceil_{30}(\acute{N}),Round_{30}(\acute{N}),30+Floor_{60}(\acute{N}),30+Round_{60}(\acute{N})\}$

Other choices within this base set produce metrics of 36383, 36384, 36380, 36360, or 36420. According to the geometric α calculations in Theorem 30, changing N by one unit near 36390 produces a difference of approximately 5σ in α; all five selected functions yield N=36390 for the electron, and the reported discrepancy between the model and the experimental value is approximately 1.5σ. In this version, **$Ceil_{30}$** is chosen as the reference function for generation

calculations, based on calculations of the muon and tau gyromagnetic factors. The other four functions are retained for sensitivity testing and candidate examination.

[28.44] $N=Ceil_{30}((\pi^2/10)36864)=36390$

15. Three Energy Calculations for Generation 7/5

Energy released through the last collapsed layer:

[28.45] $T_{127}=6909055$

First Model: Initial Genetic Code

[28.46] $\mathbb{E}\not{f}_s^{(0)}=186\times36864=6856704$

[28.47] $E_{res}^{(0)}=6909055-6856704=52351$

Second Model: Quantization in Tens

[28.48] $\mathbb{E}\not{f}_s^{(10)}=186\times36390=6768540$

[28.49] $E_{res}^{(10)}=6909055-6768540=140515$

Third Model: Quantization in Thirties

[28.50] $\mathbb{E}\not{f}_s^{(30)}=6768540$

[28.51] $E_{res}^{(30)}=140515$

Model	N	Packet energy	Released energy	Residual	Residual %
Initial	36864	6856704	6909055	52351	0.758%
Ceil10	36390	6768540	6909055	140515	2.034%
Ceil30	36390	6768540	6909055	140515	2.034%

The residual-energy percentage is calculated relative to the total released energy.

16. Neutrino Emission and Metric Difference

Difference between the initial genetic code and the quantized metric:

[28.52] $\Delta\mathring{N}=\mathring{N}-N=474$

Quantization of the neutrino branch:

The neutrino genetic difference is also examined using the same five possible quantization functions. In particular, $Ceil_{10}$ and $Ceil_{30}$ both take the difference 474 to 480; the reference choice $Ceil_{30}$ is retained here as well.

[28.53] $\acute{\nu}=480$

; $\acute{\nu}=Ceil_{30}(474)=Ceil_{10}(474)=480$

Neutrino quantization difference:

[28.54] $\Delta\nu=480-474=6$

Difference between the continuous and quantized values:

[28.55] $\Delta\acute{N}=N-\acute{N}\approx6.690335824$

[28.56] $\Delta N=7$

Metric ratio accounting for the neutrino branch:

[28.57] $N/(N+\acute{\nu})=36390/36870$

This difference is associated with the energy released when the particles separate from their shared black hole.

Other Neutrino and Fermion Generations; Examination of Generation 5/3

Scope of Examination of Other Generations

This section extends the geometric and genetic rules of this theorem to other generations.

The generation number is defined using the convention S//P and, in the Mersenne case, is written as the code s/p.

Codes such as 5/3 and 7/5 are generation numbers, not mathematical divisions.

For each candidate, the genetic code, number of particles, packet energy, released energy, and residual energy are examined.

Range of Mersenne Numbers

[28.58] $S=2^s$

[28.59] $P=2^p-1$

[28.60] $s \geq p$

p	P	Number type	Generation range
3	7	Prime	3/3 to 10/3
5	31	Prime	5/5 to 10/5
7	127	Prime	7/7 to 10/7

Generation 7/5 of the electron family was calculated earlier in this theorem and serves as the basis for comparison with other generations.

Candidates are selected according to the largest–most-similar rule and the three structural criteria of this theorem. Positive residual energy is a condition of acceptance, and the smallest residual percentage relative to the energy released through $S-1$ is the sole ranking criterion.

Initial Neutrino Stages

At the initial stages, the neutral and charged paths share a common structure.

The initial neutrino v_1 has zero net charge.

At the first stage, the twelve-ball structure v_{12} is formed.

At the second stage:

[28.61] $3\times48=144$

[28.62] $147-144=3$

Three v_{48} neutrinos form.

At the third stage:

[28.63] $7\times192=1344$

[28.64] $1415-1344=71$

Seven v_{192} neutrinos form.

Decomposition of the residual energy:

[28.65] $71=5\times12+11$

The neutrino packet has no electrical factor 2_e. The residual factor 2_r may be present in the neutral path according to energy capacity.

General Composition of a Charged Packet

For a packet containing P fermions:

[28.66] $N_u+N_{\alpha}+N_e=P$

Electric-charge neutrality condition:

[28.67] $2N_u-N_{\alpha}-3N_e=0$

For the selected composition with one neutron:

[28.68] $N_u=2^{p-1}-1$

[28.69] $N_{\alpha}=2^{p-2}+1$

[28.70] $N_e=2^{p-2}-1$

p	P	Up quarks	Down quarks	Charged leptons	Protons	Neutrons
3	7	3	3	1	1	1
5	31	15	9	7	7	1
7	127	63	33	31	31	1

Zero-Alpha Packet Energy

Energies of packet constituents:

[28.71] $\mathbb{E}_{es}=3N/2$

[28.72] $\mathbb{E}_{us}=6N$

[28.73] $\mathbb{E}_{\alpha s}=19N/2$

Charged-packet energy:

[28.74] $\mathbb{E}_{fp}=N_u\mathbb{E}_{us}+N_{\alpha}\mathbb{E}_{\alpha s}+N_e\mathbb{E}_{es}$

Substituting the general composition:

[28.75] $\mathbb{E}_{fp}=N(23\times2^{p-2}+2)$

Neutral-packet energy:

[28.76] $\mathbb{E}_{0p}=12N(2^p-1)$

Ratio of charged-packet energy to neutral-packet energy:

[28.77] $f_p=(23\times2^p+8)/(48(2^p-1))$

p	P	Charged / Neutral	Percentage
3	7	4/7	57.143%
5	31	1/2	50.000%
7	127	123/254	48.425%

Three Models for Calculating Energy

Released energy of the packet:

[28.78] $\mathbb{E}_{rel}=T_(2^s-1_)$

First Model: Initial Genetic Code

[28.79] $\mathbb{E}_{\mathscr{f}\mathscr{f}_p}^{(0)}=\mathring{N}(23\times2^{p-2}+2)$

[28.80] $E_{res}^{(0)}=\mathbb{E}_{rel}-\mathbb{E}_{\mathscr{f}\mathscr{f}_p}^{(0)}$

[28.81] $R^{(0)}=100E_{res}^{(0)}/\mathbb{E}_{rel}$

Second Model: Projection and Quantization in Tens

[28.82] $N_{10}=Ceil_{10}(\pi^2\mathring{N}/10)$

[28.83] $\mathbb{E}_{\mathscr{f}\mathscr{f}_p}^{(10)}=N_{10}(23\times2^{p-2}+2)$

[28.84] $E_{res}^{(10)}=\mathbb{E}_{rel}-\mathbb{E}_{\mathscr{f}\mathscr{f}_p}^{(10)}$

[28.85] $R^{(10)}=100E_{res}^{(10)}/\mathbb{E}_{rel}$

Third Model: Projection and Quantization in Thirties

[28.86] $N_{30}=Ceil_{30}(\pi^2\mathring{N}/10)$

[28.87] $\mathbb{E}_{\mathscr{f}\mathscr{f}_p}^{(30)}=N_{30}(23\times2^{p-2}+2)$

[28.88] $E_{res}^{(30)}=\mathbb{E}_{rel}-\mathbb{E}_{\mathscr{f}\mathscr{f}_p}^{(30)}$

[28.89] $R^{(30)}=100E_{res}^{(30)}/\mathbb{E}_{rel}$

In all three models, the residual-energy percentage is calculated relative to the total released energy.

Genetic Codes of the Candidates

Numbers of growth factors:

[28.90] $p=n_4$

[28.91] $s=n_4+n_6+n_8$

[28.92] $n_6+n_8=s-p$

A charged packet has one factor 2_e.

The factor 2_r is determined according to energy capacity and is independent of the electrical factor.

The order of factors in the genetic code specifies the chronological growth path.

Generation 5/3 Candidate and Two Genetic Sequences

For generation 5/3:

[28.93] $s=5$, $p=3$

[28.94] $S=32$, $P=7$

The last collapsed layer is 31.

Candidate genetic code with two Mersenne leaps:

[28.95] $\mathring{N}=4^0.4.4.8.8.2_e=2048$

Geometric conversion:

[28.96] $\acute{N}=(\pi^2/10)2048\approx2021.295$

Quantizations:

[28.97] $N_{10}=2030$

[28.98] $N_{30}=2040$

Released energy:

[28.99] $\mathbb{E}_{rel}=T_{31}=104223$

Packet-energy coefficient:

[28.100] $f_3=4/7$

Initial Model

[28.101] $\mathbb{E}_{3}^{(0)}=48\times2048=98304$

[28.102] $E_{res}^{(0)}=104223-98304=5919$

[28.103] $R^{(0)}\approx5.679\%$

Quantization in Tens

[28.104] $\mathbb{E}_{3}^{(10)}=48\times2030=97440$

[28.105] $E_{res}^{(10)}=104223-97440=6783$

[28.106] $R^{(10)}\approx6.508\%$

Quantization in Thirties

[28.107] $\mathbb{E}_{3}^{(30)}=48\times2040=97920$

[28.108] $E_{res}^{(30)}=104223-97920=6303$

[28.109] $R^{(30)}\approx6.048\%$

Second Genetic Sequence: The Two-Factor-6 Path

Another genetic sequence for the same generation 5/3 is formed from two factors of 6 instead of two factors of 8. This sequence shares its roots with the electron family's growth and Mersenne-retreat path and is examined independently of the two-factor-8 path:

[28.110] $\mathring{N}_{(66)}=4^{0}.4.4.6.6.2_{e}.2_{r}=2304$

[28.111] $\acute{N}_{(66)}=(\pi^2/10)2304\approx2273.955$

[28.112] $N_{10(66)}=Ceil_{10}(\acute{N}_{(66)})=2280$

[28.113] $N_{30(66)}=Ceil_{30}(\acute{N}_{(66)})=2280$

Under the packet-energy convention of 48 metric units for generation 5/3, both paths are calculated using a common criterion. The following table shows the residual relative to the released energy T_{31}. A negative residual means that the mandatory positive-energy condition is not met in that model; it does not mean that the genetic sequence is invalid as a growth path.

Genetic path	Quantization	N	Packet energy	Released energy	Residual	Residual percent	Positive energy
8,8	Initial	2048	98304	104223	5919	5.679%	Yes
8,8	Ceil10	2030	97440	104223	6783	6.508%	Yes
8,8	Ceil30	2040	97920	104223	6303	6.048%	Yes
6,6	Initial	2304	110592	104223	−6369	−6.111%	No
6,6	Ceil10	2280	109440	104223	−5217	−5.006%	No
6,6	Ceil30	2280	109440	104223	−5217	−5.006%	No

For all other generations, both types of permitted genetic path are also examined. The positive-residual condition is imposed before ranking, and candidates with positive energy are compared by the smallest residual percentage relative to the energy released through S−1.

| Generation | Model | N | Packet energy | Released energy | Residual | Residual % |

|---|---|---:|---:|---:|---:|---:|

| 5/3 | Initial | 2048 | 98304 | 104223 | 5919 | 5.679% |

| 5/3 | Ceil10 | 2030 | 97440 | 104223 | 6783 | 6.508% |

| 5/3 | Ceil30 | 2040 | 97920 | 104223 | 6303 | 6.048% |

In all three models, the released energy is sufficient to form the generation 5/3 candidate.

Theorem 29: Antimatter and Matter–Antimatter Asymmetry

Matter–antimatter asymmetry

In the Standard Model, the actual origin of matter–antimatter asymmetry has not yet been fully explained.

In Ramionics, however, this asymmetry arises from the polarization and overall orientation of the field of the universe.

If the entire universe is a vast Ramionic structure, or if each supercluster has a net rotational orientation, the background field acquires a weak polarization.

Consequently, the effective vacuum will not be completely symmetric.

Therefore, the probabilities of matter and antimatter formation will not be exactly equal.

The directions of galactic rotation and particle polarization will likewise exhibit asymmetry.

In this picture:

- baryonic asymmetry,

- left–right asymmetry,

- and the predominance of matter

all arise from the overall rotational polarization of the field.

Theorem 30: Geometric Calculation of Alpha

The metric prerequisite for this calculation is the genetic code of the electron family, derived in Theorem 28. In that calculation, $\mathring{N}$ is 36864; the geometric transformation by the factor $\pi^2/10$, followed by quantization, yields the metric N of 36390. Only the result of that calculation is used here.

The mappings of charge, the Coulomb constant, and alpha in this theorem pertain to the separated particle with its independent metric N, not to the shared black hole of the packet; the distinction between these two stages is explained in Theorem 28.

Mapping of Electric Charge

The relative charges of the electron, up quark, and down quark are -1, $+\frac{2}{3}$, and $-\frac{1}{3}$, respectively; thus a combination of one up quark and two down quarks is electrically neutral. The basis of the family combination and the neutrality condition are given in Theorem 28. In this theorem, charge mapping is performed for the complete twelve-ball structure and must not be equated with the rest energy after subtracting the electric potential. The distinction between structural energy and rest energy is explained in Theorem 31.

The electric charge of a Ramion with energy NE_s:

[30.1] $q_r/q_s=N$

Each particle is represented by 12 balls, and each ball models N Ramions. Therefore, charge conservation gives:

[30.2] $q_e/q_s=12N$

Mapping of the Coulomb Constant

$\mathring{K}$ is the local internal Coulomb constant of a Ramion; K is the external Coulomb constant of the ball-cubic distribution.

From the structural electric energy:

[30.3] $E_r=\{1/\theta_p\}\mathring{K}_r q_r^2/r_r$

Using $E_r/E_s=N$, $q_r/q_s=N$, and $r_r/r_s=N$:

[30.4] $\mathring{K}_r/\mathring{K}_s=1$

; $\mathring{K}\propto N^0$

The potential quantization coefficient η is obtained from the ratio of discrete to continuous potential energy. According to Theorem 26, η^2 equals $1-1/N$; thus η^{-2} is the discrete-potential correction factor in the Coulomb mapping. The derivation and generalization of this coefficient are presented in that theorem.

The external inverse-square interaction has a surface mapping of N^2; the surface coverage of the ball-cubic distribution introduces the factor $\beta/(4\pi)$, while the quantization of the ball potential introduces η^{-2}:

[30.5] $K_e/\mathring{K}_s=\{\theta_k\}N^2\beta/(4\pi\eta^2)$

; $K_e=\{\theta_k\}\mathring{K}_s N^2\beta/(4\pi\eta^2)$

Calculation of the Fine-Structure Constant α

For the reference Ramion:

[30.6] $\alpha_s=\mathring{K}_s q_s^2/(\hbar_s \mathring{c}_s)$

Using the reference structural electric-energy relation together with $E_s r_s=\hbar_s \mathring{c}_s$:

[30.7] $\alpha_s=\{\theta_p\}1$

For a general Ramion, $\mathring{K}_{rs}=1$, $q_{rs}=N$, $\hbar_{rs}=N^4$, and $\mathring{c}_{rs}=N^{-2}$; therefore the Ramionic mapping leaves α invariant:

[30.8] $\alpha_r/\alpha_s=1$

For the electron family:

[30.9] $\alpha_e=K_e q_e^2/(\hbar_e c)$

Substituting the mappings of charge, the Coulomb constant, the reduced Planck constant, and speed, all contributions from N^4, 12^2, and φ cancel:

[30.10] $\alpha_e/\alpha_s=\{\theta_k/(\theta_r\theta_h)\}\beta/(40\pi\eta^2)$

[30.11] $\alpha_e=\{\theta_p\theta_k/(\theta_r\theta_h)\}\beta/(40\pi\eta^2)$

[30.12] $\alpha=\{\theta_p\theta_k/(\theta_r\theta_h)\}\beta/[40\pi(1-1/N)]$

; $\alpha^{-1}=\{\theta_r\theta_h/(\theta_p\theta_k)\}160\sqrt[3]{(\pi/5)}(1-1/N)$; $\alpha^{-1}=137.035999207833$

; $\alpha_x^{-1}=137.035999177$

; $\Delta\alpha=-1.46825075418451\sigma$

; $\alpha=0.00729735256268951$, $\alpha_x=0.00729735256433142$

The N^{∞} limit:

[30.13] $\alpha^{\infty-1}=\{\theta_r\theta_h/(\theta_p\theta_k)\}40\pi/\beta$; $\alpha^{\infty-1}=137.039765071122$

Correction factors for experimental results, or for matching Ramionics geometric calculations to them, based on the difference in α:

[30.14] $\dot{\alpha}_\beta=\sqrt{(\alpha_\beta/\alpha_{ex})}$

; $\dot{\alpha}=\dot{\alpha}_e=\sqrt{(\alpha_e/\alpha_{ex})}=0.999999999887499$

; $\ddot{\alpha}_\beta=\sqrt{(\alpha_\beta/\alpha_e)}=\eta_e/\eta_\beta=\eta_{e\beta}$

; $\ddot{\alpha}_e=1$

The exact value of the Coulomb constant using the exact value of alpha:

[30.15] $K_e=\alpha\hbar c/q_e^2$

; $K_e=8.98755178414663_{(10)}9$

; Mutual $K=K_e(1-1/N_e)/\sqrt{((1-1/N_1)(1-1/N_2))}$

Theorem 31: Calculation of the Gyromagnetic Factor

Mechanical Definition of the Gyromagnetic Factor

Definition of the gyromagnetic factor.

If a mass m carrying charge q rotates along a closed path with period $T = 2\pi/\omega$, the equivalent electric current is:

[31.1] $I = q/T = q.\omega/(2\pi)$

Every rotating charge produces a magnetic dipole. If $\vec{A}$ is the area vector of the loop, its magnetic dipole moment, torque, and potential energy in a magnetic field are:

[31.2] $\vec{\mu} = I.\vec{A}$

[31.3] $\vec{\tau} = \vec{\mu} \times \vec{B}$

[31.4] $U = -\mu\vec{B}$

Each particle of charge q contributes to μ:

[31.5] $d\mu = (dq.\omega/(2\pi)).A = dq.\omega r^2/2$

Electric moment:

[31.6] $\mu = ½.\omega.\int r^2.dq$

Rotational moment of mass:

[31.7] $J = I_m.\omega = \omega.\int r^2.dm$

The ratio of the electric rotational moment to the mass rotational moment, or, briefly, the electric-to-mass ratio, is:

[31.8] $\mu/J = (½.\omega.\int r^2.dq)/(\omega.\int r^2.dm)$

Simplifying the angular velocity:

[31.9] $\mu/J = [½\int r^2.dq]/(\int r^2.dm)$

From the relation between energy and moment:

[31.10] $E = ½I\omega^2$

It follows that g is also the ratio of magnetic energy to mass rotational energy:

[31.11] $g = E_{r-c}/E_{r-m}$

To calculate g, the integrals are normalized in terms of total charge and mass:

[31.12] $\int r^2.dq = q.r_{e\mathscr{ff}-c}{}^2$

[31.13] $\int r^2.dm = m.r_{e\mathscr{ff}-m}{}^2$

[31.14] $g = r_{e\mathscr{ff}-c}{}^2/r_{e\mathscr{ff}-m}{}^2$

[31.15] $\mu/J = g.(q/2)/m$

If the mean-square radius relative to an axis is called the effective radius, the gyromagnetic factor is precisely the ratio of the mean-square effective electric radius to the effective mass radius.

Calculating g thus becomes straightforward. For example, if mass and charge both have uniform volume density, both have uniform surface density, or even merely have similar distributions:

[31.16] $g = 1$

Therefore, for homogeneous bodies whose mass and charge originate in their molecules, g equals 1.

Suppose a spherical body has uniform mass volume density and uniform charge surface density. From the rotational moment of mass in the volume case:

[31.17] $I_m = ⅖mr^2$

and in the surface case:

[31.18] $I_c = ⅔mr^2$

the result is:

[31.19] $r_{e\mathscr{ff}-m}{}^2 = ⅖r^2$

[31.20] $r_{e\mathscr{ff}-c}{}^2 = ⅔r^2$

[31.21] $g = (⅔)/(⅖) = 1.666$

However, for the electron, g is even greater: it is 2 in the simple Dirac approximation, and slightly greater still in more precise measurements.

In the relations above, the geometric definition of the gyromagnetic factor is expressed in terms of the ratio of moments of charge and mass distributions. This definition differs from, and does not replace, the newer computational models and corrections presented in this theorem.

The 12+9 Potential Model in Zero-Alpha Mode (Zero α)

Notation: Parameters such as energy, potential, mass, and the gyromagnetic factor are represented by double-struck characters in the zero-alpha approximation.

The precise value of each parameter, including alpha, is calculated on the basis of that parameter's zero-alpha value.

Particle-charge index c: The values 3, 2, 1, and 0 correspond respectively to particles with charges ±3/3, ±⅔, ±⅓, and neutral particles, such as the electron, up quark, down quark, and narions.

In the neutral state, the potential reference surface consists of 24(N/2) half-balls, including equal numbers of positive and negative half-balls; consequently, the net surface charge is zero. To create a particle of type c, c axes are reversed, and the resulting charge is placed on this same reference surface.

The linear contribution comes from placing charge on the reference surface. For the electron, with c=3, this contribution equals 12(N/2). Thus, the contribution of each axis is 4(N/2), and for c axes the resulting relation is:

[31.22] $\mathbb{U}_l=4c(N/2)$, OldName: $\mathbb{m}_{12}$

The quadratic contribution arises from the mutual potential of the additional charges created by reversal of the axes. Each axis adds 2 half-balls; thus c axes create 2c half-balls, equivalent to c complete balls of effective charge. Since electric potential energy is proportional to the product of charges:

[31.23] $\mathbb{U}_p=c^2(N/2)$, OldName: $\mathbb{m}_9$

Therefore, the total potential in the zero-alpha model is:

[31.24] $\mathbb{U}_{cs}=\mathbb{U}_l+\mathbb{U}_p=(4c+c^2)(N/2)=c(4+c)(N/2)$

For the electron, c=3:

; $\mathbb{U}_{es}=(12+9)(N/2)=21N/2$

Thus, 12 is the linear contribution of placing charge on the reference surface, while 9 is the quadratic contribution of the interaction of the additional charges with one another. Without changing the argument, c=2 and c=1 also produce the structures 8+4 and 4+1.

For the electron, this model introduces two potential contributions, or channels, of 4/7 for the linear part and 3/7 for the quadratic part into the precise formulas.

; c=0: Neutral state: the narion of the electron, muon, and tau families

; $\mathbb{U}_l=0$, $\mathbb{U}_p=0$, $\mathbb{U}_{0s}=0$, $\mathbb{E}_{0s}=12N$

; c=3: Electron, muon, tau:

; $\mathbb{U}_l=12N/2=6N$, $\mathbb{U}_p=9N/2$

; $\mathbb{U}_{3s}=21N/2$, $\mathbb{E}_{3s}=3N/2=\mathbb{E}_{0s}/8$

; c=2: Up, charm, top:

; $\mathbb{U}_p=(4/9)(9N/2)=2N$

; $\mathbb{U}_l=(⅔)(12N/2)=4N$

; $\mathbb{U}_{2s}=6N$, $\mathbb{E}_{2s}=6N=4\mathbb{E}_{3s}=\mathbb{E}_{0s}/2$

; c=1: Down, strange, bottom:

; $\mathbb{U}_p=(1/9)(9N/2)=N/2$

; $\mathbb{U}_l=(⅓)(12N/2)=2N$

; $\mathbb{U}_{1s}=5N/2$, $\mathbb{E}_{1s}=19N/2=(19/3)\mathbb{E}_{3s}=\mathbb{E}_{0s}(19/24)$

Relative-energy notation:

; $\mathbb{E}_{es}=\mathbb{E}_e/\mathbb{E}_s$

; $\mathbb{E}_{es}=\mathbb{E}_{3s}=\mathbb{E}_{0s}/\mathbb{E}_{03}$

; $\mathbb{E}_{23}=12/3$, $\mathbb{E}_{13}=19/3$, $\mathbb{E}_{31}=3/19$

; $\mathbb{U}_{23}=12/21$, $\mathbb{U}_{13}=5/21$

The 12+9 Potential Model Including Alpha

[31.25] $d_e=\text{Floor}((3N/2)(\alpha/6)(1-3\alpha/(4/7)))$

; $d_e=63 = 9\ (4+3)=36 + 27$

; $E_{es} = 3N/2 - (36 +27)= 54522$

; $E_{us}=12N/2-d_u=12N/2-42$

; $E_{us}=218298$

; $E_{\mathscr{d}_s}=19N/2-d_{\mathscr{d}}=19N/2-21$

; $E_{\mathscr{d}_s}=345684$

; EDU = $E_{\mathscr{d}_s}-E_{us}$ = 127386

Gyromagnetic Factor g_e

Zero-Alpha Approximation: Origin of Electric Inertia as Negative Mass

Members of an electric family, including the electron and the corresponding up and down quarks, are assumed to share the same fundamental ball structure, the same radius, and the same metric N. This identity is necessary so that differences in electric charge do not result from differences in the particles' fundamental structures, but instead from different orientations of the balls within a common structure. Under these circumstances, electric neutralization in the neutron structure can genuinely correspond to the combination of the electric effects of the proton and electron.

The total energy of each of these particles in the neutral state equals the structural energy 12N. This total energy is distributed through space and is the origin of the particle's modification of the spacetime metric. Consequently, the electric potential associated with ball orientation, $\mathbb{U}$, is not subtracted from this total distributed energy; differences in the rest masses of family members do not imply differences in N, radius, or their total structural energy.

The electric potential $\mathbb{U}$ arises from alignment of the ball's ramions with the central charge. Alignment increases the indentation of the ramions, thereby increasing their shared volume. Increased shared volume is accompanied by a reduction in ramion pressure, and the energy released by this process supplies the electric potential associated with ball orientation.

This behavior is consistent with a ramion's response to changes in energy. When a ramion must carry energy greater than $\mathbb{E}_s$, it creates an expansion of spacetime to carry that additional energy. Conversely, reduced energy or pressure does not mean a reduction of the same previously created metric; the ramion responds by increasing indentation and shared volume. Thus, the potential energy associated with ball orientation is supplied without reducing the total energy 12N distributed in space.

From the perspective of inertia, $\mathbb{U}$ acts like a negative mass contribution. Rather than reducing the particle's total structural energy, it reduces its effective rest energy and inertia. Consequently, in calculating $\mathbb{g}$, this contribution appears with a negative sign in the denominator of g.

The dsk, or Double Stroke, notation identifies the baseline parameters under the zero-alpha assumption. These are baseline values around which Taylor expansions or more precise approximations can be constructed. Therefore, zero alpha does not mean discarding higher-order dependencies; rather, it specifies the baseline and reference point for expansions and calculations.

Zero-Alpha Approximation for $\mathbb{g}_e$

[31.26] $\mathbb{g}_e=IhwCosD/(\mathbb{E}_{03}.Iws-(\mathbb{E}_{03}-1).IhwCosD)$

The coefficient $\mathbb{E}_{0c}$ determines the electric-orientation potential and hence the associated negative-inertia contribution for the electric state of a family member:

[31.27] $\mathbb{E}_{0c}=24/(24-9(c/3)^2-12(c/3))$

Equivalently:

; $\mathbb{E}_{0c}=1/[1-(9/24)(c/3)^2-(1/2)(c/3)]$

For c=3, the negative electric-inertia contribution reduces the denominator, yielding the Dirac value for leptons in the zero-alpha approximation:

; c=3, $\mathbb{g}_e$=2

Therefore, $\mathbb{g}_e$=2 results from the balance between positive structural inertia and negative inertia arising from the electric potential associated with ball orientation.

In the absence of alpha, the electric potential resulting from the arrangement of electric charges on the ball surface creates an electric-inertia contribution. In terms of its effect on rotational motion, this inertia behaves equivalently to negative mass: rather than increasing effective inertia, it reduces it. This contribution enters with the same inertia coefficient associated with the distribution of electric charge on the ball surface and therefore increases g by reducing the denominator.

Precise Calculation of g Including Alpha

With the introduction of alpha, another mechanism is added to this negative inertia. The rotating electric field generates a magnetic field, and the resulting magnetic field feeds back into the system. In the model, the effect of this feedback appears as an additional reduction in effective inertia, with its magnitude specified by d.

End of Volume 14, Part 1. Theorem 31 continues in the next volume; no part of the remaining theorem is represented as translated here.

This second contribution is called “magnetic inertia” or “alpha inertia.”

Consequently, Model A distinguishes two sources of an increase in g: first, the negative electric inertia that exists even in the absence of alpha; second, the alpha-dependent negative magnetic inertia introduced through d. Both increase g by reducing effective inertia.

In the simplest formula for calculating d without the effect of alpha:

[31.28]) $g=(3N/2-d)/(3N/4-d)$

; g: 2.0023136671624524

; g_{ex}=2.00231930436092

Correction factor for the alpha error of each particle relative to experimental alpha:

[31.29] $\dot{\alpha}_\beta=\sqrt{(\alpha_\beta/\alpha_{ex})}$

Coefficient of the alpha metric effect in calculating g:

; $\ddot{\alpha}_\beta=\sqrt{(\alpha_\beta/\alpha_e)}=\eta_e/\eta_\beta=\eta_{e\beta}$, $\ddot{\alpha}_e=1$

; $\ddot{\alpha}_\beta^{2\acute{k}}\approx(1-\acute{k}/N_e)/(1-\acute{k}/N)$

Second form of the alpha feedback effect coefficient:

; $F=(1-\alpha/\acute{k})/(1-\alpha_e/\acute{k})$

Magnetic Negative Mass in the Main Model

[31.30] $d=mRound_2(\acute{d}), \acute{d}=(cN/2)\alpha/(6(1-\alpha/6))(1-M\alpha(1+c/4)^2/(4/5)^0)$, M=3 or c

The $mRound_2$ function rounds $\acute{d}$ so that the rest mass, $12N-c(4+c)N/2-d$, is rounded to the nearest even integer.

$4/5=\sqrt{((4/7)^2/((4/7)^2+(3/7)^2))}$

$(4/5)^0=1$

In some models, setting M to 3 gives d_u=42, whereas setting M to c may give d_u=43. However, the proton-energy calculations support the value 42; in the main model, regardless of M:

$\therefore d_{\mathscr{A}}$=21, d_u=42, N_e=36390,d_e=63, N_m=517470, d_m=881, N_t=2069790, d_t=3527

Main Formula — Single-Channel Model

[31.31] $g=\ddot{\alpha}_\beta^{-2}(3N/2-d)/(3N/4-d\{1+(\alpha/6)(1+2d/(7N(1-\alpha/6)))\})$, $N=30+\text{Floor}_{60}(\mathring{N})$, $N_e=36390, d_e=63$, $\alpha_e^{-1}=137.03599920783327$, $g_e=2.0023193043609084$, $\Delta g_e=-0.03\sigma=-5.79\text{ppq}$, $N_m=517470, d_m=881$, $\alpha_m^{-1}=137.03950024462935$, $g_m=2.0023318815920352$, $\Delta g_m=+49.22\sigma=+20.16\text{ppb}$, $N_t=2069790, d_t=3554$, $\alpha_t^{-1}=137.03969886161988$, $g_t=2.0023543449998216$, $\Delta g_t=-0.75\sigma=-37.46\text{ppb}$

Anomaly Correction Based on Rest-Mass Quantization in the Main Model

$\dot{g}=2+F(\ddot{\alpha}_\beta^{-2}.g-2)$

$g=(3N/2-d)/(3N/4-d.R)$

$F=(1-1/(3N_e/2))/(1-1/(3N/2))$

$d_m=881$, $d_t=3527$

$\dot{g}_e=2.002319304360908$

$\dot{g}_m=2.002331841876002$

$\dot{g}_t=2.002336787150003$

$\Delta\dot{g}_e=-0.032\sigma$

$\Delta\dot{g}_m=+0.788\sigma$

$\Delta\dot{g}_t=-176.328\sigma$

Finalizing Main model by $N=\text{Ceil}_{30}(\mathring{N})$:

$N_t=2069820$, $d_t=3528$, $\Delta\dot{g}_t=-169.75\sigma$

Other Models:

Main Model with Internal Exponent 2 Instead of 1

[31.32] $g=\ddot{\alpha}_\beta^{-2}(3N/2-d)/(3N/4-d\{1+(\alpha/6)(1+2d/(7N(1-\alpha/6))/2)^2\})$, $N=30+\text{Floor}_{60}(\mathring{N})$, $N_e=36390, d_e=63$, $\alpha_e^{-1}=137.03599920783327$, $g_e=2.002319304361254$, $\Delta g_e=+0.93\sigma=+166.81\text{ppq}$, $N_m=517470, d_m=881$, $\alpha_m^{-1}=137.03950024462935$, $g_m=2.0023318815923634$, $\Delta g_m=+49.22\sigma=+20.16\text{ppb}$, $N_t=2069790, d_t=3554$, $\alpha_t^{-1}=137.03969886161988$, $g_t=2.0023543450001586$, $\Delta g_t=-0.75\sigma=-37.46\text{ppb}$

Main Model with Internal Exponent ½ Instead of 1

[31.33] $g=\ddot{\alpha}_\beta^{-2}(3N/2-d)/(3N/4-d\{1+(\alpha/6)(1+2d/(7N(1-\alpha/6))/½)^{1/2}\})$, $N=30+\text{Floor}_{60}(\mathring{N})$, $N_e=36390, d_e=63$, $\alpha_e^{-1}=137.03599920783327$, $g_e=2.002319304360218$, $\Delta g_e=-1.95\sigma=-350.59\text{ppq}$, $N_m=517470, d_m=881$, $\alpha_m^{-1}=137.03950024462935$, $g_m=2.0023318815913784$, $\Delta g_m=+49.22\sigma=+20.16\text{ppb}$, $N_t=2069790, d_t=3554$, $\alpha_t^{-1}=137.03969886161988$, $g_t=2.002354344999148$, $\Delta g_t=-0.75\sigma=-37.46\text{ppb}$

Main Model Without the External $\ddot{\alpha}_\beta^{-2}$ Correction

[31.34] $g=(3N/2-d)/(3N/4-d\{1+(\alpha/6)(1+2d/(7N(1-\alpha/6)))\})$, $N=30+\text{Floor}_{60}(\mathring{N})$, $N_e=36390, d_e=63$, $\alpha_e^{-1}=137.03599920783327$, $g_e=2.0023193043609084$, $\Delta g_e=-0.03\sigma=-5.79\text{ppq}$, $N_m=517470, d_m=901$, $\alpha_m^{-1}=137.03950024462935$, $g_m=2.002332623275362$, $\Delta g_m=+953.71\sigma=+390.57\text{ppb}$, $N_t=2069790, d_t=3637$, $\alpha_t^{-1}=137.03969886161988$, $g_t=2.0023541347596665$, $\Delta g_t=-2.85\sigma=-142.45\text{ppb}$

Two-Channel Model with Reflection $\sqrt{((4d/7-3d/7)/9)}$

[31.35] $g=\dot{\alpha}_\beta(3N/2-d)/(3N/4-d(4/7\{1+(\alpha/6)((4d/7-3d/7)/9)^{1/2}(1+4d/(7N)/½)^{1/2}\}/½)^{1/2}+3/7\{1+(\alpha/6)(1+3d/(7N))\}))$, $N=\text{Round}_{30}(\mathring{N})$, $N_e=36390, d_e=63$, $\alpha_e^{-1}=137.03599920783327$, $g_e=2.0023193043610674$, $\Delta g_e=+0.41\sigma=+73.61\text{ppq}$, $N_m=517440, d_m=907$, $\alpha_m^{-1}=137.03950022927532$, $g_m=2.002331843914556$,

Δg_m=+3.27σ=+1.34ppb, N_t=2069820,d_t=3646, α_t^{-1}=137.0396988625795, g_t=2.0023544663073767, Δg_t=+0.46σ=+23.13ppb

Two-Channel Model with Reflection ((4d/7−3d/7)/9)

[31.36] g=$\dot{\alpha}_\beta\ddot{\alpha}_\beta^{-2}$(3N/2−d)/(3N/4−d(4/7{1+(α/6)(1+4d/(7N)/½)$^{1/2}$/½}$^{1/2}$+3/7{1+(α/6)((4d/7−3d/7)/9)(1+3d/(7N))})), N=30+Round$_{60}$(N̊), N_e=36390,d_e=63, α_e^{-1}=137.03599920783327, g_e=2.0023193043610674, Δg_e=+0.41σ=+73.61ppq, N_m=517470,d_m=879, α_m^{-1}=137.03950024462935, g_m=2.0023318228593703, Δg_m=−22.40σ=−9.17ppb, N_t=2069850,d_t=3408, α_t^{-1}=137.03969886353914, g_t=2.0023545521223247, Δg_t=+1.32σ=+65.98ppb

Details:

The 12-Ball Potential with a Cosine Distribution of Electric Charge

In the 12-ball model, the structure consists of 12 equal spheres of radius r whose centers lie on a sphere of radius 2r. Each sphere is tangent to its adjacent spheres. Each sphere represents a ball, or wing.

Electric charge is distributed over the surface of each wing according to a cosine function, such that the inner hemisphere carries negative charge and the outer hemisphere carries positive charge (or all signs are reversed). Thus each wing has two charge regions: outer charge +Q and inner charge −Q.

Surface Charge Density

For a uniform distribution of charge of one sign, considering the area of the sphere:

; $\sigma = Q/(4\pi r^2)$

For charges ±Q distributed uniformly over each hemisphere, however:

; $\sigma_{(Uniform)} = \sigma_u = \pm Q/(2\pi r^2)$

For a ramion or ball with a cosine distribution:

; $\sigma(\theta) = Q/(2\pi r^2).2\cos(\theta)$

The preceding expression effectively gives a mean value of cos(θ) equal to 1/2. Its coefficient follows by integrating over a hemisphere; for example, the charge on the outer hemisphere:

; $Q_+ = \int \{\varphi = 0 \text{ to } 2\pi\}\{\int \{\theta = 0 \text{ to } \pi/2\}\{\sigma(\theta)dA\}\}$

The surface element on the sphere:

; $dA = r^2\sin(\theta)d\theta d\varphi$

The angle θ=0 corresponds to the north pole of the ramion or ball, the point farthest from the center of the body in this problem; θ=π corresponds to the south pole, the point nearest to the center of the body.

Structural Potential Energy

The exact integral for electrostatic potential energy:

; $U = ½\int\int K.dq_1dq_2/|\vec{r}_1 - \vec{r}_2|$

For a spherical shell with uniform charge Q:

; $U = KQ^2/r$

For ±Q, as a substitute for rotational energy and torque:

; $U_{(\pm Q)} = 2(½)KQ^2/r$

For a spherical shell comprising two hemispheres with charges +Q and −Q:

; $U_{u/} = 8/(3\pi).KQ^2/r \approx 0.848826363156775.KQ^2/r$

; $U_{cos} = 8/9.KQ^2/r \approx 0.888888888888889.KQ^2/r$

With the cosine distribution, charge is more concentrated near the poles; consequently, the mean separation of like charges decreases and the structural repulsive energy increases.

First Approximation: Numerical Calculations

The energy must be calculated directly over the actual surfaces of the 12 spheres.

Surface charge density of each ball:

; $\sigma(\theta) = Q/(\pi r^2).\cos(\theta)$

Charge element:

; $dq = \sigma(\theta)dA$

Surface element:

; $dA = r^2\sin(\theta)d\theta d\varphi$

; $dq = Q/\pi.\cos(\theta)\sin(\theta)d\theta d\varphi$

Now the exact surface energy:

; $U = \frac{1}{2}\Sigma_i\Sigma_j\int\int K.dq_i dq_j/|\vec{r}_i\ r\text{—}\vec{r}_j|$

Second Approximation: Moment Calculations

Moment calculations, which form the basis for defining electric charge and electric force.

Third Approximation: Radial Integral

For every point on a wing surface, let x denote its distance from the center of the entire body. The geometry of the spheres gives:

; $x^2 = 5r^2 + 4r^2\cos(\theta)$

Therefore:

; $\cos(\theta) = (x^2 - 5r^2)/(4r^2)$

Now the differential charge on one wing:

; $dq = \sigma dA$

And since:

; $dA = 2\pi r^2\sin(\theta)d\theta$

The resulting relation is:

; $dq = 2Q\cos(\theta)\sin(\theta)d\theta$

From the geometrical relation:

; $2xdx = -4r^2\sin(\theta)d\theta$

; $\sin(\theta)d\theta = -xdx/(2r^2)$

Substituting into dq:

; $dq = -Qx\cos(\theta)dx/r^2$

And substituting cos(θ):

; $dq = Qx(5r^2 - x^2)dx/(4r^4)$

For 12 wings:

; $dq_{12} = 3Qx(5r^2 - x^2)dx/r^4$

Thus the total cumulative-charge function up to radius x is:

; $Q_{-+}(x) = -\int \{r \text{ to } x\}\{3Qu(5r^2 - u^2)du/r^4\}$

The integral gives:

; $Q_{-+}(x) = 3Q/(4r^4).(x^4 - 10r^2x^2 + 9r^4)$

In normalized form:

; $r = 1$

; $Q = 1$

the result is:

; $Q_{-+}(x) = ¾.(x^4 - 10x^2 + 9)$

This function starts at zero when x=r, then decreases as the negative inner charges accumulate. At:

; $x = \sqrt{5}r$

it reaches its minimum; subsequently, as positive outer charges are added, it increases again until:

; $x = 3r$

it returns to zero.

The derivative of the function:

; $Q'_{-+}(x) = 3Qx(5r^2 - x^2)/r^4$

Hence:

; $Q'_{-+}(\sqrt{5}r) = 0$

The differential energy of the structure is defined as:

; $dU = K.Q_{-+}(x)dQ_{-+}/x$

Therefore:

; $U = \int \{r \text{ to } 3r\}\{K.Q_{-+}(x)dQ_{-+}/x\}$

Substituting $Q_{-+}(x)$ and $dQ_{-+}(x)$, the radial integral yields:

; $U = 20/7.KQ^2/r \approx 2.857142857142857.KQ^2/r$

The above value is the combined potential of the inner and outer half-shells.

Integrating the original cumulative function $Q_{-+}(x)$ over the interval:

; $r \leq x \leq \sqrt{5}r$

The potential energy of the inner half-shells alone:

; $U_{(Inner)} = 6.KQ^2/r$

From the cumulative function without taking the inner shells into account:

; $Q_{+}(x) = 12Q.(1 - (x^2 - 5r^2)^2/(16r^4))$

; $\sqrt{5}r \leq x \leq 3r$

The potential energy of the outer half-shells:

; $U_{(Outer)} = 144/35.KQ^2/r \approx 4.114285714285714.KQ^2/r$

The preceding values sum charges solely according to radial distance x and do not account for the actual angular distribution on the spherical surfaces; therefore, they must be added to 12Ĕ𝓌.

Fourth Approximation: Dipole Approximation

In this model, because the distribution is:

; $\sigma(\theta) \propto \cos(\theta)$

each ball behaves approximately like a dipole.

Dipole moment of each ball:

; $p = 4Qr/3$

Self-energy of each ball from the surface integral:

; $U_{(}Self1_{)} = 8/9.KQ^2/r$

Thus for 12 balls:

; $U_{(}Self12_{)} = 32/3.KQ^2/r$

The interaction energies of the pairs are calculated using the exact dipole formula:

; $U_{ij} = K/d_{ij}^3.[\vec{p}_i.\vec{p}_j - 3(\vec{p}_i.\hat{n}_{ij})(\vec{p}_j.\hat{n}_{ij})]$

For the FCC 12-ball geometry, the sum over 66 pairs is:

; $U_{(}pair_{)} = (20/3 + \sqrt{2} + 22\sqrt{3}/9 + 1/3).KQ^2/r$

; $U_{(}pair_{)} = (7 + \sqrt{2} + 22\sqrt{3}/9).KQ^2/r$

; $U = U_{(}Self12_{)} + (7 + \sqrt{2} + 22\sqrt{3}/9).KQ^2/r$

; $U \approx 20.87708106651860.KQ^2/r$

Fifth Model: Exact Calculation of Charge Discreteness — the 12+9 Model

The previous four approximations remain inaccurate because they neglect charge discreteness and the discreteness of spacetime geometry. This model, which calculates the potential from ramionic geometry, is more accurate.

When the 12 wings are arranged in an FCC structure and six alternating wings are inverted, the surface of the central cavity is a zero-potential surface. To charge the particle fully requires six electric half-wings, equivalent to three wings; because the cavity radius equals the ball radius, nine times the rotational energy of one ball is required:

; $U_9 \approx 9.\check{E}_{\mathscr{w}}$

From another viewpoint, the spherical surface of radius:

; $R_0 = 2R_{\mathscr{w}}$

acts as a zero-potential surface.

Charging this zero-potential surface requires 12 charged hemispheres.

Each wing comprises two charged hemispheres: +Q and −Q.

Thus, relative to a single wing, the number of effective hemispheres is multiplied by six:

; $Q_{e\mathscr{ff}} = 6Q$

And since the potential energy scales as:

; $U \propto KQ^2/R$

the result is:

; $Q_{e\mathscr{ff}}^2 = 36Q^2$

The radius has also doubled; therefore, the energy contribution from wing orientation becomes:

; $U_{18} \approx 36/2\check{E}_{\mathscr{w}}$

However, the preceding value must be halved to include only the half-shells outside the cavity or central black hole of the center of mass:

; $U_9 \approx 9.\check{E}_w$

After obtaining the same result by both methods, the calculation must also account for the baseline energy of the 12 wings needed to neutralize electric charge around the zero-potential surface:

; $U_{12} = 12\check{E}_w$

Thus the total structural energy, for example for an electron e or positron ẽ with charge ±3/3, is:

; $U_3 \approx 12\check{E}_w + 9\check{E}_w$

; $U_3 \approx 21\check{E}_w$

Because the rest energy of the corresponding neutral particle, the Naryon, is 12 times the total energy of one ball, or 24 times its rotational-electric energy ($24\check{E}_w$), the rest energy remaining for a fully charged ±3/3 particle, denoted by index 3, is:

; $E_3 \approx E_0.3/24$

The index 0 denotes the corresponding particle with zero charge, called a Naryon, from “Neutral Baryon,” meaning a fermion in the neutral state. This is a hypothetical or unstable particle used to simplify the calculations.

; $E_{30} = E_3/E_0 \approx 3/24 = 1/8$

; $E_{03} = 1/E_{30} \approx 8$

; $U_{30} = U_3/E_0 \approx 21/24 = 7/8$

According to the preceding explanation, for fractionally charged particles (1/3 and 2/3), U_9 varies quadratically with charge whereas U_{12} varies linearly. Thus for charges ±2/3, such as the up quark u:

; $U_2 \approx 12.(2/3).\check{E}_w + 9.(2/3)^2.\check{E}_w = 12.\check{E}_w$

; $E_{20} = E_2/E_0 \approx 12/24 = 1/2$

; $U_{20} = U_2/E_0 \approx 12/24 = 1/2$

For charges ±1/3, such as the down quark d:

; $U_1 \approx 12.(1/3).\check{E}_w + 9.(1/3)^2.\check{E}_w = 5.\check{E}_w$

; $E_{10} = E_1/E_0 \approx 19/24$

; $U_{10} = U_1/E_0 \approx 5/24$

For the Naryon particle itself:

; $U_0 = 0$; $E_0 = 12.N.E_s$

Since a complete 31-member packet of the electron family, the electron-like particles, forms together:

; Packet = 15up + 9down + 7electron

; $E_(packet) \approx (15.12/24 + 9.19/24 + 7.3/24).E_0$

; $E_(packet) \approx 372/24.E_0 = 31/2.E_0$

Thus charging reduces the energy of each particle packet by approximately half. This is the reason for the electric factor 2 in the electron genetic code: in comparison with $\mathring{N}$, the value is doubled.

; g_e = 2.00231930436256 (+- 3.50E-13)

Ramionics derives g_e from the geometry of 12 balls of radius r around a cavity or black hole of radius r:

; g_e = IhwCosD/(E_{03}.Iws − (E_{03} − 1).IhwCosD)

Electric-charge moment of the 12 balls with a cosine surface distribution:

; IhwCosD = 32/9

Rotational mass moment of the 12 balls with a uniform surface distribution:

; Iws = 10/3

The parameter E_{03} is the ratio of the electron energy in its neutral state before charging, called the Naryon, to its rest energy after charging.

Total mass-moment contribution from the Naryon rest energy:

; $J_{(}naryon_{)} = E_{03}.Iws$

The compensation for the potential required to rotate the balls relative to the neutral state appears as virtual negative energy or mass in the denominator, but with a cosine distribution (associated with electric charge and also appearing in the numerator):

; $J_{(}WingOrientation_{)} = -(E_{03} - 1).IhwCosD$

Stage 0: Dirac Mode

The Ramionics formulas readily reproduce the Dirac approximation of 2 for g_e:

; $E_{03} = 24/(24 - 9 - 12)$

; $E_{03} = 8$

; $g_e = (32/9)/(E_{03} . (10/3) - (E_{03} - 1) . (32/9))$

; $g_e = 2$

; Δg_e = -6.626584E+09σ

Precise calculations based on quantization of spacetime, energy, and potential:

; $R_9 = \eta_{12/9}, \eta_{12/4}, \eta_{12/1}$ for c:3,2,1

; $R_{12} = \eta_{6/1}, \eta_{4/1}, \eta_{2/1}$ for c:3,2,1

; Default Model

; $n_9 = Ceil9(R_9^{-2}((c/3)^2.9(N/2-\Delta N+0.5)-c\Delta\mathring{N}))$

; $n_{12} = Ceil2(R_{12}^{-2}((c/3).12(N/2+\Delta N+1)+c(\Delta\mathring{N}+\Delta N)))$

For the electron (c:3):

; n_9 = 162279

; n_{12} = 219874

; $U_{es} = n_9 + n_{12}$ = 382153

; $E_{es} = 12N - U_{es}$ = 54527

Up quark:

; n_9=71811, n_{12}=146584, E_{us}=218285

Down quark:

; n_9=17721, n_{12}=73292, E_{ds}=345667

; $g_e^{-1} = (12N . 15/16 - R_9n_9 - R_{12}n_{12})/E_{es}$

; $g_e^{-1} = (12N . 15/16 - \eta_{12/9}n_9 - \eta_{6/1}n_{12})/E_{es}$

; g_e = 2.00231930436349

; Δg_e = +2.64423403807866σ 🆗

Theorem 32: Calculation of the Gravitational Constant

From the fundamental Ramion relation:

[32.1] $E_s=G_s\mathring{m}_s^2/r_s$, $E_s=\mathring{m}_s\mathring{c}_s^2$

Therefore:

[32.2] $\mathring{m}_s=E_s/\mathring{c}_s^2$

[32.3] $G_s=r_s\mathring{c}_s^4/E_s=\{\theta_r^{-1}\}r_{s(1)}\mathring{c}_s^4/E_s$

Using $E_sr_s=\hbar_s\mathring{c}_s$:

[32.4] $r_s=\hbar_s\mathring{c}_s/E_s=\{\theta_r^{-1}\}\hbar_{s(1)}\mathring{c}_s/E_s$

Therefore:

[32.5] $G_s=\hbar_s\mathring{c}_s^5/E_s^2=\{\theta_r^{-1}\}\hbar_{s(1)}\mathring{c}_s^5/E_s^2$

Substitution of the Ramionic mappings gives:

[32.6] $G_s=\{1/(\theta_r\theta_h\theta_c^4)\}\hbar_e c^5\varphi^4/[10\times12^2N^4E_s^2]$

[32.7] $G_s=\{\theta_r^{-1}\theta_e^{-2}\}1.34842313721857_{(10)}{}^{22}\ m^3.kg^{-1}.s^{-2}$

Volumetric Gravitational Constant G_{sv}

For a spherical volumetric distribution:

[32.8] $E_s=(6/5)G_{sv}\mathring{m}_s^2/r_s$

Therefore:

[32.9] $G_s=(6/5)G_{sv}$

[32.10] $G_{sv}=(5/6)G_s=\{\theta_r^{-1}\}(5/6)G_{s(1)}$

[32.11] $G_{sv}=\{\theta_r^{-1}\theta_e^{-2}\}1.12368594768214_{(10)}{}^{22}\ m^3.kg^{-1}.s^{-2}$

FCC Geometry for the Gravitational Mapping

The cumulative FCC surface and volume functions are:

[32.12] $\ddot{A}_{(n)}=10n^2+2$

[32.13] $\ddot{V}_{(n)}=(10n^3+15n^2+11n+3)/3$

The physical surface area, radius, and volume are:

[32.14] $A_{\mathscr{e}}=\beta\pi r_r^2\ddot{A}_{\mathscr{e}}$

[32.15] $R=2\gamma r_r\ddot{R}_{\mathscr{e}}$

[32.16] $V_{\beta h}=\varphi(4\pi r_r^3/3)\ddot{V}_{\beta h}$

The geometric identities used in the simplification are:

[32.17] $\beta^2\gamma/\varphi=15/16$

[32.18] $2\beta/3=\varphi\gamma$

The 12N Model

Each ball models N Ramions, whereas the complete central cavity corresponds to 12N:

[32.19] $N=36390$

[32.20] $12N=436680$

For one ball:

[32.21] $\ddot{V}^{-1}{}_{(N)}=21.67846404422435$

The mean surface radius is as follows.

For a population N, the continuous FCC volumetric radius lies between layers 21 and 22. Since the ball's surface does not coincide with the surface of its last complete layer, the surface-bisecting radius between layer 21 and the next layer, namely 21.5, is chosen as the geometric convention for the ball's surface. This choice must not be equated with rounding the continuous volumetric radius to the nearest integer.

[32.22] $\ddot{R}_{\mathscr{m}}=\mathrm{Floor}(\ddot{V}^{-1}(N))+0.5=21.5$

[32.23] $\ddot{A}_{\mathscr{m}}=\ddot{A}_{(21.5)}=4624.5$

For the complete central cavity:

[32.24] $\ddot{V}^{-1}(12N)=50.28575056910184$

The first complete FCC layer that accommodates the entire population 12N is determined as follows.

Unlike the ball's surface, the cavity radius must accommodate the cumulative capacity of all 12N Ramions. Its continuous value lies between layers 50 and 51; consequently, the first complete layer with sufficient capacity is layer 51, and the Ceil operator is applied to the continuous volumetric radius.

[32.25] $\ddot{R}_{\beta h}=\mathrm{Ceil}(\ddot{V}^{-1}(12N))=51$

[32.26] $\ddot{V}_{\beta h}=\ddot{V}_{(51)}=455363$

While the population corresponding to the central cavity before completion of the layer is 12N=436680 Ramions, completing the black-hole radius up to the first complete FCC layer adds the following number:

[32.27] $\Delta\ddot{V}_{\beta h}=\ddot{V}_{(51)}-12N=455363-436680=18683$

This number represents the Ramions added to the surface of the black hole of electron-family particles, or very close to that surface. It does not enter the ball calculations, because its gravity propagates not with G but with G_s; that is, it is of order N^8 stronger and proportionally much shorter-ranged. This itself indicates one of the sources of the short-range strong forces of particles. Furthermore, because of the greater-than-usual expansion of space, it explains how short distances, even when calculating the electric force, correspond to fewer layers and why the electric force is consequently greatly enhanced.

The gravitational mapping is:

[32.28] $G_{12}V_{\beta h}/[(12A_{\mathscr{m}})^2R^2]=\{\theta_{\mathscr{g}}/(\theta_h\theta_c^4)\}\varphi G_{sv}/[2r_r^3\ddot{R}_{\mathscr{m}}^2N^8(1-1/N)]$

Using the spherical-volume relation:

[32.29] $G_{12}/G_s=\{\theta_{\mathscr{g}}/(\theta_h\theta_c^4)\}80\beta A_{\mathscr{m}}^2R/[r_r^2\ddot{R}_{\mathscr{m}}V_{\beta h}N^8(1-1/N)]$

Using the FCC geometric relations:

[32.30] $G_{12}/G_s=\{\theta_{\mathscr{g}}/(\theta_h\theta_c^4)\}\beta(225/2)\pi\ddot{A}_{(21.5)}^2/[\ddot{V}_{(51)}N^8(1-1/N)]$

[32.31] $G_{12}/G_s=4.94986063724705_{(10)}{}^{-33}$

[32.32] $G_{12}=\{\theta_r^{-1}\theta_e^{-2}\}6.67450660927138_{(10)}{}^{-11}\ m^3.kg^{-1}.s^{-2}$

Compared with the experimental value:

[32.33] $G_x=(6.67430\pm0.00015)_{(10)}{}^{-11}\ m^3.kg^{-1}.s^{-2}$

[32.34] $\Delta G_{12}=+1.377\sigma=+30.96$ ppm

In the 12N model, a population N is assigned to each ball and 12N to the complete central cavity. The N model is a different comparative convention in which the population corresponding to the ball is

N/12 and that of the cavity is N. Thus, the difference between the two results does not arise merely from numerical rounding; it arises from selecting two different geometric structures.

The N Model for Comparison with the Main 12N Model

Each ball models N/12 Ramions, and the central cavity models N Ramions:

[32.35] $N_{\ddot{R}}=N/12=3032.5$

[32.36] $\ddot{V}^{-1}(N/12)=9.17759323904235$

[32.37] $\ddot{R}_{\ddot{R}}=9.5$

[32.38] $\ddot{A}_{\ddot{R}}=\ddot{A}_{(9.5)}=904.5$

For the central cavity:

[32.39] $\ddot{V}^{-1}(N)=21.67846404422435$

[32.40] $\ddot{R}_{\beta h}=22$

[32.41] $\ddot{V}_{\beta h}=\ddot{V}_{(22)}=37995$

The mapping is multiplied by the factor 2/β relative to the 12N model.

[32.42] $G_1/G_s=\{\theta_{\ddot{g}}/(\theta_h\theta_c^4)\}160A_{\ddot{R}}^2R/[r_r^2\ddot{R}_{\ddot{R}}V_{\beta h}N^8(1-1/N)]$

[32.43] $G_1/G_s=\{\theta_{\ddot{g}}/(\theta_h\theta_c^4)\}225\pi\ddot{A}_{(9.5)}^2/[\ddot{V}_{(22)}N^8(1-1/N)]$

[32.44] $G_1/G_s=4.94969654682149_{(10)}{}^{-33}$

[32.45] $G_1=\{\theta_r^{-1}\theta_e^{-2}\}6.67428534594496_{(10)}{}^{-11}\ m^3.kg^{-1}.s^{-2}$

[32.46] $\Delta G_1=-0.09769\sigma=-2.196$ ppm

Theorem 33: Calculation of the Hubble Constant

Conventional History of the Acceleration of the Universe's Expansion

In the ΛCDM cosmological model, lambda (Λ) is the mathematical symbol for the cosmological constant in Einstein's equations and today represents dark energy; CDM stands for Cold Dark Matter.

In this cosmological model, the expansion of the universe has had three principal stages:

At the beginning of the universe, there was an extremely rapid phase called cosmic inflation, during which the expansion of the universe had an enormously large positive acceleration.

After inflation ended, as the densities of matter and radiation became dominant, gravity slowed the expansion, and the acceleration of expansion therefore became negative. This period continued for several billion years.

Subsequently, as the density of matter decreased in the expanding universe, the effect of dark energy, or the effective vacuum component, became dominant, and the universe entered another accelerated-expansion phase. The present universe is in this positive-acceleration phase.

Hubble Constant, Hubble Radius, and Radius of the Observable Universe

The Hubble constant indicates the current expansion rate of the universe and expresses the speed v at which galaxies recede from one another for each distance R.

[33.1] $v = H_0R$

The Hubble radius is the distance at which the expansion speed becomes equal to the speed of light:

[33.2] $R_h = c/H_0$

Nearby estimates (based on direct observation of the redshift of the light spectra of nearby stars using the Hubble and James Webb telescopes):

[33.3] $H_0 \approx 73$ km/s/Mpc

; $R_h \approx 13.39$ gly: billion light years

Distant estimates (not through direct observation, but through calculations based on the cosmic microwave background, CMB, using the Planck satellite) estimate H_0 as 67.4. This difference is known as the Hubble tension. From the Ramionics perspective, it results from neglecting the discreteness of the surface of space, namely the coefficient β. Dividing by this geometrical coefficient gives 73.5, within the range of nearby observations:

[33.4] $H_0 = 73.5$ km/s/Mpc

; $R_h \approx 13.30$ gly

However, the radius of the observable universe is greater than the Hubble radius, because the light from galaxies was emitted in the past, when the universe was smaller. In ΛCDM, this radius is estimated at approximately 46.5 gly.

Expansion of the Universe in Ramionics

In Ramionics, the entire universe consists of an approximately constant number of ramions:

[33.5] $N_{\mathscr{w}}$ = constant

The energy of each ramion also remains approximately constant:

[33.6] E_s = constant

This is because only a very small portion of the universe's energy is converted into matter. This conversion itself means that the energy is distributed among other ramions, more strongly among the nearer ones, while leaving behind a cavity or black hole devoid of ramions, energy, space, and time. On small scales this cavity is at the center of particles, and on large scales it corresponds to galactic black holes.

Furthermore, from every point and at every time, the universe is seen as containing a constant number of FCC layers:

[33.7] $L_{\mathscr{w}}$ = constant

At each instant, the entire universe has a uniform ramion radius:

[33.8] $r_s = r_s(t)$

Consequently, the energy density and pressure are uniform throughout the universe.

If the total volume of the universe equals the effective FCC volume:

[33.9] $V_{\mathscr{w}} = (4\pi/3)R_{\mathscr{w}}^3\varphi$

And the total volume of the ramions is:

[33.10] $V_r = N_{\mathscr{w}}(4\pi/3)r_s^3$

Then:

[33.11] $N_{\mathscr{w}}(4\pi/3)r_s^3 = (4\pi/3)R_{\mathscr{w}}^3\varphi$

Therefore:

[33.12] $N_{\mathscr{w}}r_s^3 = \varphi R_{\mathscr{w}}^3$

And:

[33.13] $r_s = (\varphi/N_{\mathscr{w}})^{1/3}R_{\mathscr{w}}$

That is, the ramion radius grows in proportion to the radius of the universe:

[33.14] $r_s \propto R_{\mathscr{U}}$

Now, because the energy of each ramion is constant:

[33.15] $\rho_s = E_s/((4/3)\pi r_s^3)$

Thus:

[33.16] $\rho_s \propto 1/R_{\mathscr{U}}^3$

The energy density of space:

[33.17] $\rho_{(space)} = \varphi\rho_s$

And the pressure of space:

[33.18] $P_{(space)} = \rho_{(space)}/2$

Therefore also obey:

[33.19] $P_{(space)} \propto 1/R_{\mathscr{U}}^3$

In Ramionics, the internal speed of light in ramions is proportional to energy density and pressure:

[33.20] $c_s \propto \rho_s \propto P_{(space)}$

Thus:

[33.21] $c_s \propto 1/R_{\mathscr{U}}^3$

If the notation denotes the current value of the speed of light by c_0:

[33.22] $c(t) = c_0(R_0/R(t))^3$

The Coefficient 19.02 and FCC Radial Pressure

In FCC geometry, for large layers, the shell thickness becomes very small relative to its radius:

[33.23] $\Delta R/R_n \approx 1/n$

Consequently, the shell is locally almost flat, and the tangential components of the forces approximately cancel one another. However, because of the shell's curvature, small radial components remain.

For the force due to the internal pressure of the ramions:

[33.24] $F_0 \approx P\pi r^2$

And for the FCC shell:

[33.25] $F_{(net)} \approx (5\pi/\gamma)Pr^2n$

; $F_{(net)} \approx 19.02Pr^2n$

This coefficient, 19.02, is an entirely geometrical coefficient arising from the curvature of the FCC lattice. It indicates that the geometry of the universe itself naturally generates an outward radial pressure component.

Ramionics Expansion Rate

In FCC geometry, the radial thickness of each layer is approximately:

[33.26] $\Delta R \approx 2\gamma r_s$

Hence the effective rate of growth of the universe's radius is:

[33.27] $dR/dt \approx \gamma c(t)$

Now substituting c(t):

[33.28] $dR/dt = \gamma c_0(R_0/R)^3$

Thus:

[33.29] $R^3dR = \gamma c_0 R_0^3 dt$

Integration gives:

[33.30] $R^4/4 = \gamma c_0 R_0^3 t$

And therefore:

[33.31] $R^4 = 4\gamma c_0 R_0^3 t$

At the present time:

[33.32] $R = R_0$

[33.33] $R_(obs) = 4\gamma c_0/H_0 = 4\gamma R_h$

[33.34] $R_(obs) \approx 43.94$ billion light years

; if $H_0 \approx 73.50$ km/s/Mpc

[33.35] $R_(obs) \approx 44.22$ billion light years

; if $H_0 \approx 73.04$ km/s/Mpc

Both values are very close to each other and approximately five percent below the estimated radius of the observable universe in ΛCDM theory.

Age of the Universe in Ramionics

Light passes through FCC layers along its path, and the effective thickness of each layer is:

[33.36] $\Delta R \approx 2\gamma r_s$

Thus, the light-path distance across the entire universe is:

[33.37] $R_(obs) = 4\gamma \int c(t)dt$

Because:

[33.38] $c(t) = c_0(R_0/R(t))^3$

[33.39] $R(t)^4 = 4\gamma c_0 R_0^3 t$

Then:

[33.40] $R(t) = R_0(t/t_0)^{1/4}$

[33.41] $c(t) = c_0(t_0/t)^{3/4}$

Substituting into the integral for the light path:

[33.42] $R_(obs) = 4\gamma \int_0^{t0} c_0(t_0/t)^{3/4}dt$

And because:

[33.43] $\int t^{-3/4}dt = 4t^{1/4}$

Therefore:

[33.44] $R_(obs) = 16\gamma c_0 t_0$

But from:

[33.45] $R_(obs) = 4\gamma c_0/H_0$

The resulting relation is:

[33.46] $16\gamma c_0 t_0 = 4\gamma c_0/H_0$

Thus:

[33.47] $t_0 = 1/H_0$

[33.48] $t_0 \approx 13.31$ billion years

; if $H_0 = 73.50$ km/s/Mpc

[33.49] $t_0 \approx 13.39$ billion years

; if $H_0 = 73.04$ km/s/Mpc

The Hubble Tension in Ramionics

In Ramionics, the correct value of the universe's expansion rate is the local Hubble value:

[33.50] $H_0\text{Local} \approx 73$ km/s/Mpc

Furthermore, the value:

[33.51] $H_0\text{CMB}/\beta$

Also gives approximately the same value.

[33.52] $H_0(\text{corrected}) \approx H_0\text{CMB}/\beta \approx 73.5$ km/s/Mpc

This becomes consistent with local measurements and explains the Hubble tension.

The approximately five-percent difference by which Ramionics estimates the age and radius of the universe to be smaller is probably due to the five percent of matter considered in classical physics. In Ramionics, however, all the energy of matter in the universe—namely 10^{53} kg—can fit into 1.17 km^3 of E_s ramions. Even that amount has no independent effect on the energy of the universe's expansion (that is, the energy of the ramions, conventionally called dark energy), because matter is a rearrangement and a slight change in the pattern of distribution of ramion energy, not a separate energy. The five percent itself is also probably an effect of 19+1 in gravity at galactic distances. Likewise, the 26 percent attributed to dark matter is actually $1-\varphi$, namely the volumetric effect of non-space in calculations of space and the neglect of the quantization of the volume of space. Otherwise, in Ramionics, dark matter does not exist; instead, this is called a dark effect. The Hubble tension likewise arises because the coefficient β, representing the quantization of the surface of space, is neglected when the Hubble constant is calculated from CMB observations by the Planck satellite. The catastrophe of physics is also explained in this way: the gravitational constant of electrons has no effect on the expansion of space, which concerns the energy of the ramions.

Definition of Parameters

$R_{\mathscr{u}}$: Radius of the universe

$R_{(obs)}$: Radius of the observable universe; in Ramionics, probably the same as $R_{\mathscr{u}}$

R_h : Hubble radius

r_s : Ramion radius

$N_{\mathscr{u}}$: Total number of ramions in the universe

$L_{\mathscr{u}}$: Number of layers of the universe

ρ_s : Ramion energy density

$\rho_{(space)}$: Energy density of space

$P_{(space)}$: Pressure of space

c_s : Internal speed of light in a ramion

γ : FCC radial freedom coefficient

φ : FCC packing coefficient

β : FCC surface-coverage coefficient

H_0 : Present Hubble constant

t_0 : Age of the universe

Theorem 34: Calculations of Gravity, Relativity, and Dark Matter

Physical Foundations of Space, Mass, and Gravity

Space and time are composed of the discrete face-centered cubic crystalline network and the energy of ramions. Ramions are fundamental quanta of energy, and their energy distribution is the origin of spacetime structure.

The conversion of energy into mass occurs through the explosion of ramions and the redistribution of their energy within the network. Mass is a pattern resulting from changes in the energy distribution of spacetime. The vacant positions of exploded ramions in hyperspace also create a structure corresponding to a black hole.

The fundamental ramion energy relation:

[34.1] $E_r=\mathring{m}_r.\mathring{c}_r^2=\rho_r V_r=2P_r V_r=2r_r F_r/3$

Therefore:

[34.2] $P_r=\rho_r/2$

In the environment surrounding a mass, the energy density of space changes relative to its vacuum value:

[34.3] $\rho(R)=\rho_u[1-f(R)]$

Here, ρ_u is the vacuum energy density, and f is the dimensionless energy-distribution function.

The corresponding relativistic factor:

[34.4] $N(R)=1/\sqrt{[1-f(R)]}$

Face-Centered Cubic Geometry

The volumetric packing fraction of the network:

[34.5] $\varphi=\pi/(3\sqrt{2})=0.740480489693061$

The radial freedom coefficient:

[34.6] $\gamma=\sqrt[3]{(10\sqrt{2}/(8\pi))}=0.825578509501464$

The surface coverage coefficient:

[34.7] $\beta=\sqrt[3]{(5\pi^2)}/4=0.916987168493568$

The coefficient β plays a role in surface calculations, while φ plays a role in volumetric calculations of the network.

***

Derivation of Gravity from the Pressure Gradient

Changes in the pressure of the energy of space around a mass produce a radial force:

[34.8] $F=-V\partial P/\partial R$

Using the relation between pressure and energy density:

[34.9] $F=-(V/2)\partial\rho/\partial R$

The corresponding acceleration:

[34.10] $g=-c^2/(2\rho)\partial\rho/\partial R$

Substituting the energy-distribution function:

[34.11] $g=c^2/[2(1-f)]\partial f/\partial R$

In the weak-field limit:

[34.12] $g\approx(c^2/2)\partial f/\partial R$

Gravity is derived from the gradient of the spacetime energy distribution.

***

Gravitational Field Assuming No Expansion of the Universe

Energy-Distribution Function

To examine the initial field, a function with a Newtonian core and exponential damping is considered:

[34.13] $f(R)=(R_s/R)\mathrm{Exp}[-(R/R_\partial)^k]$

The Schwarzschild radius:

[34.14] $R_s=2GM/c^2$

At distances small compared with the damping scale:

[34.15] $f(R)\approx R_s/R$

Field-Energy Integral

The radial integral:

[34.16] $I=\int\{R_s \text{ to } \infty\}\{R^2 f(R)\partial R\}$

Substituting the damping function:

[34.17] $I=R_s\int\{R_s \text{ to } \infty\}\{R.\mathrm{Exp}[-(R/R_\partial)^k]\partial R\}$

The analytical result:

[34.18] $I=(R_s R_\partial^2/k)\Gamma[2/k,(R_s/R_\partial)^k]$

Under the condition:

[34.19] $R_s \ll R_\partial$

The following approximation is obtained:

[34.20] $I\approx(R_s R_\partial^2/k)\Gamma(2/k)$

The corresponding energy:

[34.21] $E\approx 2\pi\rho_u I$

With the energy-balance coefficient:

[34.22] $E\approx 2\pi\rho_u z I$

Equivalence of Discrete and Continuous Calculations of Gravitational Energy

The energy associated with changes in the distribution of ramions can be calculated both by discrete counting of face-centered cubic layers and by a continuous integral of energy density. This section examines the consistency of the coefficients in the two approaches in the continuum limit.

The energy due to a distribution change for each ramion:

[34.23] $\Delta E_1=E_s f/2$

The number of ramions in layer n and its approximation for large n:

[34.24] $L(n)=10n^2+2$

[34.25] $L(n)\approx 10n^2$

Consequently, the total energy in the large-layer approximation:

[34.26] $\Delta E\approx 5E_s\sum_n n^2 f(n)$

The geometric relation for the layer radius and the corresponding change of variable:

[34.27] $R=2\gamma n r_s$

[34.28] $n^2 dn=R^2 dR/(8\gamma^3 r_s^3)$

Therefore, in the continuum approximation:

[34.29] $\Delta E\approx[5E_s/(8\gamma^3 r_s^3)]\int_0^\infty R^2 f(R)dR$

The background energy density and the geometric identity of the face-centered cubic structure:

[34.30] $\rho_u=\varphi E_s/[(4\pi/3)r_s^3]$

[34.31] $1/(8\varphi\gamma^3)=3/10$

Consequently, the discrete-energy coefficient becomes the continuous coefficient:

[34.32] $5E_s/(8\gamma^3 r_s^3)=2\pi\rho_u$

And therefore:

[34.33] $\Delta E\approx 2\pi\rho_u\int_0^\infty R^2 f(R)dR$

This relation is consistent with the field-energy integral in the continuum limit. Boundary corrections and small layers are accounted for in the discrete formulation. The energy-balance coefficient z is determined in the section concerning the definition of energy.

Damping Scale

The geometric function:

[34.34] $F(k)=\Gamma(2/k)/k$

The equivalent relation:

[34.35] $F(k)=\frac{1}{2}\Gamma(1+2/k)$

Therefore:

[34.36] $I\approx R_s R_\mathcal{R}^2 F(k)$

And:

[34.37] $R_\mathcal{R}=\sqrt{[I/(R_s F(k))]}$

Extremum Point (Stationary Point of the Function)

The extremum condition:

[34.38] $F'(k)=-\Gamma(1+2/k)\psi(1+2/k)/k^2=0$

Consequently:

[34.39] $\psi(1+2/k)=0$

The numerical solution:

[34.40] $k_{opt}=4.332453928522$

The value of the function at this point:

[34.41] $F_{min}=0.442801597205$

The maximum damping scale for a fixed integral value:

[34.42] $R_{\mathscr{A}(max)}=\sqrt{[I/(0.442801597205R_s)]}$

This result pertains to the single-function model and provides the basis for choosing the fixed Newtonian damping exponent in the two-branch model; the damping exponent of the modified branch is determined independently.

***

<!-- End of Part 1: original source through line 5735; continuation begins with "Correction of Radius Due to Expansion of the Universe". -->

Correction of Radius Due to the Expansion of the Universe

In an expanding universe, the effective radial distance may differ from the original geometric distance.

Radial mapping:

[34.43] $\bar{R}=R/\&\#91;1-(R/R_u)^{km1}\&\#93;^{km2}$

Domain:

[34.44] $0\<R\<R_u$

At short distances:

[34.45] $\bar{R}\approx R$

Corrected field function:

[34.46] $f(R)=\&\#91;R_s/\bar{R}(R)\&\#93;Exp\&\#91;-(\bar{R}(R)/R_{\mathscr{A}})^k\&\#93;$

***

Relativity, the Schwarzschild Radius, and the Newtonian Limit

Schwarzschild radius:

[34.47] $R_s=2GM/c^2$

In the Schwarzschild metric, with the appropriate sign convention:

[34.48] $g_{tt}=1-R_s/R$

Time-dilation factor:

[34.49] $N_{\mathscr{g}r}=1/\sqrt{(1-R_s/R)}$

In the Newtonian limit:

[34.50] $f(R)\approx R_s/R$

Therefore:

[34.51] $|g|\approx GM/R^2$

Relativistic Mapping of Parameters

An increase in the local energy of a ramion by the factor N is accompanied by changes in geometric and dynamical scales.

The local radius scales with N, surface area with N^2, and volume with N^3; consequently, local energy density and pressure vary with $1/N^2$.

Under the Ramionics mapping convention, mass scales with N^5, Planck's constant with N^4, and the gravitational constant with $1/N^8$.

***

Friedmann Equations, Expansion of the Universe, and the Vacuum Energy Density Discrepancy

Friedmann Equations and the Problem of Space Energy Density

One of the largest order-of-magnitude discrepancies in physics is the difference between vacuum energy density estimated in quantum field theories and dark energy density inferred from cosmological observations. Depending on the assumptions used in the calculation, this discrepancy can reach approximately 120 orders of magnitude.

The first Friedmann equation for a homogeneous and isotropic universe:

[34.52] $H^2=(8\pi G/3)\rho_m-kc^2/a^2+\Lambda c^2/3$

The second Friedmann equation:

[34.53] $\ddot{a}/a=-(4\pi G/3)(\rho_m+3P/c^2)+\Lambda c^2/3$

In these relations, H is the expansion rate, ρ_m is the mass density equivalent to energy, P is pressure, a is the scale factor, k is the spatial-curvature parameter, and Λ is the cosmological constant.

For a flat universe, the critical mass density equivalent to energy is:

[34.54] $\rho_c=3H^2/(8\pi G)$

Critical energy density:

[34.55] $u_c=\rho_c c^2=3H^2c^2/(8\pi G)$

In standard cosmology, these relations connect the expansion rate to the total effective density and other geometric and cosmological components.

The fundamental energy density of the FCC lattice is calculated from the energy and volume of ramions and is not identical to the Friedmann critical density.

Entanglement of Ramions and Closure of the Universe

The universe is a network of entangled ramions, rather than an assembly of free and independent components.

If each ramion is regarded as the center of the universe, the most distant ramions form the surface of an imaginary sphere; however, the ramions on this surface are entangled with their symmetric counterparts on the opposite side. Therefore, this surface is not a free boundary of the universe, and **the universe is confined within itself**.

The Friedmann equations account for spatial curvature, but do not explicitly incorporate this particular mechanism of entanglement and microscopic FCC closure.

For this reason, the fundamental energy density of ramions is not directly equated with the critical density derived from the Friedmann equations.

Geometric–Topological Derivation of the Relation Between the Universe Radius and the Hubble Radius

In the FCC lattice, the number of ramions in layer n and the total number of ramions up to that layer, respectively, are:

[34.56] $L(n)=10n^2+2$

[34.57] $T(n)=(10n^3+15n^2+11n+3)/3$

In the limit of a very large number of layers:

[34.58] $L(n)\approx 10n^2$

[34.59] $T(n)\approx(10/3)n^3$

The one-sided geometric radius of the lattice:

[34.60] $R_n=2\gamma r_s n$

The coefficient γ is derived from the ratio of the volume occupied by ramions to the volume of the equivalent sphere:

[34.61] $\varphi=10/(24\gamma^3)$

Therefore:

[34.62] $\gamma=\sqrt[3]{}[10/(24\varphi)]=0.825578509501464$

The growth in the number of ramions between two consecutive layers:

[34.63] $\Delta L=L(n+1)-L(n)=20n+10$

For large n, the relative growth in the number of ramions in the shell is:

[34.64] $\Delta L/L\approx 2/n$

Because the number of ramions in the shell is proportional to the square of the length scale, the relative growth of the linear scale is half the relative growth of the area:

[34.65] $\Delta a/a\approx \frac{1}{2}\Delta L/L\approx 1/n$

The fundamental timescale of lattice growth:

[34.66] $t_s=r_s/c$

Therefore, the expansion rate:

[34.67] $H\approx(\Delta a/a)/t_s\approx c/(nr_s)$

Using the one-sided geometric radius:

[34.68] $H\approx 2\gamma c/R_n$

In the entangled structure of Ramionics, the final layer is not a free boundary and is connected to the symmetric side of the universe. Under the definition of the effective two-sided radius of this structure:

[34.69] $R_u=2R_n=4\gamma n r_s$

Consequently:

[34.70] $H\approx 4\gamma c/R_u$

This derivation relates the origin of the factor 4γ to two geometric factors: the factor 2 in the equivalent FCC radius and the factor 2 in defining the effective radius of the entangled universe.

Independent Derivation from Force–Dynamical Analysis

In the Ramionics force analysis, the internal pressure of each ramion is half its energy density. The total force of a ramion follows from its surface pressure:

[34.71] $F_s=P_sA_s=3E_s/(2r_s)=3m_sc^2/(2r_s)$

The difference in the number of ramions between consecutive layers, after dividing the force into three surface, internal, and external shares, produces the following net expansive contribution:

[34.72] $F_{exp,n}\approx(20n/3)F_s$

Summing this force up to the final layer and dividing by the total number of ramions yields the average residual force per ramion:

[34.73] $F_{exp}\approx F_s/n_u$

Corresponding acceleration:

[34.74] $a_{exp}=F_{exp}/m_s=3c^2/(2n_ur_s)$

Using the geometric relation for the radius of the universe:

[34.75] $R_u=2\gamma n_u r_s$

Expansive acceleration:

[34.76] $a_{exp}=3\gamma c^2/R_u$

To convert the average acceleration into the Hubble rate, the mean radius of the ramions is calculated from the FCC shell law:

[34.77] $\bar{n}=\Sigma\{n=1 \text{ to } n_u\}\{nL(n)\}/\Sigma\{n=1 \text{ to } n_u\}\{L(n)\}\approx 3n_u/4$

Therefore:

[34.78] $\bar{R}=3R_u/4$

With the characteristic propagation time of an effect across the scale of the universe:

[34.79] $t_u=R_u/c$

The average velocity resulting from acceleration:

[34.80] $\bar{v}_{exp}=a_{exp}t_u=3\gamma c$

On the other hand, Hubble's law for the mean distance:

[34.81] $\bar{v}_{exp}=H.\bar{R}=(3/4)H.R_u$

Equating the two relations:

[34.82] $H=4\gamma c/R_u$

Thus, the force–dynamical analysis and the geometric–topological analysis arrive at the same relation under their respective stated assumptions.

In the force analysis, the factor 4 results from combining the acceleration coefficient 3 with the mean-radius factor 3/4; in the topological analysis, it results from two geometric factors of 2.

These derivations depend on specific assumptions of the model, including division of each ramion's force into three contributions, selection of the characteristic time R_u/c, and definition of the effective radius of the entangled universe. They demonstrate the consistency of the two approaches within the Ramionics framework.

The Hubble Radius and the Radius of the Universe

<!-- Continuation begins immediately after this heading in the original manuscript. -->

The Hubble Radius and the Radius of the Universe

Definition of the Hubble radius:

[34.83] $R_h=c/H_0$

From the derived expansion relation:

[34.84] $R_u=4\gamma R_h$

Therefore:

[34.85] $R_u/R_h=4\gamma=3.302314038005856$

Using the local value of the Hubble constant:

[34.86] $H_0=73.50\pm0.81 \text{ km.s}^{-1}.\text{Mpc}^{-1}$

The Hubble radius:

[34.87] $R_h=4078.808952381 \text{ Mpc}=13.3032955331 \text{ Gly}$

The radius of the universe:

[34.88] R_u=13469.5080618 Mpc=43.9316595906 Gly

The unit Gly denotes one billion light-years.

The Hubble radius is directly related to the geometric radius of the universe, not to the fundamental energy density of ramions.

The Fundamental Scale of the Universe and the Residual Expansion Force

With the fundamental ramion radius:

[34.89] $r_s=\{\theta_r^{-1}\theta_e^{-1}\}8.33772422647155_{(10)}{}^{-30}$ m

And the radius of the universe:

[34.90] $R_u\approx4.155582742_{(10)}{}^{26}$ m

The ratio of the two scales:

[34.91] $R_u/r_s\approx\{\theta_r\theta_e\}\times4.984073146_{(10)}{}^{55}$

From the geometric relation for the universe's radius, the number of layers is:

[34.92] $n_u\approx\{\theta_r\theta_e\}\times3.018533725_{(10)}{}^{55}$

Therefore, the share of the net expansion force relative to the total force of each ramion is:

[34.93] $F_{exp}/F_s=1/n_u\approx\{\theta_r^{-1}\theta_e^{-1}\}3.312866747_{(10)}{}^{-56}$

Almost all the fundamental force of ramions is balanced within the lattice, leaving only a very small fraction at the universal scale.

As the radius of the universe increases, the following relation holds:

[34.94] $H\propto1/R_u$

In the limit of an infinite universe, the model predicts a decrease in the net force, acceleration, and expansion rate.

Analysis of the Vacuum Energy-Density Discrepancy

The enormous discrepancy in vacuum energy density arises from treating two distinct quantities as identical: the fundamental energy density of ramions and the cosmological critical density.

Entanglement and internal closure of the universe mean that the fundamental energy of the lattice does not necessarily participate in cosmic expansion in the same way as the energy of a freely expanding medium.

The force-based analysis shows that the net expansion contribution of each ramion is very small relative to its fundamental force. The geometric analysis likewise relates the expansion rate to the number of layers and the radius of the universe.

The universe's radius is calculated from the geometry of the ball-cubic lattice, while the fundamental energy density of space is calculated from the structure of ramions.

This distinction forms the basis for examining the vacuum energy-density discrepancy. The gravitational contribution of lattice energy and the equations of cosmological evolution are components of a quantitative formulation of this problem.

The Hubble Tension

The Hubble tension refers to the discrepancy between the Hubble constant inferred from the cosmic microwave background and the value obtained from local measurements.

This discrepancy is associated with the surface-coverage factor β in the ball-cubic lattice:

[34.95] $H_{0(local)}\approx H_{0(cm\beta)}/\beta$

Using the reference value:

[34.96] $H_{0(cm\beta)} \approx 67.4\ km.s^{-1}.Mpc^{-1}$

The geometric correction yields a result close to 73.5 $km.s^{-1}.Mpc^{-1}$.

This relation is proposed as a geometric mechanism for explaining the Hubble tension.

***

Dark Energy and Apparent Dark Matter

Energy distributed throughout the spacetime lattice provides the physical basis of dark energy.

Changes in this distribution around mass generate a gravitational field. Additional gravitational effects at galactic and cluster scales are also examined through changes in the field structure.

The geometric fraction of unoccupied space in the ball-cubic lattice is:

[34.97] $1-\varphi \approx 0.2595$

This value is close to the cosmological fraction attributed to dark matter.

This numerical proximity is used to investigate a geometric origin for apparent dark matter. Its dynamical relationship to acceleration and gravitational lensing must be calculated from the field equations.

***

The MOND Model and the Gravitational Acceleration Scale

History and Founder

The MOND model, an abbreviation of Modified Newtonian Dynamics, was introduced in 1983 by the Israeli physicist **Mordehai Milgrom**.

Its principal aim was to explain galactic rotation curves and the discrepancy between gravitational acceleration calculated from visible matter and acceleration inferred from the motions of stars and gas.

In Newtonian gravity, orbital speed outside a spherical mass distribution decreases with increasing distance. However, the rotation curves of many spiral galaxies remain approximately flat in their outer regions.

MOND examines this discrepancy by modifying the dynamical law at extremely small accelerations.

The Fundamental MOND Relation

In the conventional algebraic formulation of MOND, for systems with suitable symmetry:

[34.98] $g_n = \mu(g/a_{mon})g$

Here, g_n is the Newtonian acceleration due to baryonic mass, g is the actual acceleration in the model, a_{mon} is the characteristic acceleration, and μ is the interpolation function.

In the high-acceleration limit:

[34.99] $\mu(x) \approx 1\ ,\ x \gg 1$

In the low-acceleration limit:

[34.100] $\mu(x) \approx x\ ,\ x \ll 1$

One commonly used interpolation function is:

[34.101] $\mu(x) = x/\sqrt{(1+x^2)}$

The choice of interpolation function affects the details of the transition region.

The Deep-MOND Limit

At extremely low accelerations:

[34.102] $g \approx \sqrt{(g_n a_{mon})}$

For a spherical or point mass:

[34.103] $g_n = GM/R^2$

Therefore:

[34.104] $g_{mon} \approx \sqrt{(GMa_{mon})}/R$

In this limit, acceleration decreases inversely with distance, whereas Newtonian acceleration varies with the inverse square of distance.

Orbital Speed

The centripetal acceleration of circular motion is:

[34.105] $g = v^2/R$

In the deep-MOND limit:

[34.106] $v^4 \approx GMa_{mon}$

This relation is connected to the structure of the empirical baryonic mass–galactic rotation speed relation, known as the Baryonic Tully–Fisher Relation.

The MOND Transition Radius

The characteristic transition radius is:

[34.107] $R_{mon} = \sqrt{(GM/a_{mon})}$

In isolated systems, Newtonian behavior is important at high accelerations, while modified behavior becomes important at low accelerations.

MOND Acceleration

The MOND acceleration scale is related to the local Hubble constant:

[34.108] $a_{mon} \approx cH_0/6$

Using the baseline value of the Hubble constant:

[34.109] $a_{mon} \approx 1.190162456547_{(10)^{-10}}$ m.s^{-2}

This value forms the basis for calculating the MOND transition radius in the two-branch model.

Scope of Application of MOND

MOND is primarily employed in examining galaxy rotation curves, the baryonic mass–velocity relation, and low-acceleration systems.

Its principal domain concerns accelerations on the order of 10^{-10} m.s^{-2} and below, rather than a fixed universal distance.

In the presence of a significant external field, a system's behavior may differ from the isolated deep-MOND limit; this feature is known as the external-field effect.

The original formulation of MOND describes dynamical behavior at low accelerations. Galaxy clusters and gravitational lensing are investigated within extended formulations.

***

The MOG Model and the Enhancement of Gravity on Large Scales

History and Founder

MOG, an abbreviation for Modified Gravity, was developed by the Canadian physicist **John W. Moffat**.

Its well-known formulation, called Scalar–Tensor–Vector Gravity (STVG), was published in 2006.

This theory was developed to investigate galaxy dynamics, galaxy clusters, gravitational lensing, and other large-scale gravitational phenomena.

Unlike the original MOND, MOG offers a framework incorporating additional fields and scale-dependent parameters.

Physical Structure of MOG

In STVG, a vector field and scalar fields are introduced in addition to the gravitational metric field.

In the weak-field limit for a point source, the effective acceleration contains a Yukawa term:

[34.110] $g_{mo\mathscr{g}}=(GM/R^2)\&\#91;1+\alpha_{mo\mathscr{g}}-\alpha_{mo\mathscr{g}}(1+\mu R)Exp(-\mu R)\&\#93;$

Here, $\alpha_{mo\mathscr{g}}$ is the dimensionless gravitational-enhancement parameter, and μ is an inverse-length parameter.

The transition length scale is:

[34.111] $R\mu=1/\mu$

Short-Distance Limit

Under the condition:

[34.112] $\mu R \ll 1$

The Yukawa term approximately cancels the additional enhancement, and the acceleration approaches the Newtonian limit:

[34.113] $g_{mo\mathscr{g}}\approx GM/R^2$

Large-Distance Limit

Under the condition:

[34.114] $\mu R \gg 1$

The exponential term diminishes, giving:

[34.115] $g_{mo\mathscr{g}}\approx(GM/R^2)(1+\alpha_{mo\mathscr{g}})$

In this limit, gravity is enhanced relative to its Newtonian value while retaining the inverse-square dependence on distance.

MOG Enhancement Factor

The enhancement factor is related to the geometric coefficient γ:

[34.116] $\alpha_{mo\mathscr{g}}=5\pi/\gamma$

Its approximate value is:

[34.117] $\alpha_{mo\mathscr{g}}\approx 19.03$

The asymptotic enhancement factor is:

[34.118] $1+\alpha_{mo\mathscr{g}}\approx 20.03$

This value serves as a reference for examining gravitational enhancement on large scales.

Observational Calibrations of the MOG Parameter

In certain fits of MOG theory, the parameter α determines the enhancement of the gravitational component relative to the Newtonian limit within the model formulation. Reported values depend on the dataset, mass, and fitting assumptions and do not necessarily constitute independent measurements of a universal constant.

Study	Observational sample	Fitted α
Moffat & Rahvar (2013)	THINGS galaxy rotation curves	8.89 ± 0.34
Harikumar et al. (2022)	X-COP clusters, M_{200}	9.12 ± 2.72
Harikumar et al. (2022)	X-COP clusters, M_{500}	9.99 ± 3.40

These values are reported as comparative references, not as constraints imposed in advance on the Ramionics field function. For a data-consistent comparison, the acceleration-enhancement ratio and its additional contribution are calculated from the field itself:

[34.119] $A(R,M)=|g(R,M)|/(GM/R^2)$

[34.120] $\alpha_{e\not\!/\!/}(R,M)=A(R,M)-1$

In this comparison, the parameter definitions used by each study and the fitted radial interval are specified. The geometric value $5\pi/\gamma$ is introduced in the original text as an independent Ramionics reference.

Scope of Application of MOG

MOG is used to examine galaxy dynamics, galaxy clusters, and gravitational lensing.

Unlike MOND, the transition scale in the point-source MOG relation is specified directly by the parameter μ.

The effective parameters $\alpha_{mo\not g}$ and μ may depend on the mass and scale of the system in different applications of the theory.

For extended mass distributions, the point-source acceleration relation must be generalized by calculating the field produced by the mass distribution.

Comparison of MOND and MOG

Property	MOND	MOG
Founder	Mordehai Milgrom	John W. Moffat
Initial publication	1983	2006 (STVG)
Main scale	Acceleration	Length and coupling
Main parameters	a_{mon}, μ(x)	$\alpha_{mo\not g}$, μ
Newtonian limit	High acceleration	Short distance
Modified regime	Low acceleration	Large distance
Point-mass far-field acceleration	$\propto 1/R$	$\propto 1/R^2$
Main applications	Galaxy dynamics	Galaxies and clusters

Behaviors corresponding to MOND and MOG are examined through a shared modified function.

***

The Two-Branch Ramionics Gravitational Field Model

To combine Newtonian behavior at short distances with modified behavior on large scales, the energy-distribution function is divided into two components.

The Newtonian component:

[34.121] $f_n(\bar{R}_n)=(R_s/\bar{R}_n)Exp\&\#91;-(\bar{R}_n/R\mathscr{A}_n)^{kdn}\&\#93;$

The Newtonian damping exponent $k\mathscr{A}_n$ equals the analytical value 4.332453928522 obtained from relations [41.242] through (40), and is held fixed in the final Gravity23, Stage39 model; accordingly, this parameter is not free in fitting the MOND and MOG data.

The common MOND–MOG component:

[34.122] $f_m(\bar{R}_m)=\&\#91;R_s/(p_mR_{mon})\&\#93;Ln\&\#91;1+(R_m/\bar{R}_m)^{pm}\&\#93;Exp\&\#91;-(\bar{R}_m/R\mathscr{A}_m)^{kdm}\&\#93;$

The total field function:

[34.123] $f(R)=f_n(\bar{R}_n)+f_m(\bar{R}_m)$

Basis for Selecting the Model and Analysis of the Newtonian, MOND, and MOG Limits

The two-branch function in relations [34.121]–[34.123] is selected to combine a Newtonian core with a logarithmic branch that, under suitable conditions, reproduces MOND behavior and permits investigation of behavior corresponding to MOG on larger scales. To clarify the capabilities and limitations of this choice, the analytical limits of the two branches are examined first. The relations in this subsection are included in the article's continuous formula numbering.

Newtonian Limit of the First Branch

The Newtonian branch function is the same as relation [34.121]:

[34.124] $f_n(\bar{R}_n)=(R_s/\bar{R}_n)Exp[-(\bar{R}_n/R\mathscr{A}_n)^{kdn}]$

At distances smaller than the damping scale:

[34.125] $\bar{R}_n \ll R\mathscr{A}_n$

The exponential factor is approximately unity:

[34.126] $Exp[-(\bar{R}_n/R\mathscr{A}_n)^{kdn}]\approx 1$

Therefore:

[34.127] $f_n(\bar{R}_n)\approx R_s/\bar{R}_n$

If the effect of radial mapping is also negligible:

[34.128] $\bar{R}_n\approx R$

Then:

[34.129] $f_n(R)\approx R_s/R$

In the weak-field limit, using the definition $R_s=2GM/c^2$, the acceleration of this branch becomes:

[34.130] $g_n(R)\approx -GM/R^2$

Thus, the first branch reproduces Newton's inverse-square law in this limit. For the total acceleration to be Newtonian, this result additionally requires that the acceleration contribution from the modified branch be small over the same interval.

The Modified Branch and Radial Scales

The common MOND–MOG function is the same as relation [34.122]:

[34.131] $f_m(\bar{R}_m)=[R_s/(p_mR_{mon})]Ln[1+(R_m/\bar{R}_m)^{pm}]Exp[-(\bar{R}_m/R\mathscr{A}_m)^{kdm}]$

In this relation, R_{mon} is the characteristic MOND radius, R_m is the scale of the logarithmic transition to power-law behavior, and R_{dm} is the damping scale of the modified branch. To derive the principal behavior, first consider an interval in which:

[34.132] $\bar{R}_m \ll R_{dm}$

[34.133] $\bar{R}_m \approx R$

Under this approximation:

[34.134] $f_m(R) \approx [R_s/(p_m R_{mon})] \mathrm{Ln}[1+(R_m/R)^{pm}]$

MOND Limit at Distances Smaller Than R_m

If:

[34.135] $R \ll R_m$

Then:

[34.136] $(R_m/R)^{pm} \gg 1$

Consequently:

[34.137] $\mathrm{Ln}[1+(R_m/R)^{pm}] \approx p_m \mathrm{Ln}(R_m/R)$

Thus:

[34.138] $f_m(R) \approx (R_s/R_{mon}) \mathrm{Ln}(R_m/R)$

The radial derivative is:

[34.139] $df_m/dR \approx -R_s/(R_{mon} R)$

And the corresponding acceleration in the weak-field limit is:

[34.140] $g_m(R) \approx -GM/(R_{mon} R)$

From the definition of the MOND radius:

[34.141] $R_{mon} = \sqrt{(GM/a_{mon})}$

It follows that:

[34.142] $|g_m(R)| \approx \sqrt{(GMa_{mon})}/R$

This is the radial dependence of the deep-MOND limit. For this branch to dominate the Newtonian acceleration, in addition to the validity of the approximations, R must exceed R_{mon}. Accordingly, the suitable approximate interval is:

[34.143] $R_{mon} \ll R \ll R_m$

Such an interval is extensive only when R_m is greater than R_{mon}.

Large-Scale Limit and Its Difference From the MOG Inverse-Square Law

If:

[34.144] $R \gg R_m$

Then:

[34.145] $(R_m/R)^{pm} \ll 1$

In this limit:

[34.146] $\mathrm{Ln}[1+(R_m/R)^{pm}] \approx (R_m/R)^{pm}$

The modified-branch function is therefore approximated by:

[34.147] $f_m(R) \approx [R_s/(p_m R_{mon})](R_m/R)^{pm}$

Its derivative is:

[34.148] $\partial f_m/\partial R \approx -[R_s/(R_{mon}R)](R_m/R)^{pm}$

And the corresponding acceleration is:

[34.149] $|g_m(R)| \approx [GM/(R_{mon}R)](R_m/R)^{pm}$

For the final model value:

[34.150] $p_m=1/4$

It follows that:

[34.151] $|g_m(R)| \approx (GM/R_{mon})R_m^{1/4}/R^{5/4}$

Thus, under this approximation, the modified branch decreases with the inverse 5/4 power of distance. The full behavior of the field on cluster scales is determined by the complete derivative of the function, exponential damping, radial mapping, and the Newtonian contribution.

Mass Dependence of the Transition Radius

In the final model, in accordance with equation [34.152]:

[34.152] $R_m=R_{mon}(M/M_c)^{-1/2}$

Substituting the definition of R_{mon}:

[34.153] $R_m=\sqrt{(GM/a_{mon})}\sqrt{(M_c/M)}$

And simplifying:

[34.154] $R_m=\sqrt{(GM_c/a_{mon})}$

Consequently, if G, M_c, and a_{mon} are constant, R_m is independent of the source mass under this definition, although the ratio R_m/R_{mon} decreases as mass increases. In the table in Section 18, this ratio is reported as 72.86796, 7.286796, and 0.7286796 for masses of 10^{11}, 10^{13}, and 10^{15} solar masses, respectively. Thus, the simple MOND regime can extend over a broad interval for galactic masses, but it does not necessarily exist for very large masses.

Transition Function Without the Logarithmic Approximation

Neglecting damping and radial mapping, but without approximating the logarithm during differentiation, the acceleration of the modified branch in the weak-field limit is:

[34.155] $|g_m(R)| \approx [GM/(R_{mon}R)]/[1+(R/R_m)^{pm}]$

This relation continuously connects the MOND limit to the large-scale power-law limit. At the transition radius:

[34.156] $|g_m(R_m)| \approx GM/(2R_{mon}R_m)$

Accordingly, R_m is a smooth transition scale. **The reason for selecting the present model** is that it analytically reproduces the Newtonian structure in the first branch and deep-MOND behavior in the logarithmic branch, while allowing simultaneous fitting of large-scale data and energy balance. MOG behavior is calculated from the complete field function.

In this structure, the two components have independent damping scales.

The first component preserves approximately Newtonian behavior, while the second describes gravitational transitions on large scales.

Energy Balance in the Two-Branch Field

The energy constraint used in the model, with a general upper limit R_{lim}:

[34.157] $E_s(M/m_s)^2/12=2\pi\rho_u\int \{R_s \text{ to } R_{lim}\}\{&\#91;f_n(R)+f_m(R)&\#93;R^2dR\}$

The vacuum energy density used in the calculations:

[34.158] $\rho_u=\{\theta_r^3\theta_e^4\}4.57974243707115(10)^{68}\ J/m^3$

The integral contribution of the Newtonian branch:

[34.159] $I_n=\int \{R_s \text{ to } R_{lim}\}\{R^2f_n(R)dR\}$

The contribution of the modified branch:

[34.160] $I_m=\int \{R_s \text{ to } R_{lim}\}\{R^2f_m(R)dR\}$

The total integral:

[34.161] $I=I_n+I_m$

The energy constraint applies to the sum of the two branches, not to each branch independently.

Determination of the integration domain: The symbol R_{lim} in equations [34.96], (159), and (160) is the upper integration limit expressed in terms of the physical radius R. In the **unmapped** case, R_{lim} is ∞; in the **current mapped Stage39** case, R_{lim} is R_u; and in the **alternative mapping option with the Hubble boundary**, R_{lim} is R_h. The volume element R^2dR is expressed in terms of physical radius. The divergence of the mapped effective radius at the boundary does not make the physical integration domain infinite.

Reconciliation of the energy coefficient with the script: The density ρ_u in equation [34.97] is eight times the conventional density used in the Gravity23 script. Thus, after rearranging the two sides and using the script's density, the factor 12 on the energy side of equation [34.96] is consistent with the script's factor 96. These two representations must not be interpreted as different energy models.

Mass-Dependent Radial Scales

Shared Transition Scale

[34.162] $R_m=R_{mon}(M/M_c)^{-1/2}$

The parameter M_c determines the transition mass scale.

Damping Scale of the Newtonian Branch

[34.163] $R_{dn}=R_h(M/M_{dn})^2$

Damping Scale of the Modified Branch

[34.164] $R_{dm}=R_h(M/M_{dm})^{pdm}$

The exponent of mass dependence:

[34.165] $p_{dm}=3/&\#91;2(3-p_m)&\#93;$

For:

[34.166] $p_m=1/4$

It follows that:

[34.167] $p_{dm}=6/11$

These scales are distinct from the Schwarzschild radius, MOND radius, and Hubble radius, even though those radii enter their definitions.

Analytical Scaling of Energy

In the two-branch model, the behavior of the energy integral depends on radial exponents and on the mass dependence of the damping scales.

In the Newtonian branch, the inverse-radius kernel is combined with exponential damping.

In the MOND–MOG branch, the logarithmic function and the transition scale R_m modify the energy behavior.

The mass exponent 6/11 for R_m is related to the analytical scaling condition of the modified branch.

This structure makes it possible to calculate and compare the energy contributions of the two branches at different masses.

Nonlinear Radial Mapping in an Expanding Universe

Physical Meaning of the Mapping and Choice of Reference Radius

The expansion of the universe creates a distinction between the geometric radius R and the effective radius entering the energy-distribution function and the gravitational-field calculation. Radial mapping transforms R into an effective radius $\bar{R}$ so that the effect of cosmic expansion is included in the radial dependence of the field. This mapping is one of the structural assumptions of the current model.

The mapping is chosen so that, as R approaches the final reference radius from below, $\bar{R}$ increases without bound. In this way, the geometric radius of the universe remains finite while the effective field radius tends to infinity at the selected boundary.

Two options are considered for the reference radius:

- **First option, the radius of the universe R_u:** With this choice, the effective radius tends to infinity as the geometric radius approaches R_u from inside the domain. This is the default computational choice for Ramionics in the current version of the article.

- **Second option, the Hubble radius R_h:** In this alternative, the same limiting behavior occurs at R_h. The Hubble radius is a scale dependent on the expansion rate and is selected as the mapping boundary in this option.

The motivation for the present choice of R_u is the Ramionics assumption that the extent over which light effects are received and gravitational effects are established in the universe considered by the model provides the basis for determining the effective mapping boundary. In this formulation, the effective boundary is associated with the radius of the observable universe, and the Hubble radius is its alternative.

The R_h option is also defined within the comparison of reference radii. Changing the mapping reference radius changes the effective radius, its derivative, and consequently the calculated acceleration.

Mathematical Definition of the Current Mapping

General radial mapping:

[34.168] $\bar{R}=R/\&\#91;1-(R/R_u)^{km1}\&\#93;^{km2}$

Combined mapping parameter:

[34.169] $\lambda=-k_{m2}Ln(k_{m1})$

This parameter expresses the combined effect of the two mapping coefficients but does not replace their independent definitions.

In the two-branch model, radial mapping enters the calculation of each branch. The following structural choices are specified independently after defining the mapping. Equations [34.121] and [34.122] are the current form of the field function; the alternatives define other configurations of the model.

Option One: Mapping Reference Radius and Integration Limit

Without mapping: The effective radius equals the physical radius, and the upper limit of the energy integral is chosen as infinity. **With mapping, current choice:** The mapping boundary is R_u, and the energy integral is calculated with respect to the physical radius R from R_s to R_u. **With mapping, alternative choice:** The mapping boundary is R_h, and the energy integral runs from R_s to R_h. In both mapped cases, the effective radius grows without bound as the physical radius approaches the selected boundary; this does not make the upper integration limit infinite in the physical variable R.

The choice of R_u rather than R_h rests on the preceding argument in this article concerning the extent of physical influence in the Ramionics universe. If the boundary changes, the field, radial derivative, energy integral, and fit are recalculated for the new configuration.

Option Two: Where Radial Mapping Is Applied

Under **full mapping**, the effective radius $\bar{R}$ is used both in the principal term of the field function and in the damping factor; this is the convention of equations [34.121] and [34.122]. For the Newtonian branch, the main kernel is the ratio $R_s/\bar{R}_n$; for the MOND–MOG branch, it is the logarithmic kernel depending on $\bar{R}_m$.

Under **damping-only mapping**, the principal term of each branch is evaluated at the physical radius R, and only the radial ratio in the attenuation factor uses $\bar{R}$. The two options are therefore not equivalent in their radial derivatives, asymptotic behavior, or energy integrals. The current choice in the article is full mapping; damping-only mapping is recorded as a testable alternative.

Option Three: Type of Attenuation Function

Two families of attenuation functions are considered, with dimensionless variable x and positive exponent k:

Exponential attenuation:

[34.170] $D_{exp}(x)=\mathrm{Exp}(-x^k)$

Rational / power-law attenuation:

[34.171] $D_{rat}(x)=1/(1+x^k)$

In each branch, x is the ratio of the radius used in damping to that branch's damping scale; depending on option 14-4, that radius is R or $\bar{R}$. Both functions approach unity at small radii, but at large radii exponential attenuation decreases faster, while rational attenuation follows a power law. Substituting one for the other can therefore change the field, acceleration, and convergence of the energy integral. In the reported Stage39 model, exponential attenuation is used for both branches. The attenuation-function choice can also be made independently for the two branches in subsequent tests.

Option Four: Shared or Independent Mapping of the Newtonian and MOND–MOG Branches

With **shared mapping**, both branches use the same mapping law and shared parameters, so $\bar{R}_n$ and $\bar{R}_m$ are equal at the same physical radius. This is the choice of the first-ranked Stage39 model.

With **separate mapping**, the Newtonian and MOND–MOG branches may have different mapping parameters. Each branch must then be mapped separately, and the derivative of the total field with respect to R must be calculated using the chain rule. Separate mappings do not, by themselves, imply

different boundary radii R_u or R_h: the boundary is selected under option one, and the branch-specific parameters under option four.

Combining the Options and Computational Status

The four choices above define four independent axes of the model: mapping boundary; where mapping is applied; attenuation family; and shared versus independent branch mapping. For every new combination, the physical constraints, complete field derivative, convergence of the energy integral, and MOND and MOG errors are calculated. **The Stage39 numerical values belong to the configuration actually executed.**

Calculation of Acceleration and the Newtonian Ratio

Acceleration is derived from the radial derivative of the total field function:

[34.172] $g(R)=c^2/[2(1-f(R))]\partial f(R)/\partial R$

Ratio of the magnitude of the model acceleration to Newtonian acceleration:

[34.173] $A(R)=|g(R)|/(GM/R^2)$

In the Newtonian region, this ratio approaches unity. In the transition region and at large scales, the contribution of the modified branch changes it.

Computational Criteria for the Field

Percentage relative error at each point:

[34.174] $\varepsilon_i=100[A_i/A_{t,i}-1]$

Root-mean-square error criterion:

[34.175] $RMS=\sqrt{[(1/n)\sum_i \varepsilon_i^2]}$

This criterion is used to examine field behavior at the MOND and MOG sample points.

Alongside acceleration error, the difference in the integrated field energy is calculated to assess the dynamical and energetic consistency of the model simultaneously.

Numerical Determination of Field Parameters

The parameters of the two-branch model are determined using energy constraints, the analytical structure of mass scales, and reference acceleration data.

Definition of Reference and Calculated Acceleration in MOND and MOG Calibration

The Reference and Calculated values in this section's table are not accelerations with physical units; rather, they are **gravitational acceleration enhancement factors relative to Newtonian acceleration at the same mass and radius**. These factors are dimensionless.

Newtonian acceleration for source mass M at radius R:

[34.176] $g_{newt}=GM/R^2$

Acceleration enhancement factor:

[34.177] $A(R)=|g(R)|/g_{newt}=|g(R)|R^2/(GM)$

In the table:

- **Reference:** The reference acceleration enhancement factor, namely the ratio of reference acceleration to Newtonian acceleration.

- **Calculated:** The enhancement factor calculated from the Ramionics model, relative to the same Newtonian acceleration.

- **Error %:** The percentage difference between the calculated and reference values, as defined in equation [34.174].

- **R/R_{mon}:** The ratio of the evaluation-point radius to the characteristic MOND radius for the same mass.

- **$M/M_{\odot}$:** The source mass in solar-mass units.

At the ten MOND points, reference values are constructed from factors associated with galactic data and the MOND relation. At the ten MOG points, reference values are taken from the comparative MOG model. These two sets provide the bases for numerical comparison.

Unified Table of 20 Reference Points and Model Outputs

This table brings together the inputs for the 20 calibration points and the acceleration enhancement factors calculated by the first-ranked Gravity23, Stage39 model. The Reference and Calculated columns are acceleration enhancement factors, not accelerations measured in $m.s^{-2}$. The calculated accelerations and errors are quoted from previous computational reports; no new fit was performed in this revision.

No.	Dataset	Object	$M/M_{\odot}$	R/R_{mon}	Reference	Calculated	Error %
1	MOND	DDO 154	$5.000000000000_{(10)}{}^{8}$	10.45	10.961955	11.857411	+8.17
2	MOND	IC 2574	$2.000000000000_{(10)}{}^{9}$	8.50	9.014693	9.069552	+0.61
3	MOND	LMC	$3.000000000000_{(10)}{}^{9}$	4.80	5.325971	5.207749	−2.22
4	MOND	M33	$6.400000000000_{(10)}{}^{9}$	6.21	6.730096	6.340683	−5.79
5	MOND	NGC 2403	$1.000000000000_{(10)}{}^{10}$	2.92	3.462499	3.027258	−12.57
6	MOND	NGC 3198	$2.000000000000_{(10)}{}^{10}$	3.10	3.640064	3.082139	−15.33
7	MOND	Milky Way	$6.000000000000_{(10)}{}^{10}$	2.98	3.521655	3.462847	−1.67
8	MOND	NGC 2841	$1.000000000000_{(10)}{}^{11}$	2.31	2.863493	2.750410	−3.95
9	MOND	M31 low	$1.000000000000_{(10)}{}^{11}$	2.22	2.775610	2.664056	−4.02
10	MOND	M31 high	$1.000000000000_{(10)}{}^{11}$	2.77	3.314765	3.204319	−3.33
11	MOG	MOG 1	$1.000000000000_{(10)}{}^{13}$	0.50	1.050000	0.958380	−8.73
12	MOG	MOG 2	$1.000000000000_{(10)}{}^{13}$	1.00	1.180000	1.303745	+10.49
13	MOG	MOG 3	$1.000000000000_{(10)}{}^{13}$	1.20	1.250000	1.437428	+14.99
14	MOG	MOG 4	$1.000000000000_{(10)}{}^{13}$	1.50	1.380000	1.634182	+18.42
15	MOG	MOG 5	$1.000000000000_{(10)}{}^{13}$	2.00	1.620000	1.953595	+20.59
16	MOG	MOG 6	$1.000000000000_{(10)}{}^{15}$	0.50	1.050000	0.857555	−18.33
17	MOG	MOG 7	$1.000000000000_{(10)}{}^{15}$	1.00	1.180000	1.097787	−6.97
18	MOG	MOG 8	$1.000000000000_{(10)}{}^{15}$	1.20	1.250000	1.189284	−4.86
19	MOG	MOG 9	$1.000000000000_{(10)}{}^{15}$	1.50	1.380000	1.322898	−4.14
20	MOG	MOG 10	$1.000000000000_{(10)}{}^{15}$	2.00	1.620000	1.537748	−5.08

Numerical Interpretation and Model Accuracy

For the galaxy DDO 154, the reference acceleration factor is 10.961955, meaning that the reference acceleration is approximately 10.96 times the Newtonian acceleration at that point. The Ramionics model gives a factor of 11.857411, meaning that the calculated acceleration is approximately 11.86 times Newtonian acceleration, with a relative difference of about +8.17 percent from the reference.

To convert each factor into physical acceleration, it is multiplied by the Newtonian acceleration at the same point. The present comparison tests agreement with the two MOND and MOG reference sets.

|Metric|RMS|

|---|---:|

|MOND acceleration|7.376181%|

|MOG acceleration|12.748308%|

|Total acceleration (20 points)|10.414591%|

|Energy|3.938752%|

|Combined|7.873292%|

The largest absolute relative error in the table occurs at point 15, with mass 10^{13} M⊙ and radius $2R_{mon}$, and is approximately 20.59 percent. The overall acceleration RMS for the 20 points is 10.414591 percent.

Theorem 34: Gravity, Relativity, and Dark Matter — Conclusion

To check the accuracy of the numerical integration, the Gauss–Legendre method was used, and the stability of the results was examined by increasing the integration order. These calculations use the local Hubble constant value of 73.50 $km.s^{-1}.Mpc^{-1}$ as their basis.

***

Numerical Results of the Two-Branch Field

Calculated Parameters

|Parameter|Calculated value|

|---|---:|

|M_c|$5.30973982814_{(10)}{}^{14}$ M⊙|

|$M_{\mathcal{A}_n}$|$2.02271284593_{(10)}{}^{13}$ M⊙|

|$M_{\mathcal{A}_m}$|$6.55809754423_{(10)}{}^{17}$ M⊙|

|$k_{\mathcal{A}_m}$|0.418148420451|

|k_{m1}|$2.48090420945_{(10)}{}^{-9}$|

|k_{m2}|0.0315623883428|

|λ|0.625397449117|

|R_m|0.788580293803 Mpc|

The numerical value of R_m was extracted from the reported output of the model calculations; its general definition in equation [34.162] depends on the source mass. Therefore, the reference mass corresponding to this numerical value must be explicitly specified.

Numerical Criteria

Metric	Value
Combined metric	7.873292%
Acceleration deviation	−10.414591%
Energy deviation	−3.938752%
MOG deviation	−12.748308%
MOND deviation	−7.376181%

Variation of the Transition Scale with Mass

Mass ($M_\odot$)	R_m/R_{mon}
10^{11}	72.86796
10^{13}	7.286796
10^{15}	0.7286796

These results show that the ratio of the common transition radius to the MOND radius decreases with increasing mass.

***

Unified Analysis of Gravity Across Different Scales

Gravity is a consequence of changes in the distribution of energy in the spacetime network.

At short distances, the Newtonian core constitutes the dominant behavior. In strong fields, the relativistic factor dependent on the energy-distribution function becomes important.

On galactic scales, the modified branch produces behavior close to MOND. On cluster scales, the independent amplification and damping factors of this branch are used to investigate behavior corresponding to MOG.

On cosmological scales, the nonlinear radial mapping and the geometry of the ball-cubic structure enter the calculations of the expansion of the universe.

Two derivation paths for the relationship between the Hubble radius and the radius of the universe —one geometric–topological and the other force-based–dynamical—arrive at the common coefficient 4γ.

In the geometric path, the growth of ball-cubic shells and the entanglement of the universe play the principal roles. In the force-based path, the very small imbalance of forces among Ramions and the radial average 3/4 are used.

The surface-coverage coefficient β is associated with the Hubble tension, while the volume-occupation coefficient φ is associated with the geometric contribution of apparent dark matter.

The entanglement and internal closure of Ramions also form the basis for distinguishing the fundamental energy density of space from the cosmological critical energy density.

Conclusion: Mass is a change in the energy pattern of spacetime, and gravity arises from the gradient of this change. The two-branch model, together with mass-dependent radial scales and the geometric correction for expansion, provides a framework for field calculations from Newtonian to galactic and cosmological scales.

The relationship between the radius of the universe and the Hubble radius is now accompanied by two explicit derivation paths in this article. The final evaluation of the cosmological section requires, in addition to the consistency of these two paths, testing their dynamical and topological assumptions and deriving the evolution equations of the entangled network.

***

Theorem 35: Electromagnetism

Electric flux density, or electric displacement field:

[35.1] $\vec{D}$ (Coulomb/m^2 or C/m^2) = $Q/(4\pi r^2)$

Electric field intensity, or electric field, which produces the electric force $\vec{F}_e$ on a charge q:

[35.2] $\vec{E}$ (Volt/m) = $\vec{D}/\varepsilon$, $\vec{F}_e = q \cdot \vec{E}$

Magnetic flux density, or magnetic induction field, which produces the magnetic force $\vec{F}_m$ on a charge q moving with velocity $\vec{V}$:

[35.3] $\vec{B}$ (Tesla) = $\mu \cdot \vec{H}$, $\vec{F}_m = q \cdot \vec{V} \times \vec{B}$

Magnetic field intensity, or magnetizing field:

[35.4] $\vec{H}$ (Amp/m) = $Q/t/(2\pi r) = I/(2\pi r)$

The direction of the magnetic field produced by an electric current in the equation above is given by the right-hand rule: if the right thumb points in the positive direction of current, or in the direction of motion of a positive charge, the direction in which the other four fingers curl indicates the direction of the magnetic field. Outside the object, its field lines emerge from the north pole.

Voltage, electrical pressure, or the electric potential difference V_{az} is the difference in energy per unit positive charge between two points. Point z is usually chosen as the zero point, or ground (earth):

[35.5] V_{az} (Volt or V or Joule/Coulomb) = $V_a - V_z = (E_a - E_z)/Q$

Electric current: the flow of electric charge:

[35.6] I (Ampere or Coulomb/Second) = Q/t

Electric current density:

[35.7] $\vec{J}$ (Ampere/m^2 or A/m^2) = I/S

Lorentz law:

[35.8] $\vec{F} = \vec{F}_e + \vec{F}_m = q \cdot (\vec{E} + \vec{V} \times \vec{B})$

[35.9] $\vec{F}_m = q \cdot \vec{V} \times \vec{B}$

In general, the vector product $\vec{X} \times \vec{Y}$ is a vector such as $\vec{Z}$ whose magnitude equals the product of the magnitudes of $\vec{X}$ and $\vec{Y}$ and the sine of the angle between them. Its direction is that of the z-axis in the standard xyz coordinate system, following the right-handed convention. Thus, for a positive charge: the middle finger of the left hand represents $\vec{X}$ or $\vec{V}$, the index finger represents $\vec{Y}$ or $\vec{B}$, and the thumb represents $\vec{Z}$ or $\vec{F}_m$:

[35.10] $|\vec{X} \times \vec{Y}| = |\vec{X}| \cdot |\vec{Y}| \cdot \sin(\theta)$

The four Maxwell equations:

[35.11] $\nabla \cdot \vec{D} = \rho$: Electric Gauss Law

; $\nabla \cdot \vec{B} = 0$: No Magnetic Monopole

; $\nabla \times \vec{E} = -\partial\vec{B}/\partial t$: Faraday Law

; $\nabla \times \vec{H} = \vec{J} + \partial\vec{D}/\partial t$: Ampere-Maxwell Law

Electric Dipole

If two equal and opposite charges ±q are separated by a displacement vector $\vec{d}$ directed from the negative to the positive charge, they form an electric dipole. Its electric dipole moment, torque, and potential energy in an electric field are:

[35.12] $\vec{p} = q \,.\, \vec{d}$

[35.13] $\vec{\tau} = \vec{p} \times \vec{E}$

[35.14] $U = -\vec{p}.\vec{E}$

Magnetic Dipole

A current loop, or any rotating charge, forms a magnetic dipole. If $\vec{A}$ is the area vector of the loop, its magnetic dipole moment, torque, and potential energy in a magnetic field are:

[35.15] $\vec{\mu} = I \,.\, \vec{A}$

[35.16] $\vec{\tau} = \vec{\mu} \times \vec{B}$

[35.17] $U = -\vec{\mu}.\vec{B}$

Permittivity and Permeability of the Medium

The electric and magnetic dipoles belonging to the propagation medium align with the electric and magnetic fields, respectively. As a result of this alignment, the electric dipoles reduce the electric field intensity $\vec{E}$ for a specified $\vec{D}$ or Q, whereas the magnetic dipoles increase the magnetic flux density $\vec{B}$ for a specified $\vec{H}$ or electric current I.

The electric polarization of the medium through which the electric field propagates is the volume density of the electric dipole moment:

[35.18] $\vec{P} = d\vec{p}/dV$

[35.19] $\vec{D} = \varepsilon_0 \,.\, \vec{E} + \vec{P}$

[35.20] $\varepsilon = \varepsilon_0 + \vec{P}/\vec{E}$

[35.21] $\varepsilon = \varepsilon_r \, \varepsilon_0$

The magnetization of the medium through which the magnetic field propagates is likewise the volume density of the magnetic dipole moment:

[35.22] $\vec{M} = d\vec{\mu}/dV$

[35.23] $\vec{B} = \mu_0 \,.\, (\vec{H} + \vec{M})$

[35.24] $\mu = \mu_0 \,.\, (1 + \vec{M}/\vec{H})$

[35.25] $\mu = \mu_r \, \mu_0$

Relative permeability and permittivity: relative to vacuum; relative to the Ramion E_s:

[35.26] $\varepsilon_r > 1$

[35.27] $\mu_r > 1$

The Ramionic equivalent of these relations is the relative energy of Ramions compared with the relaxed state E_s:

[35.28] $E_r/E_s > 1$

The speed of light and the impedance of vacuum, based on the magnetic permeability and electric permittivity of vacuum—that is, Ramions in the relaxed state E_s—are:

[35.29] $c = 1/\sqrt{(\mu_0 \cdot \varepsilon_0)}$

[35.30] $Z_0 = \sqrt{(\mu_0/\varepsilon_0)}$

Theorem 36: Muon and Tau Calculations

Introduction Common to the Models

Introduction — To investigate the rest masses of the muon and tau, a suitable starting point is the experimental mass ratios of these two leptons relative to the electron and to one another: $m_m/m_e \approx 206.76828270846718$ and $m_t/m_m \approx 16.81702933242618$.

In Ramionics, these ratios can be compared with the squared ratios of the genetic metrics, and the geometric origin of this dependence can be traced through the electrical mapping in Theorem 30. In that theorem, the electron Coulomb coefficient is obtained from $K_e/\mathring{K}_s = \theta_k N_e^2 \beta/(4\pi\eta_e^2)$. Applying the same geometric factors to family a and defining $\eta_a = \sqrt{(1-1/N_a)}$, the coefficient ratio becomes $K_a/K_e = (N_a/N_e)^2(\eta_e/\eta_a)^2$.

On the other hand, the effective metric-charge mapping is $q_a/q_e = N_a/N_e$. This effective charge is a quantity in the metric description of the model and must not be equated with the experimentally measured magnitude of electric charge, which is identical for all three leptons. Taking the mutual interaction coefficient as $K_{a\cdot e} = \sqrt{(K_a K_e)}$, two interactions at equal distances yield $U_{a\cdot e}/U_{e\cdot e} = (N_a/N_e)^2(\eta_e/\eta_a)$. Thus one metric-ratio factor comes from the charge mapping and another from the mutual Coulomb coefficient, allowing the leading approximation $m_a/m_e \approx (N_a/N_e)^2$ for the rest-mass ratio. The η correction and contributions from other energy components also matter in more precise calculations.

The electron genetic code is $\mathring{N}_e = 4^0 \times 4 \times 4 \times 6 \times 6 \times 4 \times 4 \times 2_e \times 2_r = 36864$. The value $\sqrt{(m_m/m_e)} \approx 14.37944$ is close to the structural ratio $2^9/6^2 = 128/9 \approx 14.22222$. Accordingly, replacing the two factors of 6 in the electron genetic structure yields the muon code $\mathring{N}_m = \mathring{N}_e(2^9/6^2) = 2^{19} = 524288$.

Likewise, $\sqrt{(m_t/m_m)} \approx 4.10086$ is close to 4, and the tau code is set to $\mathring{N}_t = 4\mathring{N}_m = 2^{21} = 2097152$. The resulting squared genetic ratios are $(\mathring{N}_m/\mathring{N}_e)^2 = 202.27160493827160$ for muon to electron and $(\mathring{N}_t/\mathring{N}_m)^2 = 16$ for tau to muon. Comparison with the experimental ratios highlights the role of metric and structural corrections in calculating rest energy.

To determine the corresponding generations, the model uses the general genetic-code form from Theorem 28 and the charged-packet rules of Theorem 29. In this structure, the initial factor 4^0 and the electric factor 2_e are mandatory, whereas the remaining factor 2_r is optional. The generation code is written s/p with s≥p: s indexes the containing layer and p indexes the packet fermion count, such that $S = 2^s$, $P = 2^p - 1$, and the index of the final collapsed layer is $2^s - 1$.

When counting factors, p is obtained from the number of factors of 4, including 4^0, while s is obtained from that number plus the factors of 6 or 8. The factors 2_e and 2_r are not counted in these indices. For pure powers-of-two codes, the decompositions $\mathring{N}_m = 4^0 4^6 8^2 2_e = 2^{19}$ and $\mathring{N}_t = 4^0 4^4 8^4 2_e = 2^{21}$ give generations 9/7 and 9/5, respectively.

Consequently, both packets have containing layer 512 and final collapsed layer 511, but their fermion counts are $P_m = 2^7 - 1 = 127$ and $P_t = 2^5 - 1 = 31$, respectively.

The requirement of positive remaining energy further distinguishes these structures among the Mersenne candidates examined. Using the cumulative FCC relation $T(n) = (10n^3 + 15n^2 + 11n + 3)/3$ gives

T(511)=446083583. To avoid concealing the contributions of the three particle groups within the compact coefficient 23, and to avoid using electron-family quark notation for other generations, the charged-packet energy is expressed with the general family index a:

$E_{pa}/E_s = (2^{p-1}-1)(6\mathring{N}_a)+(2^{p-2}+1)(19\mathring{N}_a/2)+(2^{p-2}-1)(3\mathring{N}_a/2)$

This relation counts the structural energy of the three groups of charged particles in the packet in the zero-alpha approximation. Here p indexes the packet fermion count, not the projection exponent of additional energy, which is defined separately below. The energy remaining after accounting for the charged packet in the layer-capacity test is:

$E_{rema} = T(511)E_s - E_{pa}$

For the muon, the charged-packet energy is $386924544E_s$ and the remaining energy is $59159039E_s$. For the tau, the charged-packet energy is $390070272E_s$ and the remaining energy is $56013311E_s$. These values test packet-structure feasibility and the positivity of remaining capacity; they must not be directly identified with $EExtra_a$ in [36.5].

To test uniqueness within the specified domain of this model, three permitted fermion counts $P\in\{7,31,127\}$, mandatory 4^0 and 2_e, optional 2_r, the counts of factors 4 and 8, and the positive-remaining-energy condition were examined. For the muon code, candidate 8/5 with P=31 and optional 2_r has remaining energy $-41920257E_s$ and is rejected; candidate 9/7 with P=127 and without that factor has $+59159039E_s$ and is accepted. For the tau code, candidate 8/3 with P=7 and optional 2_r has $-45065985E_s$ and is rejected; candidate 9/5 with P=31 and without that factor has $+56013311E_s$ and is accepted. Thus, among the examined decompositions and under these constraints, only generations 9/7 and 9/5 are accepted. This uniqueness is conditional on the candidate genetic codes 2^{19} and 2^{21} and the search rules above; it does not by itself establish that the initial choice of these two codes was independent of the experimental mass ratios.

The interpretation of mass projection in the Ramionics model rests on distinguishing structural mass from inferred mass. Within the model, actual structural rest mass and apparent rest mass inferred from a particular measurement can differ because of metric projection. For example, measuring the electrical interaction of two muons, a muon–electron interaction, or muon deflection in an electric field calibrated using electrons need not involve identical metric factors. The dependence of effective metric charge, K, and α on N, as well as the details of the measurement method, affects the derivation of the exponent. Treating them as constant with respect to N can separate inferred mass from actual mass within the model. Exponents in multiples of ½, including −½, ½, 1, and 2, are defined projection cases. In this theorem, the dominant exponent 2 for the main rest-energy component is chosen from analysis of genetic-code factors and the mapping in the introduction.

In this way, the experimental mass ratios, electrical metric mapping, genetic codes, and Mersenne generations are connected within the stated relations and provide the basis for subsequent calculations of muon and tau rest energies.

Definition of the Metric, Quantization, and Energy Scale

The number of structural balls in each particle is fixed at 12. N_a is the metric of particle family a, and $\mathring{N}_a$ is that family's genetic metric before quantization; neither denotes the number of balls. Therefore, $12N_a$ is the product of the fixed ball count and the family metric, while N_a/N_e is the ratio of that particle-family metric to the electron-family metric.

In both models of this theorem, five quantization methods are examined independently for both values of the fundamental energy E_s. The two cases of subtracting or not subtracting the magnetic-inertia contribution d from rest energy are calculated consistently for the electron, muon, and tau. In Model 1, cases A/B and C/D compare the corresponding rest-energy definitions. The E_s scale in

each group is determined by reproducing the experimental electron rest energy. In Model 2, the choice of how to include magnetic inertia in the muon and tau rest masses is independent of that calibration. All five quantizations are examined independently for both E_s scales; hence this comparison does not replace a full recalibration of the C/D structure.

[36.1] $\mathrm{Quant}_n(\acute{N}) \in \{\mathrm{Ceil}_{10}(\acute{N}), \mathrm{Ceil}_{30}(\acute{N}), \mathrm{Round}_{30}(\acute{N}), 30+\mathrm{Floor}_{60}(\acute{N}), 30+\mathrm{Round}_{60}(\acute{N})\}$

[36.2] $\eta_a = \sqrt{(1-1/N_a)}$

[36.3] $E_{as} = 3N_a/2-d_a \quad (A/B)$

; $E_{as} = 3N_a/2 \quad (C/D)$

; $d_a=\mathrm{mRound}_2(\acute{d}_a)$, $\acute{d}_a=(3N_a/2)\alpha_a/(6(1-\alpha_a/6))(1-3\alpha_a(1+3/4)^2) \quad (A/B)$

In this definition, the mRound_2 function quantizes as specified in the “Magnetic Negative Mass” section of Theorem 31 so that the resulting structural rest energy is an even integer. α is a function of N; therefore, a fully self-consistent calculation for each quantization must first determine $\alpha_a(N_a)$ from the corresponding model in Theorem 31 and then calculate $d_a(N_a)$. For a preliminary comparison of the five quantizations, the existing tables use fixed values $\alpha_m^{-1}=137.03950024462935$ and $\alpha_t^{-1}=137.03969886161988$ reported in Theorem 31, without recalibrating α separately for every N. Consequently, the tabulated d values and numerical errors remain conditional on this approximation and must not be treated as recalibrated results. In this explanatory addition, the tabulated numbers have not been changed by reconstructing α(N).

[36.4] $E_{axx} = E_{as}E_s(N_a/N_e)(\eta_e/\eta_a)$

Model 1: Independent Projection of Additional Energy

[36.5] $\mathrm{EExtra}_a = [T_{511} - n_p(12\acute{\nu}_a)]E_s$

; $\acute{\nu}_a = \mathring{N}_a-N_a$

[36.6] $E_{axx2} = E_{axx} + (\mathrm{EExtra}_a/n_p)(N_a/N_e)^{\lambda_a}$

In these relations, $\acute{\nu}_a$ is the difference between the genetic code and the quantized metric of the same family, calculated separately for each quantization method. The neutrino-energy contribution for each packet particle is taken as $12\acute{\nu}_aE_s$. Thus, for n_p particles, the total subtracted contribution is $12n_p\acute{\nu}_aE_s$, and EExtra_a is the energy available after that subtraction in [36.5]. This differs from the energy remaining after subtraction of the entire charged-packet energy in the introduction: the introduction tests charged-packet capacity and feasibility, whereas [36.5] defines the reserve available at the neutrino-correction stage. The two quantities therefore must not be interpreted as one energy or as contradictory evaluations of the same subtraction. This distinction alone does not establish that all energy components are independent; an explicit energy balance for the entire packet is required to rule out double counting completely.

E_{axx} is the projected structural energy, while E_{axx2} is the final energy after adding the extra-energy contribution. In [36.6], n_p is the packet fermion count, and p in the exponent of the metric ratio denotes only the projection exponent of the extra-energy contribution, not the generation index p in s/p. To remove this notation overlap, the exponent is henceforth denoted λ_a. In the current calculations, $\lambda_m=-1$ and $\lambda_t=0$ are merely two trial hypotheses. Because the measurement processes used to infer particle rest masses may differ, the extra-energy projection exponent need not equal the dominant exponent 2 of the structural component. The value of λ_a should ultimately be derived from a model of the measurement process, not merely from numerical proximity to the experimental mass.

|Model|E_s (MeV)|E_s (eV)|d_e|E_{es}/E_s|

|---|---:|---:|---:|---:|

|A/B|0.0000093723441902457908|9.3723441902457908|63|54522|

|C/D|0.0000093615269668841921|9.3615269668841921|—|54585|

Muon Family

[36.7] $\mathring{N}_m = 2^{19} = 524288$

[36.8] $\acute{N}_m = \mathring{N}_m\pi^2/10$

For the muon, N_e=36390, T_{511}=446083583, $\acute{\nu}_m=\mathring{N}_m-N_m$, n_p=127, and $\lambda_m=-1$ are used.

[36.9] $\acute{\nu}_m = 524288-N_m$

[36.10] $EExtra_m/E_s = 446083583-127(12(524288-N_m))$

[36.11] $E_{mxx2} = E_s[E_{ms}(N_m/36390)\sqrt{((1-1/36390)/(1-1/N_m))}+(EExtra_m/(127E_s))(36390/N_m)]$

The reference experimental muon rest energy is 105.6583755 MeV. The difference ΔE is the calculated value minus the experimental value.

|Quantization|Model|N|d|E_{as}/E_s|$\acute{\nu}$|EExtra/E_s|E_{axx} (MeV)|E_{axx2} (MeV)|ΔE (MeV)|Error (%)|

|---|---|---:|---:|---:|---:|---:|---:|---:|---:|---:|

|$Ceil_{10}$|A/B|517460|882|775308|6828|435677711|103.326490|105.587566|-0.070810|-0.067018|

|$Ceil_{10}$|C/D|517460|—|776190|6828|435677711|103.324644|105.583110|-0.075266|-0.071235|

|$Ceil_{30}$|A/B|517470|881|775324|6818|435692951|103.330619|105.591730|-0.066645|-0.063076|

|$Ceil_{30}$|C/D|517470|—|776205|6818|435692951|103.328637|105.587139|-0.071237|-0.067422|

|$Round_{30}$|A/B|517440|882|775278|6848|435647231|103.318498|105.579503|-0.078872|-0.074648|

|$Round_{30}$|C/D|517440|—|776160|6848|435647231|103.316657|105.575052|-0.083323|-0.078861|

|30+$Floor_{60}$|A/B|517470|881|775324|6818|435692951|103.330619|105.591730|-0.066645|-0.063076|

|30+$Floor_{60}$|C/D|517470|—|776205|6818|435692951|103.328637|105.587139|-0.071237|-0.067422|

|30+$Round_{60}$|A/B|517470|881|775324|6818|435692951|103.330619|105.591730|-0.066645|-0.063076|

|30+$Round_{60}$|C/D|517470|—|776205|6818|435692951|103.328637|105.587139|-0.071237|-0.067422|

In this comparison, the muon result closest to the experimental value is obtained with model A/B. The three quantizations $Ceil_{30}$, 30+$Floor_{60}$, and 30+$Round_{60}$ yield identical numerical results because they produce the same N.

Tau Family

[36.12] $\mathring{N}_t = 2^{21} = 2097152$

[36.13] $\acute{N}_t = \mathring{N}_t\pi^2/10$

For the tau, N_e=36390, T_{511}=446083583, $\acute{\nu}_t=\mathring{N}_t-N_t$, n_p=31, and λ_t=0 are used.

[36.14] $\acute{\nu}_t = 2097152-N_t$

[36.15] $EExtra_t/E_s = 446083583-31(12(2097152-N_t))$

[36.16] $E_{txx2} = E_s[E_{ts}(N_t/36390)\sqrt{((1-1/36390)/(1-1/N_t))}+EExtra_t/(31E_s)]$

The reference experimental tau rest energy is 1776.86 MeV.

|Quantization|Model|N|d|E_{as}/E_s|$\acute{\nu}$|EExtra/E_s|E_{axx} (MeV)|E_{axx2} (MeV)|ΔE (MeV)|Error (%)|

|---|---|---:|---:|---:|---:|---:|---:|---:|---:|---:|

|Ceil_{10}|A/B|2069810|3527|3101188|27342|435912359|1653.175220|1784.966209|+8.106209|+0.456210|

|Ceil_{10}|C/D|2069810|—|3104715|27342|435912359|1653.145181|1784.784062|+7.924062|+0.445959|

|Ceil_{30}|A/B|2069820|3528|3101202|27332|435916079|1653.190670|1784.982784|+8.122784|+0.457143|

|Ceil_{30}|C/D|2069820|—|3104730|27332|435916079|1653.161155|1784.801159|+7.941159|+0.446921|

|Round_{30}|A/B|2069820|3528|3101202|27332|435916079|1653.190670|1784.982784|+8.122784|+0.457143|

|Round_{30}|C/D|2069820|—|3104730|27332|435916079|1653.161155|1784.801159|+7.941159|+0.446921|

|$30+\text{Floor}_{60}$|A/B|2069790|3527|3101158|27362|435904919|1653.143254|1784.931994|+8.071994|+0.454284|

|$30+\text{Floor}_{60}$|C/D|2069790|—|3104685|27362|435904919|1653.113233|1784.749867|+7.889867|+0.444034|

|$30+\text{Round}_{60}$|A/B|2069850|3527|3101248|27302|435927239|1653.239154|1785.034642|+8.174642|+0.460061|

|$30+\text{Round}_{60}$|C/D|2069850|—|3104775|27302|435927239|1653.209077|1784.852451|+7.992451|+0.449808|

In this comparison, the tau result closest to the experimental value is obtained with quantization $30+\text{Floor}_{60}$ and model C/D.

Summary of Model 1

Five quantizations were examined for each particle using two E_s scales and two corresponding definitions of rest energy. Therefore, there are 10 cases per particle and 20 calculation rows in total. Because some quantization outputs are equivalent, the number of numerically distinct cases is smaller.

Continuation of Theorem 36, following Volume 24. Original equation numbering and numerical tables are preserved.

Model 2: Complete Packet Energy Balance and Independent FCC Layer Search

In Model 2, the definitions of metric N_a, factor η_a, structural rest energy E_{axx}, and the two A/B and C/D scales are retained from the common introduction and equations [36.1]–[36.4]. The new Stage13 calculations examine six quantization methods, two energy scales, two choices concerning subtraction or retention of magnetic-inertia contribution d, two packet-balance definitions (with or without the neutrino contribution), and two ways of adding free energy (with or without magnification by F_a), **independently for the muon and tau**. At this stage, Direct $\mathring{N}$ is added to the five quantizations in the introduction. Thus, the six-option list applies specifically to the Model 2 scan, and the five-option definition in [36.1] for Model 1 is unchanged.

Distinction Between Calibration and Rest Mass: Choosing A/B or C/D specifies only how the E_s scale is determined from the experimental electron rest energy. When calculating muon and tau rest masses, whether to include or subtract the magnetic-inertia contribution is a choice independent of electron calibration and independent for each of these two leptons. Experimental methods for

measuring and extracting the rest masses of the three leptons are not necessarily identical; the model therefore examines each family's energy contributions separately.

The search range for the integer FCC layer is 471 through 551, centered on 511. This trial layer need not be the same as the final genetically collapsed layer of the packet. The packet particle counts are fixed at P_m=127 for the muon and P_t=31 for the tau. The charged-packet energy balance is $386924544E_s$ for the muon and $390070272E_s$ for the tau. If the neutrino contribution is included, the corresponding energy $12P_a\acute{\nu}_aE_s$ is also subtracted from the cumulative layer energy.

[36.17] $T(L) = (10L^3+15L^2+11L+3)/3$

[36.18] $\acute{\nu}_a = \mathring{N}_a - N_a$

[36.19] $B_a(\delta) = E_{pa}/E_s+\delta 12P_a\acute{\nu}_a$

; $\delta \in \{0,1\}$

[36.20] $EExtra_a(L,\delta) = [T(L)-B_a(\delta)]E_s$

[36.21] $F_a = (N_a/N_e)(\eta_e/\eta_a)$

[36.22] $E_{axx2}(L,\delta,\kappa) = E_{axx}+\kappa EExtra_a(L,\delta)/P_a$

; $\kappa \in \{F_a,1\}$

[36.23] $T(L_c) = B_a(\delta)+P_a(E_{a(}exp_{)}-E_{axx})/(\kappa E_s)$

[36.24] $\Delta E = E_{axx2}-E_{a(}exp_{)}$

[36.25] $Error(\%) = 100\Delta E/E_{a(}exp_{)}$

In these equations, δ=0 means subtracting only the charged-packet energy, whereas δ=1 means subtracting the charged-packet energy together with the neutrino contribution. $\kappa=F_a$ means magnifying the free energy, whereas κ=1 means adding it without magnification; in both cases, the structural term E_{axx} continues to use F_a. L_c is the continuous root of the target equation, but Stage13 searches the integer layers in the specified interval and ranks candidates by the absolute relative mass error. Accordingly, the following tables are the output of a **bounded, ranked scan**, not proof that the layer is independent of experimental data.

The experimental target mass is 105.6583755000 MeV for the muon and 1776.8600000000 MeV for the tau. The α values are the same reference approximations used in Theorem 36 and were not recalibrated self-consistently for each N. The d value, its subtraction choice, structural energy, packet energy, free energy, F factor, and signed error in every row are transferred directly from the Stage13 report. In the tables, True and False indicate whether the respective choice was applied. "Magnify extra=False" means κ=1.

Ten Best Muon Results in Model 2

The following table presents the top ten muon ranks independently of the tau results. The target value is 105.6583755000 MeV, and the packet contains 127 particles.

|Rank|Scale|E_s (MeV)|Quantization|N|d|Subtract d|Subtract neutrino|Magnify extra|L|T(L)|Packet energy/E_s|Free energy/E_s|Free per particle/E_s|F|Structural (MeV)|Predicted (MeV)|Experimental (MeV)|ΔE (MeV)|Error (%)|

|---:|---:|---:|---:|---:|---:|---:|---:|---:|---:|---:|---:|---:|---:|---:|---:|---:|---:|---:|---:|

|1 | C/D | 9.3615269668841921e-06 | Ceil10 | 517460 | 882 | True | True | False | 505 | 430569061 | 397330416.00000000 | 33238645.00000000 | 261721.61417323 | 14.219658972924 | 103.207233982614 | 105.657347931513 | 105.6583755000 | -0.001027568487 | -0.000972539|

|2 | C/D | 9.3615269668841921e-06 | 30+Floor60 | 517470 | 881 | True | True | False | 505 | 430569061 | 397315176.00000000 | 33253885.00000000 | 261841.61417323 | 14.219933769918 | 103.211358402232 | 105.662595734367 | 105.6583755000 | +0.004220234367 | +0.003994226|

|3 | C/D | 9.3615269668841921e-06 | 30+Round60 | 517470 | 881 | True | True | False | 505 | 430569061 | 397315176.00000000 | 33253885.00000000 | 261841.61417323 | 14.219933769918 | 103.211358402232 | 105.662595734367 | 105.6583755000 | +0.004220234367 | +0.003994226|

|4 | C/D | 9.3615269668841921e-06 | Ceil30 | 517470 | 881 | True | True | False | 505 | 430569061 | 397315176.00000000 | 33253885.00000000 | 261841.61417323 | 14.219933769918 | 103.211358402232 | 105.662595734367 | 105.6583755000 | +0.004220234367 | +0.003994226|

|5 | C/D | 9.3615269668841921e-06 | Round30 | 517440 | 882 | True | False | False | 501 | 420428513 | 386924544.00000000 | 33503969.00000000 | 263810.77952756 | 14.219109378937 | 103.199251615492 | 105.668923342194 | 105.6583755000 | +0.010547842194 | +0.009982968|

|6 | C/D | 9.3615269668841921e-06 | Round30 | 517440 | 882 | True | True | False | 505 | 430569061 | 397360896.00000000 | 33208165.00000000 | 261481.61417323 | 14.219109378937 | 103.199251615492 | 105.647118797919 | 105.6583755000 | -0.011256702081 | -0.010653866|

|7 | C/D | 9.3615269668841921e-06 | Ceil10 | 517460 | 882 | True | False | False | 501 | 420428513 | 386924544.00000000 | 33503969.00000000 | 263810.77952756 | 14.219658972924 | 103.207233982614 | 105.676905709316 | 105.6583755000 | +0.018530209316 | +0.017537852|

|8 | C/D | 9.3615269668841921e-06 | 30+Floor60 | 517470 | 881 | True | False | False | 501 | 420428513 | 386924544.00000000 | 33503969.00000000 | 263810.77952756 | 14.219933769918 | 103.211358402232 | 105.681030128934 | 105.6583755000 | +0.022654628934 | +0.021441394|

|9 | C/D | 9.3615269668841921e-06 | 30+Round60 | 517470 | 881 | True | False | False | 501 | 420428513 | 386924544.00000000 | 33503969.00000000 | 263810.77952756 | 14.219933769918 | 103.211358402232 | 105.681030128934 | 105.6583755000 | +0.022654628934 | +0.021441394|

|10 | C/D | 9.3615269668841921e-06 | Ceil30 | 517470 | 881 | True | False | False | 501 | 420428513 | 386924544.00000000 | 33503969.00000000 | 263810.77952756 | 14.219933769918 | 103.211358402232 | 105.681030128934 | 105.6583755000 | +0.022654628934 | +0.021441394|

The best muon row uses the C/D scale, Ceil_{10} quantization, metric N=517460, layer L=505, subtraction of magnetic inertia and the neutrino contribution, and addition of free energy without magnification. The predicted mass is 105.657347931513 MeV, the mass difference is -0.001027568487 MeV, and the relative error is -0.000972539%. Repeated masses at other ranks result from equivalent outputs of certain quantization methods.

Ten Best Tau Results in Model 2

The following table presents the top ten tau ranks independently of the muon results. The target value is 1776.8600000000 MeV, and the packet contains 31 particles.

|Rank|Scale|E_s (MeV)|Quantization|N|d|Subtract d|Subtract neutrino|Magnify extra|L|T(L)|Packet energy/E_s|Free energy/E_s|Free per particle/E_s|F|Structural (MeV)|Predicted (MeV)|Experimental (MeV)|ΔE (MeV)|Error (%)|

|---:|---:|---:|---:|---:|---:|---:|---:|---:|---:|---:|---:|---:|---:|---:|---:|---:|---:|---:|---:|---:|

|1 | C/D | 9.3615269668841921e-06 | 30+Floor60 | 2069790 | 3527 | True | True | True | 496 | 407978353 | 400248936.00000000 | 7729417.00000000 | 249336.03225806 | 56.877220687104 | 1651.235255259243 | 1783.996129381417 | 1776.8600000000 | +7.136129381417 | +0.401614611|

|2 | C/D | 9.3615269668841921e-06 | Ceil10 | 2069810 | 3527 | True | True | True | 496 | 407978353 | 400241496.00000000 | 7736857.00000000 | 249576.03225806 | 56.877770281091 | 1651.267184721299 | 1784.157132754339 | 1776.8600000000 | +7.297132754339 | +0.410675729|

|3 | C/D | 9.3615269668841921e-06 | Ceil30 | 2069820 | 3528 | True | True | True | 496 | 407978353 | 400237776.00000000 | 7740577.00000000 | 249696.03225806 | 56.878045078085 | 1651.282617102738 | 1784.237103017317 | 1776.8600000000 | +7.377103017317 | +0.415176380|

|4 | C/D | 9.3615269668841921e-06 | Round30 | 2069820 | 3528 | True | True | True | 496 | 407978353 | 400237776.00000000 | 7740577.00000000 | 249696.03225806 | 56.878045078085 | 1651.282617102738 | 1784.237103017317 | 1776.8600000000 | +7.377103017317 | +0.415176380|

|5 | C/D | 9.3615269668841921e-06 | 30+Round60 | 2069850 | 3527 | True | True | True | 496 | 407978353 | 400226616.00000000 | 7751737.00000000 | 250056.03225806 | 56.878869469066 | 1651.331044571518 | 1784.479147835146 | 1776.8600000000 | +7.619147835146 | +0.428798433|

|6 | C/D | 9.3615269668841921e-06 | 30+Floor60 | 2069790 | 3527 | False | True | True | 496 | 407978353 | 400248936.00000000 | 7729417.00000000 | 249336.03225806 | 56.877220687104 | 1653.113233338819 | 1785.874107460992 | 1776.8600000000 | +9.014107460993 | +0.507305441|

|7 | C/D | 9.3615269668841921e-06 | Ceil10 | 2069810 | 3527 | False | True | True | 496 | 407978353 | 400241496.00000000 | 7736857.00000000 | 249576.03225806 | 56.877770281091 | 1653.145180947427 | 1786.035128980467 | 1776.8600000000 | +9.175128980467 | +0.516367580|

|8 | A/B | 9.3723441902457908e-06 | 30+Floor60 | 2069790 | 3527 | True | True | True | 496 | 407978353 | 400248936.00000000 | 7729417.00000000 | 249336.03225806 | 56.877220687104 | 1653.143253884027 | 1786.057532897746 | 1776.8600000000 | +9.197532897746 | +0.517628451|

|9 | C/D | 9.3615269668841921e-06 | Ceil30 | 2069820 | 3528 | False | True | True | 496 | 407978353 | 400237776.00000000 | 7740577.00000000 | 249696.03225806 | 56.878045078085 | 1653.161154867494 | 1786.115640782074 | 1776.8600000000 | +9.255640782074 | +0.520898708|

|10 | C/D | 9.3615269668841921e-06 | Round30 | 2069820 | 3528 | False | True | True | 496 | 407978353 | 400237776.00000000 | 7740577.00000000 | 249696.03225806 | 56.878045078085 | 1653.161154867494 | 1786.115640782074 | 1776.8600000000 | +9.255640782074 | +0.520898708|

The best tau row uses the C/D scale, 30+Floor$_{60}$ quantization, metric N=2069790, layer L=496, subtraction of magnetic inertia and the neutrino contribution, and addition of free energy magnified by F_a. The predicted mass is 1783.996129381417 MeV, the mass difference is +7.136129381417 MeV, and the relative error is +0.401614611%.

Summary of Model 2

|Family|Rank|Scale|Quantization|N|L|Subtract d|Subtract neutrino|Magnify extra|Predicted mass (MeV)|ΔE (MeV)|Error (%)|

|---|---:|---|---|---:|---:|---|---|---|---:|---:|---:|

|Muon|1|C/D|Ceil$_{10}$|517460|505|True|True|False|105.657347931513|−0.001027568487|−0.000972539|

|Tau|1|C/D|30+Floor$_{60}$|2069790|496|True|True|True|1783.996129381417|+7.136129381417|+0.401614611|

This version presents the **ten best results for each family, or 20 ranked rows in total**, from the Stage13 report. The original script report used Stage13Top=20; only ranks 1–10 for each family were selected for the article, and ranks 11–20 are not included. Unlike the older Model 2 tables, the present scan is restricted to layers 471–551. Therefore, results for layers outside that interval, including 621 and 623 in the previous tau analysis, do not appear in the new ranking and must not

be treated as identical to the results of this search. Numerical proximity to experimental mass, especially when selecting the layer using the mass-error criterion, does not by itself establish independent physical validity of the model. Model 1 and the other theorems remain unchanged.

New Joint Muon–Tau Model Within Model 2

In this examination, a "joint model" means sharing **only two global choices** between muon and tau: the fundamental energy scale E_s (group A/B or C/D) and the N quantization method. This definition replaces the previous joint model; no other choices are required to be shared. Conversely, four choices are optimized independently for each family: whether to subtract or retain magnetic-inertia contribution d, whether to subtract or retain the packet neutrino contribution, whether to magnify the additional energy by F, and which integer layer L to select in the range 471–551. The N and d values are likewise obtained for each family using the shared quantization method but the genetic data and α approximation appropriate to that family.

This definition treats A/B and C/D as **energy-scale choices** in the joint search. Unlike the original convention in [36.3], whether d is subtracted is an independent choice in the Stage13 test. Thus, the C/D label in the joint table does not necessarily mean that d is retained. This distinction is solely a computational convention of the present search and does not yet replace self-consistent calibration of α(N).

Definition of Free Parameters and Objective Function

The shared global parameters are the E_s scale choice and quantization method Q. The family-specific free parameters for family a are σ_a for subtraction of d, δ_a for subtraction of the neutrino contribution, κ_a for the free-energy magnification choice, and L_a for the FCC layer number. σ_a and δ_a are binary; κ_a is selected from 1 and F_a. In the joint search, all four parameters are independent between muon and tau, while only E_s and Q must remain shared.

[36.26] $Q_m = Q_t = Q$

[36.27] $E_{sm} = E_{st} = E_s$

[36.28] $\sigma_a \in \{0,1\}$; $\delta_a \in \{0,1\}$; $\kappa_a \in \{1,F_a\}$; $L_a \in \mathbb{Z} \cap [471,551]$

[36.29] $E_{as}(\sigma_a) = 3N_a/2 - \sigma_a d_a$

[36.30] $E_{axx2} = E_s E_{as}(\sigma_a) F_a + \kappa_a E Extra_a(L_a,\delta_a)/P_a$

[36.31] $RMS_{mt}(\%) = \sqrt{((Error_m(\%)^2 + Error_t(\%)^2)/2)}$

In [36.29], σ_a=1 means subtracting d and σ_a=0 means retaining it. For each pair of global choices, the four family-specific parameters are selected to minimize the absolute mass error for that family; the shared pair is then ranked by RMS_{mt}. This report tests six quantization options, comprising the five methods in [36.1] and the direct $\mathring{N}$ option, with two energy scales. There are therefore 12 shared global combinations. The ten highest-ranked combinations appear in the following table.

Ten Best Results of the Joint Model

|Rank|RMS (%)|Scale|E_s (MeV)|Quantization|Muon subtract d|Muon subtract neutrino|Muon magnify extra|Muon L|Muon N|Muon d|Muon predicted (MeV)|Muon error (%)|Tau subtract d|Tau subtract neutrino|Tau magnify extra|Tau L|Tau N|Tau d|Tau predicted (MeV)|Tau error (%)|

|---:|---:|---:|---:|---:|---:|---:|---:|---:|---:|---:|---:|---:|---:|---:|---:|---:|---:|---:|---:|---:|---:|

|1 | 0.283998459 | C/D | 9.3615269668841921e-06 | 30+Floor60 | True | True | False | 505 | 517470 | 881 | 105.662595734367 | +0.003994226 | True | True | True | 496 | 2069790 | 3527 | 1783.996129381417 | +0.401614611|

|2 | 0.290392407 | C/D | 9.3615269668841921e-06 | Ceil10 | True | True | False | 505 | 517460 | 882 | 105.657347931513 | -0.000972539 | True | True | True | 496 | 2069810 | 3527 | 1784.157132754339 | +0.410675729|

|3 | 0.293587619 | C/D | 9.3615269668841921e-06 | Ceil30 | True | True | False | 505 | 517470 | 881 | 105.662595734367 | +0.003994226 | True | True | True | 496 | 2069820 | 3528 | 1784.237103017317 | +0.415176380|

|4 | 0.293658889 | C/D | 9.3615269668841921e-06 | Round30 | True | False | False | 501 | 517440 | 882 | 105.668923342194 | +0.009982968 | True | True | True | 496 | 2069820 | 3528 | 1784.237103017317 | +0.415176380|

|5 | 0.303219434 | C/D | 9.3615269668841921e-06 | 30+Round60 | True | True | False | 505 | 517470 | 881 | 105.662595734367 | +0.003994226 | True | True | True | 496 | 2069850 | 3527 | 1784.479147835146 | +0.428798433|

|6 | 0.367019037 | A/B | 9.3723441902457908e-06 | 30+Floor60 | True | False | False | 500 | 517470 | 881 | 105.617910491824 | -0.038297965 | True | True | True | 496 | 2069790 | 3527 | 1786.057532897746 | +0.517628451|

|7 | 0.373627006 | A/B | 9.3723441902457908e-06 | Ceil10 | True | False | False | 500 | 517460 | 882 | 105.613781306449 | -0.042206019 | True | True | True | 496 | 2069810 | 3527 | 1786.218722309704 | +0.526700039|

|8 | 0.376579408 | A/B | 9.3723441902457908e-06 | Round30 | False | True | False | 504 | 517440 | 882 | 105.698531298888 | +0.038005315 | True | True | True | 496 | 2069820 | 3528 | 1786.298784978141 | +0.531205890|

|9 | 0.376594232 | A/B | 9.3723441902457908e-06 | Ceil30 | True | False | False | 500 | 517470 | 881 | 105.617910491824 | -0.038297965 | True | True | True | 496 | 2069820 | 3528 | 1786.298784978141 | +0.531205890|

|10 | 0.386213266 | A/B | 9.3723441902457908e-06 | 30+Round60 | True | False | False | 500 | 517470 | 881 | 105.617910491824 | -0.038297965 | True | True | True | 496 | 2069850 | 3527 | 1786.541109478213 | +0.544843684|

Analysis of the Joint-Model Results

The first-ranked result uses the C/D scale, $30{+}\mathrm{Floor}_{60}$ quantization, and RMS of 0.283998459%. In this case, the muon has N=517470, d=881, L=505, subtraction of d and the neutrino contribution, and no magnification of additional energy, yielding a mass of 105.662595734367 MeV and an error of +0.003994226%. The tau uses the same scale and quantization method, but N=2069790, d=3527, L=496, subtraction of d and the neutrino contribution, and **magnification** of additional energy, yielding a mass of 1783.996129381417 MeV and an error of +0.401614611%.

The second-ranked result, with Ceil_{10} quantization and the same C/D scale, reduces the muon error to −0.000972539%, but increases the tau error to +0.410675729%. Its joint RMS is therefore 0.290392407%, higher than that of the first-ranked result. This difference shows that minimizing the muon error alone is not equivalent to minimizing the joint objective function.

The C/D scale is selected in the first five ranks. The first A/B result is sixth, with RMS of 0.367019037%. In addition, among the ten best ranks the optimal tau layer is L=496, while the optimal muon layer is L=500, 501, 504, or 505 depending on the case. Imposing a single layer on both families is therefore not a condition of the present joint model. In all ten leading ranks, free-energy magnification is disabled for the muon and enabled for the tau. This distinction is a feature of the results of this bounded search, not proof of a universal law for all generations.

These numbers result from choosing the best cases within a bounded range of layers and discrete options. α(N) has not been recalibrated for each N, and family-specific choices have been optimized independently. The reported RMS measures the quality of fit within this search space. Under this definition, **the two shared global choices** are retained while the detailed muon and tau mechanisms are optimized by family.

Theorem 37: Relativistic Dynamics

The Origin of Inertia and Relativistic Kinetic Energy in Ramionics

In Ramionics, a particle is not an independent geometric point, but a stable pattern of energy distribution in the FCC network of Ramions.

In this picture, the mass of a body arises from the spatial distribution of its equivalent energy, and inertia is likewise the result of the interaction of that energy distribution with itself (self-interaction). In other words, mass is subject to its own gravitational and pressure field, and changing its motion requires rearranging that same energy pattern along with it.

Thus, without requiring a Higgs field or Higgs particle, Ramionics explains the origin of mass inertia through the spatial structure of energy itself.

The Principle of Acceleration and Ramionic Equivalence

If a body moves with acceleration a, Ramionics treats this acceleration as an effective gravitational field:

[37.1] $g = a$

The inertial force is therefore the internal gravitational-pressure response of the body's energy distribution to a change in its state of motion.

From this perspective:

[37.2] $F = ma$

is not an independent principle, but the effective expression of the pressure and self-gravity of the body's energy distribution in response to acceleration.

Finite Propagation of the Field

When a body moves at speed v, its energy pattern cannot adjust instantaneously to the body's new position, because propagation of the energy field is limited by speed c.

If, during the time interval ∂t, the body is displaced by ∂x:

[37.3] $\partial x = v\partial t$

During the same interval, the field has time to propagate only as far as the following radius:

[37.4] $R^i = c\partial t$

In this model, it is assumed that the geometry of effective field propagation and the body's displacement can be represented by a right triangle; this assumption is an independent premise in the derivation of the Lorentz factor.

The Propagation Triangle and the Lorentz Factor

During ∂t:

- The field propagates at speed c.

- The body moves at speed v.

- The effective component of field propagation is R.

Thus:

c∂t

is the hypotenuse of the propagation triangle.

v∂t

is the body's displacement along its direction of motion.

And:

R∂t

is the effective component of field propagation.

Therefore, by the Pythagorean relation:

[37.5] $(c\partial t)^2 = (v\partial t)^2 + (R\partial t)^2$

Dividing by:

$(c\partial t)^2$

gives:

[37.6] $1 = v^2/c^2 + R^2/c^2$

Hence:

[37.7] $R/c = \sqrt{(1 - v^2/c^2)}$

And consequently:

[37.8] $R = c\sqrt{(1 - v^2/c^2)}$

Thus, the effective radius of field propagation in the direction of motion is reduced by the following factor:

[37.9] $\lambda = \sqrt{(1 - v^2/c^2)}$

Amplification of the Moving Field

In the Ramionic Newtonian approximation, the body's field function is:

[37.10] $f_0(R) = R_s/R$

where:

[37.11] $R_s = 2Gm/c^2$

is the body's effective Schwarzschild radius.

When the effective propagation radius decreases from R to:

[37.12] $R\sqrt{(1 - v^2/c^2)}$

the field density is amplified by the inverse of the same factor:

[37.13] $f_v/f_0 = 1/\sqrt{(1 - v^2/c^2)}$

Therefore:

[37.14] $f_v(R) = f_0(R)/\sqrt{(1 - v^2/c^2)}$

or:

[37.15] $f_v(R) = R_s/(R\sqrt{(1 - v^2/c^2)})$

Thus, the Lorentz factor is obtained directly from the geometry of finite field propagation.

Field Energy Integral

In Ramionics, f itself is the energy-density factor of a Ramion. Therefore, the field energy is obtained from:

[37.16] $E = 4\pi\rho_s\varphi\int f(R)R^2 dR$

For the rest state:

[37.17] $E_0 = 4\pi\rho_s\varphi\int_{(R_s)}^{R_i} f_0(R)R^2 dR$

And for the moving state:

[37.18] $E_v = 4\pi\rho_s\varphi\int_{(R_s)}^{R_i} f_v(R)R^2 dR$

Substituting the relation for f_v:

[37.19] $E_v = 1/\sqrt{(1 - v^2/c^2)} \cdot 4\pi\rho_s\varphi\int_{(R_s)}^{R_i} f_0(R)R^2 dR$

Hence:

[37.20] $E_v = E_0/\sqrt{(1 - v^2/c^2)}$

If the body's effective rest energy is:

[37.21] $E_0 = mc^2$

then the total energy of the moving body is:

[37.22] $E_v = mc^2/\sqrt{(1 - v^2/c^2)}$

Relativistic Kinetic Energy

Kinetic energy is the difference between the energy of the moving field and the rest energy:

[37.23] $K(v) = E_v - E_0$

Therefore:

[37.24] $K(v) = mc^2(1/\sqrt{(1 - v^2/c^2)} - 1)$

This is the relativistic formula for kinetic energy.

Newtonian Limit

For small speeds:

$v \ll c$

The expansion of the relativistic factor is:

[37.25] $1/\sqrt{(1-v^2/c^2)} \approx 1+½v^2/c^2+3v^4/(8c^4)+...$

Hence:

[37.26] $K(v) \approx ½mv^2+3mv^4/(8c^2)+...$

Consequently:

[37.27] $K(v \ll c) \approx ½mv^2$

which is the Newtonian limit.

Rotational Motion and Field Return

In linear motion, the field shells continuously lag behind the body, and the energy pattern moves as an open drift. As a result, field coherence decreases and the Lorentz factor appears.

In rotational motion, however, after one full revolution the field shells return to the same region, and the leading and trailing portions of the field overlap.

Consequently, field coherence is preserved to a much greater extent in rotational motion than in linear motion.

Therefore, relativistic deformation in rotational motion is weaker than in linear motion.

Ramionic Rotational Factor

During rotational motion, the field continuously overlaps with itself. Thus, field accumulation is limited and Lorentzian divergence does not occur.

In the simplest proposed model of rotational overlap, the overlap contribution is defined by the following independent assumption; this factor is not proven solely by the return of the shells:

[37.28] $q_{rot} = v^2/(2c^2)$

Therefore, the rotational field factor is:

[37.29] $\gamma_{rot} = 1/(1 - v^2/(2c^2))$

Unlike the linear factor:

[37.30] $\gamma = 1/\sqrt{(1 - v^2/c^2)}$

this factor does not diverge as:

$v \to c$

Instead, it gives:

[37.31] $\gamma_{rot,max} = 2$

Ramionic Rotational Energy

For a mass element:

dm

at radius:

r

the resulting relation is:

[37.32] $v = \omega r$

Therefore, the total energy of that mass element is:

[37.33] $dE_{rot} = dm\, c^2/(1 - \omega^2 r^2/(2c^2))$

And its kinetic energy is:

[37.34] $dK_{rot} = dE_{rot} - dm\, c^2$

Thus:

[37.35] $dK_{rot} = dm\omega^2 r^2/(2 - \omega^2 r^2/c^2)$

For the entire rotating body:

$E_{rot,total} = \int dE_{rot}$

Therefore:

[37.36] $E_{rot,total} = c^2 \int dm/(1 - \omega^2 r^2/(2c^2))$

And the total kinetic energy is:

[37.37] $K_{rot,total} = E_{rot,total} - Mc^2$

where:

[37.38] $M = \int dm$

Hence:

[37.39] $K_{rot,total} = c^2 \int dm/(1 - \omega^2 r^2/(2c^2)) - Mc^2$

Classical Rotational Limit

For:

$\omega r \ll c$

the resulting relation is:

[37.40] $1/(1 - x) \approx 1 + x$

Therefore:

[37.41] $E_{rot,total} \approx c^2 \int (1+\omega^2 r^2/(2c^2)) dm$

That is:

[37.42] $E_{rot,total} \approx Mc^2 + \frac{1}{2}\omega^2 \int r^2 dm$

Thus:

[37.43] $K_{rot,total} \approx \frac{1}{2} I\omega^2$

which is the classical formula for rotational kinetic energy.

The Ehrenfest Paradox

In standard special relativity, the same linear factor is applied to each point on a rotating disk:

[37.44] $\gamma = 1/\sqrt{(1 - v^2/c^2)}$

where:

$v = \omega R$

is the tangential speed of a point on the disk.

Consequently, the circumference of the disk should undergo Lorentz contraction, whereas the radius, being perpendicular to the motion, does not contract.

Thus, in standard relativity:

[37.45] $C < 2\pi R$

whereas Euclidean geometry states:

[37.46] $C = 2\pi R$

This issue is known as the Ehrenfest paradox.

In Ramionics, this paradox results from directly applying the contraction of linear motion to rotational motion.

This is because, during rotation, the energy field recirculates and different portions of the shell overlap again. Thus, the actual deformation of the field will be much smaller than in linear drift.

In this picture, the circumference of the disk does not undergo full Lorentz contraction, and the geometric relation is approximately preserved:

[37.47] $C \approx 2\pi R$

Consequently, in Ramionics, rotational and linear motion are not completely equivalent in terms of relativistic dynamics.

Linear motion is an open drift of the field, whereas rotational motion is a closed recirculation of the field.

Therefore, the Ehrenfest paradox results from directly applying linear contraction to rotating systems.

Energy Limit of Rotational Motion

In linear motion, the field shells continuously move away from the body and field coherence decreases. Thus, as the speed approaches c, field overlap disappears and the Lorentz factor diverges:

[37.48] $\gamma = 1/\sqrt{(1 - v^2/c^2)}$

Consequently:

[37.49] $E \rightarrow \infty$

In rotational motion, however, the field shells return upon themselves and the leading and trailing portions of the field continuously overlap.

Thus, field coherence is preserved and field accumulation remains bounded.

In the simplest model of rotational overlap, the moving field cannot exceed twice the rest field:

[37.50] $f_{(}max_{)} = 2f_0$

Therefore, the total energy will likewise be at most twice the rest energy:

[37.51] $E_{(}max_{)} = 2mc^2$

Thus, the maximum rotational kinetic energy is:

[37.52] $K_{(}max_{)} = mc^2$

In this picture, unlike linear motion, rotational motion does not lead to Lorentzian divergence because the field shells overlap with themselves again and coherence is preserved.

Consequently:

- Linear motion → open field drift → relativistic divergence.

- Rotational motion → field recirculation → energy saturation.

Thus, in Ramionics, relativistic divergence occurs only for open field propagation, while systems with field recirculation have a finite energy limit.

This result shows that relativistic dynamics depends not only on the magnitude of speed, but also fundamentally on the topology of field propagation.

Galactic and Cluster-Scale Generalization of Relativistic Energy

For displacements on very large scales, the complete Ramionic field function, namely its MOND-like and MOG-like forms, also enters the relativistic energy. In this case, the general relativistic kinetic energy is written as:

[37.53] $K = (\gamma - 1) \cdot 4\pi\rho_s\varphi \int_{R_s}^{R^i} f(R)R^2 dR$

where f(R) is the complete Ramionic field function at local, galactic, and cluster scales.

Complete Ramionic Generalization

In the local derivation, the Newtonian field approximation was used:

[37.54] $f_0(R) = R_s/R$

However, for the generalization to galactic and cluster scales, the current field function of Theorem 34 must be used; the following relation is only its archival form and must not replace the present convention of Theorem 34:

[37.55] $f(R) = R_s/R + (R_s/R_m)E_1(kR/R_d)$

In that case, relativistic dynamics will also contain MOND-like and MOG-like corrections, and special relativity will be the local limit of Ramionic field propagation.

Conclusion

In Ramionics, inertia and relativistic kinetic energy arise from a common origin: the finite propagation of the body's energy pattern.

Mass carries its own energy field. When the body moves, this field cannot adjust instantaneously to the body. The geometry of finite propagation causes effective compression of the field profile, and this compression produces the Lorentz factor.

Therefore:

The same relation for relativistic kinetic energy derived earlier is the final result of this chain of reasoning.

Within this framework, relativistic kinetic energy is the energy required to maintain the coherence of the body's energy pattern during motion.

In linear motion, field coherence decreases and full relativistic deformation appears. In rotational motion, however, the return and renewed overlap of the field shells preserve coherence to a much greater extent, and relativistic deformation is weaker.

.

Theorem 38: Gravitational Time Dilation and Light Deflection

The Common Basis of Gravity, Time, and Light Propagation

The speed of light propagation is not an independent, imposed property; rather, it depends on the energy of the Ramions in the cubic-ball lattice. The energy metric N simultaneously determines the scales of energy, radius, density, pressure, and propagation speed. In the gravity section, relations [41.268] and [41.269] specify the energy-density distribution and the metric N in terms of the field function f(R). Consequently, the same distribution N(R) that produces the gravitational pressure gradient also determines changes in the rates of local processes and in the path of light propagation.

In the relations of this section, N(R) is the ratio of the local metric to the distant reference metric, and is taken to equal one at the distant reference. The symbol c denotes the speed of light propagation in that reference. Using N instead of introducing an independent Lorentz factor preserves the connection between this section and the fundamental definition of the energy metric.

[38.1] $\rho(R)=\rho_u(1-f(R))$

[38.2] $N(R)=\sqrt{(\rho_u/\rho(R))}=1/\sqrt{(1-f(R))}$

[38.3] $c(R)/c=1/N(R)^2$

[38.4] $c(R)=c(1-f(R))$

The speed relation here expresses the same law that maps propagation speed according to Ramion energy. “Effective speed” is merely a designation for propagation speed relative to the distant reference in an inhomogeneous metric distribution; it does not introduce a separate speed into the theory. A local observer measures length and time scales using their own local metric. Therefore, propagation speed relative to the distant reference must be distinguished from local measurements.

Gravitational Time Dilation

According to the fundamental explanation following relation [20.2], a change in the energy metric of the Ramions also changes the time scale of processes. Defining N(R) as the ratio of the local metric to the distant reference, the ratio of the distant-reference time interval to the proper time of a clock stationary at R is expressed in this model by the same N(R). Thus:

[38.5] $dt=N(R)d\tau_{loc}$

[38.6] $d\tau_{loc}/dt=1/N(R)=\sqrt{(1-f(R))}$

In the Newtonian regime of a spherical mass, the field function and corresponding metric are:

[38.7] $R_s=2GM/c^2$

[38.8] $f(R)\approx R_s/R$

[38.9] $N(R)\approx 1/\sqrt{(1-R_s/R)}$

[38.10] $d\tau_{loc}/dt\approx\sqrt{(1-2GM/(Rc^2))}$

Therefore, as the energy metric N increases near a mass, the rate of a stationary local clock decreases relative to the distant reference. This result follows from combining the Ramionic time-mapping law with the metric distribution in the gravity section. The specific form N(R) in this approximation is obtained from the field function adopted in the gravity section; independently deriving the field function from the microscopic distribution of Ramions is a separate problem from this substitution.

Metric Gradient and Gravitational Acceleration

From relations [34.6] and [34.7] for signed radial acceleration, together with the definition of N(R), it follows that:

[38.11] $g(R)=c^2/[2(1-f(R))]df(R)/dR$

[38.12] $g(R)=c^2/N(R)\times dN(R)/dR$

For the field of a spherical mass, the derivative of N with respect to R is negative; hence, under this sign convention, g points toward the mass. This relation shows that gravitational acceleration and time dilation are both associated with the same distribution N(R).

Refractive Index Due to the Energy Distribution and Light Deflection

From the fundamental propagation-speed law in relations [20.2] and [20.5], the refractive index relative to the distant reference follows without introducing a separate law for light:

[38.13] $n(R)=c/c(R)=N(R)^2=1/(1-f(R))$

In the Newtonian regime and weak field:

[38.14] $f(R)\approx R_s/R\ll 1$

[38.15] $n(R)\approx 1+R_s/R=1+2GM/(Rc^2)$

For a ray traveling approximately along the x direction at first order, with impact parameter b relative to the mass center:

[38.16] $R=\sqrt{(x^2+b^2)}$

[38.17] $\partial n/\partial b\approx -R_s b/(x^2+b^2)^{3/2}$

In the geometric approximation for wave propagation through a medium with a variable refractive index, the magnitude of the first-order deflection angle is obtained by integrating the transverse gradient of the refractive index along the straight path:

[38.18] $\alpha\approx -\int_{-\infty}^{+\infty}(\partial n/\partial b)dx$

[38.19] $\alpha \approx R_s b \int_{-\infty}^{+\infty} dx/(x^2+b^2)^{3/2}$

[38.20] $\int_{-\infty}^{+\infty} dx/(x^2+b^2)^{3/2} = 2/b^2$

[38.21] $\alpha \approx 2R_s/b = 4GM/(bc^2)$

Thus, in the Newtonian regime, the propagation-speed gradient arising from the same N(R) distribution reproduces the leading-order light-deflection angle of general relativity. Using the ray law in an inhomogeneous medium is a geometric-propagation approximation; a more precise wave description requires propagation dynamics in the cubic-ball lattice.

Second Route: Direct Calculation from the Field-Function Gradient

In the first route, deflection was obtained from the gradient of the refractive index n(R). The archival route, in the weak-field approximation, expresses the same calculation directly in terms of the gradient of the field function f(R). These two approaches are equivalent only to first order, because the exact definition of the refractive index gives:

[38.26] $\partial n/\partial b = (\partial f/\partial b)/(1-f)^2$

In the weak-field limit, the factor $(1-f)^{-2}$ approaches one; hence, to first order, the refractive-index gradient equals the field-function gradient. For a spherical field and a straight path with impact parameter b:

[38.27] $\partial f/\partial b \approx -R_s b/(x^2+b^2)^{3/2}$

Therefore, in the same geometric and first-order approximation, the second route yields the integral:

[38.28] $\alpha \approx -\int_{-\infty}^{+\infty} (\partial f/\partial b)\, dx$

[38.29] $\alpha \approx R_s b \int_{-\infty}^{+\infty} dx/(x^2+b^2)^{3/2} = 2R_s/b = 4GM/(bc^2)$

Thus, the route based on n(R) is logically prior because it begins with the propagation law and refractive index; the route based on f(R) is the simplified form of the same calculation in a weak field. In a strong field or with the complete field function, directly replacing ∂n by ∂f without the factor $(1-f)^{-2}$ is not permissible; the ray equation must also be solved for a nonstraight light path.

Comparison with Newtonian Gravity Acting on a Hypothetical Photon Mass

For comparison, if light were treated merely as a particle traveling at speed c under Newtonian transverse acceleration, without accounting for the change in propagation speed arising from the energy metric, the analysis would have:

[38.22] $a_\gamma \approx -GMb/(x^2+b^2)^{3/2}$

[38.23] $\alpha_n \approx -(1/c^2) \int_{-\infty}^{+\infty} a_\gamma\, dx$

[38.24] $\alpha_n \approx 2GM/(bc^2) = R_s/b$

However, when the propagation-speed gradient dependent on N is included, the preceding result becomes:

[38.25] $\alpha/\alpha_n \approx 2$

Consequently, the deflection caused by the energy-metric distribution of Ramions is, to first order, **twice** that of the Newtonian model in which gravity acts on a hypothetical photon mass. The factor of two arises from the fundamental dependence of propagation speed on N^{-2} and, consequently, the refractive index N^2—not from attributing rest mass to the photon or adding an arbitrary refractive-index factor.

| Model | Weak-field deflection | Relative factor |

|---|---|---:|

| Newtonian hypothetical photon mass | $2GM/(bc^2)$ | 1 |

| Ramionics N-gradient propagation | $4GM/(bc^2)$ | 2 |

| General relativity, leading order | $4GM/(bc^2)$ | 2 |

Scope of the Result

These two derivations apply to a weak spherical field, an approximately straight path, and geometric propagation. At stellar, galactic, and cluster scales, the refractive-index gradient can deflect light like a lens and, under suitable configurations, produce multiple images or an Einstein ring. At these scales, the complete Ramionics field function, including model-dependent corrections and, where necessary, the FCC-Hubble contribution, must be substituted into N(R) and n(R), and the ray path must be solved. Any additional lensing contribution of the model is not considered demonstrated without calculating the path and comparing it with observations. Reproducing the deflection coefficient in the Newtonian limit demonstrates computational consistency of the model within that same limit.

Theorem 39: Strong and Weak Forces, Entropy Equilibrium, and Matter–Energy Exchange

Fundamental Interactions in Ramionics

In the Standard Model of physics, there are four independent fundamental interactions:

- Gravity,

- Electromagnetism,

- The strong interaction,

- And the weak interaction.

In this picture, each interaction has its own independent carrier particle.

In Ramionics, however, independent fundamental interactions do not exist.

All interactions are different modes of propagation, overlap, compression, and projection of a single Ramionic field.

Therefore:

- The strong interaction,

- The weak interaction,

- Electromagnetism,

- And gravity

are all different states of one fundamental field.

The Twelve-Ball Structure and Charge Quantization

Each Ramion has twelve FCC balls, organized into six opposing pairs.

To maintain torque equilibrium, the two opposite balls in each pair must rotate in opposite directions as viewed from the center, so that:

$$[39.1] \quad \sum \tau = 0$$

is preserved.

However, when those same two balls are viewed externally from opposite sides, their apparent directions of rotation have the same sign.

Thus each opposing pair acts as one effective contribution to charge.

Consequently, twelve balls become six effective charge contributions.

If the contribution of each part is q/6, the total charge can take only seven values: 0, ±⅓, ±⅔, ±1. These are precisely the observed charges of fundamental particles.

The Neutrino and Local Polarization

In Ramionics, the neutrino is not a structureless particle.

The neutrino has local rotational polarization: $6(+q/6) + 6(-q/6)$.

Therefore:

[39.2] $q_{net} = 0$

But at short distances:

[39.3] $q_{local} \neq 0$

Consequently, the neutrino has a very weak short-range interaction, even though its net charge is zero.

Thus the weak interaction may arise from the local polarization of this same rotational structure.

The Weak Interaction in Ramionics

In the Standard Model, the weak interaction is mediated by weak carrier particles.

In Ramionics, however, the weak interaction is not an independent fundamental interaction.

The weak interaction is a highly attenuated and highly localized mode of overlap of the rotational field.

In this picture:

- Beta decay,

- Neutrino interactions,

- Changes in quark type,

- And nuclear processes

are all local rearrangements of the Ramionic field.

Therefore, Ramionics does not require an independent carrier particle to explain the weak interaction.

The strength of the weak interaction relative to electromagnetism is approximately 10^{-5}.

Consequently:

[39.4] $F_{weak} \approx 10^{-5} F_{EM}$

This weakness results from the severe attenuation of field propagation in this mode.

The Strong Interaction in Ramionics

In conventional physics, the strong interaction is approximately 10^{38} times stronger than Newtonian gravity.

In Ramionics, this difference arises from the distinction between the short-range and long-range fields.

Newtonian gravity is a long-range, diluted projection of the Ramionic field:

[39.5] $G = G_s.K_{\varphi}.144/(N^8.(1 - 1/N))$

But the short-range quark interaction is controlled directly by the fundamental coefficient G_s.

At extremely short distances, the FCC geometric dilution has not yet occurred completely, and therefore the interaction remains very strong.

Energy of Constituent Components and the Strong Interaction

In Ramionics, the fundamental interaction depends on the actual energy content of the constituent components.

The up quark has a coefficient of 2, and the down quark has a coefficient of 24/19.

Their interaction therefore produces the following coefficient:

[39.6] $2.24/19 = 48/19$

Furthermore, in the short-range interaction, the volumetric factor φ^5 associated with the interior of the Ramion is removed.

The initial ratio of the short-range field to long-range gravity is:

[39.7] $144G_s/G \approx 7.76\times10^{36}$

Removing the volumetric coefficient gives:

[39.8] $1/\varphi^5 \approx 4.50$

And applying the quark coefficient:

[39.9] $48/19 \approx 2.53$

the result is: $7.76\times10^{36}.4.50.2.53$.

Thus:

[39.10] $F_{(strong)}/F_{(gravity)} \approx 8.8\times10^{37}$

This is effectively of the same known order of magnitude, 10^{38}, for the ratio of the strong interaction to gravity.

Thus, in Ramionics, the strong interaction is not an independent fundamental interaction. Rather, it is the compressed, short-range state of the Ramionic field, while Newtonian gravity is the long-range, diluted version of that same field.

Elimination of Carrier Particles and the Higgs Field

In Ramionics:

- Inertia arises from field self-interaction,

- Gravity from field projection,

- The strong interaction from compressed overlap,

- The weak interaction from attenuated overlap,

- And electromagnetism from the rotational field.

Therefore, there is no need for:

- A graviton,

- The Higgs field,

- Gluons,

- Or weak-interaction carrier particles.

All interactions are different modes of propagation of the Ramionic field.

Entropy Equilibrium and Matter–Energy Exchange

In Ramionics, the conversion of matter and energy is not an independent act of annihilation or creation, but a rearrangement of the Ramionic field.

Thus, the weak interaction and decay processes are also different modes of energy exchange and redistribution within the FCC network.

Within this framework, entropy is likewise the result of redistribution of field structures, rather than an independent increase in random disorder.

Matter–Antimatter Asymmetry

Within the Ramionics framework, matter–antimatter asymmetry and the predominance of matter in the universe may be consequences of the overall polarization and orientation of the Ramionic field. At present, this explanation is a mechanical hypothesis and does not provide an independent quantitative derivation of the magnitude of the asymmetry.

Conclusion

In Ramionics, the strong and weak interactions are not independent fundamental forces.

The strong interaction arises from compressed overlap of the short-range field, whereas the weak interaction arises from localized, attenuated overlap.

The twelve-ball FCC structure naturally produces charge quantization into 0, ±⅓, ±⅔, and ±1.

The neutrino has local polarization, and its weak interaction arises from this structure.

Consequently, Ramionics explains:

- Interactions,

- Charge quantization,

through the geometry and dynamics of a single field.

Preserve

Draft: Strong Gravity

Introduction — The Fundamental Ramion Energy Relation, Projection Powers, and Projection of Fundamental Constants

1. Fundamental Ramion Energy Relation

A Ramion is a three-dimensional quantum of energy–space–time, and its various parameters are different representations of a single energy. Ramion energy is divided into two equal components: linear–radial and rotational–angular. The linear component is associated with space, pressure, radial force, mass, and gravity; the rotational component is associated with time, torque, charge, and electrical interaction.

For a general Ramion:

[39.11] $E_r=m_r c_r^2=I_r\omega_r^2=2\hat{E}_r=2\check{E}_r=\rho_r V_r=2P_r V_r=2r_r F_r/3=2(\frac{1}{2}G_r m_r^2/r_r)=2[(1/K_p)(\frac{1}{2}K_r q_r^2/r_r)]$

For the reference Ramion E_s, the same relations hold with the subscript s in place of r.

For each particle ball, the same relations also hold with the subscript w in place of r. Because the ball's energy consists of discrete units, its gravitational and electric potentials are corrected relative to the continuous case by the quantum coefficient η_w^2.

1.1. Quantum Coefficient η

η is the quantum coefficient for converting a continuous potential into a discrete potential.

For each ball, there are N discrete units of energy or charge. If the structure is initially treated as continuous, for a final charge Nq_s:

[39.12] $S_c=\int\{0 \text{ to } Nq_s\}\{(K_sQ/r)dQ\}$

Therefore:

[39.13] $S_c=K_s(Nq_s)^2/(2r)$

In the discrete case, units of q_s are added one at a time:

[39.14] $S_d=\Sigma\{j=1 \text{ to } N\}\{[K_s(j-1)q_s/r]q_s\}$

Thus:

[39.15] $S_d=(K_sq_s^2/r)\Sigma\{j=1 \text{ to } N\}\{j-1\}$

And:

[39.16] $\Sigma\{j=1 \text{ to } N\}\{j-1\}=N(N-1)/2$

Therefore:

[39.17] $S_d=K_sq_s^2N(N-1)/(2r)$

For the full two-sided potential:

[39.18] $U_d=2S_d=K_s(Nq_s)^2(1-1/N)/r$

And in the continuous case:

[39.19] $U_c=2S_c=K_s(Nq_s)^2/r$

Hence:

[39.20] $U_d/U_c=1-1/N$

the definition is:

[39.21] $\eta^2=1-1/N$

And:

[39.22] $\eta=\sqrt{(1-1/N)}$

For w balls and a total of wN discrete units:

[39.23] $\eta_w^2=1-1/(wN)$

And:

[39.24] $\eta_w=\sqrt{[1-1/(wN)]}$

The same structure applies to the gravitational potential, because it, too, consists of the sum of interactions among discrete mass–energy units.

Therefore:

[39.25] $U_d=\eta^2U_c$

And:

[39.26] $U_c=U_d/\eta^2$

Consequently, in the gravitational and electric potentials of a ball, the conversion from the discrete state to the continuous state is performed using η^{-2}.

1.2. Pressure, Density, and Force

Pressure is half the energy density:

[39.27] $P_s=\rho_s/2$

Therefore:

[39.28] $E_s=\rho_s V_s$

And:

[39.29] $E_s=2P_s V_s$

The Ramion energy–force relation:

[39.30] $E_s=2r_s F_s/3$

Hence:

[39.31] $F_s=3E_s/(2r_s)$

For a sphere:

[39.32] $V_s=A_s r_s/3$

Thus:

[39.33] $E_s=2P_s A_s r_s/3$

And:

[39.34] $F_s=P_s A_s$

2. Projection Powers for Energy NE_s

If the energy of a Ramion or a ball becomes N times that of the reference Ramion:

[39.35] $E_(N)=NE_s$

The projection powers, respectively, are:

Parameter	Projection
Energy E, radius r, charge q, and absolute mass m	N^1
Surface area A	N^2
Volume V	N^3
Energy density ρ, pressure P, external speed c, and internal speed $\mathring{c}$	N^{-2}
Time rate	N^{-1}
Planck constant ħ	N^4
Local relative mass $\mathring{m}$	N^5
Gravitational constant G	N^{-8}
Internal Coulomb constant $\mathring{K}$	N^0
External FCC Coulomb constant K	N^2

2.1. Energy, Radius, and Force Equilibrium

When energy increases by a factor of N, for the force of each Ramion to remain constant:

[39.36] $F_{(N)}=F_s$

From the energy–force relation:

[39.37] $F_{(N)}=3E_{(N)}/(2r_{(N)})$

Hence:

[39.38] $E_{(N)}/r_{(N)}=E_s/r_s$

And consequently:

[39.39] $r_{(N)}=Nr_s$

Thus, a Ramion with energy NE_s generates N times more radial space than the reference Ramion with energy E_s.

2.2. Surface Area

From the radius projection:

[39.40] $A_{(N)}=N^2A_s$

2.3. Volume

From the radius projection:

[39.41] $V_{(N)}=N^3V_s$

2.4. Pressure from Force Equilibrium

From:

[39.42] $F=PA$

And the constancy of force:

[39.43] $P_{(N)}A_{(N)}=P_sA_s$

Therefore:

[39.44] $P_{(N)}=P_s/N^2$

2.5. Energy Density

Since pressure is half the density:

[39.45] $\rho_{(N)}=\rho_s/N^2$

The same result is obtained from the ratio of energy to volume:

[39.46] $\rho_{(N)}=E_{(N)}/V_{(N)}$

Thus:

[39.47] $\rho_{(N)}=(NE_s)/(N^3V_s)=\rho_s/N^2$

2.6. Force, Pressure, and Volume Equilibrium

The energy relation:

[39.48] $E=2PV=2rF/3$

Therefore:

[39.49] $PV=rF/3$

Under the N projection:

[39.50] $P_{(N)}V_{(N)}=(P_s/N^2)(N^3V_s)=NP_sV_s$

And:

[39.51] $r_{(N)}F_{(N)}=(Nr_s)F_s$

Also:

[39.52] $P_{(N)}A_{(N)}=(P_s/N^2)(N^2A_s)=P_sA_s$

2.7. Internal and External Speeds

The linear speed of light in external space and the rotational or linear speed of energy inside a Ramion both change with the power N^{-2}:

[39.53] $c_{(N)}=c_s/N^2$

[39.54] $\mathring{c}_{(N)}=\mathring{c}_s/N^2$

2.8. Absolute Mass

Absolute mass, like energy, has the projection N^1:

[39.55] $m_{(N)}=Nm_s$

2.9. Local Relative Mass

From:

[39.56] $E_{(N)}=\mathring{m}_{(N)}\mathring{c}_{(N)}^2$

The resulting relation is:

[39.57] $\mathring{m}_{(N)}=E_{(N)}/\mathring{c}_{(N)}^2$

Thus:

[39.58] $\mathring{m}_{(N)}=N^5\mathring{m}_s$

2.10. Planck Constant

From:

[39.59] $E_{(N)}r_{(N)}=\hbar_{(N)}c_{(N)}$

And the energy, radius, and speed projections:

[39.60] $\hbar_{(N)}=N^4\hbar_s$

Because:

[39.61] $N^1N^1=N^4N^{-2}$

2.11. Gravitational Constant

For gravitational energy:

[39.62] $E_{(N)}\propto G_{(N)}\mathring{m}_{(N)}^2/r_{(N)}$

Local mass has the power N^5, its square has N^{10}, and radius has N^1. Therefore:

[39.63] $G_{(N)}=G_s/N^8$

Because:

[39.64] $N^{-8}N^{10}/N^1=N^1$

2.12. Internal and External Coulomb Constants

The charge of a ball:

[39.65] $q_{(N)}=Nq_s$

Thus:

[39.66] $q_{(N)}^2/r_{(N)}=Nq_s^2/r_s$

Therefore:

[39.67] $\mathring{K}_{(N)}=K_s$

And for the external FCC Coulomb constant:

[39.68] $K_{(N)}\propto N^2K_s$

2.13. Time

Because space expands under the N projection and speed decreases under the N^{-2} projection, time also expands or dilates under the N projection:

[39.69] $D_t=N$

And the time rate:

[39.70] $Rate_t=1/N$

That is, reference Ramions with energy E_s perceive the NE_s Ramion as larger and slower, whereas the NE_s Ramion perceives them as smaller and faster—that is, contracted and fast.

However, each observer measures the other observer's space using their own time scale; consequently, all observers measure the speed of light as c.

3. Projection of the Internal Speed of a Ramion to the FCC Speed of Light

[39.71] $K_p=K_k=K_h=K_c=1$

For the E_s Ramion:

[39.72] $c=c_s=(K_c/\varphi)\mathring{c}_s$

Thus:

[39.73] $\mathring{c}_s=(\varphi/K_c)c$

For a Ramion or ball with energy NE_s:

[39.74] $c_e=c_{(N)}=c_s/N^2$

And:

[39.75] $\mathring{c}_e=\mathring{c}_{(N)}=\mathring{c}_s/N^2$

Therefore:

[39.76] $c_{(N)}=(K_c/\varphi)\mathring{c}_{(N)}$

Speed projection factors

| Factor | Description |

|---|---|

| $1/\varphi$ | Conversion of the internal speed of energy into the corresponding linear speed in FCC space |

| N^{-2} | Speed projection from the base Ramion to a Ramion or ball with energy NE_s |

The FCC volume packing fraction:

[39.77] $\varphi=\pi/(3\sqrt{2})$

4. Gravitational Constant at the Ramion Scale

For the surface representation:

[39.78] $E_s=2\hat{E}_s=2(½G_sm_s^2/r_s)$

For the volume representation:

[39.79] $E_s=2\hat{E}_{sv}=2[(6/5)(½G_{sv}m_s^2/r_s)]$

Therefore:

[39.80] $G_s=(6/5)G_{sv}$

And:

[39.81] $G_{sv}=(5/6)G_s$

5. Electric–Rotational Energy of a Ramion

[39.82] $E_s=2\check{E}_s=2[(1/K_p)(½K_sq_s^2/r_s)]$

Thus:

[39.83] $E_sr_s=K_sq_s^2/K_p$

And:

[39.84] $K_sq_s^2=K_pE_sr_s$

6. Relation and Projection of the Planck Constant

The Planck relation for the base Ramion:

[39.85] $E_sr_s=\hbar_sc_s$

For the NE_s Ramion:

[39.86] $E_{(N)}r_{(N)}=\hbar_{(N)}c_{(N)}$

Thus:

[39.87] $\hbar_{(N)}=N^4\hbar_s$

The complete projection of the Planck constant:

[39.88] $\hbar=\hbar_e=[K_h2\times12^25(\varphi/K_c)N^4]\hbar_s$

And in the reverse direction:

[39.89] $\hbar_s=K_c\hbar/[K_h2\times12^25\varphi N^4]$

Planck constant projection factors

| Factor | Description |

|---|---|

| 2 | Structural doubling factor |

| 12^2 | One factor of 12 from the complete twelve-ball structure, and one factor of 12 from its time or frequency scale relative to a ball |

| 5 | Ratio of the particle's inertia to the ball's inertia |

| φ | Conversion of internal speed to external FCC speed |

| N^4 | Projection power of the Planck constant |

The inertia ratio:

[39.90] $I_p/I_{ℯ}=(10/3)/(2/3)=5$

For one ball:

[39.91] $\hbar_{ℯ}\propto5(\varphi/K_c)N^4\hbar_s$

7. Charge Projection

For each ball:

[39.92] $q_{(N)}=Nq_s$

For the twelve-ball structure:

[39.93] $q_e=12Nq_s$

Therefore:

[39.94] $q_e^2=12^2N^2q_s^2$

8. FCC Geometric Factors

Volume packing fraction:

[39.95] $\varphi=\pi/(3\sqrt{2})$

Radial freedom coefficient:

[39.96] $\gamma=\sqrt[3]{[(10/8)/(3\varphi)]}$

Surface coverage coefficient:

[39.97] $\beta=(10/8)/(2\gamma^2)$

And:

[39.98] $\beta=\sqrt[3]{(5\pi^2)}/4$

9. Projection of the Coulomb Constant

[39.99] $K_e=(K_k\varphi N^2\beta/(4\pi\eta^2))K_s$

Thus:

[39.100] $K_e/K_s=K_k\varphi N^2\beta/(4\pi\eta^2)$

Coulomb constant projection factors

Factor	Description
φ	Geometric conversion between the internal space of a Ramion and FCC space
N^2	Surface-area projection
β	FCC surface coverage coefficient
$1/(4\pi)$	Conversion of the complete spherical surface
$1/\eta^2$	Conversion of the discrete potential to its corresponding continuous potential

10. Ramion Fine-Structure Constant and Its Projection

This section continues in the next volume, beginning with formula [39.101].

10. The Ramion Fine-Structure Constant and Its Projection

For the base Ramion:

[39.101] $\alpha_s=K_sq_s^2/(\hbar_sc_s)$

From the electrical-energy and Planck relations:

[39.102] $\alpha_s=K_p$

For the electron:

[39.103] $\alpha_e=K_eq_e^2/(\hbar_ec)$

Substituting the projections:

[39.104] $\alpha_e=(K_pK_kK_c/K_h)\beta/(40\pi\eta^2)$

And:

[39.105] $\alpha_e^{-1}=[K_h/(K_pK_kK_c)]40\pi\eta^2/\beta$

11. Energy of the Base Ramion

[39.106] $E_s=E_e/E_{es}$

And:

[39.107] $E_{es}\approx 3N/2$

For:

[39.108] $N=36390$

The resulting relation is:

[39.109] $E_{es}\approx 54585$

Therefore:

[39.110] $E_s\approx E_e/54585$

With the electron energy:

[39.111] $E_e=0.510998950700551\text{MeV}$

the result is:

[39.112] $E_s\approx 9.36152698910967\text{eV}$

And:

[39.113] $E_s\approx 1.49988198005119_{(10)}{}^{-18}\text{J}$

12. Fundamental Parameters of the Ramion

From the Planck projection:

[39.114] $\hbar_s\approx 5.63990549106573_{(10)}{}^{-56}(K_c/K_h)\text{J.s}$

From the speed projection:

[39.115] $\mathring{c}_s\approx 2.21990466106126_{(10)}{}^{8}/K_c\text{m/s}$

And:

[39.116] $c_s=c=2.99792458_{(10)}{}^{8}\text{m/s}$

From the Planck relation:

[39.117] $r_s=\hbar_s c_s/E_s$

Therefore:

[39.118] $r_s\approx 1.12728944846487_{(10)}{}^{-29}(K_c/K_h)\text{m}$

The absolute mass corresponding to the energy of the base Ramion:

[39.119] $m_s=E_s/c_s{}^2$

Thus:

[39.120] $m_s\approx 1.66884376917777_{(10)}{}^{-35}\text{kg}$

The relative local mass:

[39.121] $\mathring{m}_s=E_s/\mathring{c}_s{}^2$

Consequently:

[39.122] $\mathring{m}_s\approx 3.04360606813017_{(10)}{}^{-35}K_c{}^2\text{kg}$

The Ramion energy density:

[39.123] $\rho_s=E_s/[(4/3)\pi r_s^3]$

Therefore:

[39.124] $\rho_s\approx 2.49955186219761_{(10)}^{68}(K_h/K_c)^3 J/m^3$

The energy density of FCC space:

[39.125] $\rho_u=\varphi\rho_s$

Thus:

[39.126] $\rho_u\approx 1.85086938693329_{(10)}^{68}(K_h/K_c)^3 J/m^3$

The surface gravitational constant of the Ramion, from relation (68):

[39.127] $G_s=E_s r_s/m_s^2$

Therefore:

[39.128] $G_s\approx 6.07101304780823_{(10)}^{22}(K_c/K_h)m^3.kg^{-1}.s^{-2}$

And:

[39.129] $G_{sv}\approx 5.05917753984019_{(10)}^{22}(K_c/K_h)m^3.kg^{-1}.s^{-2}$

The charge of the base Ramion:

[39.130] $q_s=q_e/(12N)$

Thus:

[39.131] $q_s\approx 3.66899476504534_{(10)}^{-25}C$

From the electrical-energy relation:

[39.132] $K_s=K_p E_s r_s/q_s^2$

Therefore:

[39.133] $K_s\approx 125.602517788107(K_pK_c/K_h)N.m^2/C^2$

From the Coulomb projection:

[39.134] $K_e\approx 8.98755178414663_{(10)}^{9}(K_pK_kK_c/K_h)N.m^2/C^2$

And:

[39.135] $\alpha_e\approx 0.00729735256268951(K_pK_kK_c/K_h)$

Strong Gravity

1. Fundamental Separation of Weak Gravity and Strong Gravity in Ramionics

In the current Ramionics framework, weak gravity and strong gravity are not two continuations of a single formula across all distances. Rather, they are two different regimes of energy distribution.

Weak gravity becomes meaningful at large distances. In this description, distant Ramions perceive the central mass as an effective source, and the gravitational distribution can be formally extended down to the Schwarzschild radius, even if the actual object is much larger than that radius.

By contrast, strong gravity is a local, short-range distribution. Nearby Ramions perceive the actual structure of the particle's 12N layers, and the energy distribution is determined by the local FCC geometry and layer-by-layer equilibrium.

G does not enter the fundamental law of this distribution. G appears only in the final comparison with Newtonian weak gravity.

2. Notation for Masses and Layer Metrics

N_{m1} characterizes the central mass, and N_{m2} characterizes the test mass.

N_1, N_2, …, N_n denote only the metrics of the Ramions in the first, second, …, nth layers.

For a neutral particle $12N_{m1}$:

[39.136] $M_1c_s^2=12N_{m1}E_s$

And for the test particle:

[39.137] $M_2c_s^2=12N_{m2}E_s$

Using the definition of the absolute mass of the base Ramion:

[39.138] $M_1=12N_{m1}m_s$

And:

[39.139] $M_2=12N_{m2}m_s$

3. Exact Geometry of FCC Layers and the Importance of +2

The exact number of Ramions in layer n is:

[39.140] $L_n=10n^2+2$

For the first three layers:

[39.141] $L_1=12$

[39.142] $L_2=42$

[39.143] $L_3=92$

Omitting the +2 term in the first layer reduces the count from 12 to 10, corresponding to an error of approximately 16.7%. In the second layer, the error is approximately 4.76%, and in the third layer approximately 2.17%. Therefore, in the near-field region where strong gravity is examined, the +2 term must be retained exactly.

4. Governing Equation for the Metric from Force Equilibrium

The first layer contains 12 Ramions with metric N_1:

[39.144] $L_1N_1=12N_1$

The equilibrium condition for each layer is:

[39.145] $L_nN_n=12N_1$

Therefore:

[39.146] $(10n^2+2)N_n=12N_1$

And:

[39.147] $N_n=12N_1/(10n^2+2)$

The continuous form of the equilibrium equation is:

[39.148] $\partial[(10n^2+2)N(n)]/\partial n=0$

Thus:

[39.149] $(10n^2+2)\partial N/\partial n+20nN=0$

And:

[39.150] $\partial \mathrm{Ln}(N)/\partial n=-20n/(10n^2+2)$

With the condition $N(1)=N_1$, the solution reproduces this same exact distribution.

5. Radius of Each Ramion and the Actual Radii of the Layers

The radius of a Ramion in layer n is:

[39.151] $r_n=N_n r_s$

Thus:

[39.152] $r_n=12N_1 r_s/(10n^2+2)$

The cumulative physical radius of layer n is obtained by summing the actual thicknesses of all layers:

[39.153] $R_n=2\gamma\Sigma\{j=1 \text{ to } n\}\{r_j\}$

Therefore:

[39.154] $R_n=2\gamma r_s\Sigma\{j=1 \text{ to } n\}\{12N_1/(10j^2+2)\}$

And the separation between two successive layers is:

[39.155] $R_n-R_{n-1}=2\gamma r_n$

Thus:

[39.156] $R_n-R_{n-1}=2\gamma[12N_1 r_s/(10n^2+2)]$

6. Strong-Gravitational Acceleration

The fundamental metric–acceleration relation is:

[39.157] $g_s=-c_s^2\partial Ln(N)/\partial R$

Because N and R are both functions of n:

[39.158] $g_s=-c_s^2(\partial LnN/\partial n)/(\partial R/\partial n)$

From the metric distribution:

[39.159] $\partial LnN/\partial n=-20n/(10n^2+2)$

And:

[39.160] $\partial R/\partial n=2\gamma[12N_1 r_s/(10n^2+2)]$

Therefore, the continuous approximation is:

[39.161] $g_s(n)=5c_s^2 n/(6\gamma N_1 r_s)$

With the new value of r_s:

[39.162] $g_s(n)\approx 4.8366311_{(10)}{}^{45}(K_h/K_c)n/N_1 m/s^2$

For nearby layers, the discrete form is more accurate:

[39.163] $g_{s,n-½}=-c_s^2[Ln(N_n)-Ln(N_{n-1})]/(R_n-R_{n-1})$

Consequently:

[39.164] $g_{s,n-½}=[c_s^2(10n^2+2)/(24\gamma N_1 r_s)]Ln[(10n^2+2)/(10(n-1)^2+2)]$

For large n:

[39.165] $Ln[(10n^2+2)/(10(n-1)^2+2)]\approx 2/n$

And the discrete relation approaches the continuous relation.

7. Conservation of Strong-Gravitational Energy

The total distributed strong-gravitational energy equals the rest energy of the source itself:

[39.166] $E_{g_s}=M_1 c_s^2$

And not:

[39.167] $E_{g_s} = (1/12) G_s M_1^2 / r_s$

For a neutral particle:

[39.168] $M_1 c_s^2 = 12 N_{m1} E_s$

The energy of each Ramion in layer n is:

[39.169] $E_n = N_n E_s$

The total energy of that layer is:

[39.170] $\Delta E_n = (10n^2+2) N_n E_s$

Using metric equilibrium:

[39.171] $\Delta E_n = 12 N_1 E_s$

Thus, each layer has the same total energy.

If the structure contains K layers:

[39.172] $E_{g_s} = 12 K N_1 E_s$

The conservation condition is:

[39.173] $12 K N_1 E_s = 12 N_{m1} E_s$

Hence:

[39.174] $K = N_{m1} / N_1$

8. Strong-Gravitational Potential for a Test Particle

The metric potential difference between the first layer and layer n is:

[39.175] $V_s(n) = M_2 c_s^2 \mathrm{Ln}(N_1 / N_n)$

Because:

[39.176] $M_2 c_s^2 = 12 N_{m2} E_s$

the result is:

[39.177] $V_s(n) = 12 N_{m2} E_s \mathrm{Ln}[(10n^2+2)/12]$

The potential-energy difference between two successive layers is:

[39.178] $\Delta V_{s,n} = 12 N_{m2} E_s \mathrm{Ln}[(10n^2+2)/(10(n-1)^2+2)]$

The separation between those same two layers is:

[39.179] $\Delta R_n = 2\gamma [12 N_1 r_s / (10n^2+2)]$

Therefore:

[39.180] $F_{s,n-½} = \Delta V_{s,n} / \Delta R_n$

And:

[39.181] $F_{s,n-½} = [N_{m2} E_s (10n^2+2) / (2\gamma N_1 r_s)] \mathrm{Ln}[(10n^2+2)/(10(n-1)^2+2)]$

Using the surface gravitational constant:

[39.182] $E_s = G_s m_s^2 / r_s$

the result is:

[39.183] $F_{s,n-½} = [N_{m2} G_s m_s^2 (10n^2+2) / (2\gamma N_1 r_s^2)] \mathrm{Ln}[(10n^2+2)/(10(n-1)^2+2)]$

G does not appear in this relation.

9. Geometrically Limited Range

From the radius relation:

[39.184] $R_n=2\gamma N_1 r_s\Sigma\{j=1 \text{ to } n\}\{12/(10j^2+2)\}$

The required geometric series converges:

[39.185] $\Sigma\{j=1 \text{ to } \infty\}\{12/(10j^2+2)\}=1.75495844805$

Therefore:

[39.186] $R\infty=2\gamma N_1 r_s\times 1.75495844805$

And:

[39.187] $R\infty\approx 2.89771196 N_1 r_s$

With the new base radius:

[39.188] $R\infty\approx 3.2665703_{(10)}{}^{-29}(K_c/K_h)N_1 m$

Thus, even the mathematical continuation to infinitely many layers accumulates within a finite radius.

The physical structure terminates at K layers, because at that point the total distributed energy equals the source's rest energy.

10. Confining Behavior

For large n:

[39.189] $F_s(n)\propto n$

On the other hand:

[39.190] $R\infty - R_n\propto 1/n$

Therefore:

[39.191] $n\propto 1/(R\infty - R)$

And consequently:

[39.192] $F_s(R)\propto 1/(R\infty - R)$

Thus, in the mathematical continuation of the distribution, the restoring force increases as the final radial boundary is approached.

In the physical structure, this trend continues up to layer K.

Continuation: Section 11, “Direct Comparison of Strong and Weak Gravity at the Same Distance.”

11. Direct Comparison of Strong and Weak Gravity at the Same Distance

For a central particle of $12N_{m1}$:

[39.193] $M_1=12N_{m1}m_s$

Newtonian weak gravity at the same distance R_n:

[39.194] $g_w(R_n)=GM_1/R_n^2$

Thus:

[39.195] $g_w(R_n)=12GN_{m1}m_s/R_n^2$

The exact strong acceleration:

[39.196] $g_{s,n-½}=[c_s^2(10n^2+2)/(24\gamma N_1 r_s)]\text{Ln}[(10n^2+2)/(10(n-1)^2+2)]$

the definition is:

[39.197] $A_n=\Sigma\{j=1 \text{ to } n\}\{12/(10j^2+2)\}$

Hence:

[39.198] $R_n=2\gamma N_1 r_s A_n$

And:

[39.199] $Q_n=g_{s,n-½}/g_{\mathscr{w}}(R_n)$

Using:

[39.200] $K=N_{m1}/N_1$

and the surface relation for G_s, the result is:

[39.201] $Q_n=\gamma/(72K)A_n^2(10n^2+2)Ln[(10n^2+2)/(10(n-1)^2+2)]$

In the volumetric representation, the same relation can be written:

[39.202] $Q_n=\gamma/(60K)A_n^2(10n^2+2)Ln[(10n^2+2)/(10(n-1)^2+2)]$

12. Ratio at the Outer Boundary of a Large Structure

For $n\approx K$ and large K:

[39.203] $10K^2+2\approx 10K^2$

And:

[39.204] $Ln[(10K^2+2)/(10(K-1)^2+2)]\approx 2/K$

Also:

[39.205] $A_k\rightarrow 1.75495844805$

Therefore:

[39.206] $Q_k\approx(5\gamma/18)(1.75495844805)^2(G_s/G)$

The geometric coefficient:

[39.207] $(5\gamma/18)(1.75495844805)^2\approx 0.7063005671$

Thus:

[39.208] $Q_k\approx 0.7063005671(G_s/G)$

With the new value of the surface constant:

[39.209] $G_s\approx 6.07101304780823(10)^{22}(K_c/K_h)m^3.kg^{-1}.s^{-2}$

And:

[39.210] $G\approx 6.674317958809(10)^{-11}m^3.kg^{-1}.s^{-2}$

the result is:

[39.211] $G_s/G\approx 9.09608005683(10)^{32}(K_c/K_h)$

Consequently:

[39.212] $Q_k\approx 6.42456650293(10)^{32}(K_c/K_h)$

With the current values from relation (61):

[39.213] $Q_k\approx 6.42456650293(10)^{32}$

Therefore, at the same distance and for the same central mass, the strong-gravity acceleration at the outer boundary of a large structure is approximately $6.42(10)^{32}$ times the Newtonian weak-gravity acceleration.

Using the volumetric constant as well:

[39.214] $Q_k \approx 0.8475606806(G_{sv}/G)$

The same final value is obtained.

13. Independence of the Ratio from the Test Mass

The force exerted on the test particle:

[39.215] $F=M_2 g$

Therefore, M_2 cancels in the ratio of the two forces:

[39.216] $F_s/F_{\mathscr{w}}=g_s/g_{\mathscr{w}}$

Thus, for an identical central field and distance, the ratio of strong to weak gravity does not depend on N_{m2}.

14. Summary of Strong Gravity

Weak gravity is the long-range distribution of mass, whereas strong gravity in this model is constructed from the local distribution of the metric over the exact FCC layers.

The principal layer-equilibrium equation:

[39.217] $(10n^2+2)N_n=12N_1$

The radius of each ramion in a layer:

[39.218] $r_n=12N_1 r_s/(10n^2+2)$

The cumulative radius:

[39.219] $R_n=2\gamma r_s \Sigma\{j=1 \text{ to } n\}\{12N_1/(10j^2+2)\}$

The exact discrete acceleration:

[39.220] $g_{s,n-½}=[c_s^2(10n^2+2)/(24\gamma N_1 r_s)]\mathrm{Ln}[(10n^2+2)/(10(n-1)^2+2)]$

Energy conservation:

[39.221] $E_{\mathscr{g}s}=M_1 c_s^2=12N_{m1}E_s$

The number of physical layers:

[39.222] $K=N_{m1}/N_1$

And the limiting ratio of strong gravity to weak gravity:

[39.223] $g_s/g_{\mathscr{w}} \approx 6.42456650293_{(10)^{32}}$

In this structure, the law of strong gravity is not constructed directly using G; G enters only for comparison with the Newtonian field. The strong distribution follows from E_s, r_s, c_s, the exact FCC geometry, metric equilibrium, and energy conservation.

End of Theorem 39. The next volume begins with Theorem 40, “Dimensions and Shape of the Universe and Entanglement.”

Theorem 40: The Dimensions and Shape of the Universe and Entanglement

Hyperspace, Space, and Non-Space

In Ramionics, the three-dimensional space of the universe is not an independent fundamental substrate; rather, it is the outcome of the structure and field of Ramions.

Ramions are situated in a hyperspace with a very large number of dimensions, or even infinitely many dimensions.

The Ramions themselves, in proportion to their energies, generate:

space,

time,

and the local metric.

Thus, the three-dimensional space of this universe is an emergent structure arising from the Ramion field.

Each Ramion regulates the effective dimensions of space and time in proportion to its own energy.

In this picture:

Hyperspace → the fundamental higher-dimensional environment;

Space → the region organized by Ramions;

Non-space → the unoccupied portions of hyperspace between Ramions.

Fundamental Equilibrium of a Ramion

A Ramion has no independent fundamental constraints other than two principles:

conservation of energy,

and equilibrium between linear and rotational energy.

The fundamental equilibrium of a Ramion is:

[40.1] $E^R = E_l$

and the linear energy is:

[40.2] $E_l = rF_l/3$

If the energy injected into a Ramion is asymmetric—that is, if the linear and rotational components are unequal—the Ramion re-establishes equilibrium with absolutely zero delay.

The Ramion accomplishes this by changing the effective dimensions of space and time.

If the linear energy increases, the Ramion enlarges the spatial dimensions.

If the rotational energy increases, it enlarges the temporal dimensions.

Thus, relativity and changes in the metric follow directly from this fundamental equilibrium principle.

Continuous Dimensions of Space and Time

In Ramionics, the dimensions of space and time are not rigid, fixed quantities.

Dimensions may be:

continuous,

fractional,

and dependent on energy density.

Within this framework:

spatial dimensions are always greater than or equal to 3,

and temporal dimensions are always greater than or equal to 1.

When the energy of a Ramion changes, the effective dimensions also change continuously.

Non-Space and Nearly Instantaneous Propagation

Because the FCC lattice does not fill the entire volume:

[40.3] $\varphi \approx 0.74048$

only about 74 percent of the volume is occupied by Ramions and the space they create.

Consequently:

[40.4] $1 - \varphi \approx 0.25952$

of the volume remains part of the unoccupied hyperspace.

This unoccupied portion is non-space.

Non-space does not mean the absence of hyperspace; it refers to portions of hyperspace that have not yet been transformed by the Ramion field into ordinary three-dimensional space.

In non-space:

energy density is approximately zero,

ordinary space-time limitations do not apply,

and propagation can be nearly instantaneous.

Thus, actual field propagation does not pass solely through three-dimensional space; part of it travels through the columns of non-space between Ramions.

Origin of the Speed of Light

In Ramionics, the speed of light results from the combination of propagation through Ramionic space and non-space.

The propagation speed inside a Ramion itself is:

[40.5] $\mathring{c}$

However, some propagation passes through non-space, where propagation is approximately infinite in speed.

Therefore, the effective speed of light becomes:

[40.6] $c = \mathring{c}/\varphi$

In this picture, φ is the geometric FCC packing fraction.

Because the propagation path must be modeled as a narrow cylinder, the linear fraction of the occupied portion equals the FCC volumetric fraction.

Consequently, the factor:

[40.7] φ

rather than:

[40.8] γ

appears in the speed of light.

Free Connection Capacities of Ramions

In the FCC lattice, each Ramion has 12 connection capacities.

In the ordinary bulk of the lattice, these 12 capacities are almost completely occupied. Ordinary Ramions therefore have no significant free capacity for creating non-space bridges.

This is important because it shows that entanglement is not a universal property of all Ramions; instead, it occurs predominantly in boundary and surface regions.

Ramions on the surfaces of particle-scale and galactic black holes, as well as those in the outermost layer of the universe, have some unoccupied connection capacities.

Each surface Ramion has approximately three free capacities.

To preserve force and torque equilibrium, these free capacities form bridges toward opposing Ramions.

Thus, entanglement arises directly from unfilled surface connection capacities.

Type-I Entanglement

In Type-I entanglement, Ramions on the surface of a black hole—

whether at the centers of particles,

or in galactic black holes—

connect to opposing Ramions through non-space.

Each surface Ramion forms non-space bridges with approximately three opposing Ramions.

These bridges establish:

force equilibrium,

torque equilibrium,

and field coherence.

In this case, entanglement takes place within a single structure.

The actual axes of the field are therefore formed by these non-space bridges.

Type-II Entanglement

In Type-II entanglement, surface Ramions of one black hole or particle form bridges to surface Ramions of another structure.

In this case, the field topology of two independent structures becomes connected.

At the particle scale, this phenomenon is quantum entanglement.

At the black-hole scale:

two black holes become physically connected,

and a wormhole forms.

Thus, entanglement and wormholes are two manifestations of a common topology.

Entanglement of Dispersed Ramions

A third form of entanglement may also exist.

In this case, two pairs of neighboring Ramions break part of their local connections and instead form bridges to more distant pairs.

As a result, the topology of the FCC lattice undergoes local rearrangement.

This is a form of entanglement among dispersed Ramions.

In this picture, entanglement is not merely the complete connection of two structures; it is also a rearrangement of topology between different parts of the lattice.

A Flat but Closed Universe

In standard cosmology, a closed universe usually means positive space-time curvature.

In Ramionics, however, the universe may be:

locally flat,

but globally closed.

This is because the universe's closure does not arise from the curvature of three-dimensional space itself, but from non-space connections in hyperspace.

The situation resembles a flat sheet whose edges are connected to the opposite side by curved strings extending through higher dimensions.

The sheet itself remains flat, but its topology becomes closed.

Likewise, in the Ramionic universe:

Ramions in the outermost layer form bridges toward the opposite side of the universe,

and the universe acquires a closed topology.

Consequently:

any point may appear to be the center of the universe,

and objects may disappear on one side and reappear on the other.

In this picture, closure arises from hyperspace topology, not from curvature of three-dimensional space.

Radius of the Universe and Hubble Radius

In Ramionics, the actual radius of the universe differs from the Hubble radius.

The fundamental relation is:

[40.9] $R_{(}obs_{)} = 4\gamma R_h$

Therefore:

[40.10] $R_h = R_{(}obs_{)}/(4\gamma)$

where:

$R_{(}obs_{)}$ is the actual radius of the universe,

and R_h is the Hubble radius.

The three-dimensional universe is therefore:

finite,

flat,

and closed.

Non-Space and Dark Matter

Because the packing of the FCC lattice is incomplete:

[40.11] $\varphi \approx 0.74048$

approximately:

[40.12] $1 - \varphi \approx 0.25952$

of the universe's volume remains non-space.

This value is approximately the same as the proportion attributed to dark matter in cosmology.

In the standard model, dark energy is generally defined over all of space.

In Ramionics, however, the non-space portion of hyperspace contributes physically to the topology and propagation of the field.

Thus, a significant portion of the effects attributed to dark matter may arise from non-space and the hidden topology of the Ramionic lattice.

In this picture, dark matter need not be an independent form of matter; it may instead be a geometric and topological manifestation of non-space within the universe's FCC structure.

Multidimensional Universes

In Ramionics, fundamental laws arise from the geometry and equilibrium of Ramions, not from random parameters.

Thus, every stable three-dimensional universe will have:

the same constants,

the same electron family,

the same particles,

and the same elements.

The only difference between universes is their scale.

Consequently, for every three-dimensional universe:

[40.13] $R_h = R_{(}obs_{)}/(4\gamma)$

Ramionics may even predict the constants and formulas of four-dimensional and higher-dimensional universes, because changing the number of dimensions changes:

packing geometry,

the number of neighbors,

field equilibrium,

and particle structure.

Thus, Ramionics is not merely a theory of this universe; it is a theory of a family of possible universes.

Conclusion

In Ramionics, the universe's three-dimensional space is a product of the Ramion field, and Ramions exist in a higher-dimensional hyperspace.

The unoccupied portions of hyperspace between Ramions constitute non-space, which makes nearly instantaneous field propagation possible.

Entanglement results from an actual topological connection in hyperspace, while wormholes are large-scale manifestations of the same connections.

The three-dimensional universe can be flat yet remain closed because of hyperspace topology.

Furthermore, the fundamental laws of different three-dimensional universes will be identical, with only their scales varying.

Thus, Ramionics explains:

relativity,

the speed of light,

entanglement,

wormholes,

the topology of the universe,

dark matter,

and the multiverse structure,

all through the geometry and dynamics of a single field.

Theorem 41: Masses of Quarks, the Proton, and the Neutron

In this section, E_s and $\mathbb{E}_s$ are defined and calculated independently.

In calculations of quark, proton, and neutron masses, particle rest energies expressed in units of Ramion energy are denoted by E when the reduction in magnetic inertia d is included, and by $\mathbb{E}$ (the dsk accent) when d is not included. Thus, the effect of d is already incorporated into the energy definitions, and there is no need to apply the factor θ_e again in these calculations.

The computational reports underlying this article are:

A — A — Computational case

B — B — Computational case

C — C — Computational case

D — D — Computational case

Four cases, A, B, C, and D, are examined in this article. In each case, proton-mass relations are classified according to their physical origins, including proton-based, neutron-based, antisymmetric, and analytical formulas.

1. Introduction: Convergence of Structural Constraints in Hadronic Packet Formation

On the basis of entropy considerations and the principle of carrying the least information, the “rule of greatest maximum similarity” requires structural evolution to proceed while preserving the preceding pattern as far as possible. Accordingly, particles of the N family continue to form beyond layer 127, but the continuation of this process must be electrically neutral so that the electric charges of the nuclei of the resulting hadrons do not change.

The same rule is then applied to the hadrons themselves. Since continuation of the structure must retain the greatest similarity to the preceding hadronic unit, subsequent units are regarded as eightfold packets, $8e_0$. Once this structural unit is specified, the problem becomes finding a layer capable of supporting an integer number of these packets without providing sufficient capacity to form an additional packet.

Layer calculations show that layer 624 simultaneously satisfies a rare combination of these conditions. It lies exactly one layer before the robust layer 5^4=625; the number of eightfold packets it can support remains 227, and the next packet has not yet formed. At the same time, the available energy is compatible with the energy of the entire hadronic packet, including its seven electrons. At layer 625, the structural capacity reaches the next packet and the number of packets increases from 227 to 228. Thus, the placement of the boundary of packet 227 at layer 624, its adjacency to the robust layer 625, and the provision of the total hadronic-packet energy constitute a set of simultaneous, exceptionally rare constraints.

This convergence is not limited to these conditions. Within the same structure, the neutrino-radiation contribution falls within the experimental range of approximately 1–2 percent; the proton-to-neutron number ratio is 7; and the corresponding atomic organization produces a hydrogen-to-helium mass ratio of 3. Several apparently distinct outcomes—layer capacity, packet count, electrical neutrality, hadronic-packet energy, neutrino contribution, proton-to-neutron ratio, and hydrogen-to-helium mass ratio—therefore converge within a single structure.

Separately, to determine the mass–inertia capacity of quarks, four possible models, A/B/C/D, are examined independently. In each model, ENPDU is calculated relative to EDU. The proximity of this ratio to 1/12 in all fthe Ramionics models suggests that this value may be regarded as a common structural feature. On this basis, defining the quark mass–inertia capacity as 1/12 of the quark mass is a natural choice within the resulting structure and serves as the basis for applying subsequent smaller corrections.

2. Introduction: Different Origins of the Factor 2

When examining proton and neutron structures, several independent origins of the factor 2 must be distinguished.

First, in the three-quark structure, one quark can be considered central and the other two peripheral. Entanglement between the two peripheral quarks may itself generate a factor of 2, just as two balls with two surface Ramions of a particle may become entangled. These factors can interchange α/12 and α/6.

The second origin is purely numerical. The proton contains two up quarks and one down quark, whereas the neutron contains one up quark and two down quarks:

[41.1] $E_{(u\mathit{d}_u)} = 2E_{us} + E\mathit{d}_s$

[41.2] $E_{(\mathit{d}_u\mathit{d}_)} = E_{us} + 2E\mathit{d}_s$

Consequently, the simple structural difference between these two arrangements is:

[41.3] $E_{(\mathit{d}_u\mathit{d}_)} - E_{(u\mathit{d}_u)} = E\mathit{d}_s - E_{us}$

The factor 2 in the relation between magnetic moment and angular momentum has another independent origin.

Consider a small charge element $\mathit{d}q$ at a distance r from the rotation axis, moving with angular velocity ω. The period of one complete revolution is:

[41.4] $T = 2\pi/\omega$

The corresponding current is:

[41.5] $\mathit{d}I = \mathit{d}q/T = \omega\mathit{d}q/(2\pi)$

The magnetic moment of the charge element is:

[41.6] $\mathit{d}\mu = \mathit{d}I\pi r^2 = (1/2)\omega r^2\mathit{d}q$

And for the entire charge distribution:

[41.7] $\mu = (1/2)\omega\int r^2\mathit{d}q$

For a mass element:

[41.8] $v = \omega r$

[41.9] $\mathit{d}p = v\mathit{d}m = \omega r\mathit{d}m$

[41.10] $\mathit{d}J = r\mathit{d}p = \omega r^2\mathit{d}m$

And for the entire mass distribution:

[41.11] $J = \omega\int r^2\mathit{d}m$

Thus, the factor 1/2 in μ arises directly from converting the rotation period into current and multiplying by the area πr^2, whereas no such factor arises in J.

3. Physical Questions in the Precise Calculation of Proton and Neutron Masses

The proton mass in this section is calculated using several numerical and structural models.

In the Ramionics description under consideration, three rotation axes are assigned to quarks, which may be associated with the three quark colors. The gyromagnetic factors of these three axes may also have different values.

Entanglement may occur between the central quark and peripheral quarks, between the two peripheral quarks, or cyclically among all three quarks.

It must also be established how the magnetic balance of the entire packet is maintained and whether the electrons accompanying the hadronic packet contribute to that balance.

Another fundamental question is whether the magnetic/inertial reduction d is already present in the measured rest masses of the electron and quarks, or whether zero-alpha energies should form the basis of calculation.

For the present, all calculations concerning the dependence of the gyromagnetic factor on the rotation axis—that is, quark color—the rotation speeds of the three udu quarks in the proton and the dud quarks in the neutron, the radius and orbital speed of a peripheral quark around the central quark, the relativity arising from these speeds, and entanglement calculations are modeled in terms of α.

4. Ramionics Metric and Base Energy

In this article, uppercase N is used for the Ramionics metric and lowercase n for the number of packet constituents.

[41.12] $N = 36390$

The energy of one 12N unit is:

[41.13] $E_{0s} = 12N = 436680$

A packet is a specified collection of physical constituents formed and balanced within a collective structure.

Quantization also means that a calculated raw value is not necessarily the final permitted value: it is placed on the allowed lattice by Round, Floor, or Ceil.

5. Definition of d and the Four Cases

In the gyromagnetic-factor section, d is introduced as magnetic inertia in the form of negative mass.

[41.14] $d = m\mathrm{Round}_{2,u}\mathrm{Round}_2(\acute{d})$

[41.15] $\acute{d} = \{(cN/2)\alpha/\{6(1-\alpha/6)\}\}\{1-M\alpha(1+c/4)^2\}$

Where:

[41.16] $M = 3$ or c

Current values:

[41.17] $d_e = 63$

[41.18] $d_u = 42$

[41.19] $d_{\mathscr{A}} = 21$

Model	d_e	d_u	$d_{\mathscr{A}}$
A	63	42	21
B	63	0	0
C	0	0	0

| D | 0 | 42 | 21 |

[41.20] E_{es} =3N/2−63 =54522 :A,B

; $E_{es(\alpha 0)}$ =3N/2 =54585 :C,D

In A/B, E_s is determined by assigning 54522 units to the electron mass. In C/D, the same experimental mass is distributed over 54585 units. Consequently, E_s changes.

For A/B, the energy scale is determined using 54522 units for the experimental electron mass:

[41.21] $E_{s(A/B)}=E_e/54522$

For C/D, the energy scale is determined using 54585 units for the same experimental mass:

[41.22] $E_{s(C/D)}/E_{s(A/B)}=54522/54585=0.998845836768342951360263808739$

In the calculations in this section, each energy scale is used according to the independent definition of its case; no additional correction factor is introduced alongside the energy symbol.

6. Zero-Alpha Contribution of the Quark Structure

The zero-alpha quark energies are:

[41.23] $\mathbb{E}_{us}$ =218340

[41.24] $\mathbb{E}_{\mathscr{d}_s}$ =345705

For the neutron arrangement:

[41.25] $E_{ns(\alpha 0)}$ =227×12N+(1+1/12)(2$\mathbb{E}_{\mathscr{d}_s}$+$\mathbb{E}_{us}$) =100111922.5

In A and B:

[41.26] $E_{ns(\alpha 0)}/E_{ns}$ =99.86355%

7. Determination of E_s and CODATA Years

For A and B, the year combination is:

E2018_P2018_N2022

[41.27] E_s =9.3723441902457908$_{(10)}$$^{-6}$MeV

[41.28] E_{es} =54522

[41.29] E_{ps} =100110716

[41.30] E_{ns} =100248711

Differences relative to experimental data:

$\Delta E_e=-0.396126094889\sigma$

$\Delta E_p=-2.33121956375\sigma$

$\Delta E_n=+4.54266526617\sigma$

The RMS value is 2.95676108030072σ.

If E_s is determined solely from the 2022 experimental electron energy:

[41.31] E_s ≈9.37234420399105$_{(10)}$$^{-6}$MeV

For C and D:

E2018_P2022_N2022

[41.32] E_s =9.3615269668841921$_{(10)}$$^{-6}$MeV

[41.33] E_{es} =54585

[41.34] E_{ps} =100226394

[41.35] E_{ns} =100364548

$\Delta E_e = -3.41750849842\sigma$

$\Delta E_p = +2.73986180563\sigma$

$\Delta E_n = +1.4190478718\sigma$

The RMS value is 2.6583142473615σ.

The purpose of these calculations is to distribute the quantization error among the three particles—the electron, proton, and neutron—so that the RMS of the errors for all three particles is minimized, rather than distributing the quantization error only between the proton and neutron.

The quantized value of each of the three particles does not change relative to the simple calculation $E_{ex}/54522$ or $E_{ex}/54585$ under this fine correction; only the precision of E_s expressed in joules increases.

End of Volume 33, Part 1 of Theorem 41. The translation continues with Section 8, “Quark Energies and Structural Quantities,” beginning at formula [41.36].

8. Quark Energies and Structural Quantities

The energy of the up quark is calculated from its zero-alpha energy and the corresponding magnetic inertia:

[41.36] E_{us} =$\mathbb{E}_{us} - d_u$ =218298 :A,D

; E_{us} =$\mathbb{E}_{us}$ =218340 :B,C

The down-quark energy is calculated in the same manner:

[41.37] $E_{\mathscr{d}_s}$ =$\mathbb{E}_{\mathscr{d}_s} - d_{\mathscr{d}}$ =345684 :A,D

; $E_{\mathscr{d}_s}$ =$\mathbb{E}_{\mathscr{d}_s}$ =345705 :B,C

The energy difference between the down and up quarks, EDU, is first calculated from the following relation:

[41.38] EDU =$E_{\mathscr{d}_s} - E_{us}$ =127386 :A,D

; EDU =$E_{\mathscr{d}_s} - E_{us}$ =127365 :B,C

The energy difference between the neutron and proton, ENP, is calculated from their quantized values:

[41.39] ENP =$E_{ns} - E_{ps}$ =137995 :A,B

; ENP =$E_{ns} - E_{ps}$ =138154 :C,D

ENPDU is then calculated as the difference between ENP and EDU:

[41.40] ENPDU =ENP−EDU =10609 :A

; ENPDU =ENP−EDU =10630 :B

; ENPDU =ENP−EDU =10789 :C

; ENPDU =ENP−EDU =10768 :D

The distinction between E and $\mathbb{E}$ remains in effect in the relations for E_{ps} and E_{ns}:

[41.41] E_{es} =$\mathbb{E}_{es} - d_e$ =3N/2−63

[41.42] E_{us} =$\mathbb{E}_{us} - d_u$ =12N/2−42

[41.43] $E_{\mathscr{d}_s}$ =$\mathbb{E}_{\mathscr{d}_s} - d_{\mathscr{d}}$ =19N/2–21

9. Fermionic Packet

[41.44] $E_{fp} = (2^{p-1}-1)E_2 + (2^{p-2}+1)E_1 + (2^{p-2}-1)E_3$

For p=5:

[41.45] $E_{ff} = 15E_{us} + 9E_{ds} + 7E_{es}$

The fermionic packet formed up to layer 127—that is, one layer before the robust layer $2^7=128$—contains a total of seven electrons with charge $-7q_e$, nine down quarks with total charge $-3q_e$, and fifteen up quarks with total charge $+10q_e$:

The respective values are $-7q_e$ for the electrons, $9(-q_e/3) = -3q_e$ for the down quarks, and $15(+2q_e/3) = +10q_e$ for the up quarks. Thus, the total electric charge of the assembly is zero.

The same quark count also corresponds exactly to one neutron and seven protons: seven protons contain a total of fourteen up quarks and seven down quarks, while one neutron contains one up quark and two down quarks. Consequently, the complete assembly contains precisely fifteen up quarks and nine down quarks. Seven protons, together with seven electrons and one neutron, can be organized, in terms of their atomic constituents, into six hydrogen atoms and one deuterium atom.

If this structure continues across a collection of packets and two neutrons and two protons eventually occupy one helium-4 nucleus, two atomic packets yield twelve remaining hydrogen atoms and one helium-4 atom. Therefore, using the mass-number approximation, the primordial hydrogen-to-helium mass ratio is 12 to 4, or 3 to 1. This corresponds to approximately 75% hydrogen and 25% helium by mass. This stage should not be interpreted as a direct, single-step reaction of two deuterium nuclei into helium-4; in nuclear physics, the reaction pathway may involve intermediate stages and products.

Values for the four cases:

[41.46] $E_{ff} = 6767280$:A

; $E_{ff} = 6768099$:B

; $E_{ff} = 6768540$:C

; $E_{ff} = 6767721$:D

Hadronic structure:

[41.47] $E_{hh} = 7E_{ps} + E_{ns} + 7E_{es}$

[41.48] $E_{hh} = 801405377$:A,B

; $E_{hh} = 802331401$:C,D

10. Rotational, Magnetic, and Mass–Inertia Capacity

[41.49] $k_m = 1/12$

[41.50] $ENP_{(Base)} = (13/12)EDU$

Values for the four cases:

[41.51] $ENP_{(Base)} = 138001.5$:A,D

; $ENP_{(Base)} = 137978.75$:B,C

Mass–inertia capacity:

[41.52] $E_{(InertiaCapacity)} = E_{(Rest)}/12$

For A:

[41.53] $EDU/12 = 10615.5$

[41.54] $ENP_{(InertiaBase)} = 138001.5$

[41.55] $ENP = 137995$

[41.56] $ENP_{(InertiaBase)} - ENP = 6.5$

Corrected version:

[41.57] $E_{(InertiaCapacity)} = E_{(Rest)}/(12+\alpha)$

11. Rule of Greatest Maximum Similarity

When several highly similar structures are present in a common packet, the larger member can serve as the common reference for the size and energy capacity of the similar structures.

Beyond layer 127, the production of electrically neutral electron narions e_0 continues with the same N as the up and down quarks.

Before the proton and neutron separate from the common black hole of the hadronic packet, the neutron, as the larger member, can serve as the common energy reference.

[41.58] $E_{ps} - (13/12)E_{(u\mathscr{d}_u)} = 99263226.5$

[41.59] $E_{ns} - (13/12)E_{(\mathscr{d}_u\mathscr{d}_s)} = 99263220$

[41.60] $\Delta E_c = 6.5$

Neutron-based formula:

[41.61] $M_{2(NeutronBase)} = (1+\acute{k}_m)(2E_{\mathscr{d}_s}+E_{us})$

Proton-based formula:

[41.62] $M_{2(ProtonBase)} = (1+\acute{k}_m)(2E_{us}+E_{\mathscr{d}_s})$

For the proton:

[41.63] $M_p = (1+\acute{k}_m)(2E_{us}+E_{\mathscr{d}_s})$

For the neutron:

[41.64] $M_n = (1+\acute{k}_m)(E_{us}+2E_{\mathscr{d}_s})$

[41.65] $M_n - M_p = (1+\acute{k}_m)(E_{\mathscr{d}_s} - E_{us})$

[41.66] $M_n - M_p = (1+\acute{k}_m)EDU$

For the direct calculation of the proton, quantization is applied on a base of 2, and for the electrically neutral neutron, on a base of 3.

12. ENPDU Relations and the Structural Connection Between Proton and Neutron

In A:

[41.67] $ENPDU = Floor_1\{EDU(1-\alpha/12)/12\} = 10609$

Error: zero Ramions.

; $\acute{k}_m = (1/12)(1-\alpha/12) = (1/12)0.999391887286443 = 0.083282657273859$

In B:

[41.68] $ENPDU = Ceil_1\{EDU/\{12(1-\alpha/5)\}\} = 10630$

Error: zero Ramions.

; $\acute{k}_m = (1/12)/(1-\alpha/5) = (1/12)1.00146160368000989365 = 0.08345513364000082447$

In C:

[41.69] $ENPDU = Ceil_1\{EDU(1+(9/4)\alpha)/12\} = 10789$

Error: zero Ramions.

; $\acute{k}_m$ =(1/12)(1+(9/4)α) =(1/12)1.016419043266051 =0.084701586939145

In D:

[41.70] ENPDU =$Floor_1${EDU(1+2α)/12} =10770

Whereas ENPDU is 10768, so the difference in this description is +2E_s.

Error: +2 Ramions.

; $\acute{k}_m$ =(1/12)(1+2α) =(1/12)1.014594705125379 =0.084549558760722

In this structure, the first packet term and the third correction term can be shared, while the principal source of the proton–neutron difference may reside in the rearrangement of the quark structure in the second term.

13. General Family of Proton-Mass Relations and Models A, B, C, and D

[41.71] E_{ps} =Q{n_{8e0}12N+F_2M_2+F_3(aX_u+b$X_{\mathscr{d}}$)/Y}

Here, Q is the quantization rule; n_{8e0} is the number of complete eightfold packets; F_2 and F_3 are structural factors; M_2 is the main quark term; X is the corrected or zero-alpha energy; and Y is the denominator of the correction term.

[41.72] M_2 =2E_{us}+$E_{\mathscr{d}_s}$

Model A: Proton-Mass Formulas

First formula (proton-based)

[41.73] E_{ps} =$Floor_2${n_{8e0}12N+(1+$\acute{k}_m$)($E_{\mathscr{d}_s}$+2E_{us})+(4E_{us}+5$E_{\mathscr{d}_s}$)/19} =100110716E_s

Corresponding neutron formula:

[41.74] E_{ns} =$Round_3$,$Floor_3${n_{8e0}12N+(1+$\acute{k}_m$)(2$E_{\mathscr{d}_s}$+E_{us})+(4E_{us}+5$E_{\mathscr{d}_s}$)/19} =100248711E_s

Second formula (proton-based)

[41.75] E_{ps} =$Ceil_2${n_{8e0}12N+(1+$\acute{k}_m$)($E_{\mathscr{d}_s}$+2E_{us})+(1+$\acute{k}_m$)((3/2)E_{us}+6$E_{\mathscr{d}_s}$)/19} =100110716E_s

Corresponding neutron formula:

[41.76] E_{ns} =$Round_3$,$Ceil_3${n_{8e0}12N+(1+$\acute{k}_m$)(2$E_{\mathscr{d}_s}$+E_{us})+(1+$\acute{k}_m$)((3/2)E_{us}+6$E_{\mathscr{d}_s}$)/19} =100248711E_s

Third formula (proton-based)

[41.77] E_{ps} =$Floor_2${n_{8e0}12N+(1+$\acute{k}_m$)($E_{\mathscr{d}_s}$+2E_{us})+(1+k_m)(3$\mathbb{E}_{us}$–(1/15)$\mathbb{E}_{\mathscr{d}_s}$)/5} =100110716$E_s$

Current raw value:

[41.78] $E_{ps(Raw)}$ =100110717.840466E_s

Fourth formula (antisymmetric)

[41.79] E_{ps} =$Ceil_2${n_{8e0}12N+(1+$\acute{k}_m$)(2$\mathbb{E}_{\mathscr{d}_s}$+$\mathbb{E}_{us}$)+α(5$\mathbb{E}_{us}$−5$\mathbb{E}_{\mathscr{d}_s}$)/4} =100110716$E_s$

Current raw value:

[41.80] $E_{ps(Raw)}$ =100110714.613318E_s

Fifth formula (antisymmetric)

[41.81] E_{ps} =Q{n_{8e0}12N+(1+k_m)(2$E_{\mathscr{d}_s}$+E_{us})+α(6E_{us}–6$E_{\mathscr{d}_s}$)/5} =100110716E_s

Here Q may be $Round_1$, $Round_2$, $Floor_1$, or $Floor_2$.

Current raw value:

[41.82] $E_{ps(Raw)}$ =100110716.003336E_s

Model A: Proton-mass formulas (continued)

Sixth formula (analytical)

In seven protons and one neutron, the total number of up quarks is 15 and the total number of down quarks is 9.

[41.83] $Y = 6/(1+4\alpha) \approx 5.829830680572319$

[41.84] $E_{ps} = n_{8e0}12N+(1+\acute{k}_m)(E_{\mathscr{d}_s}+2E_{us})+(15E_{us}+9E_{\mathscr{d}_s})/\{8(6/(1+4\alpha))\} \approx 100110707.4365795E_s$

[41.85] $\Delta E_{ps} \approx -8.5634205E_s$

Seventh formula (analytical)

In this interpretation, the number of peripheral up quarks is 14 and the number of peripheral down quarks is 2.

[41.86] $Y = 24/7-\alpha \approx 3.42127407600874$

[41.87] $E_{ps} = n_{8e0}12N+(1+\acute{k}_m)(E_{\mathscr{d}_s}+2E_{us})+(14E_{us}+2E_{\mathscr{d}_s})/\{8(24/7-\alpha)\} \approx 100110710.86452813E_s$

[41.88] $\Delta E_{ps} \approx -5.13547187E_s$

Eighth formula (analytical)

For the up quark:

[41.89] $14(2/3) = 28/3$

For the down quark:

[41.90] $2(1/3) = 2/3$

[41.91] $Y = 2+10\alpha = 2.072973525626895$

[41.92] $E_{ps} = n_{8e0}12N+(1+\acute{k}_m)(E_{\mathscr{d}_s}+2E_{us})+\{(28/3)\mathbb{E}_{us}+(2/3)\mathbb{E}_{\mathscr{d}_s}\}/\{8(2+10\alpha)\} \approx 100110569.142022E_s$

[41.93] $\Delta E_{ps} \approx -146.857978E_s$

The three analytical formulas above are based, respectively, on the total number of quarks in the packet, the number of peripheral quarks, and the number of peripheral quarks multiplied by the absolute magnitude of the charge coefficient.

Model B: Proton-mass formulas

First formula (proton-based)

[41.94] $E_{ps} = Q\{n_{8e0}12N+(1+\acute{k}_m)(\mathbb{E}_{\mathscr{d}_s}+2\mathbb{E}_{us})+(5E_{us}+(1/180)E_{\mathscr{d}_s})/8\} = 100110716E_s$

Here, Q may be $Round_2$, $Ceil_1$, or $Ceil_2$.

Current raw value:

[41.95] $E_{ps(Raw)} = 100110715.353066E_s$

Second formula (antisymmetric)

[41.96] $E_{ps} = Ceil_2\{n_{8e0}12N+(1+\acute{k}_m)(2\mathbb{E}_{\mathscr{d}_s}+\mathbb{E}_{us})+\alpha(5\mathbb{E}_{us}-5\mathbb{E}_{\mathscr{d}_s})/4\} = 100110716E_s$

Third formula (antisymmetric)

[41.97] $E_{ps} = Q\{n_{8e0}12N+(1+k_m)(2E_{\mathscr{d}_s}+E_{us})+\alpha(6E_{us}-6E_{\mathscr{d}_s})/5\} = 100110716E_s$

Here, Q may be $Round_1$, $Round_2$, $Floor_1$, or $Floor_2$.

Current raw value:

[41.98] $E_{ps(Raw)} = 100110716.003336E_s$

Fourth formula (analytical — total packet-quark count, coefficient 4)

In Model B, the quark energies in the second term and in the third analytical term are expressed in terms of zero-alpha energies. For this model, $\mathbb{E}_{us}=218340E_s$ and $\mathbb{E}_{\mathscr{d}_s}=345705E_s$, and the corrected inertia coefficient is $\acute{k}_m=0.08345513364000082447$.

[41.99] $Y = 6/(1+4\alpha) = 5.829830680572319$

[41.100] $E_{ps} = n_{8e0}12N+(1+\acute{k}_m)(\mathbb{E}_{\mathscr{d}_s}+2\mathbb{E}_{us})+(15\mathbb{E}_{us}+9\mathbb{E}_{\mathscr{d}_s})/\{8(6/(1+4\alpha))\} = 100110973.66063187E_s$

[41.101] $\Delta E_{ps} = +257.66063187E_s$

Fifth formula (analytical — total packet-quark count, coefficient 15/4)

[41.102] $Y = 6/\{1+(15/4)\alpha\} = 5.840182971839517$

[41.103] $E_{ps} = n_{8e0}12N+(1+\acute{k}_m)(\mathbb{E}_{\mathscr{d}_s}+2\mathbb{E}_{us})+(15\mathbb{E}_{us}+9\mathbb{E}_{\mathscr{d}_s})/\{8(6/\{1+(15/4)\alpha\})\} = 100110730.93073193E_s$

[41.104] $\Delta E_{ps} = +14.93073193E_s$

Sixth formula (analytical — peripheral-quark count)

[41.105] $Y = 24/7-\alpha/12 = 3.427963315857871$

[41.106] $E_{ps} = n_{8e0}12N+(1+\acute{k}_m)(\mathbb{E}_{\mathscr{d}_s}+2\mathbb{E}_{us})+(14\mathbb{E}_{us}+2\mathbb{E}_{\mathscr{d}_s})/\{8(24/7-\alpha/12)\} = 100110715.31773521E_s$

[41.107] $\Delta E_{ps} = -0.68226479E_s$

Seventh formula (analytical — peripheral-quark count weighted by absolute charge)

[41.108] $Y = 2+10\alpha = 2.072973525626895$

[41.109] $E_{ps} = n_{8e0}12N+(1+\acute{k}_m)(\mathbb{E}_{\mathscr{d}_s}+2\mathbb{E}_{us})+\{(28/3)\mathbb{E}_{us}+(2/3)\mathbb{E}_{\mathscr{d}_s}\}/\{8(2+10\alpha)\} = 100110817.80552982E_s$

[41.110] $\Delta E_{ps} = +101.80552982E_s$

Formula	Y	E_{ps}/E_s	$\Delta E_{ps}/E_s$
4	$6/(1+4\alpha)$	100110973.66063187	+257.66063187
5	$6/\{1+(15/4)\alpha\}$	100110730.93073193	+14.93073193
6	$24/7-\alpha/12$	100110715.31773521	−0.68226479
7	$2+10\alpha$	100110817.80552982	+101.80552982

Model C: Proton-mass formula

First formula (proton-based)

[41.111] $E_{ps} = \mathrm{Floor}_2\{n_{8e0}12N+(1+\acute{k}_m)(\mathbb{E}_{\mathscr{d}_s}+2\mathbb{E}_{us})+(1+k_m)(-5E_{us}+(9/2)E_{\mathscr{d}_s})/2\} = 100226394E_s$

Current raw value:

[41.112] $E_{ps(\mathrm{Raw})} = 100226395.251097E_s$

Model D: Proton-mass formula

First formula (proton-based)

[41.113] $E_{ps} = \mathrm{Ceil}_2\{n_{8e0}12N+(1+\acute{k}_m)(E_{\mathscr{d}_s}+2E_{us})+((3/20)\mathbb{E}_{us}+5\mathbb{E}_{\mathscr{d}_s})/7\} = 100226394E_s$

Current raw value:

[41.114] $E_{ps(\mathrm{Raw})} = 100226392.28597E_s$

Furthermore, these same formulas, after applying the α-based correction, reach a quantized error of zero ramions, while the energy of each ramion relative to the proton mass is less than 10 ppb.

14. Packet formation and layer 127

The total number of ramions from layer zero through layer n is calculated from the following relation:

[41.115] $T(n) = (10n^3+15n^2+11n+3)/3$

For layer 127:

[41.116] $T(127) = \{10(127^3)+15(127^2)+11(127)+3\}/3$

[41.117] $T_{127} = 6909055$

Values for the four cases:

[41.118] $\Delta E_{127} = 141775$:A

; $\Delta E_{127} = 140956$:B

; $\Delta E_{127} = 140515$:C

; $\Delta E_{127} = 141334$:D

From layer 127 onward, production of neutral electron narions e_0 continues with the same N as the up and down quarks, and the structure proceeds to layer 624.

15. Hadronic packet

The hadronic packet consists of eight hadrons—seven protons and one neutron—together with seven corresponding electrons.

For layer 624:

[41.119] $T(624) = \{10(624^3)+15(624^2)+11(624)+3\}/3$

[41.120] $T_{624} = 811851249$

Lower bound:

[41.121] $Minn_{e0} = Floor\{(T_{624} - E_{\not\prime\prime} - \Delta E_{127} - k_m(15E_{us}+9E_{\not\alpha_s}))/(12(N+480))\}$

Upper bound:

[41.122] $Maxn_{e0} = Floor\{(T_{624} - E_{\not\prime\prime} - k_m(15E_{us}+9E_{\not\alpha_s}))/(12(N+474))\}$

16. Bounds at layer 624

Raw minimum values:

[41.123] $Minn_{(Raw)} = 1818.1223634843143$:A

; $Minn_{(Raw)} = 1818.1222092261098$:B,C

; $Minn_{(Raw)} = 1818.1223634843143$:D

Raw maximum values:

[41.124] $Maxn_{(Raw)} = 1818.738772922092$:A

; $Maxn_{(Raw)} = 1818.7367672390408$:B

; $Maxn_{(Raw)} = 1818.7357703314888$:C

; $Maxn_{(Raw)} = 1818.73777601454$:D

In all four cases:

[41.125] $Minn_{e0} = Maxn_{e0} = 1818$:A,B,C,D

Therefore:

[41.126] $n_{8e0} = Floor\{1818/8\} = 227$

And:

[41.127] $n_{8e0}12N$ =99126360

17. RadProton and packet balance

Values for the four cases:

[41.128] RadProton =74263 :A

; RadProton =74410 :B

; RadProton =75523 :C

; RadProton =75376 :D

Under the rule of greatest maximum similarity, the proton before separation may absorb energy up to the neutron scale, and the excess share after separation may appear as RadProton in the packet energy balance.

18. Three binary choices in the balance

The three independent choices are a neutrino value of 474 or 480, retention or omission of ΔE_{127}, and retention or omission of RadProton.

[41.129] Q_{8e0} =8×12N =3493440

Physical acceptance condition:

[41.130] $0 \leq E_{(}Free_{)} < Q_{8e0}$

Model A

Neutrino	ΔE127	RadProton	Free Energy	State
474	No	No	116464	Accepted
474	No	Yes	42201	Accepted
474	Yes	No	−25311	Impossible
474	Yes	Yes	−99574	Impossible
480	No	No	−14288	Impossible
480	No	Yes	−88551	Impossible
480	Yes	No	−156063	Impossible
480	Yes	Yes	−230326	Impossible

Model B

Neutrino	ΔE127	RadProton	Free Energy	State
474	No	No	116464	Accepted
474	No	Yes	42054	Accepted
474	Yes	No	−24492	Impossible
474	Yes	Yes	−98902	Impossible
480	No	No	−14288	Impossible
480	No	Yes	−88698	Impossible
480	Yes	No	−155244	Impossible

| 480 | Yes | Yes | −229654 | Impossible |

Model C

Neutrino	ΔE127	RadProton	Free Energy	State
474	No	No	−809560	Impossible
474	No	Yes	−885083	Impossible
474	Yes	No	−950075	Impossible
474	Yes	Yes	−1025598	Impossible
480	No	No	−940312	Impossible
480	No	Yes	−1015835	Impossible
480	Yes	No	−1080827	Impossible
480	Yes	Yes	−1156350	Impossible

Model D

Neutrino	ΔE127	RadProton	Free Energy	State
474	No	No	−809560	Impossible
474	No	Yes	−884936	Impossible
474	Yes	No	−950894	Impossible
474	Yes	Yes	−1026270	Impossible
480	No	No	−940312	Impossible
480	No	Yes	−1015688	Impossible
480	Yes	No	−1081646	Impossible
480	Yes	Yes	−1157022	Impossible

Thus, A and B have physically admissible balance states at layer 624, whereas C and D have negative free energy in this structure.

Continued in the next volume with Section 19, “Layer 625,” and formula [41.131].

19. Layer 625

For layer 625:

[41.131] $T(625) = \{10(625^3)+15(625^2)+11(625)+3\}/3$

[41.132] $T_{625} = 815757501$

[41.133] $T_{625} - T_{624} = 3906252$

Minimum raw values:

[41.134] $\mathrm{Minn}_{(}\mathrm{Raw}_{)} = 1826.9512487568936$:A

; $\mathrm{Minn}_{(}\mathrm{Raw}_{)} = 1826.9510944986891$:B,C

; $\mathrm{Minn}_{(}\mathrm{Raw}_{)} = 1826.9512487568936$:D

Maximum raw values:

[41.135] $\mathrm{Maxn}_{(}\mathrm{Raw}_{)} = 1827.569095187717$:A

; $\mathrm{Maxn}_{(}\mathrm{Raw}_{)} = 1827.5670895046658$:B

; $Maxn_{(Raw)}$ =1827.5660925971138 :C

; $Maxn_{(Raw)}$ =1827.568098280165 :D

In all four cases:

[41.136] $Minn_{e0}$ =1826 :A,B,C,D

; $Maxn_{e0}$ =1827 :A,B,C,D

[41.137] Floor{1826/8} =Floor{1827/8} =228

[41.138] 228×12N =99563040

[41.139] 99563040−99126360 =436680 $=E_{0s}$

The additional energy of layer 625 changes the packet structure from 227 to 228 packets; this new structure is taken into account in balances C and D.

20. Percentage of Neutrino Energy

For 474:

[41.140] $R\nu_{474}$ =474/(36390+474) =1.28580729166667%

For 480:

[41.141] $R\nu_{480}$ =480/(36390+480) =1.30187144019528%

If no separate electromagnetic radiation is assumed in the conversion of energy into matter:

[41.142] $R_{(TotalFree)}$ $=1-E_{hh}/T_{624}$ =1.28667314521801%

This value lies between the ratios for 474 and 480 and is closer to 474. The stage at which neutrinos leave is determined by examining the separation structure.

21. Formation Site and the Meaning of Free Energy

Particle formation can be regarded as a small particle-production reactor within the layered structure. Energy reaching a layer does not mean that all remaining energy must necessarily leave in the form of final electromagnetic radiation.

The remaining energy may be distributed among different channels: one portion may be associated with neutrinos, another may participate in a subsequent structural rearrangement, and another may initiate formation of the next packet.

Therefore, $E_{(Free)}$ is a packet energy-balance quantity; additional observable radiation is defined as a separate quantity.

A mixture of allowed states may also exist in nature, and a single state need not represent all packet-formation events.

Other Energy-Balance Models in P1

P1 refers to energy packets containing 8×1 particles, in which each hadron contributes one e_0 particle. These are the packets used in the preceding sections; however, this section proposes other methods of energy balancing.

Objective and Common Assumptions

This section examines four assumptions concerning the proton rest energy and the hadronic packet energy, in order to establish which structure can supply the energy required to form 227 eight-particle packets, equivalent to 1816 particles, within the common cavity.

This investigation is based on the calculations in Texts 85, 91, 92, 94, 98, 99, 100, 101, 102, and 103 dated 2026/10/15.

The hadronic packet contains seven protons, one neutron, and seven corresponding electrons. The stopping energy at layer 624, the neutron rest energy, and the electron rest energy in models A and B are, respectively:

[41.143] $T_{624}=811851249E_s$

[41.144] $E_{ns}=100248711E_s$

[41.145] $E_{es}=54522E_s$

The proton rest energy in models A and B is:

[41.146] $E_{ps}=100110716E_s$

In all calculations, whether ΔE_{127} remains in or leaves the common cavity is an independent physical choice. Retention means that ΔE_{127} is not subtracted from the cavity energy budget; departure means that the corresponding energy is subtracted from the cavity.

Energy Required for 227 Eight-Particle Packets

Number of particles:

[41.147] $n_{e0}=227\times8=1816$

The two metrics examined are ν_{474} and ν_{480}.

Energy per particle in the first metric:

[41.148] $E_{v474}=12\times474=5688E_s$

Total required energy:

[41.149] $E_{1816}(474)=1816\times5688=10329408E_s$

For the second metric:

[41.150] $E_{v480}=12\times480=5760E_s$

[41.151] $E_{1816}(480)=1816\times5760=10460160E_s$

Thus, the difference between the required energies of the two metrics is:

[41.152] $E_{1816}(480)-E_{1816}(474)=130752E_s$

First Assumption: Equal Proton and Neutron Rest Energies

Under the first assumption, the proton rest energy is taken to be exactly equal to the neutron rest energy, while the energy of seven electrons is added separately to the packet energy.

[41.153] $E_{ps}=E_{ns}$

[41.154] $E_{hh}=8E_{ns}+7E_{es}$

[41.155] $E_{hh}=8\times100248711+7\times54522=802371342E_s$

With ΔE_{127} retained in the cavity:

[41.156] $E_{(}Remain_{)}=811851249-802371342=9479907E_s$

Balance for metric ν_{474}:

[41.157] $\Delta E_{474}=9479907-10329408=-849501E_s$

Balance for metric ν_{480}:

[41.158] $\Delta E_{480}=9479907-10460160=-980253E_s$

Equivalent number of particles that can be supplied:

[41.159] $n_{474}=9479907/5688=1666.65031646$

[41.160] $n_{480}=9479907/5760=1645.8171875$

Therefore, under this assumption, the cavity energy is insufficient for either metric.

Second Assumption: Proton Energy Equals Neutron Energy Minus EDU

Under the second assumption, the energy difference between the down and up quarks is subtracted from the neutron energy:

[41.161] $EDU=E_{\mathcal{d}_s}-E_{us}$

[41.162] $E_{ps}=E_{ns}-EDU$

For model A:

[41.163] $EDU(A)=345684-218298=127386E_s$

[41.164] $E_{ps}(A)=100248711-127386=100121325E_s$

For model B:

[41.165] $EDU(B)=345705-218340=127365E_s$

[41.166] $E_{ps}(B)=100248711-127365=100121346E_s$

Hadronic packet energy:

[41.167] $E_{hh}=7E_{ps}+E_{ns}+7E_{es}$

For model A:

[41.168] $E_{hh}(A)=801479640E_s$

[41.169] $E_{(}Remain_{)}(A)=811851249-801479640=10371609E_s$

For model B:

[41.170] $E_{hh}(B)=801479787E_s$

[41.171] $E_{(}Remain_{)}(B)=811851249-801479787=10371462E_s$

Balance for metric ν_{474}:

[41.172] $\Delta E_{474}(A)=10371609-10329408=+42201E_s$

[41.173] $\Delta E_{474}(B)=10371462-10329408=+42054E_s$

Balance for metric ν_{480}:

[41.174] $\Delta E_{480}(A)=10371609-10460160=-88551E_s$

[41.175] $\Delta E_{480}(B)=10371462-10460160=-88698E_s$

Equivalent number of particles that can be supplied:

[41.176] $n_{474}(A)=10371609/5688\approx1823.4193038$

[41.177] $n_{474}(B)=10371462/5688\approx1823.3934599$

[41.178] $n_{480}(A)=10371609/5760=1800.6265625$

[41.179] $n_{480}(B)=10371462/5760\approx1800.6010417$

Under this assumption, metric ν_{474} has a positive balance in both models A and B, whereas metric ν_{480} still faces an energy deficit.

Third Assumption: The Rest Energy of Each Proton–Electron Pair Equals That of One Neutron

Under the third assumption, each proton–electron pair is taken to be exactly equivalent to one neutron in terms of rest energy.

[41.180] $E_{ps}+E_{es}=E_{ns}$

Consequently, the energy of seven proton–electron pairs plus one neutron is exactly equivalent to the energy of eight neutrons:

[41.181] $E_{hh}=7(E_{ps}+E_{es})+E_{ns}=8E_{ns}$

[41.182] $E_{hh}=801989688E_s$

[41.183] $E_{(}Remain_{)}=811851249-801989688=9861561E_s$

Balances for the two metrics:

[41.184] $\Delta E_{474}=9861561-10329408=-467847E_s$

[41.185] $\Delta E_{480}=9861561-10460160=-598599E_s$

Equivalent number of particles that can be supplied:

[41.186] $n_{474}=9861561/5688\approx1733.74806610$

[41.187] $n_{480}=9861561/5760=1712.0765625$

Under this assumption, too, the energy is insufficient for the complete formation of 1816 particles.

Allowing the metric to vary, the value required for zero balance is:

[41.188] $1816\times12x=9861561$

[41.189] $x=9861561/(1816\times12)\approx452.52372467$

For the two adjacent integer metrics:

[41.190] $\Delta E_{452}=9861561-1816\times12\times452=+11457E_s$

[41.191] $\Delta E_{453}=9861561-1816\times12\times453=-10335E_s$

Thus, 453 is the integer metric closest to zero balance.

Fourth Assumption: Actual Proton and Neutron Energies with an Electron Factor of 13/12

Under the fourth assumption, the calculated proton and neutron rest energies themselves are retained, and the energy contribution of each electron enters the packet with a factor of 13/12.

[41.192] $E_{hh}=7E_{ps}+E_{ns}+7(13/12)E_{es}$

[41.193] $E_{hh}=801437181.5E_s$

If ΔE_{127} remains in the cavity:

[41.194] $E_{(}Remain_{)}=811851249-801437181.5=10414067.5E_s$

Balance for metric ν_{474}:

[41.195] $\Delta E_{474}=10414067.5-10329408=+84659.5E_s$

Balance for metric ν_{480}:

[41.196] $\Delta E_{480}=10414067.5-10460160=-46092.5E_s$

Equivalent particle counts:

[41.197] $n_{474}=10414067.5/5688\approx1830.88387834$

[41.198] $n_{480}=10414067.5/5760\approx1807.99782986$

Therefore, with ΔE_{127} retained, metric ν_{474} has surplus energy, whereas metric ν_{480} has a deficit.

The following analysis examines the departure of ΔE_{127}.

In model A:

[41.199] $\Delta E_{127}(A)=141775E_s$

[41.200] $E_{(}Remain_{)}(A)=10414067.5-141775=10272292.5E_s$

[41.201] $\Delta E_{474}(A)=10272292.5-10329408=-57115.5E_s$

[41.202] $\Delta E_{480}(A)=10272292.5-10460160=-187867.5E_s$

In model B:

[41.203] $\Delta E_{127}(B)=140956E_s$

[41.204] $E_{(}Remain_{)}(B)=10414067.5-140956=10273111.5E_s$

[41.205] $\Delta E_{474}(B)=10273111.5-10329408=-56296.5E_s$

[41.206] $\Delta E_{480}(B)=10273111.5-10460160=-187048.5E_s$

Complete Comparison Table for the Four Assumptions

The following table presents all calculated cases with fully English headings and entries and separate columns.

Hadronic Assumption	Model	ΔE_{127} State	Remaining (E_s)	ν_{474} Balance (E_s)	ν_{480} Balance (E_s)
Equal Proton–Neutron; Electrons Separate	Common	Retained	9,479,907	−849,501	−980,253
Neutron Minus EDU	A	Retained	10,371,609	+42,201	−88,551
Neutron Minus EDU	B	Retained	10,371,462	+42,054	−88,698
Proton–Electron Pair Equals Neutron	Common	Retained	9,861,561	−467,847	−598,599
Physical Proton–Neutron; Electron Factor 13/12	Common	Retained	10,414,067.5	+84,659.5	−46,092.5
Physical Proton–Neutron; Electron Factor 13/12	A	Removed	10,272,292.5	−57,115.5	−187,867.5
Physical Proton–Neutron; Electron Factor 13/12	B	Removed	10,273,111.5	−56,296.5	−187,048.5

A positive sign indicates surplus energy after supplying 1816 particles, while a negative sign indicates an energy deficit.

The table shows that, for metric ν_{474}, only two families of the examined assumptions yield a positive balance: subtracting EDU from the neutron energy, and using the proton and neutron energies themselves with the 13/12 electron factor, provided ΔE_{127} remains in the cavity.

Determining the Exact Electron Factor for Zero Balance

Next, the proton and neutron energies themselves are retained, ΔE_{127} remains in the cavity, and only the electron energy factor is varied.

The notation denotes the electron factor by k_e:

[41.207] $E_{hh}=7E_{ps}+E_{ns}+7k_eE_{es}$

Exact-balance condition for metric ν_{474}:

[41.208] $811851249-(7\times100110716+100248711+7k_e\times54522)=10329408$

Therefore:

[41.209] $k_e=249059/190827\approx1.3051559789757214$

For metric ν_{480}:

[41.210] $811851249-(7\times100110716+100248711+7k_e\times54522)=10460160$

Consequently:

[41.211] $k_e=183683/190827\approx0.9625629496874132$

| Metric | Initial Electron Factor | Exact Zero-Balance Electron Factor |

|---|---:|---:|

| ν_{474} | 13/12 | 1.3051559789757214 |

| ν_{480} | 13/12 | 0.9625629496874132 |

Thus, for ν_{474}, the electron energy factor must increase relative to 13/12, whereas for ν_{480} it must decrease.

Continued in the next volume with “Structural Approximation of the Electron Factor Using α,” beginning at formula [41.212].

Structural Approximation of the Electron Factor Using α

For the factor required by metric ν_{474}, three families of approximations are examined.

First case: Outer factor 0.3

[41.212] $k_e=1+0.3(1+\alpha x)$

Required value of x:

[41.213] $x\approx2.35518244$

Simple rational approximation:

[41.214] $x=33/14$

[41.215] $k_e\approx1.30516027074$

[41.216] $\Delta k_e\approx+0.00000429177$

[41.217] $\text{Error}\approx+0.000328832\%$

A more accurate approximation using a larger fraction:

[41.218] $x=73/31$

[41.219] $k_e\approx1.30515522649$

[41.220] $\Delta k_e\approx-0.00000075249$

Second case: Outer factor 1/3

[41.221] $k_e=1+(1/3)(1+\alpha x)$

Required value:

[41.222] $x\approx-11.5839357283$

Selected rational approximation:

[41.223] $x=-139/12$

[41.224] $k_e\approx1.30515744427$

[41.225] $\Delta k_e\approx+0.00000146530$

Third case: Outer factor 1/4

[41.226] $k_e=1+(1/4)(1+\alpha x)$

Required value:

[41.227] $x\approx30.2334187649$

More accurate rational approximation:

[41.228] $x=907/30$

[41.229] $k_e \approx 1.30515582311966$

[41.230] $\Delta k_e \approx -0.00000015585606$

Another approximation:

[41.231] $x=514/17$

[41.232] $k_e \approx 1.30515940025327$

[41.233] $\Delta k_e \approx +0.00000342127755$

Selection of a Simple Fraction Based on the Criterion of Structural Simplicity

When the criterion of structural simplicity is applied, a fraction is not selected solely on the basis of the smallest numerical discrepancy. Rather, smaller numerators and denominators and a simpler structure take priority.

For the family with outer factor 1/4, the integer 30 is selected instead of the fraction 907/30.

[41.234] $x=30$

Therefore:

[41.235] $k_e=1+(1/4)(1+30\alpha)$

With the value of alpha used:

[41.236] $\alpha^{-1}=137.03599920783327$

The resulting factor is:

[41.237] $k_e \approx 1.304725104637568$

The difference from the factor required for zero balance is:

[41.238] $\Delta k_e \approx -0.0004308743381534$

The effect of this difference on the energy of seven electrons is:

[41.239] $\Delta E_{474}=-7E_{es}\Delta k_e \approx +164.449038E_s$

The relative balance error with respect to the energy required for 1816 particles is:

[41.240] $\text{Error} \approx +0.00159204\%$

Comparison Table of Electron-Factor Approximations

Outer Factor	x	Electron Factor	Factor Error	Selection
0.3	33/14	1.30516027074	+0.00000429177	Simple Rational
0.3	73/31	1.30515522649	−0.00000075249	Higher Accuracy
1/3	−139/12	1.30515744427	+0.00000146530	Simple Rational
1/4	907/30	1.30515582311966	−0.00000015585606	Higher Accuracy
1/4	514/17	1.30515940025327	+0.00000342127755	Alternative
1/4	30	1.304725104637568	−0.00043087433815	Simple Structural Model

In this table, the factor error is reported relative to the exact value required for zero balance in metric ν_{474}.

Relationship Between EDU and the Proton-to-Neutron Conversion Threshold

In models A and B, the difference between the neutron and proton rest energies is:

[41.241] $ENP=E_{ns}-E_{ps}=137995E_s$

The energy difference between the down and up quarks accounts for most of this gap.

For model A:

[41.242] $ENP-EDU(A)=137995-127386=10609E_s$

For model B:

[41.243] $ENP-EDU(B)=137995-127365=10630E_s$

These values are the ENPDU quantities of models A and B.

For seven protons:

[41.244] $7EDU(A)=891702E_s$

[41.245] $7EDU(B)=891555E_s$

And the total shortfall of the seven protons relative to the complete neutron–proton energy difference is:

[41.246] $7ENPDU(A)=74263E_s$

[41.247] $7ENPDU(B)=74410E_s$

This balance describes the structural energy of the model. The conventional kinematic threshold for the antineutrino–proton reaction is approximately 1.806 MeV and depends on the rest energies of the final particles and the conditions of energy and momentum conservation.

Summary

Comparison of the four assumptions shows that, with metric ν_{474} and ΔE_{127} remaining in the common cavity, two families of models can supply the energy needed for 227 eight-member packets.

The first family determines the proton rest energy from the neutron energy minus EDU. In this case, model A has 42201 ramions of excess energy and model B has 42054 ramions of excess energy.

The second family retains the proton and neutron rest energies themselves and calculates the electron contribution with a factor of 13/12. In this case, 84659.5 ramions of excess energy remain.

When the electron energy factor is allowed to vary, the exact values 1.3051559789757214 for metric ν_{474} and 0.9625629496874132 for metric ν_{480} establish zero balance.

Among the α-based approximations, the simple model selected on the basis of the numerical calculations is:

[41.248] $k_e=1+(1/4)(1+30\alpha)$

This model establishes the ν_{474} balance with approximately 164.449038 ramions of excess energy.

The principal result of this section is that **the balance of the hadronic packet depends on the definition of the proton rest energy, the electron energy contribution, and whether ΔE_{127} leaves or remains in the cavity**. Accordingly, these three choices must remain independent in subsequent investigations.

Different Energy Packets

Objective and Definition of the Packets

In this section, unlike Section 22, in which the packet structure was fixed, **the formats of the energy packets are varied**. All packets examined consist of eight structurally identical sets, and the total electric charge of each packet is zero. The charges of the proton and neutron arise solely from the sum of the charges of the quarks in their udu or dud cores; consequently, no new charge is assigned

to the hadron for neutralization. The earlier reference packet model is retained only in comparison tables.

There are two independent choices in the model nomenclature: the particle composition of the packet (index 31, 7, or 2), and the basis of the hadron's second term (E or 𝔼). The symbol ℙ denotes a packet whose component energies are calculated using zero-alpha values; the choice E or 𝔼 determines the basis of the second term.

Definition of Alternative Packet Energies

Energies are expressed in units of E_s. The constants, quark energies, electron energy, N, and α are as specified in the preceding sections of the article; the table of fundamental constants is not repeated.

[41.249] $P_{31}=8(15E_{us}+9E_{ds}+7E_{es})=54138240E_s$

[41.250] $\mathbb{P}_{31}=8(15\mathbb{E}_{us}+9\mathbb{E}_{ds}+7\mathbb{E}_{es})=54148320E_s$

[41.251] $P_7=8(3E_{us}+3E_{ds}+E_{es})=13971744E_s$

[41.252] $\mathbb{P}_7=8(3\mathbb{E}_{us}+3\mathbb{E}_{ds}+\mathbb{E}_{es})=13973760E_s$

[41.253] $P_2=8(2E_{es})=872352E_s$

[41.254] $\mathbb{P}_2=8(2\mathbb{E}_{es})=873360E_s$

Packet 31 consists of 15 up quarks, 9 down quarks, and 7 electrons in each unit. Packet 7 consists of 3 up quarks, 3 down quarks, and one electron. In packet 2, the energy relation $2E_{es}$ is used for each packet unit. The electrical neutrality of all packets is assumed by definition of their complete structures; the electric-charge composition must not be inferred solely from the energy expression.

Capacity, Packet Count, and the Share per Hadron

The energy capacity between layers 127 and 624 is taken from the preceding sections. The number of complete packets and the first term of the share assigned to each hadron are:

[41.255] $n_i=\text{Floor}(E_t/P_i)$

[41.256] $F_i=n_iP_i/8$

Packet	Packet Energy/E_s	Packets	First Term/E_s
P_1	3493440	227	99126360
P_{31}	54138240	14	94741920
$\mathbb{P}_{31}$	54148320	14	94759560
P_7	13971744	56	97802208
$\mathbb{P}_7$	13973760	56	97816320
P_2	872352	910	99230040
$\mathbb{P}_2$	873360	909	99235530

(A noteworthy feature of the electron packet model P_2 is the appearance of **910 injected energy packets**, obtained from an independent calculation of energy capacity and exactly equal to the product 7×10×13. In the 31-member structure comprising 7 electrons, 9 down quarks, and 15 up quarks, the number 7 is the absolute electric charge outside the core, 13 is the sum of the absolute charges inside the core, and 10 is the absolute charge of each of the two sets of positive and negative charges. This numerical correspondence may indicate a deeper relationship between the number of injected energy packets and the balance of energy, electric charge, momentum, and magnetism in the proton and neutron structures.)

The table retains the reference model solely to measure the difference in energy shares; no separate formula or discussion concerning it is repeated in this section.

Common Structure for Mass Calculation

For each packet, the first term is F_i. The second term is calculated using either the corrected-energy or zero-alpha basis, together with the magnetic coefficient corresponding to that basis. These definitions are kept consistent with the preceding relations:

[41.257] $\acute{K}_m(E)=(1-\alpha/12)/12$

[41.258] $\acute{K}_m(\mathbb{E})=1/\{12(1-\alpha/5)\}$

[41.259] $M_p(E)=(1+\acute{K}_m(E))(2E_{us}+E\mathscr{a}_s)$

[41.260] $M_n(E)=(1+\acute{K}_m(E))(E_{us}+2E\mathscr{a}_s)$

[41.261] $M_p(\mathbb{E})=(1+\acute{K}_m(\mathbb{E}))(2\mathbb{E}_{us}+\mathbb{E}\mathscr{a}_s)$

[41.262] $M_n(\mathbb{E})=(1+\acute{K}_m(\mathbb{E}))(\mathbb{E}_{us}+2\mathbb{E}\mathscr{a}_s)$

[41.263] $E_{ps}=Q_p\{F_i+M_p+C\}$

[41.264] $E_{ns}=Q_n\{F_i+M_n+C\}$

In these relations, C is the shared third term, while Q_p and Q_n are the independent quantization rules for the two particles.

Target Value of the Third Term in Fourteen Cases

The target value of C is the mean of two residuals and **does not, by itself, constitute an independent physical formula**:

[41.265] $C_t=(E_{ps}+E_{ns}-2F_i-M_p-M_n)/2$

Model	Second Proton/E_s	Second Neutron/E_s	Third Target/E_s
P_1E	847430.357132	985425.401712	136925.620578
$P_1\mathbb{E}$	847679.044733	985673.307829	136677.323719
$P_{31}E$	847430.357132	985425.401712	4521365.620578
$P_{31}\mathbb{E}$	847679.044733	985673.307829	4521117.323719
$\mathbb{P}_{31}E$	847430.357132	985425.401712	4503725.620578
$\mathbb{P}_{31}\mathbb{E}$	847679.044733	985673.307829	4503477.323719
P_7E	847430.357132	985425.401712	1461077.620578
$P_7\mathbb{E}$	847679.044733	985673.307829	1460829.323719
$\mathbb{P}_7E$	847430.357132	985425.401712	1446965.620578
$\mathbb{P}_7\mathbb{E}$	847679.044733	985673.307829	1446717.323719
P_2E	847430.357132	985425.401712	33245.620578
$P_2\mathbb{E}$	847679.044733	985673.307829	32997.323719
$\mathbb{P}_2E$	847430.357132	985425.401712	27755.620578
$\mathbb{P}_2\mathbb{E}$	847679.044733	985673.307829	27507.323719

The fixed difference between the proton and neutron second terms means that fitting their average does not necessarily make both particles' unquantized energies equal their experimental values simultaneously. The final criterion is the energy after quantization.

Continuation: First Family — Combination of Corrected Energies, beginning at [41.266].

First Family: Combination of Corrected Energies

The candidate structures of this family take the following form:

[41.266] $C_{(E)}=(aE_{us}+bE_{\mathcal{d}_s})/Y$

Model	Third-Term Formula	C/E_s
P_1E	$(4E_{us}+5E_{\mathcal{d}_s})/19$	136926.947368
$P_1\mathbb{E}$	$(5E_{us}+E_{\mathcal{d}_s}/180)/8$	136676.308333
$P_{31}E$	$(222E_{us}+56E_{\mathcal{d}_s})/15$	4521364.000000
$P_{31}\mathbb{E}$	$(-305E_{us}+258E_{\mathcal{d}_s})/5$	4521116.400000
$\mathbb{P}_{31}E$	$(224E_{us}+67E_{\mathcal{d}_s})/16$	4503723.750000
$\mathbb{P}_{31}\mathbb{E}$	$(327E_{us}+28E_{\mathcal{d}_s})/18$	4503477.666667
P_7E	$(171E_{us}-15E_{\mathcal{d}_s})/22$	1461077.181818
$P_7\mathbb{E}$	$(99E_{us}+22E_{\mathcal{d}_s})/20$	1460827.500000
$\mathbb{P}_7E$	$(259E_{us}-151E_{\mathcal{d}_s})/3$	1446966.000000
$\mathbb{P}_7\mathbb{E}$	$(138E_{us}-16E_{\mathcal{d}_s})/17$	1446716.470588
P_2E	$(6E_{us}-E_{\mathcal{d}_s})/29$	33244.965517
$P_2\mathbb{E}$	$(4E_{us}/3+9E_{\mathcal{d}_s}/80)/10$	32995.345000
$\mathbb{P}_2E$	$(E_{us}-5E_{\mathcal{d}_s}/72)/7$	27756.023810
$\mathbb{P}_2\mathbb{E}$	$(2E_{us}-5E_{\mathcal{d}_s}/72)/15$	27506.011111

These formulas are candidates obtained from a numerical search. Some rows contain large coefficients or nested fractions; consequently, neither their structural simplicity nor zero error for every row under a common quantization rule has been established.

Second Family: Combination of Zero-Alpha Energies

[41.267] $C_{(\mathbb{E})}=(a\mathbb{E}_{us}+b\mathbb{E}_{\mathcal{d}_s})/Y$

Model	Third-Term Formula	C/E_s
P_1E	—	—
$P_1\mathbb{E}$	$(45\mathbb{E}_{us}/8+\mathbb{E}_{\mathcal{d}_s}/180)/9$	136675.898148
$P_{31}E$	—	—
$P_{31}\mathbb{E}$	—	—
$\mathbb{P}_{31}E$	—	—
$\mathbb{P}_{31}\mathbb{E}$	—	—
P_7E	—	—
$P_7\mathbb{E}$	—	—
$\mathbb{P}_7E$	—	—
$\mathbb{P}_7\mathbb{E}$	—	—
P_2E	$(2\mathbb{E}_{us}+4\mathbb{E}_{\mathcal{d}_s}/3)/27$	33245.185185

| $P_2\mathbb{E}$ | $(\mathbb{E}_{us}/144+2\mathbb{E}_{\mathcal{A}_s})/21$ | 32996.488095 |

| $\mathbb{P}_2E$ | $(3\mathbb{E}_{us}+9\mathbb{E}_{\mathcal{A}_s}/80)/25$ | 27756.472500 |

| $\mathbb{P}_2\mathbb{E}$ | $(9\mathbb{E}_{us}/8+\mathbb{E}_{\mathcal{A}_s}/180)/9$ | 27505.898148 |

Third Family: Combination of N and α

[41.268] $C_{\ell}N_{\jmath}=N(a+b\alpha)/Y$

| Model | Third-Term Formula | C/E_s |

|---|---|---:|

| P_1E | $N(15+7\alpha)/4$ | 136927.213655 |

| $P_1\mathbb{E}$ | $N(34-27\alpha)/9$ | 136676.681354 |

| $P_{31}E$ | $N(1367-38\alpha)/11$ | 4521367.188630 |

| $P_{31}\mathbb{E}$ | $N(3230+35\alpha)/26$ | 4521115.164350 |

| $\mathbb{P}_{31}E$ | $N(495+7\alpha)/4$ | 4503727.213655 |

| $\mathbb{P}_{31}\mathbb{E}$ | $N(1114-27\alpha)/9$ | 4503476.681354 |

| P_7E | $N(321+28\alpha)/8$ | 1461078.177309 |

| $P_7\mathbb{E}$ | $N(522-18\alpha)/13$ | 1460830.776010 |

| $\mathbb{P}_7E$ | $N(159+7\alpha)/4$ | 1446967.213655 |

| $\mathbb{P}_7\mathbb{E}$ | $N(358-27\alpha)/9$ | 1446716.681354 |

| P_2E | $N(11-5\alpha)/12$ | 33246.853892 |

| $P_2\mathbb{E}$ | $N(8+22\alpha)/9$ | 32995.790502 |

| $\mathbb{P}_2E$ | $N(3+7\alpha)/4$ | 27757.213655 |

| $\mathbb{P}_2\mathbb{E}$ | $N(12+13\alpha)/16$ | 27508.259911 |

Among these relations, the compact candidate for model P_2E is:

[41.269] $C_{\ell}P_2E_{\jmath}=N(11-5\alpha)/12$

This algebraic structure represents a compact form of the relations obtained from the search.

Re-examination of Raw Energy and Quantization

The first table shows the differences between raw energy and the target proton and neutron energies for the N family. Nonzero entries in this table may become zero-error results after quantization.

| Model | Proton Raw Error | Neutron Raw Error |

|---|---:|---:|

| P_1E | +1.570787 | +1.615366 |

| $P_1\mathbb{E}$ | −0.273913 | −1.010817 |

| $P_{31}E$ | +1.545762 | +1.590342 |

| $P_{31}\mathbb{E}$ | −1.790917 | −2.527821 |

| $\mathbb{P}_{31}E$ | +1.570787 | +1.615366 |

| $\mathbb{P}_{31}\mathbb{E}$ | −0.273913 | −1.010817 |

| P_7E | +0.534441 | +0.579021 |

| $P_7\mathbb{E}$ | +1.820743 | +1.083839 |

| $\mathbb{P}_7$E | +1.570787 | +1.615366 |

| $\mathbb{P}_7\mathbb{E}$ | −0.273913 | −1.010817 |

| P_2E | +1.211024 | +1.255603 |

| $P_2\mathbb{E}$ | −1.164765 | −1.901669 |

| $\mathbb{P}_2$E | +1.570787 | +1.615366 |

| $\mathbb{P}_2\mathbb{E}$ | +1.304644 | +0.567740 |

For a uniform and comparable test, the second table applies Floor_2 to the proton and Floor_3 to the neutron:

| Model | Floor_2 Proton | Floor_3 Neutron | Both Exact |

|---|---:|---:|---|

| P_1E | 100110716 | 100248711 | Yes |

| $P_1\mathbb{E}$ | 100110714 | 100248708 | No |

| P_{31}E | 100110716 | 100248711 | Yes |

| $P_{31}\mathbb{E}$ | 100110714 | 100248708 | No |

| $\mathbb{P}_{31}$E | 100110716 | 100248711 | Yes |

| $\mathbb{P}_{31}\mathbb{E}$ | 100110714 | 100248708 | No |

| P_7E | 100110716 | 100248711 | Yes |

| $P_7\mathbb{E}$ | 100110716 | 100248711 | Yes |

| $\mathbb{P}_7$E | 100110716 | 100248711 | Yes |

| $\mathbb{P}_7\mathbb{E}$ | 100110714 | 100248708 | No |

| P_2E | 100110716 | 100248711 | Yes |

| $P_2\mathbb{E}$ | 100110714 | 100248708 | No |

| $\mathbb{P}_2$E | 100110716 | 100248711 | Yes |

| $\mathbb{P}_2\mathbb{E}$ | 100110716 | 100248711 | Yes |

In this test, **8 of the 14 models** have zero error for both particles. The other six models yield the corresponding outputs under the pair of quantization rules used in this test. For each model, its pair of rules and raw output are specified in the search report.

Selection Criteria and Conclusion

Three criteria are examined in order: first, **simultaneous** zero error in the quantized energies of the proton and neutron; second, minimization of coefficient and denominator complexity; and finally, a physical interpretation of the coefficients based on packet composition and charge. Formulas derived from the difference between the first terms of the two packets are classified as algebraic generalizations.

This section compares six alternative packet formats alongside one purely tabular reference format, with two bases for the second term. Fourteen candidates are recorded for the E family, five search candidates for the $\mathbb{E}$ family (including the reference row), and fourteen for the N family. The selection criteria include the pair of quantization rules for each candidate and the mechanism for charge neutralization in electron packets.

Experimental Values for the Muon and Tau

[41.270] $g_{mx} = 2.00233184123 \pm 82_{(10)}{}^{-11}$

; E_{mx} = 105.6583755 ±23$(10)^{-7}$ MeV

; E_{m2x} = 1273 ±4 MeV

; E_{m1x} = 93.4 ±86$(10)^{-1}$ MeV

; g_{tx} = 2.00235442 ±1$(10)^{-7}$

; E_{tx} = 1776.86 ±12$(10)^{-2}$ MeV

; E_{t2x} = 172690 ±300 MeV

; E_{t1x} = 4183 ±7 MeV

Completion of Theorem 41: Unified Proton and Neutron Energy Model

Introduction

This article presents a framework for calculating the rest energies of the proton and neutron; defining four fundamental families, A, B, C, and D; specifying energy-packet structures; transferring energy from the quark stage to the hadronic stage; accounting for magnetic corrections and neutrino radiation; and searching for the minimum Last.

The system under consideration consists of seven protons and one neutron. Energy released through layer collapse and energy transferred from the preceding stage become available, after subtraction of specified contributions, to supply the packet energies and the third terms of the hadrons.

Each hadron's energy consists of three terms:

1. Energy of the absorbed packets.

2. Quark energy corrected by the magnetic coefficient.

3. The shared third term, c_3.

In the general models, the difference between proton and neutron energies is determined using the exact coefficient $\acute{K}_m$. In the analytical models of the final section, α-dependent approximations and independent formulas for the third term are also examined.

The four families A, B, C, and D are defined by two independent choices, f and $\mathbb{M}$. Each family contains a set of parameter combinations.

The objective is to identify models that reproduce the target proton and neutron energies while satisfying energy balance and structural constraints.

All calculated numerical energies are expressed in units of E_s unless another unit is explicitly stated.

---

1. Constants, Fundamental Energies, and Experimental Data

1.1. Primary Metric and Electron Genetic Code

[41.271] N=36390

[41.272] $\mathring{N}$=36864

$\mathring{N}$ is the genetic code of the electron family and must not be identified with the geometric origin of the collapse layers.

1.2. Full Energies

[41.273] $\mathbb{E}_{es}$=3N/2=54585

[41.274] $\mathbb{E}_{us}$=12N/2=218340

[41.275] $\mathbb{E}_{\mathscr{A}s}$=19N/2=345705

[41.276] $\mathbb{E}_{e0s}=12N=436680$

1.3. Reduced Energies

The magnetic reductions for the electron, up quark, and down quark are 63, 42, and 21 units, respectively.

[41.277] $E_{es}=\mathbb{E}_{es}-63=54522$

[41.278] $E_{us}=\mathbb{E}_{us}-42=218298$

[41.279] $E_{\mathscr{d}s}=\mathbb{E}_{\mathscr{d}s}-21=345684$

[41.280] $E_{e0s}=\mathbb{E}_{e0s}=436680$

For the neutral electron, the magnetic reduction is zero.

1.4. Reference Experimental Energies

Values used from CODATA 2022:

[41.281] $E_{e(2022)}=0.51099895069$ MeV

[41.282] $E_{p(2022)}=938.27208943$ MeV

[41.283] $E_{n(2022)}=939.56542194$ MeV

---

2. Determination of Base Energy and Target Energies

The parameter f, short for *Full*, specifies the electron-energy basis used to determine E_s.

2.1. Case Without f: Families A and B

[41.284] $E_s=E_{e(2022)}/54522\approx 9.37234420399105_{(10)^{-6}}$ MeV

[41.285] $E_{p(2022)}/E_s\approx 100110716.06082$

[41.286] $E_{ps}=100110716$

Target proton quantization: Floor or Ceil with bases 1, 2, and 4.

[41.287] $E_{n(2022)}/E_s\approx 100248710.62032$

[41.288] $E_{ns}=100248711$

Target neutron quantization: Floor or Ceil with bases 1 and 3.

[41.289] $ENP=E_{ns}-E_{ps}=137995$

Optimal E_s from RMS minimization:

[41.290] $E_s=9.372344190245791_{(10)^{-6}}$ MeV

2.2. Case With f: Families C and D

[41.291] $E_s=E_{e(2022)}/54585\approx 9.36152698891605_{(10)^{-6}}$ MeV

[41.292] $E_{p(2022)}/E_s\approx 100226393.67925$

[41.293] $E_{ps}=100226394$

Target proton quantization: Floor or Ceil with bases 1, 2, 3, and 6.

[41.294] $E_{n(2022)}/E_s\approx 100364547.69103$

[41.295] $E_{ns}=100364548$

Target neutron quantization: Floor or Ceil with bases 1, 2, and 4.

[41.296] $ENP=E_{ns}-E_{ps}=138154$

Optimal E_s:

[41.297] $E_s=9.361526966884192_{(10)}{}^{-6}$ MeV

2.3. RMS Minimization

The initial base energy is calculated from the experimental electron energy. The value of E_s is then optimized using experimental electron, proton, and neutron data and their uncertainties.

For the case without f, the selected combination is "E2018_P2018_N2022".

Continuation follows in Volume 39, beginning with the subsequent discussion of RMS minimization.

2.3. RMS Minimization (continued)

For the case without f, the selected combination is "E2018_P2018_N2022".

Particle	Quantized energy	Normalized deviation
Electron	54522	-0.396126094889σ
Proton	100110716	-2.33121956375σ
Neutron	100248711	$+4.54266526617\sigma$

[41.298] $RMS_{(A,B)}=2.95676108030072\sigma$

For the case with f, the selected combination is "E2018_P2022_N2022".

Particle	Quantized energy	Normalized deviation
Electron	54585	-3.41750849842σ
Proton	100226394	$+2.73986180563\sigma$
Neutron	100364548	$+1.4190478718\sigma$

[41.299] $RMS_{(C,D)}=2.6583142473615\sigma$

This optimization does not change the target integer energies; rather, it slightly corrects the continuous value of E_s.

2.4. Electron Scale Factor

In the case without f:

[41.300] $\theta_e=1$

In the case with f:

[41.301] $\theta_e=54522/54585=0.998845836768343$

θ_e is the ratio of the two initial energy bases. Dimensional quantities dependent on E_s must change according to their scaling dependence when converting between the two bases.

---

3. Four Fundamental Families A, B, C, and D

The parameter f determines the electron energy basis.

The parameter $\mathbb{M}$ determines whether the second term of the hadrons uses the full quark energies or the reduced energies.

Family	f	$\mathbb{M}$	d_e	d_u	$d_{\mathcal{A}}$

|---|---|---|---:|---:|---:|

| A | No | No | 63 | 42 | 21 |

| B | No | Yes | 63 | 0 | 0 |

| C | Yes | Yes | 0 | 0 | 0 |

| D | Yes | No | 0 | 42 | 21 |

3.1. Quark Energy Difference

Without $\mathbb{M}$:

[41.302] $EDU=E\mathscr{A}_s-E_{us}=127386$

With $\mathbb{M}$:

[41.303] $EDU=\mathbb{E}\mathscr{A}_s-\mathbb{E}_{us}=127365$

3.2. Exact Magnetic Coefficient

Assuming that the energy difference between the two hadrons arises only from the difference between their quark terms:

[41.304] $ENP=(1+\acute{K}_m)EDU$

Therefore:

[41.305] $\acute{K}_m=ENP/EDU-1$

| Family | ENP | EDU | ENP−EDU |

|---|---:|---:|---:|

| A | 137995 | 127386 | 10609 |

| B | 137995 | 127365 | 10630 |

| C | 138154 | 127365 | 10789 |

| D | 138154 | 127386 | 10768 |

The exact value of $\acute{K}_m$ is the same for all models belonging to a given family.

3.3. Analytical Approximations Depending on α

These approximations are presented for structural comparison. In the general calculations of the article, the exact relation (35) is the basis.

Family A:

[41.306] $\acute{K}_m\approx(1-\alpha/12)/12$

[41.307] $\acute{K}_m\approx1/[12(1+\alpha/12)]$

Family B:

[41.308] $\acute{K}_m\approx(1+\alpha/5)/12$

[41.309] $\acute{K}_m\approx1/[12(1-\alpha/5)]$

Family C:

[41.310] $\acute{K}_m\approx(1+9\alpha/4)/12$

Family D:

[41.311] $\acute{K}_m\approx(1+2\alpha)/12$

The approximations for C and D correspond to the selected approximations in this model.

---

4. Physical Structure and Energy of the Packets

4.1. Definition of a Packet

An energy packet is a collection of energy contributions equivalent to particles.

The principal structures include packets of one, two, three, seven, and thirty-one components.

P_1 represents the energy of one neutral electron; P_2, the energy of an electron and a positron; P_3, the same pair together with a neutral electron; P_7, a combination of three up quarks, three down quarks, and one electron; and P_{31}, a combination of fifteen up quarks, nine down quarks, and seven electrons.

4.2. Electrical Charge Neutrality

[41.312] $Q(P_7)=3(\frac{2}{3})+3(-\frac{1}{3})-1=0$

[41.313] $Q(P_{31})=15(\frac{2}{3})+9(-\frac{1}{3})-7=0$

P_2 and P_3 also have zero net charge under their defined compositions.

4.3. The Two Families P and $\mathbb{P}$

The P family uses the reduced energies of the packet components.

The $\mathbb{P}$ family uses their full energies.

For a neutral electron, the two choices coincide.

4.4. Nine Distinct Packet Energies

[41.314] $P_1=\mathbb{P}_1=436680$

[41.315] $P_2=2E_{es}=109044$

[41.316] $\mathbb{P}_2=2\mathbb{E}_{es}=109170$

[41.317] $P_3=2E_{es}+E_{e0s}=545724$

[41.318] $\mathbb{P}_3=2\mathbb{E}_{es}+\mathbb{E}_{e0s}=545850$

[41.319] $P_7=3E_{us}+3E_{\mathscr{d}s}+E_{es}=1746468$

[41.320] $\mathbb{P}_7=3\mathbb{E}_{us}+3\mathbb{E}_{\mathscr{d}s}+\mathbb{E}_{es}=1746720$

[41.321] $P_{31}=15E_{us}+9E_{\mathscr{d}s}+7E_{es}=6767280$

[41.322] $\mathbb{P}_{31}=15\mathbb{E}_{us}+9\mathbb{E}_{\mathscr{d}s}+7\mathbb{E}_{es}=6768540$

Number of particle equivalents in the packet energy:

[41.323] $n\in\{1,2,3,7,31\}$

Packet	Particle count	Energy	Magnetic deduction
$P_1 = \mathbb{P}_1$	1	436680	0
P_2	2	109044	126
$\mathbb{P}_2$	2	109170	0
P_3	3	545724	126
$\mathbb{P}_3$	3	545850	0
P_7	7	1746468	252
$\mathbb{P}_7$	7	1746720	0
P_{31}	31	6767280	1260

| $\mathbb{P}_{31}$ | 31 | 6768540 | 0 |

4.5. Energy Difference Between Full and Reduced Packets

[41.324] $\mathbb{P}_2 - P_2 = 126$

[41.325] $\mathbb{P}_3 - P_3 = 126$

[41.326] $\mathbb{P}_7 - P_7 = 252$

[41.327] $\mathbb{P}_{31} - P_{31} = 1260$

---

5. Model Naming Standard

A model name consists of eight positions in a fixed order.

| Position | Parameter | Meaning | Default |

|---|---|---|---|

| 1 | f | Full electron energy basis | Reduced basis |

| 2 | n | New hadron layer origin | Continue from layer 128 |

| 3 | E / $\mathbb{E}$ | Transferred quark-stage energy | $T(127) - 7E_e$ |

| 4 | P_n / $\mathbb{P}_n$ | Packet energy type | Required |

| 5 | $\mathbb{M}$ | Full quark energies in hadron term | Reduced quark energies |

| 6 | ν_{450} / ν_{480} | Neutrino metric | ν_{474} |

| 7 | p | Seven-proton radiation correction | Off |

| 8 | e | Seven-electron magnetic correction | Off |

Inactive optional parameters are omitted from the name.

E and $\mathbb{E}$ in the third position specify the energy-transfer choice, whereas $\mathbb{M}$ in the fifth position determines the quark-energy type used in the second term.

5.1. Number of Combinations

[41.328] $N_{(family)} = 2 \times 3 \times 9 \times 3 \times 2 \times 2 = 324$

[41.329] $N_{(total)} = 4 \times 324 = 1296$

These numbers count nominal combinations, not physically validated models.

---

6. Layer Geometry and Cumulative Energy Function

[41.330] $T(L) = (10L^3 + 15L^2 + 11L + 3)/3$

[41.331] $T(127) = 6909055$

In the n case, the hadronic stage begins at layer zero, and the Last search starts at 1.

In the case without n, the hadronic stage continues the previous structure, and the search begins at layer 128.

In the second case, the cumulative contribution of the previous stage is subtracted from the total energy.

---

7. Energy Transfer from the Quark Stage

There are three energy-transfer choices.

Reduced transfer E:

[41.332] $E_t=15E_{us}+9E_{𝒹s}$

Full transfer 𝔼:

[41.333] $E_t=15\mathbb{E}_{us}+9\mathbb{E}_{𝒹s}$

Default case without E or 𝔼:

Without f:

[41.334] $E_t=T(127)-7E_{es}$

With f:

[41.335] $E_t=T(127)-7\mathbb{E}_{es}$

E_t is the transferred contribution and must not be confused with the total available energy E.

---

8. Total Available Energy E

E is the energy available to supply the packet groups and the third term of the eight hadrons.

8.1. Quark Contribution of Eight Hadrons

With 𝕄:

[41.336] $Q_{8}=(15\mathbb{E}_{us}+9\mathbb{E}_{𝒹s})(1+\acute{K}_m)$

Without 𝕄:

[41.337] $Q_{8}=(15E_{us}+9E_{𝒹s})(1+\acute{K}_m)$

8.2. Correction p

[41.338] $E_{p(ra𝒹)}=7(E_{ns}-E_{ps})$

This correction represents the hypothesis of radiation of the neutron–proton energy difference for seven protons.

8.3. Correction e

With 𝕄:

[41.339] $E_{e(m)}=7\mathbb{E}_{es}\acute{K}_m$

Without 𝕄:

[41.340] $E_{e(m)}=7E_{es}\acute{K}_m$

8.4. General Formula

[41.341] E=T(Last)

; −(if not n)T(127)

; +(if E)$(15E_{us}+9E_{𝒹s})$

; +(if 𝔼)$(15\mathbb{E}_{us}+9\mathbb{E}_{𝒹s})$

; +(if not E and not 𝔼)(T(127)−(if not f)$7E_{es}$−(if f)$7\mathbb{E}_{es}$)

; −(if 𝕄)$(15\mathbb{E}_{us}+9\mathbb{E}_{𝒹s})(1+\acute{K}_m)$

; −(if not 𝕄)$(15E_{us}+9E_{𝒹s})(1+\acute{K}_m)$

; −(if p)7($E_{ns}-E_{ps}$)

; −(if e and $\mathbb{M}$)7$\acute{K}_m\mathbb{E}_{es}$

; −(if e and not $\mathbb{M}$)7$\acute{K}_mE_{es}$

Conditional terms are applied only when their corresponding selections are active.

The neutrino cost is included in E_8 and must not be subtracted from E a second time.

---

9. Neutrino Metric

Difference between the electron genetic code and the Ramion metric:

[41.342] $\mathring{N}-N=474$

Three choices of neutrino metric:

[41.343] $N_\nu=474$

[41.344] $N_\nu=480$

[41.345] $N_\nu=450$

Neutrino energy per equivalent particle:

[41.346] $E_{\nu(1)}=12N_\nu$

Mode	N_ν	Energy
Default	474	5688
ν_{480}	480	5760
ν_{450}	450	5400

The absence of ν from the model name means that the default metric 474 is selected; it does not mean that neutrino radiation is omitted.

---

10. Eightfold Group Energy and Number of Packets

[41.347] $E_8=8(E_{pac}+n\times12N_\nu)$

[41.348] $n_8=\text{Floor}(E/E_8)$

Packet contribution per hadron:

[41.349] $E_{(pac)}=n_8E_{pac}$

Packet contribution for eight hadrons:

[41.350] $E_{(8pac)}=8n_8E_{pac}$

Total energy consumed by packets and neutrinos:

[41.351] $n_8E_8=8n_8E_{pac}+8n_8n\times12N_\nu$

---

11. Proton and Neutron Energy Structure

For brevity, the up- and down-quark energies in the second term are denoted by U and D, respectively.

With $\mathbb{M}$:

[41.352] $U=\mathbb{E}_{us}$

[41.353] $D=\mathbb{E}_{\acute{a}_s}$

Without $\mathbb{M}$:

[41.354] $U=E_{us}$

[41.355] $D=E_{\acute{a}_s}$

Continuous proton energy:

[41.356] $X_p=n_8E_{pac}+(2U+D)(1+\acute{K}_m)+c_3$

Continuous neutron energy:

[41.357] $X_n=n_8E_{pac}+(U+2D)(1+\acute{K}_m)+c_3$

Quantized energies:

[41.358] $\acute{E}_{ps}=Quant_p(X_p)$

[41.359] $\acute{E}_{ns}=Quant_n(X_n)$

The first and third terms are identical for the proton and neutron; the difference between the particles lies in the quark composition of the second term.

---

12. Range of c_3 and Balance Condition

Permitted range of the third term:

[41.360] $|c_3|\leq E_{pac}$

Energy-balance condition:

[41.361] $E\geq n_8E_8+8c_3$

c_3 may be positive, zero, or negative.

This condition tests the energy required for the packet groups and the sum of the third terms of eight hadrons.

---

13. Testing Quantization Pairs

For each family, Floor and Ceil methods are examined using the bases permitted for that family.

[41.362] $\acute{E}_{ps}=E_{ps}$

[41.363] $\acute{E}_{ns}=E_{ns}$

Every quantization pair satisfying both relations is recorded.

Round is not used as an independent method in the article's general search.

If c_3 has been extracted directly from the target energies, the resulting zero error does not, by itself, constitute an independent prediction.

---

14. Search for the Minimum Last

In the n case:

[41.364] $Last_{min}=1$

In the case without n:

[41.365] $Last_{min}=128$

For each Last, the cumulative energy, transferred energy, E, eightfold-group energy, packet count, c_3, balance condition, and quantization pairs are calculated.

Stopping rule:

[41.366] $|c_3|>E_{pac} \Rightarrow$ Stop

In the defined search, once the stopping condition is met, larger values of Last are not examined for that model.

The first Last satisfying all conditions is the smallest accepted Last for that model.

---

15. Fundamental Derivation of c_3

After identifying the accepted models, the objective is to derive an independent relation for c_3.

A candidate formula must be constructed from the fundamental Ramionics parameters and must not rely directly on the experimental target energies of the proton and neutron to determine its value.

At this stage, the dependence of c_3 on Last, packet count, packet type, f, and $\mathbb{M}$ is examined.

The analytical models of Section 18 are examples of proposed formulas for the third term.

Theorem 41 continues in Volume 40 with Section 16, “Computational Acceptance Criteria.”

16. Computational Acceptance Criteria

For the computational acceptance of a model, the following conditions are examined:

1. The fundamental family and all choices constituting the model name must be specified.

2. The target energies must be determined in accordance with f.

3. In the general search, the exact value of $\acute{K}_m$ must be used.

4. The energy E must be calculated for the Last under examination.

5. The number of packets must be an integer and nonnegative.

6. The value of c_3 must be determined and its permitted range respected.

7. The energy-balance condition must hold.

8. At least one permitted quantization pair must yield zero error for both hadrons.

9. Last must be the smallest accepted value in the ascending search.

10. All successful pairs and computational results must be recorded.

---

17. Conclusion of the General Framework

This framework defines four fundamental families: A, B, C, and D.

Each family has 324 nominal combinations; thus, a total of 1,296 nominal combinations can be examined.

The exact coefficient $\acute{K}_m$ is determined from the difference between the target proton and neutron energies and the difference between the quark energies.

The packets comprise five principal structures and nine distinct energy values.

The energy E is determined from the layer history, energy transfer, quark contribution, and optional corrections.

Neutrino radiation is included in E_8, and the number of packet groups is determined using Floor.

The energy of each hadron consists of the packet contribution, the magnetic quark contribution, and c_3.

The search over Last is performed to find the smallest accepted structure.

The next research stage is to find an independent fundamental relation for c_3 and examine the predictive power of the accepted models.

---

18. Analytical P_2 Models and Independent Formulas for the Third Term

18.1. P_2 Model — Family A

Principal formula for the third term:

[41.367] $c_3=N(1-(1+5\alpha)/12)$

Two alternative families:

[41.368] $c_3=(1-\alpha/n)(15E_{us}+9E_{\mathscr{A}_s})/(8\times24)$, $n\in\{19,20,21\}$

[41.369] $c_3=(15E_{us}+9E_{\mathscr{A}_s})/[8\times24(1+\alpha/n)]$, $n\in\{19,20,21\}$

Proton energy:

[41.370] $E_{ps}=Floor_2\{910(2E_{es})+(1+\acute{K}_m)(2E_{us}+E_{\mathscr{A}_s})+c_3\}=100110716$

Neutron energy:

[41.371] $E_{ns}=Round_3,Floor_3\{910(2E_{es})+(1+\acute{K}_m)(E_{us}+2E_{\mathscr{A}_s})+c_3\}=100248711$

If $Floor_3$ alone is sufficient for the neutron, n=22 is also accepted in the two alternative relations for c_3.

18.2. $P_2\mathbb{M}$ Model — Family B

Third term:

[41.372] $c_3=N(1-(1-22\alpha)/9)$

Proton energy:

[41.373] $E_{ps}=Ceil_2\{910(2E_{es})+(1+\acute{K}_m)(2\mathbb{E}_{us}+\mathbb{E}_{\mathscr{A}_s})+c_3\}=100110716$

Neutron energy:

[41.374] $E_{ns}=Ceil_3\{910(2E_{es})+(1+\acute{K}_m)(\mathbb{E}_{us}+2\mathbb{E}_{\mathscr{A}_s})+c_3\}=100248711$

18.3. $\mathbb{P}_2$ Model — Family A

Third term:

[41.375] $c_3=N(1-(1-7\alpha)/4)$

Proton energy:

[41.376] $E_{ps}=Floor_2\{909(2\mathbb{E}_{es})+(1+\acute{K}_m)(2E_{us}+E_{\mathscr{A}_s})+c_3\}=100110716$

Neutron energy:

[41.377] $E_{ns}=Floor_3\{909(2\mathbb{E}_{es})+(1+\acute{K}_m)(E_{us}+2E_{\mathscr{A}_s})+c_3\}=100248711$

18.4. $\mathbb{P}_2\mathbb{M}$ Model — Family B

Third term:

[41.378] $c_3=N(1-(1-16\alpha/5)/4)$

Proton energy:

[41.379] $E_{ps}=Ceil_4\{909(2\mathbb{E}_{es})+(1+\acute{K}_m)(2\mathbb{E}_{us}+\mathbb{E}_{\mathscr{A}_s})+c_3\}=100110716$

Neutron energy:

[41.380] $E_{ns}=Ceil_3\{909(2\mathbb{E}_{es})+(1+\acute{K}_m)(\mathbb{E}_{us}+2\mathbb{E}_{\mathscr{A}s})+c_3\}=100248711$

18.5. Contribution of Terms to Proton and Neutron Energies

| Historical comparison | Reported result |

|---|---|

| First term alone | More than 98.983856261254% |

| First and second terms with $\acute{K}_m=0$ | More than 99.891265434824% |

| First and second terms without α | More than 99.966830723696% |

| Two terms, third term omitted, after quantization | More than 99.96679% |

| Maximum relative error for preceding comparison | 332.092 ppm |

| Without explicit α corrections in second and third terms, after quantization | More than 99.9992428% |

| Maximum relative error for preceding comparison | Approximately 7.571 ppm |

Theorem 42: Calculation of Inertia in Hadrons

In Ramionics, the inertia of a particle is not merely an independent parameter associated with mass; rather, it arises from the spatial distribution of energy and the self-interaction of its Ramionic field. In Theorem 37, inertia was introduced as the response of a body's energy distribution to a change in its state of motion and, in the classical limit, rotational energy led to the conventional relation for the moment of inertia.

On the other hand, the structure of hadrons is based on the twelve-ball model. In this model, the particle's energy is distributed among twelve balls surrounding the central cavity, and opposite balls are organized into symmetric pairs to preserve force and torque equilibrium.

In Theorem 41, the mass-inertial energy capacity corresponding to one ball was also defined as one-twelfth of the particle's structural mass energy. Consequently, the twelve-ball structure enters directly into the calculation of hadronic inertia.

To calculate a hadron's moment of inertia, the analysis considers its three constituent quarks in their spatial arrangement. If, as a first approximation, the effective mass of each quark is m and the fundamental structural distance is R, one quark lies at distance R from the effective rotation axis and the other two quarks lie at distance 4R.

The moment of inertia of each component about the rotation axis is obtained by multiplying its mass by the square of its distance from the axis. Thus, for the first quark:

[42.1] $I_1=m.R^2$

And for the other two quarks:

[42.2] $I_2=I_3=m.(4R)^2=16m.R^2$

The total moment of inertia of the hadron is the sum of the three contributions:

[42.3] $I=I_1+I_2+I_3$

Hence:

[42.4] $I=m.R^2+16m.R^2+16m.R^2$

And therefore:

[42.5] $I=33m.R^2$

If the total mass of the hadron in this approximation is M=3m, the relation can also be written in terms of the total mass:

[42.6] $I=11M.R^2$

This result shows that hadronic inertia in the Ramionics model depends strongly on the geometry of the quark distribution. The two quarks located at distance 4R make the dominant contribution to the total inertia because the moment of inertia depends quadratically on distance.

The effective hadron radius can now be introduced directly into the relation. If the definition is the effective radius of the hadron as the distance from the center to the peripheral quarks, then:

[42.7] $R_h=4R$

Therefore:

[42.8] $R=R_h/4$

Substituting into the moment-of-inertia relation:

[42.9] $I=11M.(R_h/4)^2$

Consequently:

[42.10] $I=(11/16)M.R_h^2$

Thus, the dimensionless hadronic inertia coefficient in this model is 11/16:

[42.11] $I/(M.R_h^2)=11/16=0.6875$

This coefficient is a direct consequence of the assumed three-quark arrangement and remains independent of the absolute scales of mass and radius.

Furthermore, if the effective mass distribution of the balls is included in the calculation, the inertia contribution arising from the twelve-ball structure must be added separately to this point-quark model. This distinction is important because the relation above calculates the geometric moment of inertia of the three quark centers, whereas each center itself has an energy distribution and a ball structure. Thus, the complete hadronic moment of inertia generally comprises two contributions: the inertia arising from the positions of the energy centers and the internal inertia of the energy distribution around each center.

Accordingly, the present theorem provides a geometric basis for calculating hadronic inertia: a hadron's inertia is not determined by mass alone; the distances and arrangement of the energy components within the hadronic structure play a fundamental role. This structure may subsequently be connected to calculations of rotational energy, angular momentum, magnetic moment, and the gyromagnetic factor of hadrons.

Theorem 43: Proton Radius

[43.1] $\hbar$ = 1.05457181764615647E−34 J.s

[43.2] c = 2.99792458E8 m/s

[43.3] N_e = 36390

[43.4] E_{03} = 8.0092664715760264

[43.5] E_s = 1.5016193047094933E−18 J

[43.6] $\gamma = 0.82557850950146439$

[43.7] $z = 1.0011529837934436$

If the electron radius is defined as follows:

[43.8] $r_e = (16.\gamma.\hbar.c.z)/(N_e^2.E_s)$

the result is:

[43.9] $r_e = 2.10257607354081465E{-}16$ m

And if the model assumes that the proton radius is four times the electron radius:

[43.10] $r_p = 4.r_e$

Then:

[43.11] $r_p = 8.41030429416325862E{-}16$ m

For comparison, the experimental value of the proton charge radius, obtained from electron–proton scattering and spectroscopy of hydrogen and muonic hydrogen, is:

[43.12] $r_p(EX) = 8.414E{-}16$ m

With approximate uncertainty:

[43.13] $\sigma = 1.9E{-}19$ m

Therefore:

[43.14] $\Delta r_p = -1.945108335127174 51\sigma$

The conclusion is that the simple relation

[43.15] $r_p = 4.r_e$

Together with the definition

[43.16] $r_e = (16.\gamma.\hbar.c.z)/(N_e^2.E_s)$

reproduces the proton radius with an error of approximately 1.95σ.

The translation continues with Theorem 44: Quark Chromatics (Color Charge and Its Geometric Model in Ramionics).

Theorem 44: Quark Chromatics (Color Charge and Its Geometric Model in Ramionics)

1. Fundamental Structure: Twelve Bals and Six Axes

In the Ramionics geometry under consideration, the fundamental structure of a particle consists of **twelve bals**. These twelve bals are arranged in six pairs opposite one another and therefore form **six fundamental axes**. Each axis consists of two precisely opposite bals.

From this article onward, the numbering of axes **1 through 6, according to the latest approved reference image**, is regarded as fixed. Subsequent aesthetic improvements or redesigns of the image must not change this reference numbering.

The geometry of the centers of the twelve bals is based on the edge structure of a cube. The six resulting axes contain three orthogonal pairs:

1–6, 2–4, and 3–5.

Each axis makes an angle of 90° with its paired axis and an angle of 60° with each of the other four axes. Thus, the six-axis structure contains three orthogonal relationships and twelve 60° relationships.

This geometry exists before the particle type is defined. Narions, neutrinos, electrons, and quarks are not constructed by altering the base geometry; their differences concern the states and rotational directions of the bals.

2. Why Do the Two Opposite Bals on an Axis Have the Same Sign?

The twelve bals are not counted as twelve independent units of charge. Two opposite bals belong to **one and the same axis**, and their states express one axial degree of freedom.

If an axis is positive, both opposite bals are members of that same positive axial state; if the axis is negative, both belong to its negative state.

Thus, the unit used to count charge is not an individual bal; it is **an axis consisting of two opposite bals**.

The twelve bals give rise to six independent axes, so the fundamental quantum for counting charge in this structure is 1/6, not 1/12.

However, charge changes by switching an axis from one sign to the other. In such a transition, the axis contribution changes from −1/6 to +1/6, or vice versa. The resulting magnitude of change is therefore 2/6:

[44.1] $\Delta q = 2/6 = 1/3$

Accordingly, two concepts must remain distinct:

The axial quantum of charge is 1/6, whereas the quantum of charge change between the two sign states of an axis is 1/3.

This distinction provides a natural explanation, within this model, for the appearance of one-third steps in the electric charges of this family.

3. Sign, and the Inner and Outer Surfaces of a Bal

The sign of an axis is not merely an abstract label. Every bal has inner and outer regions with opposite states.

For a positive bal, the outward-facing region is positive and the inward-facing region is negative. For a negative bal, the arrangement is reversed: the outer region is negative and the inner region positive.

Consequently, even in a structure whose total charge is zero, the signs do not disappear from its interior. Zero net charge results only from the balance of their sum.

This is fundamentally important for short-range behavior.

4. Neutrality Does Not Mean Electrical and Magnetic Inactivity

Within this structure, a neutral particle such as a **narion or neutrino** is not necessarily electrically and magnetically inactive at every distance and in every direction.

Zero net charge means that the contributions of the six axes sum to zero. But when another particle or structure is brought extremely close, its distances from all twelve bals are not equal.

Under these circumstances, **the nearest bal or bals make a more dominant local contribution to the interaction**. The sign of the nearest bal, the states of its inner and outer surfaces, and its rotational direction can therefore determine the electrical and magnetic effects of the nearby interaction in that direction.

Ramionics must therefore distinguish two concepts:

A particle's net charge is a global property of its six axes, whereas **a short-range interaction** can depend on direction, the nearest bal, and the rotational state of that region.

A neutral narion or neutrino can consequently exhibit local electrical and magnetic effects at short distances without possessing nonzero net charge.

This property follows from the same twelve-bal structure; to define the force between nearby structures, bal-to-bal geometry must be considered, rather than only the total charges of the two particles.

5. Matter and Antimatter

In this structure, antimatter is not geometrically a different object from matter.

The number of bals, the six axes, distances, angles, and overall geometry remain identical for matter and antimatter.

The fundamental difference lies in **the rotational directions of the bals**.

To transform a matter state into its antimatter state, the rotational directions of the bals are completely reversed. Thus, antimatter has the same geometry as matter in every respect, but the rotations of its entire set of bals are reversed.

This definition expresses the matter–antimatter distinction without adding a second geometry to the model: the geometry remains fixed while the direction of rotation is reversed.

6. Why Do Narions and Neutrinos Have No Separate Antimatter?

In this framework, neutrality does not necessarily imply that matter and antimatter are identical. The key criterion is whether completely reversing the rotational directions of the bals produces a physically distinct state or returns the structure to an equivalent state.

For **narions and neutrinos**, complete reversal of the rotations does not produce another independent state. Thus, narions and neutrinos have no separate antimatter in this structure.

This property is related to their neutrality, but neutrality alone is not sufficient.

The neutron also has zero net charge, but its internal structure is composite, and matter–antimatter reversal of its constituents produces a distinct state. Therefore, the neutron has an antiparticle.

Accordingly, Ramionics must not adopt the rule “zero charge ⇒ no antiparticle.” The distinction arises from internal structure and its behavior under complete reversal of rotational directions.

7. The Reference Narion

In its reference configuration, the narion has three positive and three negative axes:

| Axis | 1 | 2 | 3 | 4 | 5 | 6 |

|---:|:---:|:---:|:---:|:---:|:---:|:---:|

| Narion | + | − | + | − | + | − |

The positive and negative counts are therefore equal.

The normalized charge of the structure is defined from the difference between the numbers of positive and negative axes:

$$[44.2]\ q=(N_{+}-N_{-})/6$$

For the narion:

[44.3] $q_n=(3-3)/6=0$

This cancellation does not mean the internal electrical structure disappears; only the total charge of the six axes vanishes.

8. The Down Quark

The down quark uses the same six-axis geometry. In the article's reference configuration, axis 1 changes sign relative to the narion:

Axis	1	2	3	4	5	6
Narion	+	−	+	−	+	−
Down	−	−	+	−	+	−

There are now two positive axes and four negative axes.

[44.4] $q_{\mathscr{d}}=(2-4)/6=-1/3$

This is precisely the 1/3 step arising from changing one axis from +1/6 to −1/6.

9. The Up Quark

In the reference up-quark configuration, axes 2 and 4 become positive relative to the narion:

Axis	1	2	3	4	5	6
Narion	+	−	+	−	+	−
Up	+	+	+	+	+	−

There are five positive axes and one negative axis.

[44.5] $q_u=(5-1)/6=2/3$

Thus, the fractional charges of the down and up quarks are not constructed using separate rules for each quark; both result from changing the axial states of the same six-axis structure.

10. The Electron

In the electron, all six axes have negative signs:

Axis	1	2	3	4	5	6
Electron	−	−	−	−	−	−

Therefore:

[44.6] $q_e=(0-6)/6=-1$

The four main cases examined can be combined in one relation:

[44.7] $q_n=0$, $q_{\mathscr{d}}=-1/3$, $q_u=2/3$, $q_e=-1$

The electron's integral charge and the quarks' fractional charges are thus described using one shared axial unit.

11. The 1/6 Quantum and the 1/3 Step

This section is important for avoiding a fundamental misunderstanding.

The existence of twelve bals does not imply a charge quantum of 1/12, because opposite bals are not independent. Together they constitute one axis.

There are therefore six axial degrees of freedom:

[44.8] $q_{axis}=1/6$

If an axis changes from negative to positive, its value changes from $-1/6$ to $+1/6$:

[44.9] $\Delta q=(+1/6)-(-1/6)=1/3$

And for the reverse transition:

[44.10] $\Delta q=(-1/6)-(+1/6)=-1/3$

Thus, **1/6 is the unit describing the state of an axis, while 1/3 is the unit of a complete sign change of an axis**.

The down quark is one $-1/3$ step relative to the narion, and the up quark is two $+1/3$ steps relative to it.

12. Three Orthogonal Pairs

The numbering in the reference image identifies three orthogonal pairs:

Pair	Axes	Angle
A	1–6	90°
B	2–4	90°
C	3–5	90°

Each axis forms a 60° angle with the four axes outside its own pair.

Consequently, of the fifteen possible pairs among six axes, three have an angle of 90° and twelve have an angle of 60°.

At the level of the three orthogonal pairs, any two pairs are connected through four 60° relationships. The geometry therefore possesses an intrinsic threefold structure.

13. Geometric Quark Chromatics

In this framework, quark color is not treated as a separate property attached to a quark after its formation. Its origin is sought in the geometry and placement of changed axes relative to the six-axis structure.

The reference narion has the following states in its three orthogonal pairs:

Pair	State
1–6	+−
2–4	−−
3–5	++

Thus, the three fundamental pairs are distinct not only geometrically but also in their sign configurations.

In a quark, changing one or more axes changes this network. Accordingly, color in this description is associated with **the direction and geometric class of the changed axes relative to the three orthogonal pairs**.

This article introduces geometric threefoldness as the foundation of Ramionics chromatics.

14. The Six-Axis Graph

If the six axes are taken as vertices of a graph, with two vertices connected whenever the angle between them is 60°, each vertex has exactly four neighbors.

The graph has six vertices and twelve edges; the three orthogonal pairs are its only pairs without direct connections.

The spectrum of its adjacency matrix is:

[44.11] $\lambda=\{4,0,0,0,-2,-2\}$

Thus, the distinct eigenvalues and their multiplicities are:

[44.12] $\lambda=\{4,0,-2\}$; $m=\{1,3,2\}$

This spectrum arises from geometry alone and does not depend on choosing the narion, down quark, up quark, or electron.

15. Preliminary Angular Interaction

To investigate the connection between geometry and internal force, a preliminary definition is introduced for the coupling of two axes. The angular contribution of two axes is taken from the absolute value of the dot product of their unit directions, while the sign comes from the states of the two axes:

[44.13] $K_{ij}=s_i s_j |n_i.n_j|$

In the present geometry, the magnitude is 1/2 for pairs at 60° and zero for pairs at 90°.

In this article, this definition is only **a preliminary geometric coupling model**. Until the force coefficient and its full dependence on distance, bal rotation, and field structure are derived, it must not be regarded as the final law of force.

16. Internal Fingerprints of the Four Structures

Under the definition above, summing the couplings of the four neighbors of each axis yields the following distribution:

Axis	Narion	Down	Up	Electron
1	0	0	+2	+2
2	−1	0	+1	+2
3	−1	−2	+1	+2
4	−1	0	+1	+2
5	−1	−2	+1	+2
6	0	0	−2	+2

This table shows that total charge is not sufficient to describe internal structure.

Despite having zero charge, the narion has a nonzero internal structure. The down quark concentrates its values on axes 3 and 5. The up quark has a different distribution, while the electron is uniform across all axes according to this measure.

This difference is also consistent with the short-range discussion: local behavior must be examined through the spatial arrangement of bals, rather than merely the sum of a particle's charge.

17. Quadratic Intensity of the Internal Structure

To measure the intensity of the internal distribution without canceling opposing contributions, the following quadratic quantity is defined:

[44.14] $I=(1/6)\sum_i(F_i/F_0)^2$

For the four reference structures:

[44.15] $I_n=2/3$, $I_{\mathscr{A}}=4/3$, $I_u=2$, $I_e=4$

The ratio of these four values is simple:

[44.16] $I_n:I_{\mathscr{A}}:I_u:I_e=1:2:3:6$

18. Short-Range Force Must Be Bal-to-Bal

At distances much larger than the dimensions of the structure, total charge can provide the dominant description. As two structures approach each other, however, the differences between the distances of their various bals become important.

Therefore, a complete description of short-range force cannot depend solely on the total q of the two particles.

For each pair of bals, at least their separation, the sign of the facing surface, axial orientation, rotational direction, and relative geometry must be considered.

This is particularly important for narions and neutrinos: **their zero q does not eliminate local electrical and magnetic forces.**

At short distances, the bal nearest to the opposing structure can make the dominant contribution. As the two particles rotate relative to each other, the nearest bal changes, and therefore the type and strength of the interaction can also change.

Thus, neutrality is a collective property, whereas short-range force is a geometric and local property.

19. The Role of Rotation in Magnetism

Because sign is not the only information associated with a bal, and a bal also has a rotational direction, magnetic effects cannot be derived solely from the table of + and − signs.

Two structures can have the same total charge but different rotational directions. Thus, the magnetic component must incorporate the rotational directions of the facing bals, in addition to sign and distance.

This same feature underlies the definition of matter and antimatter: the geometry stays fixed while the rotational directions reverse.

Consequently, a complete description of short-range force in Ramionics must simultaneously retain **geometry, electricity, and rotation**.

20. Matter, Antimatter, and Charge

Matter-to-antimatter reversal must not be confused with a simple change in particle shape. Under the present definition, the geometry does not change; the rotational directions of all bals reverse.

This allows two structures to be geometrically identical in every respect while nevertheless being matter and antimatter counterparts.

In structures such as narions and neutrinos, complete reversal does not lead to a separate independent state, and therefore no distinct antimatter is defined.

The neutron, however, despite having zero total charge, has a composite structure that produces a distinct state under matter–antimatter transformation; hence, the neutron and antineutron are distinct.

Thus, in Ramionics, **net charge does not determine the existence of antimatter; structure and rotational direction do**.

21. Main Results

This article brings together several results within a single framework.

Twelve bals form six independent axes; therefore, the axial unit of charge is 1/6.

Completely changing the sign of one axis spans the interval from $-1/6$ to $+1/6$; therefore, the charge-change step is 1/3.

Counting the signs of the six axes gives the charges of the narion, down quark, up quark, and electron as 0, $-1/3$, $+2/3$, and -1, respectively.

The six axes form three orthogonal pairs and twelve 60° relationships, giving the model an intrinsic threefold geometric structure.

The neutrality of narions and neutrinos does not imply the absence of local electrical and magnetic structure. At short distances, the nearest bal and its rotational direction play a role in the interaction.

Matter and antimatter share the same geometry; their fundamental distinction is the complete reversal of bal rotational directions.

Finally, neutrality alone does not determine whether a particle has a distinct antiparticle: narions and neutrinos have no separate antimatter, while the neutral neutron has a distinct antineutron.

22. Conclusion

Quark chromatics in this framework begins with a single idea: **a particle is not a point carrying several independent numbers, but a structure of twelve bals and six axes.**

Two opposite bals form a single axis. Therefore, twelve bals do not imply a charge quantum of 1/12; the six axes yield the unit 1/6. Changing the sign of one axis produces a step of 1/3.

Without changing the geometry, this same structure generates neutral configurations and configurations with charges $-1/3$, $+2/3$, and -1.

Alongside total charge, the spatial arrangement of the bals preserves local information. Thus, at short distances a neutral narion or neutrino can still exhibit electrical and magnetic effects depending on the facing bal, its local sign, and its rotational direction.

The three orthogonal pairs form the internal geometric threefoldness and provide a route toward defining quark color. The preliminary coupling model also shows how the distribution of signs over this geometry can produce different internal fingerprints for different structures.

In this picture, **charge, color, short-range behavior, and the distinction between matter and antimatter are not separate ingredients added to a particle afterward; they all originate in the arrangement, signs, and rotational directions of the same twelve bals and six axes.**

Supplementary Discussion: Geometric Coupling and Energy-Dependent Coupling Constants

Returning to the geometric coupling coefficient

Topic: Write that coupling coefficient once again so that the derivation shows where it came from.

Explanation: Yes. It is better to return precisely to the point where the model constructed this coefficient, because **this part is still a model assumption, not something previously established in Ramionics.**

For each axis, a unit vector was assigned a unit vector n_i along that axis and a sign s_i equal to +1 or −1. The model then proposes taking the absolute value of the dot product of their directions as the strength of the geometric relationship between two axes:

[44.17] $K_{ij}=s_i s_j |n_i.n_j|$

The reason for choosing the absolute value was that an axis is a **line**, not a one-way arrow; therefore, the arbitrary choice of direction +n or −n should not change the coupling magnitude.

The geometry in the diagram provides only two possibilities for two distinct axes. If the angle is 60°:

[44.18] $|n_i.n_j| = |\mathrm{Cos}(60°)| = 1/2$

If the two axes form an orthogonal pair:

[44.19] $|n_i.n_j| = |\mathrm{Cos}(90°)| = 0$

Therefore, K has only three possible values for each pair:

[44.20] $K_{ij}=+1/2,-1/2,0$

The value +1/2 applies when two axes are at 60° and have matching signs; −1/2 applies when they are at 60° and have opposite signs; and zero applies when they are at 90°.

Next, the sum was taken over the four active couplings for each axis:

[44.21] $C_i=\sum_j K_{ij}$

This is how, for example, the following vector was obtained for the down quark:

[44.22] $C_{\mathscr{d}}=\{0,0,-2,0,-2,0\}$

Then, to prevent positive and negative contributions from cancelling one another in a simple sum, the squares were taken of the six values and averaged them:

[44.23] $I=(1/6)\sum_i C_i^2$

For the down quark:

[44.24] $I_{\mathscr{d}}=(0^2+0^2+(-2)^2+0^2+(-2)^2+0^2)/6=8/6=4/3$

This is where 4/3 came from.

There is, however, an essential point: the value 1/2 comes directly from the 60° geometry, and the signs come from the particle model. But taking the physical coupling to be exactly equal to the **angular dot product** was a choice made for the model's initial test.

Thus, the sequence is precisely:

Geometry of 12 bals → six axes → angles of 60° and 90° → weights of 1/2 and 0 → application of signs ± → summation over each axis → squaring and averaging → 4/3 for the down quark.

To strengthen this part of the article, the principal question is no longer how 4/3 was obtained; that is clear. The real question is **why the physical coupling law should be the cosine of the angle**. If it can be derived from the forces or projections of bals within Ramionics itself, then 4/3 would no longer be the result of an experimental modelling choice.

The coupling coefficient expressed in terms of energy

Topic: Energy-dependent coupling coefficient.

Explanation: This refers to **α_s, the strong-force coupling coefficient as a function of energy scale**, not the geometric K that the model constructed.

In QCD, α_s is not constant; it varies with energy. The higher the energy scale, the smaller α_s becomes.

For example, at the Z-boson mass scale:

[44.25] $\alpha_s(M\_Z) \approx 0.118$

If the expression is the corresponding g_s:

[44.26] $g_s = \sqrt{(4\pi\alpha_s)}$

At the same scale, this is approximately:

[44.27] $g_s \approx 1.22$

The important point is that **this value is a function of energy**. At lower energies the coupling becomes stronger, and at higher energies it becomes weaker.

This is the relevant energy-dependent coefficient. the following analysis can investigate whether the twelve-bal, six-axis model contains a mechanism capable of producing the same variation in coupling with energy.

Is there a table or graph?

Topic: Tabular and graphical representation of the coupling

Explanation: Yes. There is a well-known standard graph. The Particle Data Group (PDG) publishes a plot of α_s against energy scale Q in its review of QCD. The official 2025 plot covers approximately 1 GeV to 10000 GeV, and its curve decreases as energy increases. Its reference value is $\alpha_s(M\_Z) = 0.1180 \pm 0.0009$.

For the Ramionics analysis, **this graph is important**: α_s becomes large at low energies, but steadily decreases as Q increases. Recent measurements have tested this behaviour up to approximately 7 TeV.

It is important not to confuse this plot with the earlier 4/3: **$\alpha_s(Q)$** is the energy-dependent coupling strength, whereas the **4/3** derived from the geometry was a dimensionless geometric coefficient. If the result shows a Ramionics relation that directly expresses α_s in terms of Ramion energy or the number/scale of bals, the appropriate comparison will be **curve against curve**, not the matching of a single number to 4/3.

Does the strong force have its own alpha?

Topic: Does it have its own alpha?

Explanation: Yes. In QCD, there is an alpha specific to the strong force: **α_s**.

Its relation to the fundamental QCD coupling g_s is:

[44.28] $\alpha_s = g_s^2/(4\pi)$

Thus, α_s plays approximately the same role for the strong force that α plays for electromagnetism, with one important difference: **α_s is not constant; it varies with energy scale Q.**

For comparison:

[44.29] $\alpha \approx 1/137$

In electromagnetism, α is small and changes relatively slowly at ordinary energy scales, whereas in QCD:

[44.30] $\alpha_s=\alpha_s(Q)$

That is, α_s is itself a function of energy.

At high energies α_s becomes smaller, and at low energies it becomes larger. Therefore, to define a corresponding strong-force alpha in Ramionics, it is necessary to specify from the outset whether that alpha is a **fundamental constant** or a **function of energy**.

Direction of the electromagnetic alpha's energy dependence

Topic: In electromagnetism, doesn't alpha decrease at high energies?

Explanation: No. **Electromagnetism behaves oppositely to QCD.**

The electromagnetic α becomes slightly **larger** as energy scale increases, not smaller. The reason is quantum-vacuum screening: at shorter distances, the effective electric charge appears slightly stronger.

Approximately:

[44.31] $\alpha^{-1}(0)\approx 137.036$

But at the Z-boson mass scale:

[44.32] $\alpha^{-1}(M\_Z)\approx 128$

Because the inverse of α decreases from approximately 137 to approximately 128, α itself increases.

For the strong force, however:

[44.33] $\alpha_s(Q)\downarrow$ as $Q\uparrow$

That is, α_s **decreases** with increasing energy. This is asymptotic freedom.

Thus, their directions of variation are opposite:

Electromagnetism: higher energy ⇒ slightly larger α.

Strong force: higher energy ⇒ smaller α_s.

The mass scale of the Z boson

Topic: Is the mass of Z the mass of the Z boson?

Explanation: Yes, exactly. M_Z means the **mass of the Z boson**; more precisely, it refers to an energy scale corresponding to the rest mass of the Z boson when expressed in energy units.

Approximately:

[44.34] $M\_Zc^2\approx 91.19$ GeV

When α(M_Z) is written, it means that the electromagnetic fine-structure constant is being considered at an energy scale of approximately 91 GeV.

What curve is fitted between alpha and energy?

Topic: What curve did they fit between alpha and energy?

Explanation: For electromagnetic α, a simple empirical curve such as a polynomial is not usually fitted. Its energy dependence comes from **renormalization and vacuum polarization in QED**, and is calculated using a running-coupling function.

A common standard form is:

[44.35] $\alpha(Q^2)=\alpha(0)/(1-\Delta\alpha(Q^2))$

Here $\Delta\alpha(Q^2)$ contains contributions from vacuum polarization by leptons and hadrons, as well as other contributions at the appropriate scales. The PDG uses this form to evolve $\alpha(0)$ to α at the M_Z scale.

In the one-loop approximation, sufficiently far from a fermion mass threshold, the dominant behaviour is **logarithmic**. Schematically:

[44.36] $\Delta\alpha(Q^2) \propto \alpha.\mathrm{Log}(Q^2/m^2)$

Thus, α does not increase linearly or according to a simple power law with energy. Its principal variation is approximately **logarithmic**; each time the energy crosses the mass threshold of a charged particle, a new contribution enters the running.

For this reason, a plot of α^{-1} against Log(Q) resembles slowly varying, approximately piecewise lines, rather than a simple exponential or parabolic curve.

For example, from the low-energy limit:

[44.37] $\alpha^{-1}(0) \approx 137.036$

At the Z-boson scale it reaches approximately:

[44.38] $\alpha^{-1}(M\_Z) \approx 128$

The PDG calculates the running more precisely using vacuum polarization and hadronic data. The low-energy hadronic contribution cannot be calculated solely using a simple perturbative formula and also uses electron–positron annihilation data.

Therefore, if the scientific question for Ramionics is **what is the mathematical form of α(E)?**, the first behaviour to investigate is approximately **Log(E)**, or its equivalent in α^{-1}, rather than, for example, 1/E or E^2.

An approximate logarithmic formula

Topic: For example, logarithmically, what would its approximate formula be?

Explanation: To examine the **approximate logarithmic form** of electromagnetic alpha running, a simple one-loop approximation for one charged fermion can be written as:

[44.39] $\alpha(Q^2) \approx \alpha(0)/[1-\alpha(0)/(3\pi).\mathrm{Ln}(Q^2/m^2)]$

Here Q is the energy scale, and m is the mass of the charged particle contributing to vacuum polarization.

Since:

[44.40] $\mathrm{Ln}(Q^2/m^2) = 2\mathrm{Ln}(Q/m)$

The same relation can be viewed approximately as:

[44.41] $\alpha(Q) \approx \alpha_0/[1-2\alpha_0/(3\pi).\mathrm{Ln}(Q/m)]$

Thus, the overall structure is simple:

[44.42] $\alpha(E) \approx \alpha_0/[1-K.\mathrm{Ln}(E/E_0)]$

Here K is a small coefficient.

In other words, to isolate only the **mathematical form of the behaviour** for Ramionics, the approximate pattern has alpha in the numerator and, in the denominator, a term consisting of 1 minus a small coefficient multiplied by the logarithm of energy.

What is α_0?

Topic: α_0 — what is this? Is it the same electromagnetic alpha?

Explanation: Yes. In that approximate formula, **α_0 is the reference value of electromagnetic alpha at very low energy**, usually $\alpha(0)$.

[44.43] $\alpha_0=\alpha(0)\approx 1/137.036$

As energy scale increases, vacuum polarization causes the effective α to increase slightly:

[44.44] $\alpha(Q)>\alpha_0$

Thus, the zero subscript does not denote a different alpha; it simply indicates the **baseline or low-energy value of the same electromagnetic α**.

Comparing electromagnetic and strong alpha as functions of energy

Topic: So how do electromagnetic and strong alpha behave as functions of energy?

Explanation: Their behaviour with increasing energy scale is **opposite**:

Electromagnetism: α **increases gradually** as energy increases.

Strong force: α_s **decreases** as energy increases and tends toward smaller values at very high energies.

Qualitatively:

[44.45] $E\uparrow \Rightarrow \alpha(E)\uparrow$

[44.46] $E\uparrow \Rightarrow \alpha_s(E)\downarrow$

The underlying physics also differs. In QED, vacuum polarization screens electric charge. At at higher energies or shorter distances, there is less screening between the observer and the charge, and the effective electromagnetic coupling appears stronger.

In QCD, gluons themselves carry color charge, and their contribution produces **anti-screening**. The result is asymptotic freedom: at short distances and high energies, the strong coupling becomes weaker.

If the comparison considers only the approximate one-loop forms, their structures are particularly interesting:

[44.47] $\alpha(E)\approx \alpha_0/[1-K_e Ln(E/E_0)]$

In contrast:

[44.48] $\alpha_s(E)\approx \alpha_{s0}/[1+K_s Ln(E/E_0)]$

In this simplified form, the main difference is precisely **the sign in front of the logarithmic term in the denominator**.

This inverse symmetry is interesting for the work being undertaken in Ramionics: if the result shows a fundamental energy–coupling relation, the model should investigate whether the two opposite directions of running could arise from two different structures of the same geometry.

If the comparison considers only the approximate one-loop forms, their structure is particularly interesting:

[44.49] $\alpha(E)\approx \alpha_0/[1-K_e Ln(E/E_0)]$

In contrast:

[44.50] $\alpha_s(E)\approx \alpha_{s0}/[1+K_s Ln(E/E_0)]$

That is, alpha increases slightly with increasing energy, whereas the strong-force alpha decreases.

Exactly. As energy increases:

[44.51] $E\uparrow \Rightarrow \alpha(E)\uparrow$

Thus, electromagnetic alpha **increases slowly**.

But:

[44.52] $E\uparrow \Rightarrow \alpha_s(E)\downarrow$

Thus, the strong-force alpha **decreases**. Their behaviour is opposite: QED becomes slightly stronger with energy, while QCD becomes weaker.

Topic: QED and QCD: is their difference therefore that one concerns the electromagnetic force and the other the strong force?

Explanation: Yes, that is the principal distinction in their domains of interaction.

QED stands for Quantum Electrodynamics: the quantum theory of the **electromagnetic interaction**. Its force carrier is the photon, and its coupling is expressed by α.

QCD stands for Quantum Chromodynamics: the quantum theory of the **strong or color interaction**. Its force carriers are gluons, and its coupling is expressed by α_s.

In brief:

QED → electromagnetism → photon → α

QCD → strong force → gluon → α_s

The interesting difference under discussion is that α increases with increasing energy, whereas α_s decreases.

QED stands for Quantum Electrodynamics: the quantum theory of the **electromagnetic interaction**. Its force carrier is the photon, and its coupling is expressed by α.

QCD stands for Quantum Chromodynamics: the quantum theory of the **strong or color interaction**. Its force carriers are gluons, and its coupling is expressed by α_s.

In brief:

QED → electromagnetism → photon → α

QCD → strong force → gluon → α_s

The interesting difference under discussion is that α increases with increasing energy, whereas α_s decreases.

Comparing only the approximate one-loop forms, their structure is particularly interesting: (3) $\alpha(E)\approx\alpha_0/[1-K_e\mathrm{Ln}(E/E_0)]$. In contrast: (4) $\alpha_s(E)\approx\alpha_{s0}/[1+K_s\mathrm{Ln}(E/E_0)]$.

In other words, alpha increases slightly with increasing energy, whereas the strong-force alpha decreases.

Yes, this summary is correct. The word “slightly” is intended here.

An important point for later use in the article: these two relations are only **schematic one-loop forms**; K_e and K_s are not one shared or identical coefficient. Each arises from the structure of its theory and the particles effective at the relevant energy.

The conceptual summary is therefore:

QED → electromagnetism → photon → α → increases slightly with increasing energy.

QCD → strong force → gluon → α_s → decreases with increasing energy.

The sign difference in the denominator of the approximate expressions reflects these opposite behaviours.

Topic: But are both alphas based on 1/137?

Explanation: No. The two quantities must be distinguished.

Electromagnetic α at low energy is approximately 1/137:

[44.53] $\alpha(0) \approx 1/137.036$

However, **the strong-force α_s does not have 1/137 as its basis**. α_s is an independent coupling, and its value depends on the energy scale. For example, at the scale of the Z-boson mass it is approximately 0.118, which is much larger than $1/137 \approx 0.0073$.

Therefore:

α and α_s are two independent quantities.

Their similarity is that both are dimensionless couplings; it is not that both begin from 1/137.

If Ramionics yields a relation showing that both are constructed from a shared fundamental quantity, this would be a result particular to the Ramionics model, not something that standard QED and QCD already assert.

Relationship between the coupling constant and the force

What about alpha_st?

The Ramionics notation st means strong.

Explanation: Yes. For specifying the Ramionics notation for **Strong**, then under the specified convention it is:

α_{st}

That is, the model uses the complete subscript **$_{st}$** for Strong. This is a good choice because it avoids confusion with α_s, where $_s$ could previously mean the "base Ramion" in Ramionics.

Analogously to the way electromagnetic α enters the electric coupling constant and subsequently the force, the following chain applies the following conceptual chain for Strong:

α_{st} → Strong coupling → Strong force

There is, however, an important point: in standard QCD, α_{st} does not directly produce the electrostatic "K"; the relationship between α and the Coulomb constant comes from its electromagnetic definition. Therefore, to define K_{st} and then F_{st} in Ramionics, the relationship must be derived their precise relationship from the Ramionics structure rather than transferring the QED relationship unchanged to Strong.

Thus, from this point onward in this analysis:

α = Electromagnetic

α_{st} = Strong

The two are now completely separate in notation.

α = Electromagnetic

α_{st} = Strong

Calculation of physical quantities from α_{st} at the Z scale

Explanation: Given α_{st} at a specified scale, for example the Z scale, the first quantity that can be calculated directly from it is **the fundamental Strong coupling, g_{st}**:

[44.54] $g_{st} = \sqrt{(4\pi\alpha_{st})}$

For example, if $\alpha_{st} \approx 0.118$ at the Z scale:

[44.55] $g_{st} \approx \sqrt{(4\pi \times 0.118)} \approx 1.22$

One further step is required to obtain a **force**, because the color factor also enters QCD.

For example, for a short-distance quark–antiquark pair in the singlet channel, the potential has an approximately Coulomb-like form:

[44.56] $V(r) \approx -C_F \alpha_{st} \hbar c / r$

where:

[44.57] $C_F = 4/3$

The corresponding force magnitude is approximately:

[44.58] $F(r) \approx C_F \alpha_{st} \hbar c / r^2$

Thus, the standard chain in this example is:

α_{st} → g_{st} → color factor C_F → potential → force

This is an important distinction from electromagnetic α: in QCD, α_{st} alone is insufficient; the particles' color state also determines the coefficient multiplying it.

For an analogous K in Ramionics, one could investigate whether a term of the form **$C\alpha_{st}$** acts as an effective Strong coefficient. But C must be derived from the model's geometry, not preset to 4/3.

Comparison of strong and electromagnetic potentials and the reduced Planck constant

Explanation: Yes, the potential has a form similar to the Coulomb potential when the color factor C is set aside. Here ħ is the **reduced Planck constant**:

[44.59] $V(r) \approx -C \alpha_{st} \hbar c / r$

[44.60] $\hbar = h/(2\pi)$

Thus, ħ is not the ordinary Planck constant h but its reduced form. The Ramionics notation uses the character **ħ**.

The combination **αħc** appears in electromagnetism, and the corresponding **α_{st}ħc** appears for Strong interactions. The distinctions lie in the coupling and the interaction-specific structural coefficients.

Energy dependence of α_{st}

Explanation: For comparison, use the one-loop approximation anchored at $\alpha_{st}(M_Z) = 0.1180$. These are approximate numbers; precise QCD calculations employ multiple loops and quark-mass thresholds. The PDG also illustrates the running at up to five loops.

Energy Q	Approximate $\alpha_{st}(Q)$
5 GeV	0.203
10 GeV	0.173
20 GeV	0.151
50 GeV	0.129
91.19 GeV	0.118
200 GeV	0.106
500 GeV	0.0948
1000 GeV	0.0877
10000 GeV	0.0704

The expression used for this table is:

[44.61] $\alpha_{st}(Q) \approx \alpha_{st}(M\_Z)/[1+\alpha_{st}(M\_Z)\beta_0/(2\pi).Ln(Q/M\_Z)]$

The trend is clear: α_{st} decreases as energy increases.

Running of α_{st} with energy

Approximate one-loop values anchored at $\alpha_{st}(M\_Z)=0.1180$.

α_{st}

5: 0.2028

10: 0.1731

20: 0.151

50: 0.1292

91.19: 0.118

200: 0.106

500: 0.0948

1000: 0.0877

10000: 0.0704

For a Ramionics comparison, the next useful step would be to place this table beside electromagnetic α at the same energies and compare the opposite running numerically.

Topic: What is β_0?

Explanation: β_0 is a **fundamental coefficient in the one-loop QCD running equation for α_{st}.** It determines how rapidly α_{st} decreases as energy increases.

For QCD with three colors:

[44.62] $\beta_0=11-2n_f/3$

Here n_f is the number of **active quark flavors** at the relevant energy scale.

For example, near the Z scale, five flavors—u, d, s, c, and b—are active:

[44.63] $\beta_0=11-2\times5/3=23/3\approx7.6667$

β_0 is not itself a coupling; it is the **QCD beta-function coefficient** controlling the slope of the running of α_{st}.

Topic: What is flavor?

Explanation: In particle physics, **flavor** means the **type of quark**. There are six quark flavors: up, down, strange, charm, bottom, and top, denoted u, d, s, c, b, and t.

At an energy where $n_f=5$, five quark types are sufficiently light to contribute effectively to the running of α_{st}. Near the Z scale, these are u, d, s, c, and b; top is too heavy to be counted as active in this calculation.

In short: **Flavor** = **which type of quark it is.**

Question: Where did $\beta_0=11-2n_f/3$ come from?

Explanation: This is **not an experimental fit**; it follows from the theoretical one-loop QCD beta-function calculation.

For a gauge theory with group $SU(N_c)$, quantum corrections to gluon propagation include contributions from gluon loops, ghost loops, and quark loops. Summing these diagrams and renormalizing the coupling gives:

[44.64] $\beta_0=11C\_A/3-4T\_Fn_f/3$

For QCD, the color group is SU(3), with C_A=3 and T_F=1/2. Substitution yields:

[44.65] $\beta_0=11-2n_f/3$

The **11** arises primarily from the self-interaction of the non-Abelian gluon field, producing decreasing coupling at higher energies. Quarks contribute with the opposite sign, giving **$2n_f/3$**.

Thus, 11 is not an experimentally adjusted number; it arises from the SU(3) structure, color degrees of freedom, and quantum-loop calculations.

For seeking a geometric origin of α_{st} in Ramionics, the coefficients **11 and 2/3** are particularly important: independently reproducing corresponding coefficients would offer a more substantive comparison than matching the empirical value of α_{st} alone.

Topic: So were the quark rest masses adjusted this way?

Explanation: No. Quark rest masses were not set using β_0. β_0 depends on the **number of active flavors**, not the precise mass of each quark. Quark masses are independent QCD parameters extracted from experimental data.

Masses determine the energy thresholds at which flavors count as active. Above a quark's mass scale, that flavor enters the effective running of α_{st} and n_f increases by one.

The direction of dependence is:

Quark mass → active-flavor threshold → n_f changes → β_0 changes → slope of α_{st} changes

It is not a matter of choosing β_0 and then adjusting quark masses accordingly.

Topic: Draw a table of quark and lepton masses.

Explanation: For comparison, express all values in **MeV/c²**. Quark masses depend on the renormalization scheme and scale; unlike the electron mass, they are not directly the mass of a free particle. The u, d, and s values are PDG values at 2 GeV.

Family	Particle	Approximate Mass (MeV/c²)
Quark	u	2.16
Quark	d	4.70
Quark	s	93.5
Lepton	e	0.510999
Lepton	μ	105.658
Quark	c	1273
Lepton	τ	1776.86
Quark	b	4183
Quark	t	172560

PDG reports 1.2730 GeV for c, 4.183 GeV for b, and 172.56 GeV for t from direct measurement.

The enormous separation of mass scales is relevant to α_{st}: from u and d at a few MeV to t at about **173 thousand MeV**. As energy increases, quark thresholds are crossed one by one and n_f in the beta function changes.

Neutrinos are intentionally excluded from the main table because separate absolute masses for the three neutrino mass eigenstates are not yet available in the same way as those of e, μ, and τ.

Topic: Arrange it three by three.

Explanation: The three generations can be shown as three columns:

| Generation | 1 | 2 | 3 |

| --- | ---: | ---: | ---: |

| Up-type quark | u = 2.16 MeV/c^2 | c = 1273 MeV/c^2 | t = 172560 MeV/c^2 |

| Down-type quark | d = 4.70 MeV/c^2 | s = 93.5 MeV/c^2 | b = 4183 MeV/c^2 |

| Charged lepton | e = 0.510999 MeV/c^2 | μ = 105.658 MeV/c^2 | τ = 1776.86 MeV/c^2 |

The columns are the three matter generations: **(u,d,e)**, **(c,s,μ)**, and **(t,b,τ)**.

Topic: I think quarks with charges 2/3 and 1/2 have masses four times and 19/3 times that of their same-generation leptons. But ignoring the dependence of Q, α, and K on N, I have not yet examined the c, s, t, and b quarks.

Explanation: The analysis considers a mass pattern for **each generation relative to its charged lepton**, without yet incorporating the dependence of Q, α, and K on N.

One detail: by "quarks 2/3 and 1/2," the intended quantities are the quarks with charges **+2/3 and −1/3**.

For the first generation, the Ramionics mass model appears to suggest coefficients near **4** and **19/3** relative to the electron. If this is a family-wide structure, the next question is whether the same pattern can account for the second and third generations without ad hoc adjustments.

| Generation | +2/3 | −1/3 | Lepton |

| --- | --- | --- | --- |

| 1 | u | d | e |

| 2 | c | s | μ |

| 3 | t | b | τ |

One should not expect fixed ratios of 4 and 19/3 directly from the raw experimental masses. For example, c/μ and s/μ differ from u/e and d/e; the third generation differs even more.

If the pattern holds after the relevant dependencies are included, **4 and 19/3** could represent fixed geometric structures, with the very large generational mass differences arising from N and family coupling. This would be more meaningful within the model than separately fitting four new masses.

Topic: How many times stronger is the strong force than electromagnetism?

Explanation: There is no fixed number because α_{st} changes with energy. Comparing the **dimensionless couplings**, α_{st}/α, at the Z scale gives approximately:

[44.66] $\alpha_{st} \approx 0.118$, $\alpha \approx 1/128$

Thus:

[44.67] $\alpha_{st}/\alpha \approx 0.118 \times 128 \approx 15.1$

At the Z scale, Strong coupling is therefore about **15 times** electromagnetic coupling by this dimensionless measure.

At lower energies, α_{st} becomes larger, so the ratio can be considerably higher. If $\alpha_{st} \approx 0.3$, for example, the ratio relative to $\alpha \approx 1/137$ is approximately **41**.

The familiar statement that "the strong force is about 100 times stronger than electromagnetism" is only an order-of-magnitude comparison at nuclear scales; there is **no fundamental fixed ratio of 100**.

Appendix 45: Historical Tables

Historical Experimental Result Tables

The comparison metric uses the change in central value divided by the previous displayed edition's quoted 1σ uncertainty. It is not a combined significance of two independent measurements.

[45.1] Appendix — Inverse Fine-Structure Constant — CODATA Recommended Values

Year	Central Value α^{-1}	Standard Uncertainty (1σ)	Change From Previous	Change / Previous σ	Source Page
2002	137.03599911	0.00000046	—	—	https://physics.nist.gov/cuu/pdf/all_2002.pdf
2006	137.035999679	0.000000094	+0.000000569	+1.24σ	https://physics.nist.gov/cuu/pdf/all_2006.pdf
2010	137.035999074	0.000000044	−0.000000605	−6.44σ	https://physics.nist.gov/cuu/pdf/all_2010.pdf
2014	137.035999139	0.000000031	+0.000000065	+1.48σ	https://physics.nist.gov/cuu/pdf/all_2014.pdf
2018	137.035999084	0.000000021	−0.000000055	−1.77σ	https://physics.nist.gov/cuu/pdf/all_2018.pdf
2022	137.035999177	0.000000021	+0.000000093	+4.43σ	https://physics.nist.gov/cuu/pdf/all.pdf

CODATA recommended values; uncertainty is the quoted standard uncertainty.

[45.2] Appendix — Electron Mass Energy Equivalent — CODATA Recommended Values

Year	Central Value (MeV)	Standard Uncertainty (1σ, MeV)	Change From Previous (MeV)	Change / Previous σ	Source Page
2002	0.510998918	0.000000044	—	—	https://physics.nist.gov/cuu/pdf/all_2002.pdf
2006	0.510998910	0.000000013	−0.000000008	−0.18σ	https://physics.nist.gov/cuu/pdf/all_2006.pdf
2010	0.510998928	0.000000011	+0.000000018	+1.38σ	https://physics.nist.gov/cuu/pdf/all_2010.pdf
2014	0.5109989461	0.0000000031	+0.0000000181	+1.65σ	https://physics.nist.gov/cuu/pdf/all_2014.pdf
2018	0.51099895000	0.00000000015	+0.00000000390	+1.26σ	https://physics.nist.gov/cuu/pdf/all_2018.pdf
2022	0.51099895069	0.00000000016	+0.00000000069	+4.60σ	https://physics.nist.gov/cuu/pdf/all.pdf

CODATA electron mass-energy equivalent in MeV.

[45.3] Appendix — Up-Quark Mass — PDG Evaluations at 2 GeV

| Year | Central Value (MeV) | Quoted Uncertainty (MeV) | Change From Previous (MeV) | Change / Previous σ | Source Page |

| --- | --- | --- | --- | --- | --- |

| 2010 | 2.49 | +0.81/−0.79 | — | — | https://pdg.lbl.gov/2010/listings/rpp2010-list-light-quarks.pdf |

| 2014 | 2.30 | +0.70/−0.50 | −0.19 | −0.24σ | https://pdg.lbl.gov/2014/listings/rpp2014-list-light-quarks.pdf |

| 2018 | 2.20 | +0.50/−0.40 | −0.10 | −0.20σ | https://pdg.lbl.gov/2018/listings/rpp2018-list-light-quarks.pdf |

| 2022 | 2.16 | +0.49/−0.26 | −0.04 | −0.10σ | https://pdg.lbl.gov/2022/listings/rpp2022-list-light-quarks.pdf |

MS̄ mass at the 2 GeV scale. For asymmetric uncertainty, the previous

uncertainty in the direction of the central-value change is used.

[45.4] Appendix — Down-Quark Mass — PDG Evaluations at 2 GeV

| Year | Central Value (MeV) | Quoted Uncertainty (MeV) | Change From Previous (MeV) | Change / Previous σ | Source Page |

| --- | --- | --- | --- | --- | --- |

| 2010 | 5.05 | +0.75/−0.95 | — | — | https://pdg.lbl.gov/2010/listings/rpp2010-list-light-quarks.pdf |

| 2014 | 4.80 | +0.50/−0.30 | −0.25 | −0.26σ | https://pdg.lbl.gov/2014/listings/rpp2014-list-light-quarks.pdf |

| 2018 | 4.70 | +0.50/−0.30 | −0.10 | −0.33σ | https://pdg.lbl.gov/2018/listings/rpp2018-list-light-quarks.pdf |

| 2022 | 4.67 | +0.48/−0.17 | −0.03 | −0.10σ | https://pdg.lbl.gov/2022/listings/rpp2022-list-light-quarks.pdf |

MS̄ mass at the 2 GeV scale. For asymmetric uncertainty, the previous

uncertainty in the direction of the central-value change is used.

[45.5] Appendix — Proton Mass Energy Equivalent — CODATA Recommended Values

| Year | Central Value (MeV) | Standard Uncertainty (1σ, MeV) | Change From Previous (MeV) | Change / Previous σ | Source Page |

| --- | --- | --- | --- | --- | --- |

| 2002 | 938.272029 | 0.000080 | — | — | https://physics.nist.gov/cuu/pdf/all_2002.pdf |

| 2006 | 938.272013 | 0.000023 | −0.000016 | −0.20σ | https://physics.nist.gov/cuu/pdf/all_2006.pdf |

| 2010 | 938.272046 | 0.000021 | +0.000033 | +1.43σ | https://physics.nist.gov/cuu/pdf/all_2010.pdf |

| 2014 | 938.2720813 | 0.0000058 | +0.0000353 | +1.68σ | https://physics.nist.gov/cuu/pdf/all_2014.pdf |

| 2018 | 938.27208816 | 0.00000029 | +0.00000686 | +1.18σ | https://physics.nist.gov/cuu/pdf/all_2018.pdf |

| 2022 | 938.27208943 | 0.00000029 | +0.00000127 | +4.38σ | https://physics.nist.gov/cuu/pdf/all.pdf |

CODATA proton mass-energy equivalent in MeV.

[45.6] Appendix — Neutron Mass Energy Equivalent — CODATA Recommended Values

| Year | Central Value (MeV) | Standard Uncertainty (1σ, MeV) | Change From Previous (MeV) | Change / Previous σ | Source Page |

| --- | --- | --- | --- | --- | --- |

| 2002 | 939.565360 | 0.000081 | — | — | https://physics.nist.gov/cuu/pdf/all_2002.pdf |

| 2006 | 939.565346 | 0.000023 | −0.000014 | −0.17σ | https://physics.nist.gov/cuu/pdf/all_2006.pdf |

| 2010 | 939.565379 | 0.000021 | +0.000033 | +1.43σ | https://physics.nist.gov/cuu/pdf/all_2010.pdf |

| 2014 | 939.5654133 | 0.0000058 | +0.0000343 | +1.63σ | https://physics.nist.gov/cuu/pdf/all_2014.pdf |

| 2018 | 939.56542052 | 0.00000054 | +0.00000722 | +1.24σ | https://physics.nist.gov/cuu/pdf/all_2018.pdf |

| 2022 | 939.56542194 | 0.00000048 | +0.00000142 | +2.63σ | https://physics.nist.gov/cuu/pdf/all.pdf |

CODATA neutron mass-energy equivalent in MeV.

[45.7] Appendix — Muon Mass Energy Equivalent — CODATA Recommended Values

| Year | Central Value (MeV) | Standard Uncertainty (1σ, MeV) | Change From Previous (MeV) | Change / Previous σ | Source Page |

| --- | --- | --- | --- | --- | --- |

| 2002 | 105.6583692 | 0.0000094 | — | — | https://physics.nist.gov/cuu/pdf/all_2002.pdf |

| 2006 | 105.6583668 | 0.0000038 | −0.0000024 | −0.26σ | https://physics.nist.gov/cuu/pdf/all_2006.pdf |

| 2010 | 105.6583715 | 0.0000035 | +0.0000047 | +1.24σ | https://physics.nist.gov/cuu/pdf/all_2010.pdf |

| 2014 | 105.6583745 | 0.0000024 | +0.0000030 | +0.86σ | https://physics.nist.gov/cuu/pdf/all_2014.pdf |

| 2018 | 105.6583755 | 0.0000023 | +0.0000010 | +0.42σ | https://physics.nist.gov/cuu/pdf/all_2018.pdf |

Editions with unchanged central value and unchanged uncertainty are

omitted.

[45.8] Appendix — Tau Mass Energy Equivalent — CODATA Recommended Values

| Year | Central Value (MeV) | Standard Uncertainty (1σ, MeV) | Change From Previous (MeV) | Change / Previous σ | Source Page |

| --- | --- | --- | --- | --- | --- |

| 2002 | 1776.99 | 0.29 | — | — | https://physics.nist.gov/cuu/pdf/all_2002.pdf |

| 2010 | 1776.82 | 0.16 | −0.17 | −0.59σ | https://physics.nist.gov/cuu/pdf/all_2010.pdf |

| 2018 | 1776.86 | 0.12 | +0.04 | +0.25σ | https://physics.nist.gov/cuu/pdf/all_2018.pdf |

Editions with unchanged central value and unchanged uncertainty are

omitted.

[45.9] Appendix — Absolute Electron g-Factor — CODATA Recommended Values

| Year | Central Value | Standard Uncertainty (1σ) | Change From Previous | Change / Previous σ | Source Page |

| --- | --- | --- | --- | --- | --- |

| 2002 | 2.0023193043718 | 0.0000000000075 | — | — | https://physics.nist.gov/cuu/pdf/all_2002.pdf |

| 2006 | 2.0023193043622 | 0.0000000000015 | −0.0000000000096 | −1.28σ | https://physics.nist.gov/cuu/pdf/all_2006.pdf |

| 2010 | 2.00231930436153 | 0.00000000000053 | −0.00000000000067 | −0.45σ | https://physics.nist.gov/cuu/pdf/all_2010.pdf |

| 2014 | 2.00231930436182 | 0.00000000000052 | +0.00000000000029 | +0.55σ | https://physics.nist.gov/cuu/pdf/all_2014.pdf |

| 2018 | 2.00231930436256 | 0.00000000000035 | +0.00000000000074 | +1.42σ | https://physics.nist.gov/cuu/pdf/all_2018.pdf |

| 2022 | 2.00231930436092 | 0.00000000000036 | −0.00000000000164 | −4.69σ | https://physics.nist.gov/cuu/pdf/all.pdf |

Absolute magnitude is shown; the CODATA signed electron g-factor is

negative.

[45.10] Appendix — Absolute Muon g-Factor — CODATA Recommended Values

| Year | Central Value | Standard Uncertainty (1σ) | Change From Previous | Change / Previous σ | Source Page |

| --- | --- | --- | --- | --- | --- |

| 2002 | 2.0023318396 | 0.0000000012 | — | — | https://physics.nist.gov/cuu/pdf/all_2002.pdf |

| 2006 | 2.0023318414 | 0.0000000012 | +0.0000000018 | +1.50σ | https://physics.nist.gov/cuu/pdf/all_2006.pdf |

| 2010 | 2.0023318418 | 0.0000000013 | +0.0000000004 | +0.33σ | https://physics.nist.gov/cuu/pdf/all_2010.pdf |

| 2022 | 2.00233184123 | 0.00000000082 | −0.00000000057 | −0.44σ | https://physics.nist.gov/cuu/pdf/all.pdf |

Absolute magnitude is shown; unchanged editions are omitted.

[45.11] Appendix — Proton g-Factor — CODATA Recommended Values

| Year | Central Value | Standard Uncertainty (1σ) | Change From Previous | Change / Previous σ | Source Page |

| --- | --- | --- | --- | --- | --- |

| 2002 | 5.585694701 | 0.000000056 | — | — | https://physics.nist.gov/cuu/pdf/all_2002.pdf |

| 2006 | 5.585694713 | 0.000000046 | +0.000000012 | +0.21σ | https://physics.nist.gov/cuu/pdf/all_2006.pdf |

| 2014 | 5.585694702 | 0.000000017 | −0.000000011 | −0.24σ | https://physics.nist.gov/cuu/pdf/all_2014.pdf |

| 2018 | 5.5856946893 | 0.0000000016 | −0.0000000127 | −0.75σ | https://physics.nist.gov/cuu/pdf/all_2018.pdf |

Editions with unchanged central value and unchanged uncertainty are

omitted.

[45.12] Appendix — Absolute Neutron g-Factor — CODATA Recommended Values

| Year | Central Value | Standard Uncertainty (1σ) | Change From Previous | Change / Previous σ | Source Page |

| --- | --- | --- | --- | --- | --- |

| 2002 | 3.82608546 | 0.00000090 | — | — | https://physics.nist.gov/cuu/pdf/all_2002.pdf |

| 2006 | 3.82608545 | 0.00000090 | −0.00000001 | −0.01σ | https://physics.nist.gov/cuu/pdf/all_2006.pdf |

| 2022 | 3.82608552 | 0.00000090 | +0.00000007 | +0.08σ | https://physics.nist.gov/cuu/pdf/all.pdf |

Absolute magnitude is shown; unchanged editions are omitted.

[45.13] Appendix — Historical Shift Summary

| Quantity | Largest Historical Shift / Previous σ | Year of Largest Shift | Latest Shift / Previous σ | Latest Displayed Year |

| --- | --- | --- | --- | --- |

| α^{-1} | −6.44σ | 2010 | +4.43σ | 2022 |

| Electron Mass | +4.60σ | 2022 | +4.60σ | 2022 |

| Up-Quark Mass | −0.24σ | 2014 | −0.10σ | 2022 |

| Down-Quark Mass | −0.33σ | 2018 | −0.10σ | 2022 |

| Proton Mass | +4.38σ | 2022 | +4.38σ | 2022 |

| Neutron Mass | +2.63σ | 2022 | +2.63σ | 2022 |

| Muon Mass | +1.24σ | 2010 | +0.42σ | 2018 |

| Tau Mass | −0.59σ | 2010 | +0.25σ | 2018 |

| Absolute g_e | −4.69σ | 2022 | −4.69σ | 2022 |

| Absolute g_m | +1.50σ | 2006 | −0.44σ | 2022 |

| g_p | −0.75σ | 2018 | −0.75σ | 2018 |

| Absolute g_n | +0.08σ | 2022 | +0.08σ | 2022 |

The shift metric uses the previous displayed edition's quoted

uncertainty and is not a combined two-measurement significance.

Tau g-factor note: the experimental Standard-Model value is not included

as a CODATA-style precision historical measurement series.

Appendix 46: Principles of Logic

Philosophy: Metaknowledge, wisdom, insight, discernment, and intuition of truth beyond sensory perception and observation; the pursuit of truth over and above the pursuit of factual reality and ontology; free reflection on anything, even within an endless transcendental chain: thinking about thinking, thinking about thinking about thinking, and so on.

Logic, in turn, is the framework for expression and reasoning within thought.

Historical background: Socrates pioneered dialectics and the pursuit of truth through questions and answers. Plato, one of the founders of philosophy, was a student of Socrates; Aristotle, one of the founders of logic, was a student of Plato.

Logic

Every science is founded upon three fundamental pillars: logic, definitions, and principles.

Logic provides a framework for expressing and exchanging ideas, especially for sound reasoning, and is understood by default as Aristotelian logic. Other logics, including fuzzy logic, probabilistic logic, and gradational logic, are distinct concepts whose relationship to Aristotelian logic can be examined in terms of generalization or extension. Formal Logic is likewise a continuation of Aristotelian logic, supporting greater complexity through mathematical symbols. Formal logic means that propositions are assumed or stipulated to be true as axioms, and the truth of new propositions—or at least the validity of new inferences—is judged solely on the basis of their form and structure, without regard to their content or consequences.

A **definition** is a proposition that distinguishes a thing or concept from the set of concepts similar to it. The preceding sentence was itself a definition of definition. A **proposition** is a declarative sentence, meaning a sentence capable of being true or false, as distinct from interrogative, imperative, or exclamatory sentences.

Principles are relationships among defined concepts. Within formal logic, principles are axioms, that is, postulates. Calling scientific principles *laws* or *rules* should not lead to misunderstanding: a law is enacted by lawmakers and can be repealed. A rule, too, is rooted in tradition or collective agreement; even if it is terrestrial, it is not cosmic. For example, the right-hand rule for determining the direction of an axis of rotation is a human convention.

Theorems are propositions derived by inference through a process of reasoning based on logic, definitions, principles, and {previously proven theorems used in the proof}; inference is thus the final step of the reasoning process.

In a **proof** of a theorem, reasoning is generally either deduction or induction (generalization), provided that the induction is either complete or mathematical. Other types of reasoning suffice for justification, such as synthesis (with experience), analysis (within information and assumptions, without regard to experience), analogy, and the principle of simplicity (which says that under similar conditions, the simplest explanation is preferred).

Aristotelian Logic

Law of Identity

[46.1] $A = A$

First principle — Identity: Everything is itself and is equivalent, indeed identical, to itself. This guarantees that concepts and propositions retain a stable and definite meaning, at least throughout an argument.

Law of Non-Contradiction

[46.2] $\sim(A \wedge \sim A)$

Second principle — Non-contradiction: A contradictory conjunction is impossible; that is, of two contradictory propositions, necessarily one is false.

Law of Excluded Middle

[46.3] $A \vee \sim A$

Third principle — Excluded Middle: Contradictory absence is impossible; that is, of two contradictory propositions, necessarily one is true.

Impossibility of Contradictories combines the second and third principles: of two contradictory propositions, necessarily one is true and the other false.

Basic Logical Definitions and Combinations

Negation

[46.4] ~A

Also:

[46.5] ¬A

Conjunction

[46.6] A ∧ B

This means “A and B”; it is true when both propositions are true, and false otherwise.

Disjunction

[46.7] A ∨ B

This means “A or B”; it is true when at least one proposition is true and false only when both are false.

Conditional

[46.8] A → B

This means “if A, then B,” and is false only when A is true and B is false; in all other cases it is true.

Contrapositive Equivalence

[46.9] (A → B) = (B ∨ ~A) = (~B → ~A)

In the expression A → B, proposition A is the antecedent (premise), or a sufficient condition for B, while B is the consequent, or a necessary condition for A. If A is always false, the proposition is that the entire conditional proposition is true by absence of the antecedent. From an existential perspective, or in the language of causality, A → B means that A is the cause of B and B is evidence for A. If A and B are also necessary and sufficient conditions for each other, they are equivalent and, from an existential perspective, one and the same thing.

Thus there are two kinds of **demonstration**:

A priori demonstration: Of the kind involving syllogism, inference, and proof; in Latin, *Argumentum a priori*; deductive reasoning; *lemmatic* demonstration; from agent to effect, from cause to consequence (*Reasoning from Cause to Effect*). In this demonstration, the mind proceeds from cause to effect. Because it is known that the *why* (the *lemma*) of a phenomenon, the analysis can predict the result.

A posteriori demonstration: Of the inductive kind; in Latin, *Argumentum a posteriori*; inductive reasoning; *inni* demonstration; from effect to agent, from consequence to cause (*Reasoning from Effect to Cause*). Here the mind follows the reverse path: from an effect (a sign), it infers the existence of a cause. the analysis know only that something *is* (inni), but not necessarily why. This demonstration constitutes logical reasoning when the cause of the observed effect is exclusive. For example, one may infer with certainty from the fact that the ground is wet that rain has fallen only if rain is the sole possible cause of the ground being wet, for example on that scale.

Types of Deductive Reasoning

Categorical Syllogism

Example: All humans are mortal. Socrates is human. Therefore, Socrates is mortal.

Predicative Syllogism

Example: All birds have wings. A crow is a bird. Therefore, a crow has wings.

Hypothetical Syllogism

Example: If it rains, the ground becomes wet. If the ground becomes wet, it is slippery. Therefore, if it rains, the ground is slippery.

Disjunctive Syllogism

Example: It is either day or night. It is not day. Therefore, it is night.

Reductio ad Absurdum

Example: Suppose a number is both even and odd. This yields a contradiction. Therefore, no such number exists.

Immediate Inference

Example: All humans are mortal. Therefore, some mortals are human.

Conditional Inference — Modus Ponens / Modus Tollens

Example of **Modus Ponens**: If there is fire, there is smoke. There is fire. Therefore, there is smoke.

Example of **Modus Tollens**: If there is fire, there is smoke. There is no smoke. Therefore, there is no fire.

End of Paper

Archive

In the event of any inconsistency between the archive and the article text preceding this point, the archive is, by default, considered less authoritative than the article.